

---

# **Characterization of Anti-Enteroviral Activity of Heparan Sulphate Mimetic Compounds**

**By:**

Hamid Reza Pourianfar

A thesis submitted in fulfillment of the  
requirements for the degree of  
Doctor of Philosophy  
2012

Environmental and Biotechnology Centre  
Swinburne University of Technology  
Australia

---

## Summary

Enterovirus 71 (EV71) infection remains a public health problem at a global level, particularly in the Asia-pacific region. The infection normally manifests as hand-foot-mouth disease (HFMD); however, it is capable of developing into potentially fatal neurological complications. There is currently no approved vaccine or antiviral substance available for prevention or treatment of EV71 infection.

There has been no research undertaken to examine the possible antiviral activity of heparan sulphate (HS) mimetics against the Human Enterovirus A (HEV-A), in particular EV71. Therefore, this PhD research began with the aim of investigating the antiviral potencies of HS mimetics against EV71 infection.

Initially, a colorimetric-based method was developed for the titration of EV71 strains, whereby the viral titre was quantified more precisely. Three soluble HS mimetics including heparin (Hep), HS, and pentosan polysulphate (PPS) were then shown to substantially inhibit a cloned strain of EV71 from infecting in Vero cells. Further investigations revealed that the compounds most likely exerted their antiviral action through interference with the EV71 attachment.

The role of cell surface HS in mediating viral infection was then studied for several clinical isolates of HEV-A and HEV-B in Vero cells as well as a human neuroblastoma cell line, SK-N-SH. The findings revealed that the clinical isolate of EV71 utilizes low sulphated domains of cellular HS to bind to Vero cells, in contrast to Coxsackievirus B4 (CVB4), Coxsackievirus A16 (CVA16), and the cloned EV71. In the neural cells, Hep and PPS significantly prevented both clinical EV71 and clinical CVA16 binding and infections, although it could not be confirmed whether the viruses utilize cellular HS to bind to the cells.

Finally, an Affymetrix DNA microarray was performed to gain insight into the mechanisms of action of Hep against the clinical EV71 infection in the neural cells. The results showed many genes with significant down- or up-regulation across the undermentioned conditions: negative control cells, compound control (cells treated with Hep only), virus control (cells treated with virus only), and treatment control (EV71-infected cells treated with Hep). Several genes were finally found to be targets for the anti-EV71 activity of Hep in SK-N-SH cells using a strict multi-level selection procedure. In parallel, the results revealed the significant induction of

more than 1000 genes by EV71 infection with expression fold changes ranged from +46.5 to -10.7. The findings of this research may suggest new directions for studies of designing molecular drug targets against EV71 infection.

## Acknowledgements

It would not have been possible to write this PhD thesis without the persistent help and support of my principle supervisor, Dr. Lara Grollo. She guided me patiently and constantly through my PhD project and helped me shape research areas for my future research career. She taught me how to professionally manage my research ideas and draw meaningful and relevant conclusions. In addition, I learned from her to display a positive and friendly attitude at all times particularly while supervising students. Hence, I would like to express my sincere and deepest gratitude to her for helping me to gain invaluable academic and research experiences during my PhD studies.

My great thanks also go to Associate Professor Enzo Palombo, my associate supervisor, for his very warm support and for displaying a professional behavior. In addition, I would like to extend my thanks to the following people: Professor Chit Laa Poh, who was my former principal supervisor, for giving me the opportunity to choose virology as my PhD research subject, Mr. John Fecondo for his very friendly support, and Dr. Jill Shaw for her significant technical advice. It is also my pleasure to thank my colleagues and friends particularly Babu, Dhivya, and Kristin. I will never forget their support during our precious weekly lab meetings.

I am proud to be awarded a tuition fee scholarship for my PhD studies from Swinburne University of Technology. In addition, I would like to appreciate the annual financial assistance I received from Faculty of Life and Social Sciences for preparing the required materials and reagents of my PhD studies. Environment and Biotechnology Centre (EBC) of Swinburne University of Technology paid part of the costs of my travel to Holland for attending a conference. I also wish to thank all the technical lab staff at EBC for providing facilities and support for conducting my experimental work.

The cloned strain of EV71 and the Vero cell line were kindly provided by Professor Peter C. McMinn (Central Clinical School, University of Sydney, Australia), which is deeply and warmly appreciated. The microarray hybridization assays were performed at Peter MacCallum Cancer Centre in Melbourne. Particularly, I would like to thank Dr. Tim Holloway and Dr. Li Jason for their great help and useful technical comments and recommendations.

I am very lucky for being always supported by my wife, Raheleh. While I had dedicated myself to research over my stay in Australia, she warmly supported me with her understating and unconditional love and patience.

Lastly, I would like to offer my regards to all of those who supported me in any form during the completion of my PhD project. Particularly, my wife and I are grateful to many Australian nice friends whose warm support eased frustrations of my PhD project as well as hardships of living in a foreign country.

## **Declaration**

I would like to declare that this thesis is my original work and has not previously been submitted for a degree. In addition, to the best of my knowledge, the thesis contains no material previously published or written by another person except where due reference is made in the text. Furthermore, where the work is based on joint research or publications, the thesis discloses the relative contributions of the respective workers or authors.

Hamid Reza Pourianfar

June 2012

## Communications

### Papers:

- **Pourianfar HR**, Poh CL, Fecondo J, Grollo L. 2011. In vitro evaluation of the antiviral activity of heparan sulphate mimetic compounds against enterovirus 71. Submitted to Virus Research, 5<sup>th</sup> of January 2012 (Ref. no. VIRUS-D-12-00016).
- Kirk K, Shaw J, **Pourianfar HR**, Fecondo J, Poh CL, Grollo L. 2012. Cross-reactive neutralizing antibody epitopes against Enterovirus71 identified by an in-silico approach. Submitted to Vaacine, 16<sup>th</sup> of Feb 2012.

### In-preparation original papers:

- **Pourianfar HR**, Javadi A, Grollo L. 2011. A rapid and accurate method for the determination of Enterovirus 71 titre.
- **Pourianfar HR et al.** Evidence for a role of heparan sulphate in mediating infection and attachment of Enterovirus 71 in Vero and neural cells.
- **Pourianfar HR et al.** Global impact of heparin on gene expression profiles induced by Enterovirus 71 in neural cells.
- **Pourianfar HR et al.** Host gene expression profiling in Enterovirus 71-infected neural cells.
- **In-preparation review papers:**
- **Pourianfar HR et al.** Two review papers on:
  - i) Enterovirus antivirals; ii) Candidate cellular receptors of Enteroviruses.

### Seminars:

- **Pourianfar HR**, Fecondo J, Poh CL, Grollo L. 2010. In vitro evaluation of the antiviral activity of heparansulphate mimetic compounds against enterovirus 71. The 30<sup>th</sup> Antiviral Congress, Amsterdam, the Netherlands, 7-9 November.

- Kirk K, Poh CL, Fecondo J, **Pourianfer HR**, Grollo L. 2011. Anin-silico derived induction of EV71 specific neutralizing antibodies from cross-reactive synthetic peptides of the picornavirus family. Third World Congress of Vaccine, Beijing, China, March.
- K. Kirk, J. Fecondo, **H. Pourianfar**, L. Grollo. 2009. Identification of novel epitopes capable of neutralising human Enterovirus71. The 2009 Australasian Society for Immunology Meeting, Conrad Jupiters, Broadbeach, QLD, Australia.
- Grollo L, **Pourianfar HR**, Kristin K. 2010. Design and development of antiviral drugs and vaccines for the prevention and treatment of Enterovirus71 infection. A Monash University seminar.



---

## Table of Contents

<b>Summary</b> .....	<b>i</b>
<b>Acknowledgements</b> .....	<b>iii</b>
<b>Declaration</b> .....	<b>v</b>
<b>Communications</b> .....	<b>vi</b>
<b>Table of Contents</b> .....	<b>viii</b>
<b>List of Tables</b> .....	<b>xii</b>
<b>List of Figures</b> .....	<b>xiii</b>
<b>List of Abbreviations</b> .....	<b>xv</b>
<b>Chapter One: Literature Review</b> .....	<b>1</b>
1.1. Enterovirus 71 taxonomy .....	1
1.2. Genome and polyprotein structure .....	1
1.3. Life cycle.....	7
1.4. Molecular epidemiology .....	9
1.5. Clinical manifestations.....	10
1.6. Control of EV71 .....	13
1.6.1. Capsid-binding compounds.....	14
1.6.2. Antiviral drugs targeting viral proteases .....	15
1.6.3. Nucleotide analogs-mediated mutagenesis: Ribavirin .....	16
1.6.4. RNA interference .....	19
1.6.5. Antiviral peptides .....	24
1.6.6. Antiviral compounds of natural origin.....	27
1.7. Glycans and glycan mimetics: a contribution to virus receptors and antivirals .....	30
1.7.1. Introduction .....	30
1.7.2. Heparan sulphate/Heparin .....	33
1.7.3. Enzymatic removal of cell surface HS.....	39
1.7.4. Sialic acids .....	42
1.7.5. Glycans as virus cell receptors.....	45
1.7.6. Enterovirus 71 receptors .....	49
1.7.7. HS mimetics as antivirals.....	54
1.7.8. The role of cell surface HS in mediating viral pathogenicity <i>in vivo</i> .....	61
1.8. DNA microarrays .....	65

1.8.1. Introduction .....	65
1.8.2. Design of a high density oligo microarray .....	66
1.8.3. The general workflow for processing of a high density oligo microarray .....	70
1.8.4. Applications of DNA microarrays in clinical virology.....	73
1.9. Aims of this PhD thesis.....	74
<b>Chapter Two: Improvements in the Enterovirus 71 Titration .....</b>	<b>76</b>
2.1. Introduction .....	76
2.2. Materials and Methods.....	79
2.2.1. Cell and virus .....	79
2.2.2. Cell seeding and infection of cell cultures .....	79
2.2.3. Conventional TCID <sub>50</sub> titration assay .....	80
2.2.4. Modified traditional TCID <sub>50</sub> titration assay .....	80
2.2.5. The MTS-based endpoint dilution assay.....	80
2.2.6. The MTT-based endpoint dilution assay.....	81
2.2.7. Virus titration via plaquing assay.....	81
2.2.8. Statistical analysis .....	82
2.3. Results .....	82
2.3.1. Traditional TCID <sub>50</sub> .....	82
2.3.2. Modified traditional TCID <sub>50</sub> .....	83
2.3.3. The colorimetric-based virus titration.....	87
2.3.4. Titration via plaquing assay .....	88
2.4. Discussion .....	96
<b>Chapter Three: Antiviral Activity of Heparan Sulphate Mimetic Compounds and Their Mechanism against Enterovirus 71.....</b>	<b>99</b>
3.1. Introduction .....	99
3.2. Materials and Methods.....	101
3.2.1. Viruses and Cells .....	101
3.2.2. Compounds .....	101
3.2.3 Cell seeding and infection of cell cultures .....	101
3.2.4. Cytotoxicity assay .....	102
3.2.5. Cytopathic effect inhibition assay.....	102
3.2.6. Time of addition assay .....	102
3.2.7. Attachment assay .....	103
3.2.8. Penetration assay.....	103

3.2.9. Statistical analysis .....	104
3.3. Results .....	104
3.3.1. Cytotoxicity assay .....	104
3.3.2. Antiviral activity assay .....	104
3.3.3. Time of addition assay .....	109
3.3.4. Virus binding assay .....	110
3.3.5. Penetration assay .....	110
3.4. Discussion .....	117
<b>Chapter Four: Contributions of Heparan Sulphate as a Candidate Receptor for Enteroviruses .....</b>	<b>121</b>
4.1. Introduction .....	121
4.2. Materials and Methods .....	127
4.2.1. Cell lines and viruses .....	127
4.2.2. Reagents .....	127
4.2.3. Cell seeding and infection of cell cultures .....	128
4.2.4. Cytotoxicity assay .....	128
4.2.5. Infectivity assay with soluble glycosaminoglycans .....	129
4.2.6. Virus binding assay .....	129
4.2.7. GAG-lytic enzyme treatment .....	129
4.2.8. Statistical analysis .....	130
4.3. Results .....	131
4.3.1. Cytotoxicity assay .....	131
4.3.2. Anti-Enteroviral activity of Hep and PPS .....	133
4.3.3. Enteroviral attachment in the presence of GAGs compounds .....	144
4.3.4. Enteroviral attachment in the absence of cell surface HS .....	152
4.4. Discussion .....	154
<b>Chapter Five: Microarray Analysis of Antiviral Activity of Heparin against Enterovirus 71 .....</b>	<b>160</b>
5.1. Introduction .....	160
5.2. Materials and Methods .....	163
5.2.1. Cell lines and viruses .....	163
5.2.2. Reagents .....	163
5.2.3. Cell seeding and infection of cell cultures .....	163
5.2.4. Cytotoxicity and antiviral activity assays .....	164
5.2.5. Total RNA isolation and purification .....	165

5.2.6. RNA qualification and quantification .....	165
5.2.7. Arrays .....	166
5.2.8. Target preparation and hybridization process .....	166
5.2.9. Statistical analysis .....	167
5.3. Results .....	167
5.3.1. Cytotoxicity and antiviral activity .....	167
5.3.2. Assessment of total RNA samples .....	168
5.3.3. Gene expression profiling of SK-N-SH cells .....	172
5.3.4. Pattern of gene expression induced by antiviral activity of Hep .....	174
5.4. Discussion .....	184
<b>Chapter Six: Final Conclusions .....</b>	<b>195</b>
6.1. Establishment of a method for improving accuracy of EV71 titration .....	195
6.2. Antiviral activities of heparan sulphate mimetics against EV71 .....	196
6.3. Contributions of HS as a candidate receptor for Enteroviruses .....	196
6.4. Microarray analysis of anti-EV71 activity of Hep .....	199
6.5. Final statement .....	201
<b>Appendices .....</b>	<b>202</b>
Appendix 1 .....	202
Use of TCID <sub>50</sub> to determine viral dilutions for plaquing assay .....	202
Appendix 2 .....	203
Observation and scoring of viral CPE in the traditional TCID <sub>50</sub> : .....	203
Appendix 3 .....	205
Drug safety index .....	205
Appendix 4 .....	206
Testing different concentrations of Hep and PPS against CVB4 .....	206
Appendix 5 .....	207
Some of microarray results .....	207
<b>Bibliography .....</b>	<b>211</b>

---

## List of Tables

Table 1.1. The current classification of <i>Picornaviridae</i> .....	3
Table 1.2. Properties/functions of the proteins encoded by the EV71 genome .....	4
Table 1.3. RNAi-based antiviral drugs that have been tested in clinical trials .....	23
Table 1.4. Examples of antiviral peptides against DNA and RNA viruses. ....	26
Table 1.5. Structural distinctions between HS and Hep sulphate groups .....	38
Table 1.6. Classification of viruses which use glycoepitopes (sialic acid or HS) as receptors .....	48
Table 1.7. Characteristics of three important HS mimetics .....	59
Table 1.8. Relationship between cellular HS usage and <i>in vivo</i> pathogenesis in mutant viruses .....	63
Table 2.1. Comparison of TCID <sub>50</sub> /mL amounts resulted from different titration assays .....	92
Table 2.2. Comparison of TCID <sub>50</sub> , PFU and MOI amounts in the clinical and cloned strains of EV71 .....	93
Table 3.1. Potency of antiviral activity of the compounds .....	108
Table 4.1. Cell receptors of members of Human Enteroviruses .....	124
Table 5.1. Effect of interaction between Hep and EV71 on genes of neural cells (well annotated genes).....	175
Table 5.2. Effect of Hep on genes of EV71-infected of neural cells (un-annotated genes) .....	176
Table 5.3. Comparison of effects of Hep on genes of normal and EV71-infected neural cells (well annotated genes) .....	178
Table 5.4. Comparison of effects of Hep on genes of normal and EV71-infected neural cells (un-annotated genes).....	179
Table 5.5. Hep-induced genes that were not induced significantly by EV71 infection of neural cells (well annotated genes).....	181

---

## List of Figures

Figure 1.1. Typical structure of the EV71 ORF .....	5
Figure 1.2. Schematic structure of an Enterovirus virion .....	6
Figure 1.3. Cellular life cycle of a typical poliovirus .....	8
Figure 1.4. Typical HFMD in a child infected with EV71 .....	12
Figure 1.5. Molecular structures of Ribavirin, Adenin and Guanin.....	18
Figure 1.6. Mechanism of siRNA silencing.....	20
Figure 1.7. A schematic demonstration of binding of GAGs to a protein core .....	32
Figure 1.8. The structure of Hep .....	35
Figure 1.9. The structure of HS.....	37
Figure 1.10. A schematic demonstration of activity of heparinase enzymes.....	40
Figure 1.11. The schematic structures of two common sialic acids.....	44
Figure 1.12. EV71 cell receptors suggested to date .....	52
Figure 1.13. Schematic representation of the design of a GeneChip .....	68
Figure 1.14. Illustration of an oligo microarray procedure compared to cDNA microarray .....	71
Figure 2.1. Depiction of the titre of the cloned EV71 virus using the conventional method of TCID <sub>50</sub> .....	83
Figure 2.2. Depiction of the titre of the cloned EV71 virus using three methods based on log <sub>2</sub> dilution.....	85
Figure 2.3. Depiction of the titre of the clinical EV71 virus using two methods based on log 2 dilution .....	86
Figure 2.4. Micrographs of cell monolayer damages following EV71 infection.....	90
Figure 2.5. The plaque formation of both cloned and clinical EV71 .....	94
Figure 3.1. Cytotoxic effects and anti-Enterovirus 71 activities of the test compounds .....	106

Figure 3.2. Antiviral effect of the compounds during different times of the virus infection..... 112

Figure 3.3. Inhibition of Enterovirus 71 binding to the Vero cells ..... 114

Figure 3.4. Effect of the test compounds on Enterovirus 71 entry into Vero cells.. 116

Figure 4.1. Comparison of the cytotoxic effects of Hep and PPS in Vero and neural cells. .... 132

Figure 4.2. Anti-Enteroviral activities of Hep and PPS in Vero cells. .... 135

Figure 4.3. Micrographs of clinical EV71 CPE inhibition by PPS in Vero cells .... 137

Figure 4.4. Anti-Enteroviral activities of Hep and PPS in neural cells. .... 143

Figure 4.5. The effect of GAGs on Enteroviral binding to Vero and neural cells. . 146

Figure 4.6. Micrographs of inhibition of Enteroviral binding to Vero cells ..... 147

Figure 4.7. Relative effect of heparinase enzymes on Enteroviral binding to Vero cells. .... 153

Figure 5.1. Gel-like images of RNA Nano assay..... 169

Figure 5.2. The electropherogram of an RNA sample, generated by the Bioanalyzer ..... 171

Figure 5.3. Frequency of gene-level intensities ..... 173

Figure 5.4. Scanned images of microarray analysis of four conditions ..... 183

## List of Abbreviations

°C	Degrees Celsius
µg	Microgram
µL	Microlitre
µM	Micromolar
aa	Amino Acid
AEV	Avian Encephalomyelitis-Like Virus
Affx	Affymetrix
AFP	Acute Flaccid Paralysis
AGO2	Endonuclease Argonaut 2
AIDS	Acquired Immunodeficiency Syndrome
AiV	Aichi Virus
ANOVA	Analysis of Variance
Arg	Arginine
ASP	Aspartic Acid
ATP	Adenosine-5'-Triphosphate
ATPase	Adenosine Triphosphatase
AVPR2	Arginine Vasopressin Receptor 2
Axn7	Annexin 7
BATF	Basic Leucine Zipper Transcription Factor, ATF-Like
BEV	Bovine Enterovirus
BHK	Baby Hamster Kidney
BSA	Bovine Serum Albumin
BVES	Blood Vessel Epicardial Substance
C1QTNF1	C1q and Tumor Necrosis Factor Related Protein 1
CAR	Coxsackievirus-Adenovirus Receptors
CC	Cell Control
CC <sub>50</sub>	50% Cytotoxic Concentration
CCR5	Chemokine (C-C Motif) Receptor 5
cDNA	Complementary Deoxyribonucleic Acid
CHO	Chinese Hamster Ovary



CHTF18	Chromosome Transmission Fidelity Factor 18 Homolog ( <i>S. cerevisiae</i> )
CHTF8	Chromosome Transmission Fidelity Factor 8 Homolog ( <i>S. cerevisiae</i> )
CMV	Cytomegalovirus
CNS	Central Nervous System
CO <sub>2</sub>	Carbon Dioxide
CPE	Cytopathic Effect
CPPs	Cell Penetrating Peptides
cRNA	Complementary Ribonucleic Acid
CVA16	Coxsackievirus A16
CVA21	Coxsackievirus A21
CVA24	Coxsackievirus A24
CVB	Coxsackievirus B
CVB3	Coxsackievirus B3
CVB3-PD	Coxsackievirus B3 Variant PD
CVB4	Coxsackievirus B4
CXCR4	Chemokine (C-X-C Motif) Receptor 4
Da	Dalton
DAF	Decay-Accelerating Factor
DF	Dilution Factor
DMEM	Dulbecco's Modified Eagle's Medium
DMSO	Dimethyl Sulfoxide
DNA	Deoxyribonucleic Acid
DSCC1	Defective in Sister Chromatid Cohesion 1 Homolog ( <i>S. cerevisiae</i> )
dsRNA	Double-Stranded Ribonucleic Acid
DYNLT3	Dynein, Light Chain, Tctex-Type 3
ECM	Extracellular Matrix
EFHD2	EF-Hand Domain Family, Member D2
EFTUD1	Elongation Factor Tu GTP Binding Domain Containing 1
EMCV	Encephalomyocarditis Virus
ERAV	Equine Rhinitis A Virus

ERBV	Equine Rhinitis B Virus
EV70	Enterovirus 70
EV71	Enterovirus 71
EVs	Enteroviruses-Echoviruses
f.p.	Footpad
FasL	Fas Ligand
FBS	Fetal Bovine Serum
FDR	False Discovery Rate
FMDV	Foot-and-Mouth Disease Virus
GAG	Glycosaminoglycan
GAS	Gamma-Activated Sequence
GEO	Gene Expression Omnibus
GGT	Ge-Gen-Tang
GIP	G Protein-Coupled Receptor-Interacting Protein
GlcA	$\beta$ -D-Glucuronic Acid
GlcN	$\beta$ -D-Glucosamine
GlcNAc	$\beta$ -D-Glucosamine <i>N</i> -acetylated
GlcNS	$\beta$ -D-Glucosamine <i>N</i> -sulphated
Gln	Glutamine
Glu	Glutamic Acid
Gly	Glycine
gp	Glycoprotein
GPCR	G-Protein-Coupled Receptors
GPNMB	Glycoprotein (Transmembrane) nmb
GPR62	G Protein-Coupled Receptor 62
GTF2IRD1	GTF2I Repeat Domain Containing 1
GTP	Guanosine-5'-Triphosphate
HAV	Hepatitis A Virus
HBDs	Heparin-Binding Domains
HBsAg	Hepatitis B Virus Surface Antigen
HBV	Hepatitis B Virus
HCC	Hepatocellular Carcinoma
HCMV	Human Cytomegalovirus

HCV	Hepatitis C Virus
Hep	Heparin
HEV-A	Human Enterovirus A
HEV-B	Human Enterovirus B
HEV-C	Human Enterovirus C
HEV-D	Human Enterovirus D
HEVs	Human Enteroviruses
His	Histidine
HIV	Human Immunodeficiency Virus
HKR1	HKR1, GLI-Kruppel Zinc Finger Family Member
HPeV	Human Parechovirus
HPRT1	Hypoxanthine PhosphoribosylTransferase 1
HPV	Human Papillomavirus
HRV	Human Rhinovirus
HS	Heparan Sulphate
HSD	Honestly Significant Difference
HSPG	Heparan Sulphate Proteoglycan
HSV-1	Herpes Simplex Virus 1
HSV-2	Herpes Simplex Virus 2
i.c.	Intracranial
i.d.	Intradermal
i.d.l.	Intradermal-Lingual
i.n.	Intranasal
i.p.	Intraperitoneal
IC <sub>50</sub>	50% Inhibitory Concentration
ICAM-1	Intercellular Adhesion Molecule-1
IdoA	$\alpha$ -L-Iduronic Acid
IFN	Interferon
IFN $\alpha$	Interferon Alfa
IFN $\beta$	Interferon Beta
IFN $\gamma$	Interferon Gamma
IgA	Immunoglobulin A
IgE	Immunoglobulin E

IgG	Immunoglobulin G
IgM	Immunoglobulin M
IL	Interleukin
IMP	Inosine Monophosphate
IRES	Internal Ribosome Entry Site
ISGs	Interferon-Stimulated Genes
ISRE	Interferon-Stimulated Response Element
IVT	<i>in vitro</i> Transcription
JEV	Japanese Encephalitis Virus
Kb	Kilo Base
KDM4D	Lysine (K)-Specific Demethylase 4D
Kdn	2-Keto-3-Deoxynononic Acid
Lys	Lysine
MC	Myocarditis
MEV	Murray Valley Encephalitis Virus
mg	Milligram
miRNA	Micro Ribonucleic Acid
mL	Millilitre
MM	Mismatch
MOI	Multiplicity of Infection
$M_r$	Relative Molecular Mass
mRNA	Messenger Ribonucleic Acid
MT1E	Metallothionein 1E
MTS	3-(4,5-dimethylthiazol-2-yl)-5-(3-carboxymethoxyphenyl)-2-(4-sulfophenyl)-2H-tetrazolium
MTSs	Membrane Translocating Sequences
MTT	3-(4, 5-Dimethylthiazol-2-yl)-2, 5-diphenyltetrazolium bromide, a yellow tetrazole
MuLV	Murine Leukemia Virus
MW	Molecular Weight
NA	<i>N</i> -Acetylated
NaPPS	Pentosan Polysulphate Sodium Salt
NCBI	National Center for Biotechnology Information

NDUFA1	NADH Dehydrogenase (Ubiquinone) 1 Alpha Subcomplex, 1, 7
Neu5Ac	<i>N</i> -Acetylneuraminic Acid
nm	Nanometre
nM	Nanomolar
NO	Nitric Oxide
NS	<i>N</i> -Sulphated
ns	Not Significant
NSV	Sindbis Variant
OAS-1	2',5'-Oligoadenylate Synthetase-1
OD	Optical Density
ORF	Open Reading Frame
p.o.i	Post Infection/Inoculation
PBS	Phosphate Buffered-Saline
PCA	Principal Component Analysis
PCNA	Proliferating Cell Nuclear Antigen
PCR	Polymerase Chain Reaction
PCV2	Porcine Circovirus Type 2
PD	Proportionate Distance
PDTs	Protein Transduction Domains
PEV	Porcine Enterovirus
PFU	Plaque Forming Unit
PG	Proteoglycan
PKR	RNA-dependent protein kinase
PM	Perfect Match
PPS	Pentosan Polysulphate
PRTFDC1	Phosphoribosyltransferase domain containing 1
PSGL	Human P-Selectin Glycoprotein Ligand-1
PTV	Porcine Teschovirus
PV	Poliovirus
qPCR	Quantitative Polymerase Chain Reaction
RBM7	RNA Binding Motif Protein 7
RBV	Ribavirin

RC	Respiratory Chain
RCSD1	RCSD Domain Containing 1
RD	Human Rhabdomyosarcoma
RefSeq	Reference Sequence
RF	Replicative Form
RIN	RNA Integrity Number
RISC	Ribonucleic Acid-Induced Silencing Complex
RNA	Ribonucleic Acid
RNAi	Ribonucleic Acid Interference
RNase	Ribonuclease
rRNA	Ribosomal Ribonucleic Acid
RRV	Ross River Virus
RSV	Respiratory Syncytial Virus
RT PCR	Reverse Transcriptase Polymerase Chain Reaction
RTP	Ribavirin Triphosphate
S (in 18S/28S rRNA)	Svedberg Units
s.c.	Subcutaneous
SAGE	Serial Analysis of Gene Expression
SARS-CoV	Severe Acute Respiratory Syndrome Coronavirus
SCARB2	Human Scavenger Receptor Class B, Member 2
SCC1	Sister Chromatid Cohesion1
SD	Standard Deviation
SDS	Sodium Dodecyl Sulphate
Ser	Serine
SFV	Swine Fever Virus
shRNA	Small Hairpin Ribonucleic Acid
SI	Selectivity Index
SIN	Sindbis Virus
siRNA	Short Interfering Ribonucleic Acid
SIV	Simian Immunodeficiency Virus
SMC1	Structural Maintenance of Chromosomes 1
SMC3	Structural Maintenance of Chromosomes 3
SMGGT	Sheng-Ma-Ge-Gen-Tang

SNP	Single Nucleotide Polymorphism
SPANXE	SPANX Family, Member E
ssRNA	Single-Stranded Ribonucleic Acid
STRING	Search Tool for the Retrieval of Interacting Genes
SVDV	Swine Vesicular Disease Virus
TAGLN	Transgelin
TCID <sub>50</sub>	50% Tissue Culture Infectious Dose
TCM	Traditional Chinese Medicine
TESK2	Testis-Specific Kinase 2
TFPI	Tissue Factor Pathway Inhibitor (Lipoprotein-Associated Coagulation Inhibitor)
Thr	Threonine
TMEV	Theiler's Murine Encephalomyelitis Virus
TNF	Tumor Necrosis Factor
TOX	Thymocyte Selection-Associated High Mobility Group Box
U	Unit
UTR	Untranslated Regions
V	Volume
VC	Virus Control
VEE	Venezuelan Equine Encephalitis Virus
VHEV	Vilyuisk Human Encephalomyocarditis Virus
VP	Viral Protein
VZV	Varicella Zoster Virus
WT	Whole Transcripts

**Single letter abbreviations (for DNA, RNA and peptides)**

A	Adenine
C	Cytosine
G	Guanine
P	Polyprotein
T	Thymine
U	Uracil

# 1. Chapter One: Literature Review

## 1.1. Enterovirus 71 taxonomy

Enterovirus 71 (EV71) is a pathogenic serotype of the *Picornaviridae* family (Table 1.1). The virus contains a single positive sense RNA genome with a length of approximately 7.5 kb (King et al., 2000). Along with EV71, there are more than 70 distinct serotypes of Enteroviruses that infect both human and non-human hosts (T.C. Chen et al., 2008b). Based on analysis of the complete sequences of the capsid protein (VP1) for 113 EV71 strains (from 1970 to 1998), Brown et al. (1999) found that EV71 consists of three genetic lineages: A, B and C. Overall, the genetic variation within the lineages was 12% or less, while it was 16.5-19.7% between the lineages. Also, strains of all these genotypes were at least 94% identical in deduced amino acid sequences (Brown et al., 1999). The prototype BrCr-CA-70 is the sole member of genotype A, while the rest belong to either genotypes B or C. These two lineages are further divided into the sub-lineages, B1-B5 and C1-C4, respectively (Mizuta et al., 2005). On the whole, EV71 has been regarded as a genetically diverse virus which is rapidly evolving (McMinn, 2002).

## 1.2. Genome and polyprotein structure

Generally, the genome structure of an EV71 prototype comprises a single open reading frame (ORF) of 7500 nucleotides that produces a 2194-amino acid polyprotein. The ORF is surrounded by the 5' and 3' untranslated regions (UTR) that are considered to be essential for the virus RNA replication (Huang et al., 2008). The 5'-UTR also contains an internal ribosome entry site (IRES) domain which is important for the initiation of the virus translation (Schmid and Wimmer, 1994); this region has also been regarded a potential drug target for EV71 infection (Lin et al., 2009). The polyprotein consists of three distinct regions, P1-P3. The P1 region encodes four viral structural proteins, 1A-1D, that are more frequently referred to as VP1-VP4, while the P2 and P3 regions encode seven non-structural proteins: 2A-2C and 3A-3D, respectively (McMinn, 2002). The P1 region is shown to be the most variable genomic region among Enteroviruses (Brown and Pallansch, 1995). The



functions of these eleven EV71 proteins are believed to be the same as those of poliovirus and other non-poliovirus Enteroviruses (McMinn, 2002). Table 1.2 lists the proposed functions of the proteins encoded by the EV71 genome, while the typical genome composition of EV71 is illustrated in Fig. 1.1. A generic model of an Enterovirus virion contains an icosahedral non-enveloped capsid that surrounds the ORF. This structure is composed of 60 repeating units (protomers) (Fig. 1.2), each consisting of VP1 through VP4 (McMinn, 2002).

Brown and Pallansch (1995) were the first to sequence the complete genomes as well as polyprotein of both EV71/7423/MS/87 (a neurovirulent isolate) and EV71/BrCr (the prototype strain). The results were then compared to those of polioviruses and other Enteroviruses. The amino acid homology of EV71 and poliovirus was 46% with the P1 capsid region and 55% with the whole polyprotein. Overall, EV71 was placed in a distinct group along with Coxsackievirus A16 rather than with poliovirus. In addition, the two tested EV71 strains were 81% identical in nucleotide and 95% in amino acid sequences.

Table 1.1. The current classification of *Picornaviridae*, adapted from Stanway et al. (2002)

Genus	Species	Serotypes
<b>Enterovirus</b>	Poliovirus	PV serotypes 1, 2, 3
	Human Enterovirus A	CVA serotypes 2, 3, 4, 5, 6, 7, 8, 10, 12, 14, 16; EV71
	Human Enterovirus B	CVB serotypes 1, 2, 3, 4, 5, 6; CVA 9 Echovirus serotypes 1, 2, 3, 4, 5, 6, 7, 9, 11, 12, 13, 14, 15, 16, 17, 18, 19, 20, 21, 24, 25, 26, 27, 29, 30, 31, 32, 33; EV 69; SVDV
	Human Enterovirus C	CVA serotypes 1, 11, 13, 15, 17, 18, 19, 20, 21, 22, 24
	Human Enterovirus D	EV 68; EV 70
	Bovine Enterovirus	BEV 1; BEV 2
	Porcine Enterovirus A	PEV 8
	Porcine Enterovirus B	PEV 9; PEV 10
<b>Rhinovirus</b>	Human Rhinovirus A	HRV serotypes 1, 2, 7, 9, 11, 15, 16, 21, 29, 36, 39, 49, 50, 58, 62, 65, 85, 89
	Human Rhinovirus B	HRV serotypes 3, 14, 72
<b>Cardiovirus</b>	Encephalomyocarditis Virus	EMCV
	Theilovirus	TMEV; VHEV
<b>Aphthovirus</b>	Foot-and-Mouth Disease Virus	FMDV serotypes O, A, C, Asia 1, SAT 1, SAT 2, SAT 3
	Equine Rhinitis A Virus	ERAV
<b>Hepatovirus</b>	Hepatitis A Virus	HAV
	Avian Encephalomyelitis-like Virus	AEV
<b>Parechovirus</b>	Human Parechovirus	HPeV 1; HPeV 2
<b>Erbovirus</b>	Equine Rhinitis B Virus	ERBV
<b>Kobuvirus</b>	Aichi Virus	AiV
<b>Teschovirus</b>	Porcine Teschovirus	PTV serotypes 1, 2, 3, 4, 5, 6, 7, 8, 9, 10, 12

**Abbreviations**

PV: poliovirus; CVA: Coxsackievirus A; CVB: Coxsackievirus B; ESVDV: swine vesicular virus; EV: Enterovirus; BEV: bovine Enterovirus; PEV: porcine Enterovirus; HRV: human rhinovirus; EMCV: encephalomyocarditis virus; TMEV: theiler's murine virus; VHEV: vilyuisk human encephalomyocarditis virus; FMDV: foot-and-mouth disease virus; ERAV: equine rhinitis A virus; HAV: hepatitis A virus; AEV: avian encephalomyelitis-like virus; HPeV: human parechovirus; ERBV: equine rhinitis B virus; AiV: aichi virus, PTV: porcine teschovirus.

**Table 1.2. Properties/functions of the proteins encoded by the EV71 genome**

<b>Protein</b>	<b>Properties/functions</b>	<b>References</b>
<b>VP4</b>	necessary for uncoating or cell entry	Moscufo et al., 1993
<b>VP2</b>	responsible for antigenic diversity of Enteroviruses	Rueckert, 1990
<b>VP3</b>	responsible for antigenic diversity of Enteroviruses	Rueckert, 1990
<b>VP1</b>	responsible for antigenic diversity of Enteroviruses; neutralization epitopes are densely clustered in VP1	Rueckert, 1990
<b>2A</b>	responsible for proteases only in Enteroviruses and rhinoviruses	Harris et al., 1990
<b>2B</b>	very little information is available but is thought to be important for RNA replication	Paul, 2002
<b>2C</b>	containing three conserved motifs (A, B and C); ATPase activity; RNA helicase activity	Paul, 2002; T.C. Chen et al., 2008b
<b>3A</b>	serving as a scaffold of the viral RNA replication complex	T.C. Chen et al., 2008b
<b>3B</b>	required for RNA replication; substrate for uridylylation	Paul, 2002
<b>3C</b>	responsible for proteases	T.C. Chen et al., 2008b
<b>3D</b>	governing RNA-dependent RNA polymerase	Palmenberg, 1990

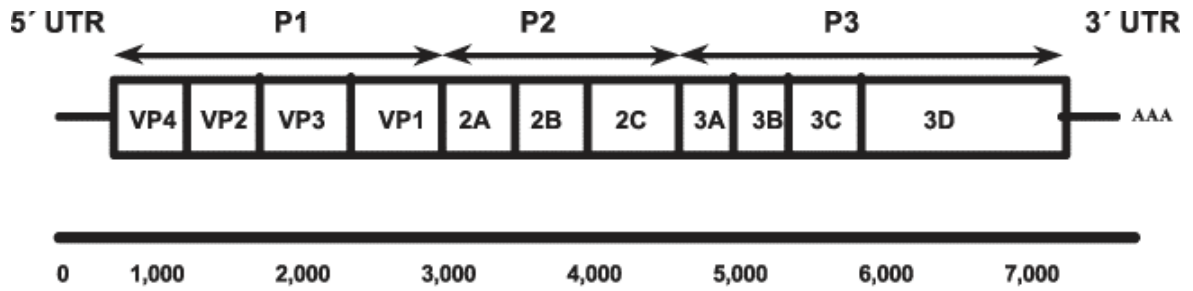


**Figure 1.1. Typical structure of the EV71 ORF**

The coding regions of the ORF are flanked by 5' UTR and 3' UTR. A poly-A tail is located at 3' UTR end. The ORF is generally divided into three regions: P1, P2, and P3. The numbers under the line represent the approximate nucleotide position relative to each protein.

Ref: McMinn, 2002 (Adapted from Brown and Pallansch, 1995)

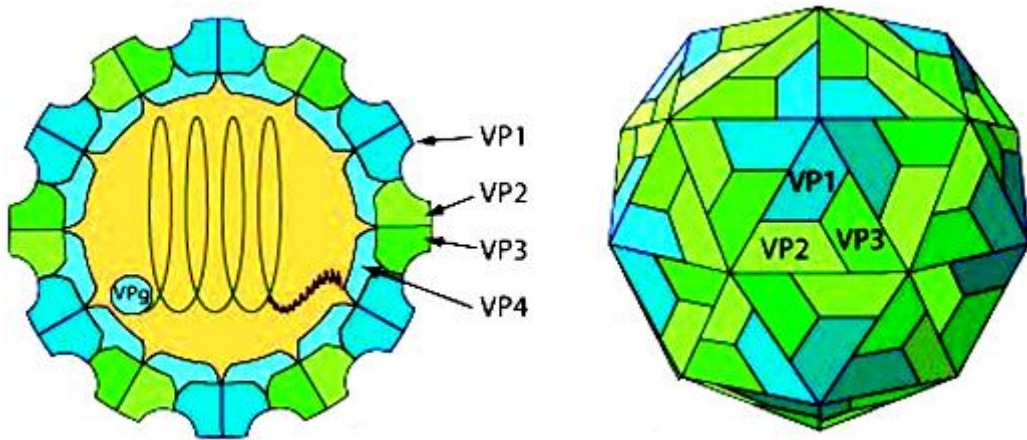


**Figure 1.2. Schematic structure of an Enterovirus virion**

An generic Enterovirus virion is composed of a protein capsid surrounding the naked RNA genome. The capsid has an icosahedral structure with 60 symmetrical units, each consisting of VP1, VP2, VP3 and VP4 (the last one is located on the internal side).

Ref: ViralZone, online at: [http://expasy.org/viralzone/all\\_by\\_species/97.html](http://expasy.org/viralzone/all_by_species/97.html)

### 1.3. Life cycle

Following binding of EV71 to the host cell receptor(s), its RNA is released into the cell cytoplasm. Then, the internal ribosome entry site (IRES) regions in 5'-UTR take control of the cell's translation machinery (Palmenberg, 1990). It is believed that host cell ribosomal subunits recognize IRES as an internal binding site where the viral proteins are synthesized (Jang et al., 1988). Initially, the viral ORF expresses a large polyprotein of which the P1, P2 and P3 regions are produced by progressive, post-translational cleavage of the polyprotein (Palmenberg, 1990; Brown and Pallansch, 1995).

Protease 2A cleaves P1 at tyrosine-glycine cleavage sites, leading to the release of P1 from the nascent polyprotein (Toyoda et al., 1986). Then, the protease 3CD acts on the P1 precursor to produce the capsid proteins VP1, VP3 and VP0 (Ypma-Wong et al., 1988). VP0 is further cleaved into VP2 and VP4 to complete the encapsidation process (Putnak and Phillips, 1981). In the mature virion, the icosahedral capsid consists of 60 copies of VP1, 60 copies of VP3, 58-59 copies of VP2, 58-59 copies of VP4 and 1-2 copies of VP0 (Chung et al., 2006, Fig. 1.2).

During the first three hours of infection of a permissive host cell, replication of the virus displays an exponential kinetics (De Jesus, 2007). Although there is no depicted life cycle for EV71 in the literature, based on a picornaviral model (Fig. 1.3) it can be assumed that the positive-sense RNA of EV71 is initially transcribed into a complementary RNA (negative) strand. This RNA negative strand then serves as a template to synthesize new positive strands of the viral genome (Andino et al., 1999), producing double-stranded RNA (replicative form, RF). The viral RNA-dependent RNA polymerase catalyzes both positive- and negative-sense RNA strands (Andino et al., 1999). The newly synthesized positive RNA strands can further serve as templates for translation of more viral proteins or can be enclosed in a capsid, which ultimately generates progeny virions. Finally, lysis of the infected host cell results in release of infectious progeny virions (De Jesus, 2007).

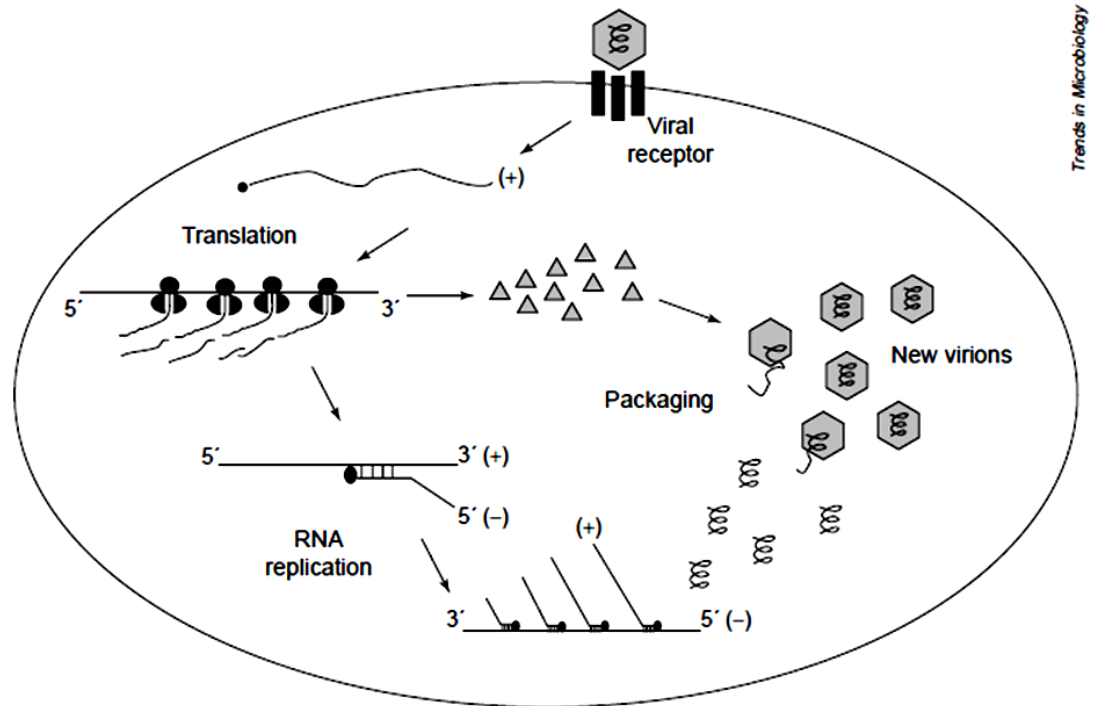


**Figure 1.3. Cellular life cycle of a typical poliovirus**

The infection process begins with the attachment of the virus to the host cells receptors. Then, the virus releases its single positive-stranded RNA into the cytoplasm. Both structural and nonstructural proteins are synthesized by translation of the positive stranded RNA that acts like mRNA. The RNA is then directly translated by the cellular protein synthesis machinery to produce specific viral proteins. This RNA strand also serves as a template to synthesize negative-stranded RNA, which, in turn, will amplify the viral genome. Finally, the newly synthesized positive RNA strands are packaged into virions formed by the synthesized proteins.

Ref: Andino et al. (1999).

### 1.4. Molecular epidemiology

The VP1 gene is the most informative region for studying evolutionary relationships and molecular epidemiology in Enteroviruses (McMinn, 2002; Thao et al., 2010). It has also been useful for distinguishing serotypes within and between Enteroviruses (McMinn, 2002). The reason lies in the fact that the VP1 protein is main Enteroviral neutralization determinant with a high degree of antigenic diversity correlated with viral serotype. In addition, the VP1 gene has an infrequent rate of homologous recombination (McMinn, 2002). For the same reason, Brown et al. (1999) used VP1 protein diversity to arrange the 113 EV71 stains into three genetic lineages, A, B, and C (Section 1.1).

It has been shown that there are molecular differences between strains of EV71 isolated from different geographic regions (McMinn, 2002). Based on this, it is hypothesized that these differences have contributed to the different clinical presentations of EV71 infection in different regions of the globe. To address this hypothesis, Zheng et al. (1995) investigated the similarity between the 5'-UTR of EV71 H from an adult patient suffering from HFMD in China and the 5'-UTR of EV71 BrCr from a patient affected by aseptic meningitis. The results of RT PCR with a unique primer pair revealed that a 397 bp product was generated from EV71 BrCr but not from EV71 H. In addition, further comparative analysis revealed that the both strains differed by 12 bases in a 154 bp product generated by a universal Enterovirus primer pair. From this study, it was concluded that the nucleotide variations within the 5'-UTR could contribute to different clinical patterns of EV71 infection such as polio-like disease in the US, Australia, and Eastern Europe, as compared to HFMD in China, Japan and Singapore (Zheng et al., 1995).

On the contrary, Shih et al. (2000) showed that there was no association of clinical manifestations and genetic differences in the 5'-UTR and VP1 region. They demonstrated a high degree (97-100%) of identity in nucleotide sequence throughout the entire genome (5'-UTR, VP4, VP2, VP3, VP1, 2A, 2B, 2C, 3A, 3B, and 3D) of the two selected strains, one from a fatal case and one from a mild case of HFMD. The only significant nucleotide substitutions were in the 3C and 3'-UTR where the identity of nucleotide sequence dropped to 90-91%. Notably, the amino acid identity was only 86% in the 3C region (Shih et al., 2000). These findings were also



supported by Yan et al. (2001) who found that there was no specific nucleotide difference between the two EV71 strains connected with HFMD and the two strains connected with encephalomyelitis, during the 1998 EV71 epidemic in Taiwan. However, the authors stated that their findings do not refute the importance of sequence and structure of 5'-UTR or other structural proteins in EV71 virulence, but rather pointed out that differences in clinical manifestations are not necessarily due to differences in pathogenicity of EV71 strains. Like many other viruses, the host-virus association can effectively determine the outcome of the disease (Yan et al., 2001).

### 1.5. Clinical manifestations

The paralytic potential of poliovirus was recognized as early as the fourteen century (Rotbart, 2000). Since the vaccines against poliovirus were introduced in the late 1950s and early 1960s, eradication plans have been considerably successful in many developed as well as developing countries (Rotbart, 2000). According to the global polio eradication initiative, poliovirus remains endemic in four countries: Pakistan, India, Nigeria and Afghanistan in 2012 (<http://www.polioeradication.org>). This being said, there has been an increase in the number of cases of non-polio infection related paralysis. EV71 is one such infection, which similar to poliovirus can cause severe neurological diseases including acute flaccid paralysis (AFP) (Pérez-Vélez et al., 2007). Therefore, the presence of this Enterovirus (and other Enteroviruses causing paralysis) in an area may negatively affect the poliomyelitis control progress (Da Silva et al., 1996). For instance, Da Silva et al. (1996) reported the presence of residual paralysis and EV71 IgM antibodies in 21.7% of AFP patients from eight geographic regions of Brazil, indicating EV71 may be causing AFP-like poliomyelitis throughout the country.

It was not until 1969-1972 that EV71 was isolated and detected as one of the most pathogenic Enterovirus serotypes during a small outbreak in California (Schmidt et al., 1974); afterward many outbreaks of EV71 infection have occurred around the world (Shen et al., 1999). EV71 infection is particularly prominent in the Asia-Pacific region (T.C. Chen et al., 2008b) with several outbreaks reported in this region (Ho, 2000). The 1997 outbreak in Malaysia caused 31 fatalities (Ho, 2000),

while an outbreak in 1998 in Taiwan left more than 100,000 hospitalized with 78 reported fatalities. Further outbreaks in 2001 and 2002 in Taiwan caused 51 fatalities in children less than 5 years old (Lin et al., 2003). The latest large outbreak of EV71 infection occurred in China in 2008. As a result, more than 600,000 HFMD cases and 126 deaths were reported in infected children from March 2008 to June 2009 (Liu et al., 2011).

Similar to other Enteroviral infections, EV71 infection may be asymptomatic or present with diarrhoea, rashes and vesicular lesions on the hands, feet, and oral mucosa (Hand Food and Mouth Disease-HFMD-) and herpangina (HA) (Ho et al., 1999). EV71-mediated HFMD (Fig. 1.4) is considered to be clinically indistinguishable from HFMD caused by Coxsackievirus A16 (CA16) (McMinn, 2002). EV71 infection might also lead to severe infections associated with the central nervous system (CNS). In a severe neurological EV71 infection, it is thought that EV71 might invade the CNS via blood or directly via cranial nerves, such as facial or hypopharyngeal nerves from day 2 to 5 of the illness (Lin et al., 2003). In addition, it has been hypothesized that EV71 might invade CNS through infecting endothelial cells (C.S. Chen et al., 2007). The EV71-caused neurological complications include aseptic meningitis (inflammation of meninges as the layers lining the brain), encephalitis (acute inflammation of the brain), polio-like paralysis, acute respiratory disease, pulmonary edema (fluid accumulation in the lungs which leads to damaged gas exchange and may even cause respiratory collapse) and myocarditis (inflammation of the heart muscle) (Ho, 2000). In the CNS, the brain stem is the most vulnerable target and the primary area involved in severe EV71 infection (Lum et al., 1998; Lin et al., 2003).



**Figure 1.4. Typical HFMD in a child infected with EV71**

The illness usually begins with a fever, poor appetite and a sore throat. Then, sores (which turn into ulcers) will appear in mouth followed by developing rashes and vesicular lesions around the palms of the hands and the soles of the feet. In all EV71 outbreaks reported to date, predominantly children under the age of 5 years old have been infected. HFMD can also be due to polioviruses, Coxsackieviruses (Particularly coxsackievirus A16), echoviruses, and other Enteroviruses.

Ref: <http://www.topnews.in/health/diseases/hfmd>

## 1.6. Control of EV71

Over the past ten years, many countries around the world have encountered outbreaks of EV71 with associated neurological complications. Thus, EV71 infection has become an important public health issue (Huang et al., 2008). Even though the application of the polio vaccine has led to effective control of poliomyelitis (T.C. Chen et al., 2008b), there is no efficient vaccine or drug for EV71 infection to date (Weng et al., 2010). There is, therefore, a need to improve the currently available drugs or develop new powerful antiviral agents for treatment of EV71 infection. It is of interest to point out that each of the crucial stages of the viral infection cycle (virus adsorption, uncoating, protein translation, polyprotein cleavage, viral RNA replication and virus assembly) could be a potential target for the field of drug development for EV71 (T.C. Chen et al., 2008b). The following is a review of some of the key groups of compounds with potential antiviral properties against EV71. It should be noted that drug-resistant variants could always emerge due to high mutation rates of Enteroviruses. Hence, in order to delay or prevent the emergence of these variants in EV71, the use of combinations of antiviral drugs based on different viral targets is of importance in antiviral therapy (T.C. Chen et al., 2008a,b).

The below are brief descriptions of the abbreviations of  $CC_{50}$ ,  $IC_{50}$ , and SI that will be used later in this review, according to the US food and drug administration (FDA) (<http://www.fda.gov>):

$CC_{50}$ : The 50% cytotoxic concentration that represents the concentration required to reduce cell growth by 50%.

$IC_{50}$ : The 50% inhibitory concentration that describes the concentration of a drug that is required for 50% inhibition (of virus) *in vitro*.

SI: Selectivity index that is calculated based on the ratio of  $CC_{50}/IC_{50}$ .

According to guidelines of FDA, it is desirable to have a high selectivity index, giving maximum antiviral activity with minimal cell toxicity. Measurement of selectivity indices of tested drugs should be conducted before the initiation of

phase 1 clinical studies. However, it is not possible to know what exactly FDA considers an acceptable SI. Generally, antiviral drugs with great selectivity and minimal toxicity have SIs of 100-1000 or better.

### 1.6.1. Capsid-binding compounds

Capsid-binding molecules are antiviral compounds that stop viral infection by preventing the uncoating of the virus and/or viral binding to cellular receptors on the host cell (T.C. Chen et al., 2008a). The importance of capsid-binding molecules lies in the fact that picornaviruses present their antigenicity through identification of specific receptors on the host cells by their capsid (Bergelson et al., 1992, Greve et al., 1989, Mendelsohn et al., 1989). In this respect, Sterling-Winthrop Pharmaceutical has developed capsid-binding compounds, commercially named the WIN series, which can interact with a hydrophobic pocket under the canyon floor in the centre of the viral protein (VP1) (Pevear et al., 1989). Among capsid-binders, the following three compounds have been reported for Enteroviruses: Pleconaril, Pyridyl Imidazolidinone, and Pirodavir (R77975).

Pleconaril was originally synthesized by Sanofi-Aventis (formerly known as Sterling Winthrop) in the early 1990s; afterward it was licensed to ViroPharma in 1997. Initially designed for the treatment of rhinovirus infections (the common cold), pleconaril was submitted to FDA in 2001 but failed to secure the approval of FDA. The reason lied in concerns raised by FDA regarding the safety of pleconaril, including: having had no statistically significant reduction in days of symptoms in non-whites after taking the drug; being better than placebo only if taken in the first 24 hours of a cold; having been limited to previously healthy volunteers that might develop resistant virus strains; and having reduced the effectiveness of oral contraceptives ([http://www.fda.gov/ohrms/dockets/ac/02/briefing/3847b1\\_02\\_FDA.pdf](http://www.fda.gov/ohrms/dockets/ac/02/briefing/3847b1_02_FDA.pdf)).

Consequently, the company did not follow licensure of Pleconaril for other indications, including Enteroviral meningitis (Desmond et al., 2006). In 2003, ViroPharma then re-licensed it to Schering-Plough in consideration as a topical (intranasal) therapy for the common cold. The Phase II clinical trial was completed in 2007. Despite not being FDA approved, pleconaril has shown notable inhibitory effects against a vast number of Enteroviruses (Pevear et al., 1999; Rogers et al.,

1999). However, it was unable to control the cytopathic effect of EV71 isolates from the 1998 outbreak in Taiwan (Shia et al., 2002).

Pyridyl imidazolidinone is a new category of capsid binders that was generated by computer-assisted drug design, based on the structure of WIN compounds and the related molecule, pleconaril, as templates (Shia et al., 2002). The efficiency of pyridyl imidazolidinone in neutralizing EV71 has been confirmed in several studies (Shia et al., 2002; Shih et al., 2004b; Chern et al., 2004; Chang et al., 2005; T.C. Chen et al., 2008a). It is believed that pyridyl imidazolidinone exerts its antiviral action by fitting into the viral hydrophobic pocket of VP1 (T.C. Chen et al., 2008a). Among the members of the pyridyl imidazolidinone family, BPROZ-101 with an  $IC_{50}$  of  $0.0012 \pm 0.0005$  ( $\mu\text{M}$ ), a  $CC_{50}$  more than 50 ( $\mu\text{M}$ ) and an SI more than 10,000; and BPROZ-074 with an  $IC_{50}$  of  $0.0008 \pm 0.0001$  ( $\mu\text{M}$ ), a  $CC_{50}$  more than 50 ( $\mu\text{M}$ ) and a SI more than 10,000 exhibited considerable antiviral activities against wild-type EV71. Taken together, the length, size, hydrophobicity and the electronic forces were concluded to contribute to binding connection and subsequently the antiviral potency of the compounds (T.C. Chen et al., 2008a). Thus far, however, there has been no report regarding effectiveness of the antiviral activity of pyridyl imidazolidinone *in vivo*.

Pirodavisir is another capsid-binding agent that presented effective activity against 16 serotypes of Enterovirus as well as rhinovirus group A and B (Andries et al., 1992). However, the use of this compound against EV71 has not yet been reported.

### 1.6.2. Antiviral drugs targeting viral proteases

In the picornavirus genome, the 2A and 3C regions are believed to encode proteases that are vital for processing the viral polyprotein (Table 1.2). The high conservation of 2A protease in rhinoviruses and Enteroviruses, and the special folding structure of 3C (varying from the other known cellular proteases), indicate these viral proteases could be potential targets for antiviral drug design (T.C. Chen et al., 2008b). In addition, 2A protease activity can be reduced by alkylating agents such as iodoacetamide and *N*-ethylmaleimide (Konig et al., 1988) as well as substrate-derived elastase inhibitors such as elastatinal and methoxysuccinyl-Ala-Ala-Pro-Val-chloromethylketone (Molla et al., 1993). However, no study has been

undertaken to examine whether such compounds inhibit EV71. On the other hand, antiviral compounds have been designed to block 3C protease through mimicking of 3C substrates (T.C. Chen et al., 2008b). An efficient antiviral agent of the compounds targeting 3C protease is AG7088 (rupintrivir) which has shown great antiviral potency against HRV, CVA21, CVB3, echovirus 11 and EV70 (Binford et al., 2005). To date, there has been no test on 3C inhibitors against EV71 infection (T.C. Chen et al., 2008b).

### 1.6.3. Nucleotide analogs-mediated mutagenesis: Ribavirin

Ribavirin (RBV) (brand names: Copegus, Rebetol, Ribasphere, Vilona and Virazole) was synthesized in 1970 (Sidwell et al., 1972) by ICN Pharmaceuticals who subsequently showed its antiviral activity (Streeter et al., 1973). To date, the potency of RBV in antiviral therapy has been presented for a wide range of RNA viruses *in vitro* and/or *in vivo*; such as poliovirus (Crotty et al., 2000 and 2001), GB virus B (Landford et al., 2001), hepatitis C virus (HCV) (Maag et al., 2001, Contreras et al., 2002; Zhou et al., 2003; Asahina et al., 2005), Hantaan virus (Severson et al., 2003), and foot-and-mouth disease virus (FMDV) (Airaksinen et al., 2003). In addition, Li and colleagues (2008) demonstrated that RBV possessed antiviral activities toward EV71 infection both *in vitro* and *in vivo*. RBV was seen to reduce the virus titre (with an  $IC_{50}$  of 65  $\mu\text{g/mL}$ ) in human and mouse cell lines and also inhibited the virus-induced cytopathic effect. Moreover, *in vivo* results revealed that RBV decreased the rate of death, morbidity and succeeding paralysis sequelae in infected mice by lowering viral loads in tissues (Li et al., 2008).

There are three possible hypotheses underlying mechanisms of antiviral action of RBV, including (i) competitive inhibition of inosine monophosphate dehydrogenase, which in turn, decreases the intracellular content of GTP; (ii) immunomodulatory activities; and (iii) interaction with viral RNA polymerase leading to lethal mutagenesis. Indeed, Crotty et al. (2000) proved the third mechanism for RBV against polioviruses. Based on this mechanism, the polio RNA polymerase incorporates RBV (in the form of ribavirin triphosphate: RTP) as a base analog of either ATP or GTP (Fig. 1.5) with the same efficiency. Therefore, RBV binds equally with either Cytosine or Uracil resulting in possible mutations in the next synthesized RNA strand: C $\rightarrow$ U (in the positive strand)/G $\rightarrow$ A (in the negative

strand); or U<sup>→</sup>C (in the positive strand)/A<sup>→</sup>G (in the negative strand). After a series of viral replications, lethal mutagenesis will possibly occur, which has also been reported for other RNA viruses such as HCV (Maag et al., 2001), FMDV (Airaksinen et al., 2003) and Hantaan virus (Severson et al., 2003).

The preference of RBV in matching with either C or U was also elucidated by Airaksinen et al. (2003), working on FMDV. The results revealed that the rates of mutations of C<sup>→</sup>U and G<sup>→</sup>A (in the positive and negative strands, respectively) were more than those of U<sup>→</sup>C and A<sup>→</sup>G (in the positive and negative strands, respectively). Thus, it could be initially explained that during FMDV negative strand synthesis, RBV has a preference to be incorporated opposite to cytidine instead of uridine. However, in order to answer why RBV shows this preference, it is essential to consider the other mechanism of action of RBV, i.e. reducing intracellular content of GTP by inhibition of inosine monophosphate (IMP) dehydrogenase. As a result, in the absence of intracellular GTP, RBV can serve as a base analog of that and match with cytidine during the negative strand synthesis. Then, during the positive strand synthesis, uridine binds to RBV more frequently than cytidine, leading to mutations of C<sup>→</sup>U and G<sup>→</sup>A (in the positive and negative strands, respectively).

As stated before, there are three possible mechanisms for the antiviral action of ribavirin and all three of these mechanisms may potentiate each other, although the possibility of interaction of RBV with RNA polymerase has been highly supported (Crotty et al., 2000; Parker, 2005). Therefore, RBV has pleiotropic effects and, due to this quality, the exact mechanism by which RBV exerts its antiviral effect is difficult to explain (Vignuzzi et al., 2005).



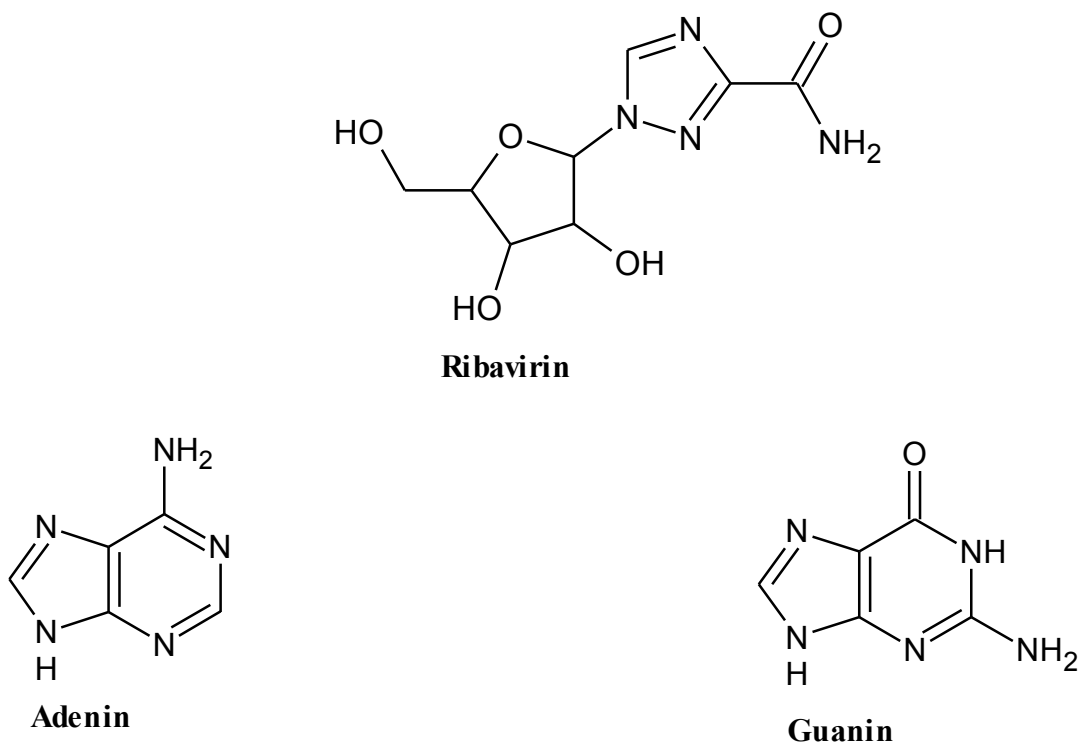


**Figure 1.5. Molecular structures of Ribavirin, Adenin and Guanin**

Ribavirin (RBV) is an analog of both nucleobases Adenin and Guanin (as purine bases). During the negative strand synthesis, RBV preferably acts like a Guanin base and matches to Cytosine. Then, RBV may act like an Adenin base, resulting in matching to Uracil. Thus, Cytosine will be replaced by Uracil in the viral RNA genome (which is positive stranded). After several rounds of viral replication, these mutations will push the virus into error catastrophe, resulting in the virus not replicating.

The structures were drawn using ACD/ChemSketch 11.01.

### 1.6.4. RNA interference

RNA interference (RNAi) is a sequence-specific silencing of genes, induced by small molecules of double-stranded RNA (dsRNA). Although this phenomenon was first observed in plants in the late 1980s, its mechanism was not elucidated until 1998 by Fire and colleagues in the nematode *Caenorhabditis elegans* (Fire et al., 1998). However, further studies gradually shed light on the exact molecular mechanism of the phenomenon. It has been clearly demonstrated that RNAi is a conserved sequence-specific silencer of genes, which holds promise as a gene-targeted therapeutic against a wide range of infectious diseases, including viruses (Ketzinel-Gilad et al., 2006). In addition, RNAi has also been used in studies to identify the role of a gene (Hokaiwado et al., 2008). Therefore, there are a vast number of the articles which have reviewed the use of RNAi in functional genomics as well as in therapeutics, including antiviral therapy, and have provided detailed explanations about the mechanism involved in RNAi cellular pathways (Ketzinel-Gilad et al., 2006).

Two distinct pathways of RNAi have been proposed: the short interfering RNA (siRNA) pathway and microRNA (miRNA) pathway. The siRNA pathway is the key pathway used in drug development (DeVincenzo, 2008; Fig. 1.6). The interference caused by siRNA begins in cytoplasm with cleavage of the dsRNA into small RNA duplexes, 21-23 nucleotides long (Zamore et al., 2000; Hammond et al., 2000), these siRNAs have two nucleotides overhanging at their 3' termini (Elbashir et al., 2001b). Dicer is the enzyme responsible for cleavage of dsRNA into siRNAs. This enzyme is a dsRNA-specific nuclease, belonging to the RNaseIII family and acting in an ATP-dependent manner (Bernstein et al., 2001). siRNAs are then incorporated into the RNA-induced silencing complex (RISC) (Hammond et al., 2000), the RISC uses one of the siRNA strands (termed the antisense strand or guide strand) to target the homologous mRNA strand (termed the sense strand or passenger strand) through base-pairing interactions. The mRNA is then cleaved by the endonuclease Argonaut 2 (AGO2) of the RISC in a homology-dependent manner, leading to degradation of the targeted mRNA (Zamore et al., 2000; Elbashir et al., 2001a). The siRNA remains within the RISC to direct several rounds of catalytic mRNA cleavage (DeVincenzo, 2008).

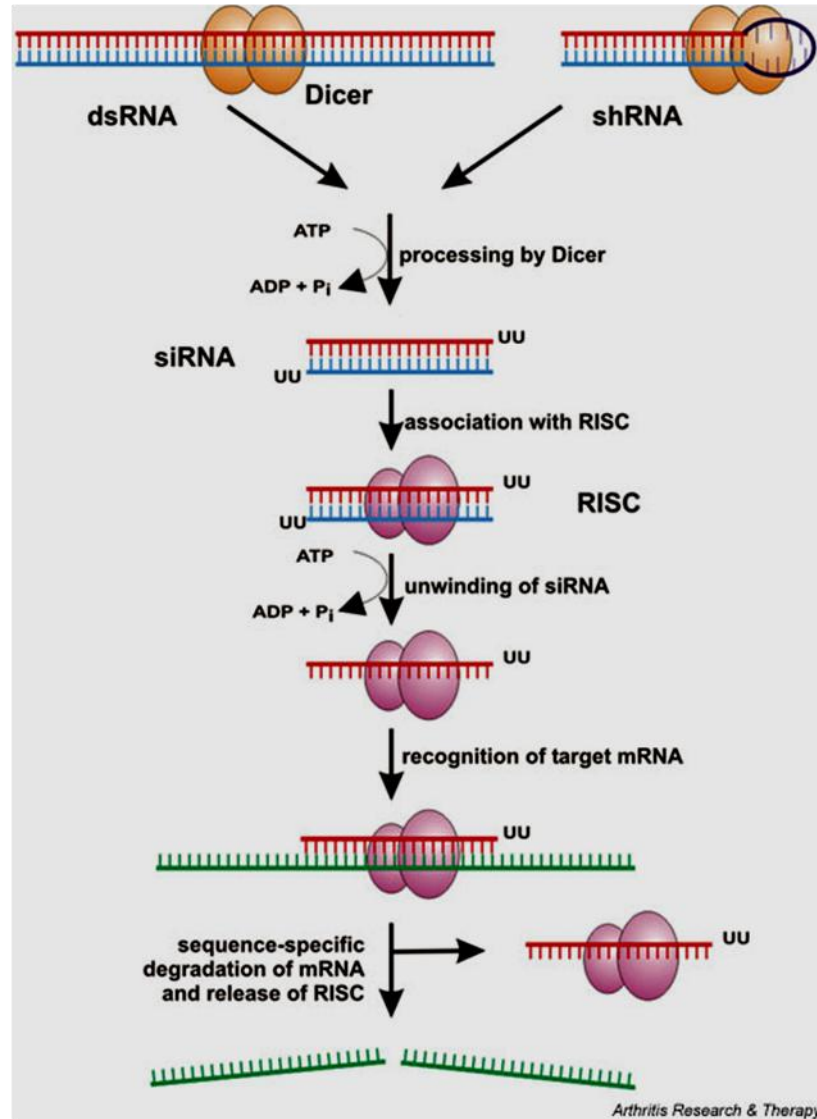


**Figure 1.6. Mechanism of siRNA silencing**

Dicer can generate a short interfering RNA (siRNA) by cleaving either long double-stranded RNA (dsRNA) or small hairpin RNA (shRNA). The siRNAs can be incorporated into RNA-induced silencing protein complex (RISC) which, in turn, mediates target sequence specificity for subsequent mRNA cleavage.

Ref: Rutz and Scheffold (2004).

The inhibitory activity of siRNAs has been shown in many viruses of different families. Recently, several RNAi-based antiviral drugs have been tested in clinical trials (Haasnoot et al., 2007; Table 1.3). The strongest *in vivo* evidence of antiviral activity of RNAi has been gained with acute viral infections such as herpes simplex virus type 2 (HSV-2) (Palliser et al., 2006) and respiratory syncytial virus (RSV) (Bitko et al., 2005). In addition, RNAi treatment of viruses such as influenza, severe acute respiratory syndrome coronavirus (SARS-CoV), Japanese encephalitis virus, and West Nile virus has been reported (reviewed by Huang, 2008). However, there are concerns with the use of these compounds, such as viral escape from RNAi, off-target effects of RNAi treatment, the delivery of the RNAi-inducer to the right target cell (Haasnoot et al., 2007), and the immune response to siRNA during *in vivo* application of siRNA (Hokaiwado et al., 2008).

The first proof-of-concept study to exploit RNAi as an antiviral tool against EV71 infection was carried out by Lu et al. (2004), who used plasmid-derived short hairpin RNA (shRNA) molecules corresponding to the EV71 genome (VP1 and 3D regions) in HeLa cells. The analyses of EV71 protein expressions demonstrated that shRNA significantly inhibited the viral protein expression in a sequence-specific and dose-dependent manner. Then, Sim et al. (2005) applied siRNA against EV71 infection; a synthetic 19-mer siRNAs (with a TT di-nucleotide overhanging at their 3' end) was designed to target the 3'UTR, 2C, 3C<sup>pro</sup> and 3D<sup>pol</sup>. The results showed a significant reduction in viral replication, gene expression and plaque formation in RD cells transfected with the siRNA in lipofectamine. Among the viral targets, 3D<sup>pol</sup> was most effectively inhibited by the siRNAs (Sim et al., 2005).

The study of RNAi against EV71 infection was followed by Tan et al. (2007a) by using 29-mer shRNAs, who demonstrated greater antiviral activity against EV71 infection in RD cells compared to both the chemically synthesized 19-mer siRNA (Sim et al., 2005) and the plasmid-derived shRNA (Lu et al., 2004). The results were promising where 10nM of 29-mer shRNAs targeted at each of the three specific sites (2C, 3C<sup>pro</sup>, and 3D<sup>pol</sup>) resulted in a 90% reduction in EV71 replication. It was concluded that the increased potency of the 29-mer shRNAs might be due to either higher affinity of the 29-mer shRNAs for the Dicer enzyme, or interaction of shRNAs with specific cellular proteins, which facilitate the delivery of shRNAs molecules to the Dicer. In terms of protection against EV71, it was also observed

that all three 29-mer shRNAs (2C, 3C<sup>pro</sup>, and 3D<sup>pol</sup>) at 10nM could protect RD cells from EV71-caused CPE up to 72 hours post infection. This time was 24 hours more than previously reported for 19-mer siRNAs (Sim et al., 2005) and for plasmid – derived 19-mer shRNAs (Lu et al., 2004). It is possible that prevention of viral replication might be due to induction of the interferon response. In order to examine this possibility, Tan et al. (2007a) used western blotting to measure expression of autophosphorylation RNA-dependent protein kinase (phospho-PKR) in RD cells transfected with 29-mer sh-RNAs as an indicator of the activated interferon response. The results showed no activation of phospho-PKR and thus it was concluded that inhibition of viral replication was mediated through action of sh-RNAs (Tan et al., 2007a).

Promising results with RNAi in silencing the EV71 genome was followed by further research evaluating activity in a murine model (Tan et al., 2007b). Twenty-four hours after infection of one-day suckling mice with EV71 via the intraperitoneal (i.p.) route, the mice were treated with 10nM of 19-mer siRNAs (targeted at the 3D<sup>pol</sup> region) or 50 µg of the plasmid-derived 19-mer shRNAs (targeted at the 3D<sup>pol</sup> region) with oligofectamine via the i.p. route. The results showed that the mice did not develop signs of weight loss or hind limb paralysis up to 14 days post infection. In another examination, mice were infected with EV71 one day after treatment with 19-mer siRNAs or plasmids-derived 19-mer shRNAs. Similar to the first group, these mice did not show signs of the infection up to 14 days post infection. Further significant findings was that similar protective effects from EV71 infections were observed in the suckling mice when 19mer-3D and psi-3D were administered without using oligofectamine as a transfection reagent.

The reduction in EV71 replication by RNAi was also confirmed and quantified by real-time RT PCR and Western blot. However, the chemically synthesized 29-mer shRNAs failed to protect the suckling mice from infection despite being previously reported to inhibit EV71 infection in RD cells *in vitro* (Tan et al., 2007a). It was speculated that suckling mice might lack certain mechanisms or cellular proteins required to deliver the 29-mer shRNAs to the Dicer enzyme (Tan et al., 2007b).

**Table 1.3. RNAi-based antiviral drugs that have been tested in clinical trials, modified from Haasnoot et al. (2007)**

<b>Virus</b>	<b>Name of inhibitor</b>	<b>Target gene</b>	<b>Stage of clinical trial</b>
Cytomegalovirus	Antisense oligonucleotide (Vitravene; formivirsen/ISIS 2922)	<i>IE2</i>	Approved
HIV-1	Ribozyme (Rz2, OZ-1)	<i>tat</i>	Phase I complete, phase 2 ongoing
HCV	Ribozyme (Heptazyme)	<i>IRES</i>	Phase 2 studied discontinued
HBV	Short-hairpin RNA ( <i>Nuc B1000</i> )	<i>Pre-gen./pre-C, Pre-S1, pre-S2/S, X</i>	Phase 1 ongoing

### 1.6.5. Antiviral peptides

Many organisms produce short, positively charged, and amphiphilic antimicrobial peptides as part of their natural defense system. These peptides are usually present at mucosal surfaces, skin, and within the granules of immune cells where they usually encounter pathogens (Jenssen et al., 2006). The diverse nature of peptides allows for easy selection of peptide ligands as therapeutic agents for any target (Hüther and Dietrich, 2007). As such, more than 140 peptides are in use and more than 400 peptides are in advanced preclinical trials worldwide. The significant advantages of peptides are their small size, high activity and specificity, and minimized non-specific side effects and immunogenicity (Hüther and Dietrich, 2007).

However, there are still limitations for oral administration of therapeutic peptides, including intestinal membrane permeability, the peptide size, intestinal metabolism (specifically enzymatic digestion of peptides) and solubility. In order to overcome these barriers, a number of approaches have been developed, such as modification of the peptide structure in order to increase its affinity for carrier proteins, specific delivery of the peptide to the most permeable part of the intestine, and controlling of metabolism of the peptide by co-administration of competitive enzyme inhibitors (Malik et al., 2007). In order to penetrate into cells, peptides require complexation with transfection molecules such as lipids, liposomes and nano-particles (Hüther and Dietrich, 2007), or the help of protein transduction domains (PTDs) [also known as cell penetrating peptides (CPPs), membrane translocating sequences (MTSs), and Trojan peptides], which have the ability to enter almost any cells independent of a membrane receptor (Sebbage, 2009).

Although antibacterial activity of cationic peptides has been widely investigated, little is known about their antiviral potencies. Moreover, the mechanism of antiviral activity of these peptides has not yet been completely elucidated (Albiol-Matanic and Castilla, 2004). Thus far, several antimicrobial peptides have been shown to exert antiviral properties against a wide range of DNA and RNA viruses (Jenssen et al., 2006; Table 1.4). In this regard, an understanding of the mechanisms of action of cationic peptides is necessary in order to consider these compounds as potential antiviral agents (Albiol-Matanic and Castilla, 2004). The most likely postulated modes of actions include interaction with heparan

sulphate and blocking of viral entry, interaction directly with specific viral receptors on host cells, and interaction with viral glycoproteins (gp) or viral envelopes (Jenssen et al., 2006).

To date, it appears that lactoferrin is the only example of an antiviral peptide against EV71 infection in the literature (Lin et al., 2002). Lactoferrin is an iron-binding glycoprotein which can be found in milk, saliva, mucous secretions, and other biological fluids of mammals. Lin et al., (2002) showed its antiviral properties against EV71 varieties from outbreaks in Taiwan and Malaysia. Both bovine and human lactoferrins significantly prevented infection with the isolates of EV71 in RD cells with an  $IC_{50}$  of 10.5-24.5 ( $\mu\text{g/mL}$ ) and 103.3-185.0 ( $\mu\text{g/mL}$ ), respectively. Further *in vivo* experiments demonstrated that lactoferrin saved seventeen-day-old ICR mice from fatal EV71 challenge (Weng et al., 2005).

The exact mode of action of lactoferrin has not been completely clarified yet. However, it was shown that lactoferrin could bind to both EV71 VP1 and the host cells. Therefore, it was proposed that lactoferrin exerts its antiviral action through prevention of viral entry by blocking cellular receptors and/or by direct binding to the virus, interfering with the interaction between virus and specific receptor (Weng et al., 2005). It has also been shown that lactoferrin can bind to heparan sulphate molecules on cell surface and inhibit HSV (Marchetti et al., 1996). Heparan sulphate molecules have a strong net negative charge and can electrostatically bind to cationic peptides, including lactoferrin.



Table 1.4. Examples of antiviral peptides against DNA and RNA viruses, modified from Jensen et al., 2006.

Peptide	Structure	Virus	Mode of action	Ref.
Megainin	$\alpha$ -Helix	HSV-1 and/or HSV-2	Cellular target	Aboudy et al., 1994; Albiol-Matanic and Castilla, 2004
		HIV	Suppresses viral gene expression	
Cecropin	$\alpha$ -Helix	Junin virus	Suppresses viral protein synthesis	Albiol-Matanic and Castilla, 2004; Wachinger et al., 1998
		HSV	Cellular target	
		HIV	Suppresses viral gene expression	
Mellitin	$\alpha$ -Helix	HSV	Cellular target	Albiol-Matanic and Castilla, 2004; Wachinger et al., 1998; Yasin et al., 2000
		Junin virus	Cellular target	
Lactoferricin	$\beta$ -Turn	HCMV	Activity at virus-cell interface	Anderson et al., 2003; Anderson et al., 2001; Jensen et al., 2004
		HIV	Unknown	
		HSV	Blocks heparan sulphate, but a secondary effect has also been indicated	

### 1.6.6. Antiviral compounds of natural origin

For thousands of years, natural products have been used to treat a variety of infectious disease all around the world. Thus, they are considered rich and mainly unexploited source of structurally novel chemicals, which are also worth investigating as potential antiviral drugs. In general, the most significant advantages of natural bioactive compounds include full biodegradability and availability from renewable sources. However, it should be noted that there are also drawbacks with natural compounds, such as their complex chemistry (having multiple components), their mostly unclear mechanism of action, and difficulties with sourcing authenticated plant materials.

There are several herbs with a good track record in folk medicine that their application to humans has been less problematic (Wu et al., 2007). Thus, such natural sources have potential to be developed as antiviral agents in the future. Regarding EV71 infection, several potential ethnobotanical sources have been reported to date (Chang et al., 2008; Su et al., 2008).

The anti-EV71 activities of allophycocyanin isolated from the cyanobacterium *Spirulina platensis* was initially reported by Shih et al., (2003a). This agent blocked the EV71-induced cytopathic effects in African green monkey kidney (Vero) cells ( $IC_{50}$  of  $0.045 \pm 0.012 \mu\text{M}$ ). It was shown that allophycocyanin had the ability to delay viral RNA synthesis in infected cells. When added at the stage of viral adsorption or post-adsorption, it also stopped plaque formation in EV71-infected Vero cells at an  $IC_{50}$  of  $0.056 \pm 0.007 \mu\text{M}$  and  $0.101 \pm 0.032 \mu\text{M}$ , respectively. A time-course assay showed that the antiviral activity was more efficient in cultures treated with allophycocyanin before viral infection compared to cultures treated after infection (Shih et al., 2003). However, since the test was only conducted *in vitro*, its application in humans remains to be evaluated.

Danshen (*Salvia miltiorrhiza*) is a well-known medicinal plant whose anti-EV71 properties were first investigated by Wu et al. (2007). Two extracts of this plant identified as SA1 and SA2 were shown to neutralize EV71 cytopathic effects at an  $IC_{50}$  of  $0.742 \pm 0.042 \text{ mg/mL}$  and  $0.585 \pm 0.018 \text{ mg/mL}$ , respectively in Vero cells. In addition, plaque formation in the EV71-infected Vero cells treated with the extracts was significantly reduced. Based on a time-course study, SA1 and SA2 were shown to inhibit viral penetration. No further mode of action for the anti-EV71

activity of these extracts has been drawn.

As it has been reported that ursolic acid blocks herpes simplex virus (HSV)-1 and human immunodeficiency virus (HIV) infections *in vitro* (Ryu et al., 1992, Xu et al., 1996), the anti-EV71 properties of ursolic acid extracted from *Ocimum basilicum* (sweet basil) was tested by Chiang et al. (2005). Ursolic acid demonstrated effective anti-EV71 action during the infection process in human skin basal carcinoma cells (BCC-1/KMC) at an IC<sub>50</sub> value of 0.5 µg/mL. Further, time-course studies between 2 hours before and 24 hours after viral infection revealed that ursolic acid exerts its function at the stage of replication of virus after infection (Chiang et al., 2005). However, the molecular mechanism of EV71 inhibition by ursolic acid has not yet been elucidated. In addition, the anti-EV71 influence of ursolic acid has not yet been studied in an animal model.

The compound Sheng-Ma-Ge-Gen-Tang (SMGGT) is a well-known traditional Chinese medicine (TCM) which has recently been shown to have antiviral activity against EV71 *in vitro* (Chang et al., 2008). Crude hot water extracts containing SMGGT were composed from the following five plants: *Pueraria lobata* Ohwi (radix), *Paeonia lactiflora* Pallas (radix), *Cimicifuga foetida* L (rhizoma), *Glycyrrhiza uralensis* Fisch (radix), and *Zingiber officinale* Roscoe (rhizoma). The results of cytopathic effect inhibitory assay on infected human foreskin fibroblast cell line showed that 0.21 µg/mL of SMGGT could cause a 50% reduction of cytopathic effect of EV71, while the cytotoxic concentration was more than 5000 µg/mL.

SMGGT was also shown not to affect the virus-induced or constitutional interferon production. Thus, it was proposed that antiviral potencies of this compound are not mediated by interferon. In addition, the results demonstrated that SMGGT was more effective before viral infection at 0.3 µg/mL. It was also found that SMGGT could inhibit viral attachment and penetration at concentrations of 0.1 and 0.3 µg/mL, respectively. However, the molecular mechanism for the antiviral activity of SMGGT against EV71 infection has not yet been elucidated (Chang et al., 2008). Similar to ursolic acid, the anti-EV71 properties of SMGGT have not been studied in an animal model.

For thousands of years, Ge-Gen-Tang (GGT) has been used in the treatment of diseases of the upper respiratory tract in ancient China. Recently, the anti-EV71

effect of this compound was reported by Su et al. (2008). Since the main source of GGT is the medicinal plant *Pueraria lobata* Ohwi, a water extract of this plant was prepared. The extract was shown to inhibit EV71-caused cytopathic effect in human foreskin fibroblast cell line with an  $IC_{50}$  of 0.028  $\mu\text{g/mL}$ , which is much lower than its cytotoxic concentration ( $> 3000 \mu\text{g/mL}$ ). According to results of time-course, attachment and penetration assays, the compound could significantly inhibit EV71 infection either before or after viral infection. It also inhibited viral attachment and penetration at concentrations higher than 0.3  $\mu\text{g/mL}$  and 0.1  $\mu\text{g/mL}$ , respectively.

Moreover, an interferon assay demonstrated that the anti-EV71 activity of GGT was not mediated by interferon, because the extract reduced the IFN production induced by EV71 infection. It has been previously reported that serum interferon levels have been significantly raised in severe cases of pulmonary edema (Wang et al., 2003; Lin et al., 2003). On the other hand, early administration of intravenous immunoglobulin decreased interferon levels resulting in lower mortality rates (Wang et al., 2006). Thus, the role that the extract of *P. lobata* plays in decreasing interferon levels might possibly be useful in treatment of EV71 infection (Su et al., 2008). However, as the authors mentioned, the molecular mechanism of the antiviral activity of GGT remains to be clarified.

One of the extracts of the medicinal plant *Rheum palmatum*, aloe-emodin, has been shown to inhibit enveloped viruses such as herpes simplex virus, influenza virus (Sydiskis et al., 1991) and human cytomegalovirus (Barnard et al., 1992). In addition, it was shown that this compound could inhibit EV71 with an  $IC_{50}$  of  $0.14 \pm 0.04$  and  $0.52 \pm 0.03 \mu\text{g/mL}$  in TE671 and HL-CZ cells, respectively (Lin et al., 2008). The study of its mode of action revealed that aloe-emodin considerably activated an interferon-stimulated response element (ISRE), induced expression of interferon-stimulated genes (ISG), and raised interferon alpha levels.

Moreover, *in vivo* signalling pathway assays revealed that aloe-emodin triggered interferon gamma-activated sequence (GAS), resulting in the production of endogenous nitric oxide (NO), which has been reported to inhibit viral replication of Japanese encephalitis virus (Lin et al., 1997) and severe acute respiratory syndrome coronavirus (Keyaerts et al., 2004). On the other hand, interferon gamma can potentiate the antiviral activity of interferons alpha and beta. Overall, aloe-emodin shows promise as a potent interferon-inducer that could activate type I and II

interferon responses and inhibit EV71 in both TE671 (human medulloblastoma cell line) and HL-CZ (promonocyte cell line) (Lin et al., 2008).

In a recent attempt to evaluate the anti-EV71 activity of 22 herbs from traditional Chinese Medicine (TCM), Lin et al. (2009) reported the successful inhibition of EV71 by an extract of *Houttuynia cordata*. This plant is native to Japan, Korea, Southern China, and Southeast Asia; and is known for its culinary and medicinal properties. An extract of *H. cordata* neutralized CPE caused by EV71 at an  $IC_{50}$  of  $125.92 \pm 27.8 \mu\text{g/mL}$  with low cytotoxicity ( $CC_{50}$ :  $12.80 \pm 0.73\text{mg/mL}$ ). Also, the extract significantly reduced EV71 plaque formation.

The mode of action bioassays showed that the *H. cordata* extract affects early stages of EV71 infection, not affecting EV71 infection after virus penetration. Therefore, the decrease in viral RNA and protein synthesis as well as reduction in cells entering the sub-G1 phase of apoptosis was assumed to be due to a decrease in viral entry. However, the active components responsible for the antiviral action of this extract need to be identified to confirm the above hypothesis. This extract could inhibit all of the three EV71 strains tested (BrCr, one strain from Genotype B, and one strain from genotype C) as well as Coxsackievirus A16.

### **1.7. Glycans and glycan mimetics: a contribution to virus receptors and antivirals**

#### **1.7.1. Introduction**

Glycan is a term that simply refers to a polysaccharide. Thus, Glycans are chains of monosaccharides, which can be homo- or hetero-polymers with a linear or branched chemical structure (Kleene and Schachner, 2004). In nature, glycans are usually found as part of glycoproteins. A glycoprotein is a protein which is covalently bound to one or more glycans. There are two major types of glycoproteins: *N*-glycans and *O*-glycans (Kleene and Schachner, 2004). However, glycans can also be found in the context of glycolipids and proteoglycans (Olofsson and Bergstrom, 2005). Notably, there is a difference between a glycoprotein and a proteoglycan in the protein/carbohydrate ratio. Glycoproteins have more protein and less carbohydrate, while proteoglycans have more carbohydrate and less protein. This review will concentrate on two important proteoglycans (PGs), heparan

sulphate (HS) and heparin (Hep).

PGs are macromolecules that exist in all types of animal tissues, in intracellular granule secretions, in extracellular matrix and on the cell surface. A PG molecule is composed of a core protein and one or more covalently linked glycosaminoglycan (GAG) chains as can be seen in Figure 1.7 (Jenssen et al., 2006). A GAG itself consists of amino sugars (glycosamino-) and uronic acids (glycurono-) which are joined in long chains (glycans) (Lamberg and Stoolmiller, 1974). Several compounds that are mostly classified as GAGs include hyaluronic acid, chondroitin 4- and 6- sulphates, dermatan sulphate, keratan sulphate, HS, and Hep (Lamberg and Stoolmiller, 1974). The net charge of a GAG molecule is negative as it has many carboxylate groups, sulphate groups, or both, which are present in the carbohydrate part of the molecule (Lamberg and Stoolmiller, 1974). The high negative charge of GAGs assist them to bind to small cations, proteins, enzymes, growth factors, cytokines, lipoproteins, and viruses (Jenssen et al., 2006).

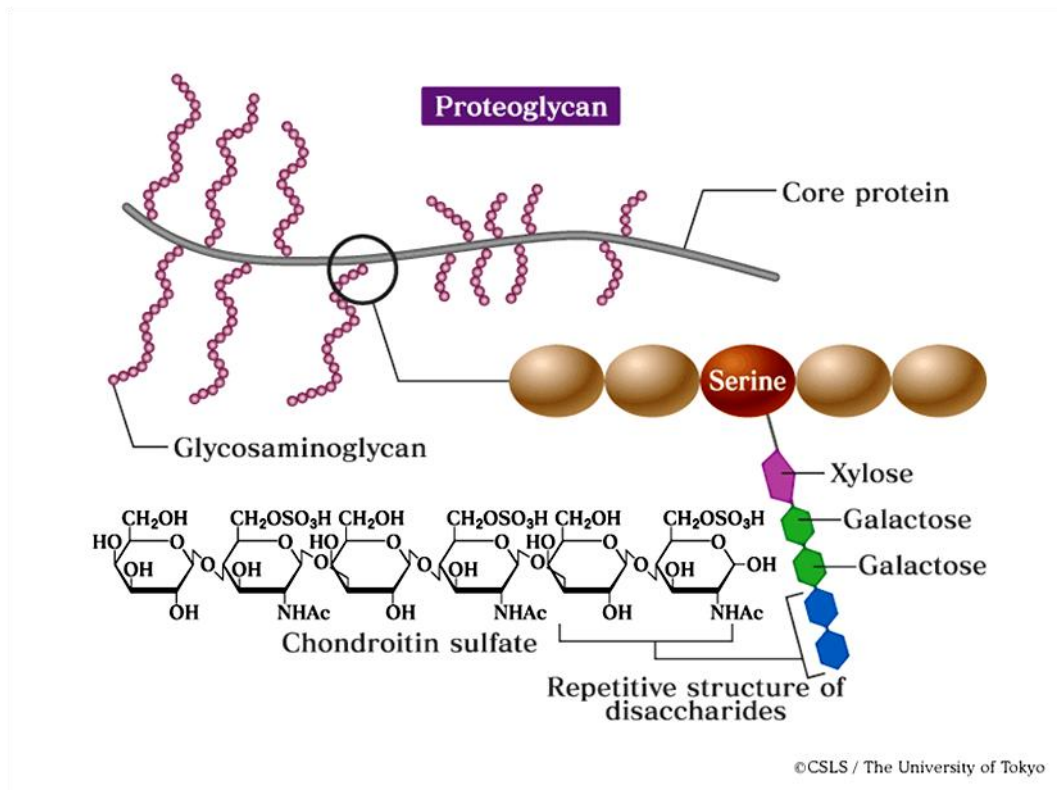


**Figure 1.7. A schematic demonstration of binding of GAGs to a protein core**

The GAGs, like chondroitin sulphate or HS, consist of a repeating disaccharide unit and bind to the amino acid Serines of the core protein via three sugars (one xylose and two galactose), forming a proteoglycan.

Ref.: The Life Science Textbook, The University of Tokyo, online at: <http://csls-text.c.u-tokyo.ac.jp/index.html>

### 1.7.2. Heparan sulphate/Heparin

Described as structurally the most complex members of the GAG family by Rabenstein (2002), Hep and HS have increasingly been the subjects of research over recent decades. The reason for this is that they are well known to be involved in numerous biological processes such as cell growth and development, angiogenesis, viral invasion, and anticoagulation (Sasisekharan and Venkataraman 2000).

Hep was discovered in 1916 and since 1935 has been used as an anticoagulant agent in humans (Rabenstein, 2002). However, HS which was initially termed heparitin sulphate (Lamberg and Stoolmiller, 1974) came to light years later (Rabenstein, 2002). HS is present as heparan sulphate proteoglycan (HSPG) in extracellular matrix (ECM) and cell surfaces. From a cellular viewpoint, HSPGs can enhance the formation of receptor-ligand signalling complexes, can direct ligands into cells and can themselves be secreted from cell surface as soluble HSPGs (Bernfield et al., 1999). On the contrary, Hep is biosynthesized by mast cells and stored intracellularly in their granules (Sasisekharan and Venkataraman, 2000). Mast cells are resident cells of several types of tissues and contain many granules rich in histamine and Hep (Qu et al., 1995). Mast cells play a critical role in IgE-dependent immediate hypersensitivity reactions as well as in phagocytizing, processing, and presenting antigens to T cells. In addition, having Hep and other coagulation-regulating factors enables mast cells to play a role in regulating blood vessel function (Maurer et al., 2003).

Considering that Hep is found only in the secretory granules of mast cells, there may be a question regarding the physiological importance of Hep-protein binding. In this respect, one answer may be related to the broad use of Hep in therapy such as modulation of angiogenesis, tumor metastasis, and viral invasion. In addition, Hep-protein binding can serve as a model for the interaction of proteins with highly sulphated domains of HS chains present on cell surface (Rabenstein, 2002) (Figs. 1.8 and 1.9).

The basic chemical structures of Hep and HS are very similar and composed of linear sulphated polymers of alternating uronic acid-(1→4)-D-glucosamine (Lamberg and Stoolmiller, 1974). Neither Hep nor HS are found as single molecules, they are instead present as a diverse family of related molecules (Rabenstein, 2002). The basic structure of Hep units is illustrated in Fig. 1.8 (a,b).



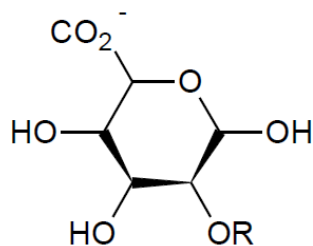
HS is made of the same repeating disaccharide subunits as Hep, illustrated in Fig. 1.9. However, in comparison to Hep, the GlcA/IdoA and GlcNAc/GlcNS ratios are higher; and the sulphate content is lower, depending on cell type and the degree of cell differentiation. Moreover, the organization of subunits of a HS molecule is different so that a HS molecule has a domain structure consisting of segregated blocks of repeating GlcA-(1 4)-GlcNAc disaccharides (NA domains) and blocks of highly sulphated, heparin-like IdoA-(1 4)-GlcNS disaccharides (NS domains) and NA/NS transition segments that consist of both GlcNAc- and GlcNS-containing disaccharides (Fig. 1.9). Thus, this diversity of HS structures allows them to participate in a wide range of biological functions (Rabenstein, 2002).

In terms of molecular mass, Hep as heparin proteoglycan complex is thought to have a relative molecular mass ( $M_r$ ) of 750,000-1,000,000. However, during post synthesis, the Hep chains are cleaved resulting in mixtures of smaller heparin polysaccharides with a  $M_r$  of 500-25000, which are stored in the cytoplasmic secretory granules of mast cells (Rabenstein, 2002). However, as mentioned above, HS is much more diverse, there are various  $M_r$  for various HS as HSPG in different locations. Normally, HS is longer than Hep and its average molecular weight is 30,000 (Gallagher and Walker, 1985).

Understanding HS- or Hep-protein interactions has long been a subject of investigation (Sasisekharan and Venkataraman 2000). One significant aspect is that Hep/HS structures are considered potential therapeutics for infectious diseases, inflammation, allergic disease, and cancer. Therefore, an understanding of the specificity and affinity of HS- or Hep-protein interactions plays a key role in designing Hep-based drugs (Coombe and Kett, 2005). Generally it is thought that the binding of protein by HS chains (or Hep) is primarily electrostatic, involving interactions between cationic ammonium, guanidinium, and imidazolium side chain functional groups of the peptide or protein with the sulphated saccharide domains of a HS/Hep chain (Kreuger et al., 2006; Rabenstein, 2002). In a molecular view, the conformational flexibility of the iduronate residue (Fig. 1.8 a) is central to the specific binding of Hep/HS to a given protein. Using X-ray crystallography and NMR studies, high-resolution structural information on HS bound to proteins has been obtained (Sasisekharan and Venkataraman, 2000).

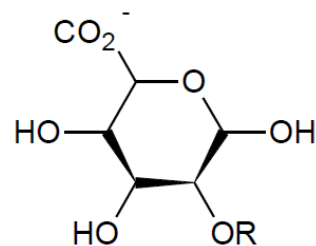
**a**

$\alpha$ -L-iduronic Acid



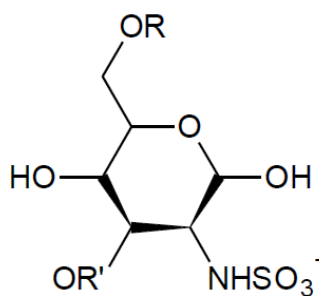
IdoA            R = H  
IdoA (2S)     R = SO<sub>3</sub><sup>-</sup>

B-D-Glucuronic Acid



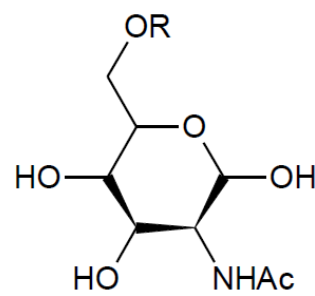
IdoA            R = H  
IdoA (2S)     R = SO<sub>3</sub><sup>-</sup>

N-sulfo- $\alpha$ -D-Glucosamine



GlcNS            R = R' = H  
GlcNS (6S)     R = SO<sub>3</sub><sup>-</sup>  
GlcNS (3S)     R = H, R' = SO<sub>3</sub><sup>-</sup>  
GlcNS (3,6 S) R = R' = SO<sub>3</sub><sup>-</sup>

N-Acetyl- $\alpha$ -D-Glucosamine



GlcNAc            R = H  
GlcNAc (6S)     R = SO<sub>3</sub><sup>-</sup>

**b**

Major repeating disaccharide of heparin

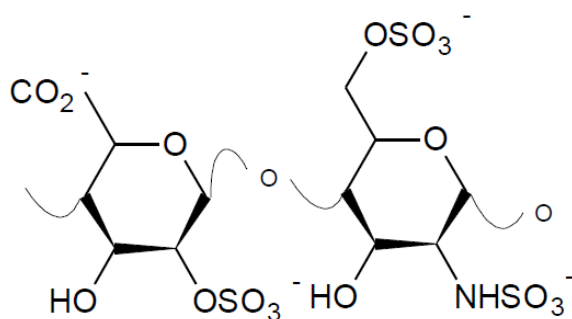


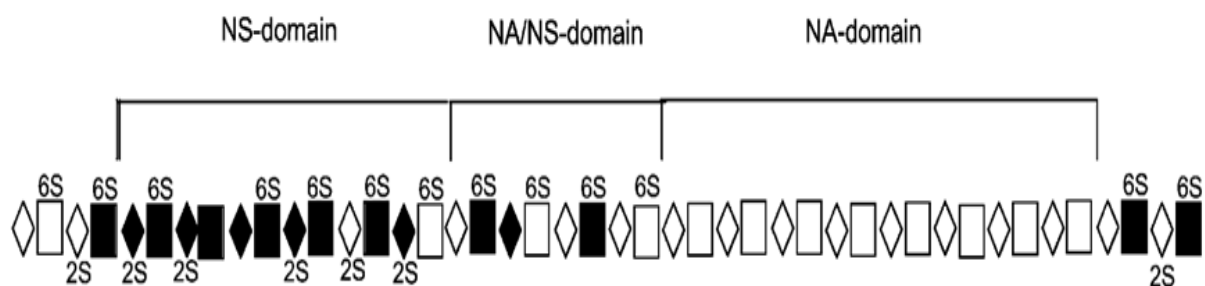
Figure 1.8. The structure of Hep

Panel a shows the basic structure of Hep which is constructed from uronic acid-(1→4)-D-glucosamine. The uronic acid portion may be either  $\alpha$ -L-iduronic acid (IdoA) or  $\beta$ -D-glucuronic acid (GlcA). It should be indicated that iduronic acid and glucuronic acid are epimers. This means they are non-mirror images of one another and differ in configuration of only one stereogenic centre, which is C5 (Wolf et al., 2007). The portion of  $\beta$ -D-glucosamine (GlcN) might be either *N*-sulphated (GlcNS) or *N*-acetylated (GlcNAc). The different Heps are made of different combinations of the monosaccharides illustrated.

Panel b depicts the disaccharide IdoA(2S)-(1 4)-GlcNS(6S) that is the most abundant combination of Hep so that 90% of Heps from bovine lung and 70% of those from porcine intestinal mucosa are composed of this structure.

The structures of this figure were drawn using ACD/ChemSketch 11.01, modified from Rabenstein (2002).

**a**



**b**

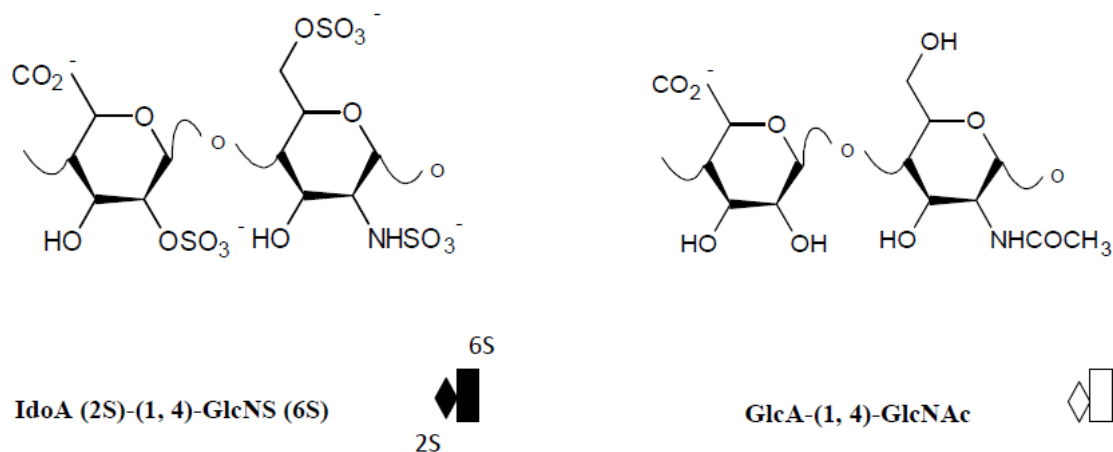


**Figure 1.9. The structure of HS**

Panel a depicts that the structure of a HS molecule is composed of highly sulphated domain (N-sulphated: NS), intermediate domain (NA/NS), and unsulphated domain (N-acetylated: NA) (Rabenstein, 2002).

Panel b shows that the highly sulphated NS domain can be IdoA(2S)-(1,4)-GlcNS(6S), which is similar to an usual Hep structure (Fig. 1.8, b); and the un-sulphated NA domain may be GlcA-(1,4)-GlcNAc. These portions together form the most common structure of HS molecules.

The structures in the section b were drawn using ACD/ChemSketch 11.01, modified from Rabenstein (2002).

**Table 1.5. Structural distinctions between HS and Hep sulphate groups, adapted from Gallagher and Walker (1985)**

Character	Sulphate groups (per 100 disaccharide units)	
	HS	Hep
Polymer sulphate	60-125	200-250
<i>N</i> -Sulphate	40-50	80-100
<i>O</i> -Sulphate	20-75	> 100
<i>N</i> -Acetylated disaccharides	Sequences > Solitary	Solitary > Sequences
Trisulphated disaccharides	Infrequent	Frequent

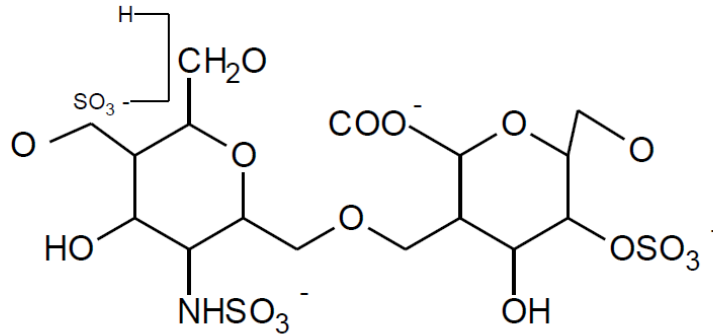
### 1.7.3. Enzymatic removal of cell surface HS

Heparinases, which are naturally produced by many sources, can degrade GAGs present on the cell surface. These enzymes have raised much interest due to their therapeutic use in blood deheparinization as well as their importance in clarification of the Hep and HS structure (Yang et al., 1985). The well-characterized heparinases that cleave Hep or HS have been isolated from four different bacteria: *Flavobacterium heparinum*, *Bacillus* spp., *Bacteroides heparinolyticus*, and an unclassified soil bacterium. Moreover, there are at least twenty-nine other bacteria which express the heparinase activity, even though these enzymes have not been isolated or characterized (Ernst et al., 1995). The heparinase enzymes can act on both Hep and HS through either eliminative cleavage by lyases, or hydrolytic cleavage by hydrolases (Ernst et al., 1995). In an eliminative mechanism, the enzyme cleaves the glucosamine-(1,4)-uronic acid glycosidic bond, leaving the glucosamine residue and the sulphate substituents intact but removes the C5 hydrogen of uronic acid, generating a terminal urinate with an unsaturated C4-C5 bond (Rabenstein, 2002) (Figure 1.10).

There are substrate specificities for each heparinase enzyme I, II or III. As such, it is known that heparinase I primarily cleaves Hep and to a lesser extent catalyzes HS with a ratio of 3:1; heparinase II acts on HS and to a lesser extent cleaves Hep with a ratio of 2:1; and heparinase III acts exclusively on HS and not on Hep (Ernst et al., 1995). It should be considered that Hep might be either an independent soluble Hep molecule or a highly sulphated domain of a cell surface HS structure (Fig. 1.9). Also, HS can be an independent HS soluble molecule or may be un-sulphated or less sulphated domains of a cell surface HS structure. Therefore, complete removal of cell surface HS may require treatment with all of the heparinase enzymes.

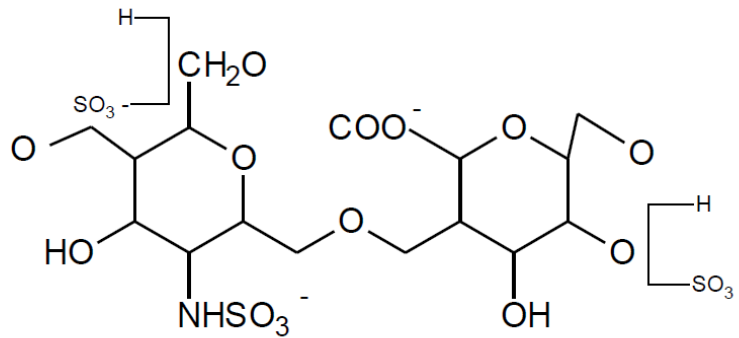
a

GlcNSO<sub>3</sub> (+/- 6-OSO<sub>3</sub>) 1-4 IdoA, 2-OSO<sub>3</sub>



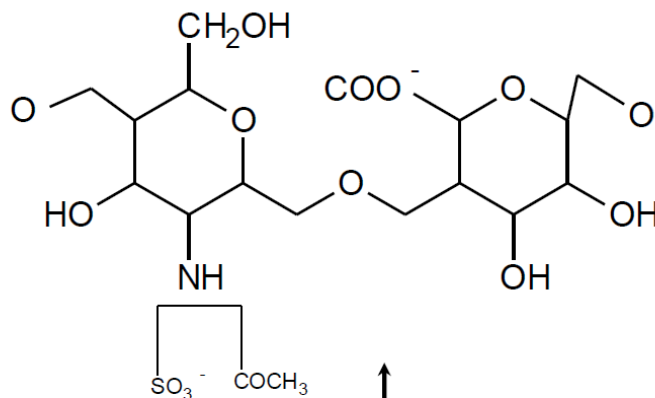
b

GlcNSO<sub>3</sub> (+/- 6-OSO<sub>3</sub>) 1-4 IdoA (+/- 2-OSO<sub>3</sub>)



c

GlcN { AC 1-4 GlcA  
SO<sub>3</sub>



Linkage cleaved by Heparinases I, II and III

Figure 1.10. A schematic demonstration of activity of heparinase enzymes

Panel a shows how heparinase I eliminates the glycosidic linkage between N-sulphated glucosamine and 2-O-sulphated iduronic acid. The disaccharide shown here is common for Hep (Fig. 1.8). In addition, it can be found in the highly sulphated domain (NS-domain) of a HS molecule (Fig. 1.9).

Panel b shows how heparinase II cleaves the glycosidic linkage between N-sulphated glucosamine and glucuronic or iduronic acid. Thus, this enzyme has a broad activity so that can catalyse Hep and most linkages in HS. The disaccharide shown here is common for both Hep and HS.

Panel c depicts the act of heparinase III on the glycosidic linkage between N-sulphated glucosamine or N-acetylated glucosamine and glucuronic acid. Thus, this enzyme mostly acts on HS in its low sulfation domains (Fig. 1.9) and has little activity against Hep or highly sulphated domains of HS.

The structures were drawn using ACD/ChemSketch 11.01, modified from Iduron technical bulletin (online at: [http://iduron.co.uk/media/catalog/category/file\\_15.pdf](http://iduron.co.uk/media/catalog/category/file_15.pdf)).



### 1.7.4. Sialic acids

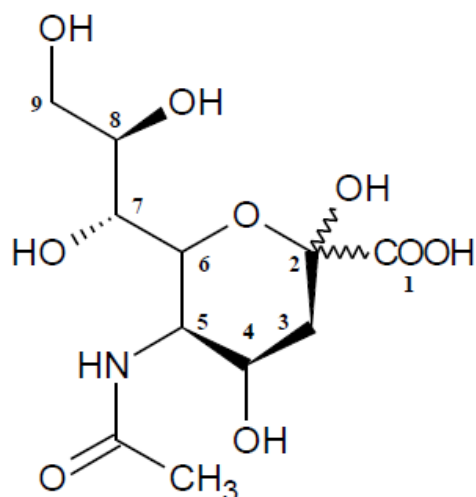
Discovered about 70 years ago, sialic acid refers to a family of derivatives of neuraminic acid, an amino acid sugar in pyranose form, with a nine-carbon carboxylated structure (Varki and Schaeue, 2009; Olofsson and Bergstrom, 2005). Sialic acids are present in the outer cell membrane at high concentration. They can be found as part of cell surface glycoproteins, gangliosides, or polysaccharides (Schauer, 1985). Like HS and Hep, sialic acids are negatively charged. Schauer (1985) stated that the negative charge of a human erythrocyte is particularly due to the presence of about 20 million sialic acid molecules on the cell surface. Sialic acids also can be found in urine and milk (Schauer, 1985). *N*-acetylneuraminic acid is the most common type of sialic acid in vertebrates (Schauer, 1985); however, 2-keto-3-deoxynononic acid is another common type of sialic acid in animal cells (Fig. 1.11). All other sialic acids are derivatives of these two forms (Varki and Schaeue, 2009). Combinations of different glycosidic linkages with the huge number of possible modifications have generated hundreds of different forms of sialic acid. This chemical diversity might contribute to the vast variety of glycan structures on cell surfaces and the distinctive makeup of different cell types (Varki and Schaeue, 2009).

The presence of sialic acid with a broad range of derivatives along with their strong negative charge suggests they are involved in several cellular functions (Schauer, 1985). As sialic acid is negatively charged, it is possible that it plays a key role in binding and transport of positively charged ions and drugs (Schauer, 1985), stabilizing the conformation of proteins including enzymes, and enhancing the viscosity of mucins (Varki and Schaeue, 2009). Sialic acids also provide protection for molecules and cells against proteases or glycosidases, extending their lifetime and function. In addition, sialic acids are important receptors for human viruses. Most sialic acid-based virus receptors contain a terminal sialic acid bound to a galactose through either  $\alpha$ 2-6-linkage or  $\alpha$ 2-3 linkage (Olofsson and Bergstrom, 2005). Historically, George Hirst and Frank Macfarlane Burnet in the 1940s stated that sialic acid serves as the cellular receptor for the human influenza viruses (Varki and Schaeue, 2009).

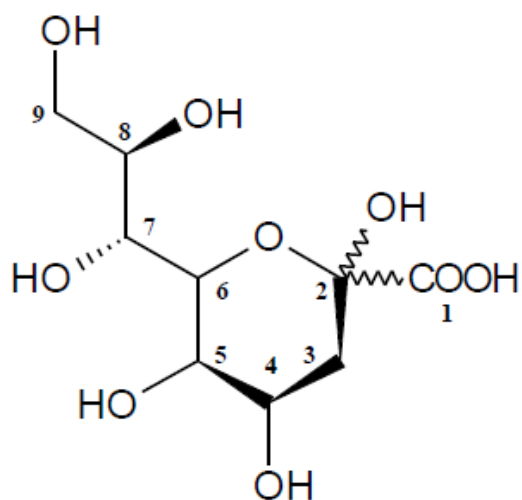
Similar to HS/Hep, there are certain enzymes that can remove sialic acids

from the cell surface, including sialidases (also called neuraminidases) that cleave the glycosidic linkages of neuraminic acids (Varki and Schaefer, 2009). There are two major classes of neuraminidase that cleave exo or endo poly-sialic acids (Cabezas, 1991): (i) Exo hydrolysis of  $\alpha$ -(2 $\rightarrow$ 3)-,  $\alpha$ -(2 $\rightarrow$ 6)-,  $\alpha$ -(2 $\rightarrow$ 8)-glycosidic linkages of terminal sialic acid residues, (ii) Endo hydrolysis of (2 $\rightarrow$ 8)- $\alpha$ -sialosyl linkages in oligo- or poly(sialic) acids. Noteworthy, neuraminidase is also found on the surface of influenza virus particles and is considered a receptor-destroying enzyme. It allows the virus to be released from the host cells. As such, zanamivir and oseltamivir, two known drugs for influenza, are designed to block the influenza neuraminidase and avoid the cleavage of sialic acid residues, thus interfering with the release of progeny virus from the infected host cells. This leads to a reduction in viral infectivity (McNicholl and McNichol, 2001).

a

*N*-acetylneuraminic acid (Neu5Ac)

b

2-keto-3-deoxynononic acid (Kdn)

**Figure 1.11. The schematic structures of two common sialic acids**

Panel a depicts *N*-acetylneuraminic acid, (Neu5Ac), while panel b shows 2-keto-3-deoxynononic acid (Kdn). The difference between the two molecules is the substitution at the C-5 position where Neu5Ac has an acetyl group and Kdn has a hydroxyl group. All other sialic acids are derivatives of these two forms. *N*-acetylneuraminic acid is more common than 2-keto-3-deoxynononic acid in human cells.

The structures were drawn using ACD/ChemSketch 11.01, modified from Varki and Schae (2009).

### 1.7.5. Glycans as virus cell receptors

The attachment of viruses to their specific receptors on the surface of susceptible host cells is a basic requirement for successful viral infection (Schneider-Schaulies, 2000). Thus, virus receptors can simply be defined as surface cellular targets that specifically bind to viruses, enabling the virus particle to attach to the host cell (Mettenleiter, 2002). As such, initial capture (attachment) receptor(s) mediate binding virions to target cells. Following this, fusion (entry) receptor(s) may be involved in penetration of the virus into the cell (Olofsson and Bergstrom, 2005). However, this definition is a simplified portrait of viral receptors. In fact, virus-receptor interactions are complex and dynamic and viral binding to cell receptors determines the host range and tissue tropism of viruses (Wu et al., 2010).

Most viral receptors belong to the family of glycoconjugates (Olofsson and Bergstrom, 2005), which are one of most significant constituents of biological membranes. As a functionally neutral term, glycoconjugate simply indicates that sugar residues are covalently bound to proteins or lipids. As such, there are three major groups of glycoconjugates, including glycolipids, glycoproteins, and proteoglycans (Fry, 1996). Regardless of the type of glycoconjugate, the carbohydrate portion (glycoepitope) is the main target of viral binding. However, sometimes a protein portion might act as a target for viruses.

As stated by Olofsson and Bergstrom (2005), viruses that use glycoepitopes as receptors (with a few important exceptions) bind to either sialylated glycans or to sulphated glycans. Table 1.6 illustrates an overview of the distribution of carbohydrate receptors in several families of viruses; however, it is not complete and research goes on to find new receptors for viruses. HS represents sulphated glycans, whereas sialic acid represents sialylated glycans. Both of these glycoepitopes are highly negatively charged due to having the carboxyl group as well as sulphate group in their molecular structure.

Influenza A virus is one of the most studied viruses that use sialic acid as a receptor. The target glycoepitope for human Influenza A virus is glycoprotein or glycolipids-linked sialic acid bound to a penultimate galactose residue (Table 1.6). In fact, the virus uses its haemagglutinin (a glycoprotein) to bind to cell surface sialic acid and then uses its neuraminidase to release sialic acid from potential virus receptors.

HS is considered the second largest group of carbohydrate receptors for human viruses of various families (Olofsson and Bergstrom, 2005). Since the chemical structure of HS/Hep gives them the ability to interact with cationic molecules, it is not surprising that many bacteria, protozoa, and viruses have been confirmed to bind to the HS of host cells. This binding may be selective for either a HS structure or a cellular location (Bernfield et al., 1999). However, for some viruses, the HS interaction is not essential for infection and might be a product of viral adaptation to *in vitro* cell culture (Bernfield et al., 1999).

The *in vitro* and/or *in vivo* antiviral potencies of soluble HS or HS mimetic compounds can be useful in understanding of the related viral receptors. Soluble HS mimetics are a group of the synthetic (or semi-synthetic) compounds that are structurally related to HS/Hep. They are polyanionic compounds where their polysaccharide backbone contains sulphate, carboxylate and hydroxyl functionalities, offering them the ability to simulate the HS/Hep functions (Papy-Garcia et al., 2005). Therefore, the assumption is that the anionic sugar residues of a soluble HS-derived compound can compete with the cellular HS chain in binding to the proteins of virus, leading to prevention of viral infection of the cell (Adamiak et al., 2007). This assumption is also true of sialic acid so that antiviral action of soluble sialic acid-derived compounds can represent the viral use of sialic acid as receptor. However, to confirm the viral use of HS or sialic acid as a receptor, other confirmatory bioassays need to be performed, such as using heparinase or sialidases enzymes to remove HS or sialic acid from the cell surface, respectively.

There are numerous examples of the role of HS mimetics or sialic acid-derived compounds in identification of the relevant viral invasion receptors. Focusing on Enteroviruses, one can mention Coxsackievirus B3 variant PD (CVB3-PD). Inhibition of CVB3-PD by the anionic HS mimetic compounds was one of the reasons that Zautner et al., (2003) justified their conclusion that HS acts as a receptor for this virus, in addition to the Coxsackievirus-Adenovirus receptor (CAR). Similarly, Goodfellow et al. (2001) concluded that HS is a possible surface receptor for viruses from the *Enterovirus* genus based on observation of the antiviral action of HS-like compounds against the viruses. In addition, recently, it was reported by Yang et al. (2009) that sialylated glycans (containing sialic acid) could be receptors for EV71 in DLD-1 intestinal cells. As one confirmatory assay for this conclusion,

they demonstrated that sialic acid-derived glycans from human milk could inhibit EV71 infection *in vitro*.

From a clinical viewpoint, the identification of a virus receptor(s) results in significant insight into the pathology of the virus infection. The knowledge gained can potentially lead to the development of clinically effective antiviral drugs against the virus (Norkin, 1995). For example, in the case of EV71, an undefined cell receptor(s) has been considered one of the critical reasons for lack of a potent antiviral against this virus (Yang et al., 2009). However, knowledge of virus-receptor interactions does not always lead to the development of clinically successful antiviral treatments. For example, although CD4 is well known to serve as the major receptor for HIV-1, soluble forms of this receptor have failed to inhibit HIV-1 infection in clinical trials. Thus, one key impediment is that often with viruses, if one receptor is removed, another may be used. Thus, treatment may need to block multiple receptors without damaging normal cell function. This shows that inhibition of viral infection by blocking viral receptors can be a very complex process.

**Table 1.6. Classification of viruses which use glycoepitopes (sialic acid or HS) as receptors, modified from Olofsson and Bergstrom (2005)**

Virus family	Virus type	Receptor
Adenoviridae	Adenovirus 37	( $\alpha$ 2-3)-linked sialic acid
	Adenovirus types 2 and 5	HS
Coronaviridae	Coronavirus OC43	9- <i>O</i> -acetylated sialic acid
Flaviviridae	Hepatitis C virus	HS
	Dengue virus	HS
	Japanese encephalitis virus	HS
	West Nile virus	HS
Herpesviridae	Herpes simplex virus	HS
Orthomyxoviridae	Influenza A virus: in birds	( $\alpha$ 2-3)-linked sialic acid
	Influenza A virus: in humans	( $\alpha$ 2-6)-linked sialic acid
	Influenza B virus	( $\alpha$ 2-6)-linked sialic acid; ( $\alpha$ 2-3)-linked sialic acid
	Influenza C virus	9- <i>O</i> -acetylated sialic acid
Papillomaviridae	Human papillomavirus types 11, 16, 33	HS
Paramyxoviridae	Paramyxovirus types 1-3	Sialic acid
	Respiratory syncytial virus	HS
Picornaviridae	Enterovirus 70	Sialic acid
	Rhinovirus 87	Sialic acid
Reoviridae	Rotavirus	Sialic acid
Retroviridae	HIV-1	Galactosylceramide/sulfatide; HS

Note: receptors mentioned in this table are not necessarily the only ones which the viruses use. For example, in the case of HIV-1, CD4 is main receptor in CD4<sup>+</sup> host cells along with a co-receptor, either CCR5 or CXCR4. These are all glycoproteins expressed on the surface of T helper cells, macrophages and dendritic cells. However, in CD4<sup>-</sup> host cells, the virus can binds to HS (Crublet et al., 2008).

### 1.7.6. Enterovirus 71 receptors

In 2009, three independent groups suggested candidates for EV71 receptors. Yamayoshi et al. (2009) proved that the human scavenger receptor class B, member 2 (SCARB2) is a protein receptor for a clinically isolated EV71 (SK-EV006). SCARB2 is a type III double-transmembrane glycoprotein with *N*- as well as *C*-terminal cytoplasmic tails, located primarily in lysosomes and endosomes (Yamayoshi et al., 2009). They followed a strategy similar to that which was used in the identification of the poliovirus receptor. The Mouse L929 cells were transformed with genomic DNA from RD cells, which are frequently used to culture EV71 strains. The EV71-susceptible cell lines were detected and subjected to a microarray analysis to identify the human gene(s) responsible for offering EV71 susceptibility to L929 cells. Among those analyzed, 22 genes were selected whose expression was significantly increased, but only the genes SCARB2, CCL2, and MEPCE were amplified and transfected into L9292 cells. Finally, it was demonstrated that SCARB2 is enough to make the cells susceptible to EV71. Further analyses demonstrated that SCARB2 could serve as a receptor for EV71 isolates from A, B and C genotypes. Additionally, it was also detected that SCARB2 had a leading role in the early stages of EV71 infection in some other cell lines, including HeLa, HEp-2, 293T, and HepG2 cells. The study also showed that CVA16 can infect cells through SCARB2 receptor but this was not true of most other human Enterovirus A viruses (Yamayoshi et al., 2009).

In parallel, human P-selectin glycoprotein ligand-1 (PSGL; also called CD162) was demonstrated to act as a receptor for EV71 (Nishimura et al., 2009). PSGL is a sialomucin membrane protein located on leukocytes and endothelial cells, which can be linked to P (platelet)-selectin, a cell adhesion molecule. Sialomucins represent various glycoproteins containing sialic acid in connective tissue, saliva, mucus, etc., that lubricate and protect the body. The complex PSGL is naturally involved in adhesion and transmigration of leukocytes into inflamed tissues. Because a neurological EV71 infection can cause a significant reduction in T cells and high levels of pro-inflammatory cytokines, Nishimura et al. (2009) established a cDNA library from Jurkat T cells that are susceptible to EV71 infection. Then four colonies of mouse myeloma P3X63Ag8U.1 transfected with the Jurkat cDNA library showed susceptibility to EV71, all of which encoded human PSGL-1. Further tests



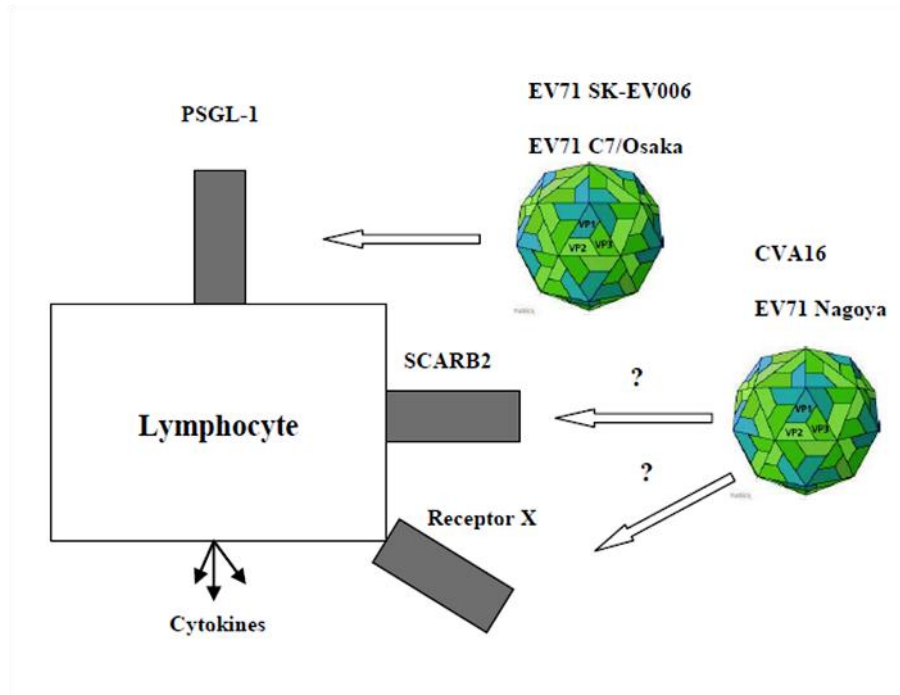
confirmed that the *N*-terminal region (amino acids 42-61) of human PSGL-1 is important for EV71 binding. However, it was shown that some EV71 strains did not use PSGL-1 as the primary receptor, also non-leukocytes such as RD, HEp-2c, SK-N-MC and Vero cells did not support EV71 replication through PSGL-1 (Nishimura et al., 2009). Figure 1.12.a,b illustrates binding EV71 to the receptors SCARB-2 and PSGL-1.

The third report suggested that EV71 can use sialic acid as a receptor in DLD-1 intestinal cells (Yang et al., 2009). The fact that many viruses use carbohydrate receptors, either sulphated or sialylated glycans as well as the fact that sialic acid- $\alpha$ 2,3 galactose is a receptor for Coxsackievirus A24 (Nillson et al., 2008) encouraged Yang et al., (2009) to work with intestinal cells epithelial cells, which contain abundant sialylated glycans. To test whether *O*-glycans, *N*-glycans, or glycolipid are involved in EV71 infection in DLD-1 cells, these compounds were reduced by benzyl *N*-acetyl- $\alpha$ -D-galactosaminide, tunicamycin and phosphatidylinositol-specific phospholipase, respectively. The results showed that depletion of glycolipids and particularly *O*-linked glycans reduced EV71 infection of DLD-1 cells. These findings may be in agreement with Nishimura et al. (2009) who found that PSGL-1 (an *O*-linked glycoprotein) acts as a receptor for EV71. Then, treatment of the cells with the  $\alpha$ 2,3 and  $\alpha$ 2,6 sialidase, to remove surface sialic acids linked to galactose, resulted in reduced EV71 infection of the cells, confirming sialic acids as a receptor for EV71. Furthermore, sialic acid  $\alpha$ 2,3 and sialic acid  $\alpha$ 2,6 from human milk (0.25 mg/mL) could significantly inhibit EV71 in DLD-1 cells (Yang et al., 2009). These findings led Yang et al. (2009) to conclude that natural sialic acids containing glycans in human milk could have a role in preventing EV71 infection in infants, in addition to other antibodies present in human milk. Therefore, a strategy was suggested by which an anionic sialylated residue could compete with EV71 invasion receptors. Then, the galactose portion can be linked to a cationic protein such as lactoferrin that can target the EV71 envelope (Weng et al., 2005). This is illustrated in Figure 1.12c.

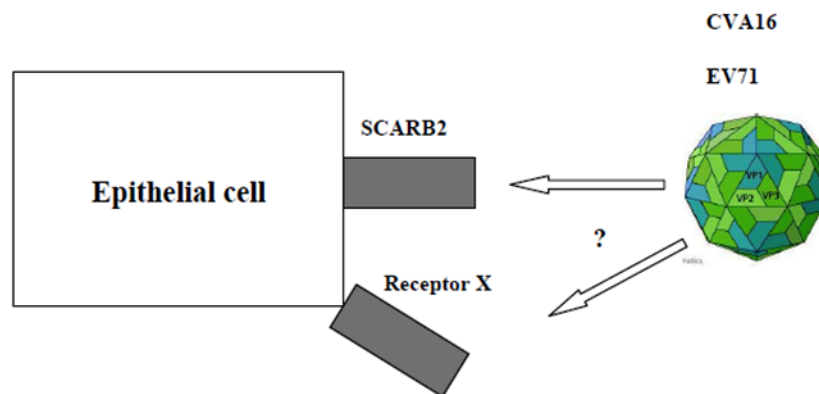
The discovery of these EV71 receptors has shed new light on the design of antivirals against EV71. However, these receptors are not localized exclusively to neural cells. Thus, the question remains how these receptors contribute to neurotropism of EV71 where it can cause neurological complications (Patel and

Bergeson, 2009). Thus, further studies need to be undertaken in order to find neural specific receptor(s) for EV71 (Weng et al., 2010). An additional consideration is that some strains of EV71 may use cellular receptors different than those reported so far, as clearly stated by Nishumura et al. (2009) and Yamayoshi et al. (2009). Thus, it could be of interest to investigate other potential cell receptors for different EV71 strains in different cell lines.

**a**



**b**



**c**

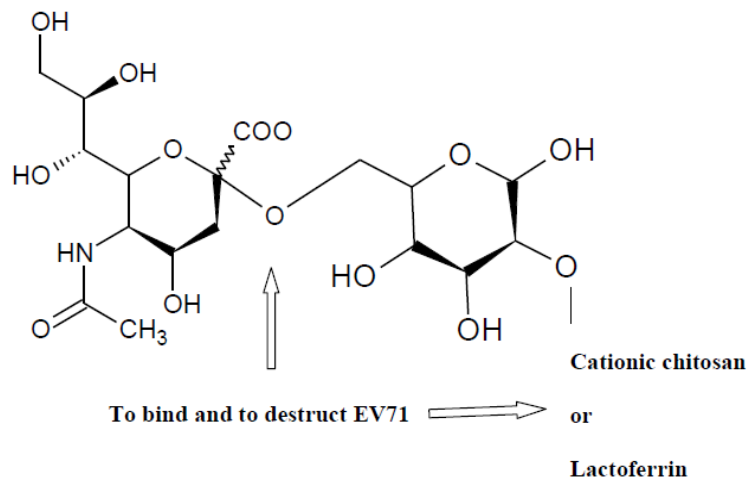


Figure 1.12. EV71 cell receptors suggested to date

a: as the picture depicts, while several isolates of EV71 were shown to bind to human P-selectin glycoprotein ligand-1 (PSGL-1) on lymphocytes, some EV71 strains (such as EV71 Nagoya) and CVA16 did not use PSGL-1 as the primary receptor. They may or may not interact with SCRB2 or another undefined receptor.

It is believed that interaction of the virus with PSGL-1 receptor induces significant high levels of pro-inflammatory cytokines, which is important for EV71 pathogenesis (Patal and Bergelson, 2009).

b: Located on epithelial cells and fibroblasts, SCARB2 can serve as a receptor for EV71 isolates from A, B and C genotypes as well as CVA16. However, most other human Enterovirus A viruses did not utilize this receptor, suggesting the possibility of presence of another receptor (Patal and Bergelson, 2009).

c: EV71 can use sialic acid as receptor in DLD-1 intestinal cells. The galactose portion in a "sialic acid  $\alpha$ 2,6-linked galactose" can be linked to cationic compounds such as chitosan or lactoferrin, to bind to and destroy EV71 (Yang et al., 2009).

The schematic pictures a and b were re-drawn and modified according to Patel and Bergelson (2009). The structure of sialic acid  $\alpha$ 2,6-linked galactose was drawn using ACD/ChemSketch 11.01, modified from Yang et al. (2009).

### 1.7.7. HS mimetics as antivirals

As described before, theoretically an anionic soluble HS-like compound can compete with the cellular HS chain in binding to the virus, leading to prevention of viral infection of the cell. Accordingly, synthetic HS mimetics have been applied in antiviral experiments against a broad range of viruses (Urbinati et al., 2008). The knowledge about antiviral activity of these compounds dates back many years (Ginsberg et al., 1947; Green and Wooley, 1947; De Somer et al., 1968; Nahmias and Kibrick, 1964). However, investigation into the specific mechanisms underlying their antiviral activity has been relatively recent.

Table 1.7 summarizes characteristics and properties of three major HS mimetics, including Hep, HS, and pentosan polysulphate (PPS). Hep has a relatively long antiviral history, particularly for its inhibitory action against HIV-1 that dates back to the mid-80's (Ito et al., 1987; Ueno et al., 1987). Baba et al. (1988a) carried out further studies to determine the molecular mechanism of anti-HIV action of Hep and its relationship with anticoagulant activity. They proved that Hep (and dextran sulphate) inhibited HIV-1 infection *in vitro*. Hep could protect MT-4 (a type of human T-cell) cells against CPE caused by HIV-1 at 25 µg/mL with an IC<sub>50</sub> of 7 µg/mL and no significant cytotoxicity. Hep exerted its anti-HIV activity through inhibition of the virus attachment process but this was not attributed with the CD4 antigen receptor. It was also shown that both the antiviral and anticoagulant activities of Hep increased with increasing molecular weight so that the normal non-fragmented Hep (MW: 15,000) showed highest anti-coagulant activity as well as highest antiviral activity (Baba et al., 1988a). In addition, Baba et al. (1988b) evaluated the antiviral activity of several anionic glycans including Hep and PPS against a range of viruses. The tested sulphated polysaccharides generally demonstrated potent and broad-spectrum antiviral activities against enveloped viruses, such as HSV, HIV, vesicular stomatitis virus, and sindbis virus in different cell types (Baba et al., 1988b).

Schols et al. (1990) demonstrated that Hep, PPS, and some other Hep-like compounds prevented the binding of anti-gp120 monoclonal antibodies to the persistently HIV-1-infected HUT-78 cells. Nevertheless, the compounds did not directly bind to the CD4 receptor. It was speculated that the compounds were able to bind to HIV gp120 and prevent its subsequent interaction with the cell surface

receptor CD4. Further research revealed that PPS is able to bind to the extracellular Tat protein of HIV-1, inhibiting its cell surface interaction, internalization, and biological activity *in vitro* in HL3T1 cells and *in vivo* (Rusnati et al., 2001). Tat protein is thought to be released from HIV-infected cells; it can enter the cell and nucleus to stimulate the transcriptional activity of HIV-LTR, it also plays a role in the pathogenesis of AIDS. Thus, the authors concluded that PPS might represent a prototypic molecule for the development of novel Tat antagonists with therapeutic implications in AIDS and AIDS-associated pathologies, including Kaposi's sarcoma (Rusnati et al., 2001).

The antiviral activity of Hep, HS and other HS mimetics was also evaluated against dengue virus infection in a study to find their potential role as binding targets for dengue virus envelope glycoprotein (Chen et al., 1997). Hep displayed potent competitive antagonism against binding of a recombinant surface glycoprotein of dengue virus-2 to Vero cells (with an  $IC_{50}$  of 0.3  $\mu\text{g/mL}$ ), while HS and other GAGs failed to display such effect. This was an unexpected result, as HS and Hep are structurally very similar. To test this further, Chen et al. (1997) tested another HS derivative with an unusually high sulphate content. The new HS considerably inhibited the recombinant surface glycoprotein to binds to Vero cells with an  $IC_{50}$  of 4  $\mu\text{g/mL}$ , suggesting highly sulphated HS domains (and Hep) were able to mimic critical structural characteristics of the cellular receptor (Chen et al., 1997). These findings were then coupled with inhibition of dengue virus infection in Vero cells by Hep (99%) and highly sulphated form of HS (87%).

Further research focused on the role of HS in the binding of infectious dengue virus-2 to cells (Germi et al., 2002). It was observed that Hep displayed an inhibitory effect on the attachment of dengue virus-2 and yellow fever virus. Hep also inhibited yellow fever virus infection by 97% with an  $IC_{50}$  of about 0.2  $\mu\text{g/mL}$ .

Lee et al., (2006) evaluated the antiviral activities of four HS mimetic compounds including Hep, PPS, PI-88 (an anti-cancer drug with a low molecular weight of 2400 Da that mimics HS) and suramin against dengue virus and some other encephalitis flaviviruses. The results revealed that  $IC_{50}$  values of Hep, PPS and PI-88 against dengue infection in baby hamster kidney-21 cells (BHK-21) were approximately 1  $\mu\text{g/mL}$ , 30  $\mu\text{g/mL}$ , and 200  $\mu\text{g/mL}$ , respectively. The results with

Japanese encephalitis virus were approximately 10 µg/mL, 7 µg/mL and 40 µg/mL, respectively.

These results clearly showed that Hep exerted a potent antiviral activity against both dengue virus and Japanese encephalitis virus infections, whereas PPS showed its most potent antiviral activity against only Japanese encephalitis virus infection. It was then concluded that the greater molecular size of Hep and PPS, compared to PI-88, might have contributed to their potent *in vitro* antiviral activities. However, the *in vitro* anti-flaviviral activities of the HS mimetics do not necessarily correlate with their *in vivo* therapeutic value, as in murine models for dengue virus and flaviviral encephalitis, only PI-88 demonstrated a significant effect for survival of infected mice (Lee et al., 2006). It was interpreted that the mode of action of HS mimetics was through interfering with the viral attachment, following binding of the compounds to regions enriched in basic residues on the viral surface. Thus, The HS mimetics antiviral activity is greatly determined by their affinity for the flavivirus E protein (Lee et al., 2006).

Barth et al., (2003) used recombinant glycoproteins of Hepatitis C virus (HCV) envelope and HCV-like particles (LPs) to show that HS acts as a capture receptor for HCV. It was demonstrated that the glycoprotein E2 of HCV binds to sulphate-HS and this interaction plays an important role in the attachment of HCV to target cells. Hep at a concentration of 10 µg/mL could inhibit HCV-LP binding to both HepG2 and MOLT-4 cells by more than 95% while its IC<sub>50</sub> was at nano-levels: 3 ng/mL in HepG2 cells and 4 ng/mL in MOLT-4 cells, respectively. The same observation was obtained with highly sulphated HS, but Hep was much more potent in inhibiting E2 binding to target cells, when compared to HS, due to the high sulphation level. Since there is limited treatment and no vaccine for chronic HCV, understanding the virion interaction with the host cell is imperative for the design and development of effective drugs (Zeisel et al., 2009).

The inhibition of herpes simplex viruses (HSV-1 and HSV-2) infection by sulphated polysaccharides has been long known (Takemoto and Fabisch, 1964; Vaheri, 1964; WuDunn and Spear, 1989). However, little is known about the effect of these compounds on the intercellular transmission of HSV. Thus, Nyberg et al., (2004) evaluated this with PI-88, which caused a more efficient reduction of cell-to-cell spread of HSV infection in Vero cells, even though Hep was a better inhibitor of

HSV infection. PI-88 has a shorter chain length and a higher degree of sulphation than most HS derivatives. Having these features, the authors concluded that PI-88 might be able to access the narrow intercellular space leading to inhibition of cell-to-cell spread of viral infection. It was speculated that, like most other HS mimetics, PI-88 inhibits HSV infection through interfering with the binding of the viral glycoproteins gC and gB to the host cells (Nyberg et al., 2004).

Similar to many other viral families and genera, the antiviral action of HS-like compounds against viruses from the *Enterovirus* genus has been studied, confirming HS as a possible surface receptor for these viruses (Goodfellow et al., 2001; Zautner et al., 2003). It was previously shown that viruses of the *Enterovirus* genus bind to decay-accelerating factor (DAF; CD55). As such, the affinity of echovirus (EV) 11 (EV11) to DAF has previously been determined (Lea et al., 1998). However, further studies have also suggested that the EV6 strain can bind to murine NIH 3T3, CHO, and RD cells in a DAF-independent manner (Goodfellow et al., 2001). Thus, in their search for other candidate surface receptors, Goodfellow et al. (2001) found that HS is the molecule that the virus might bind to. The results revealed that EV7 could not bind to NIH 3T3 and CHO cells in the absence of DAF, while EV6 was capable of binding in a DAF-independent manner. To confirm the viral usage of HS, the cell surface HS was removed by heparinase-I, resulting in the blockage of viral binding to the cell surface. Additionally, the concentrations of Hep needed to inhibit RD cell infection by a range of Enteroviruses were determined, demonstrating that while 1mg/mL of Hep could block infection caused by EV6 by 95%, the strain EV7 was insensitive to Hep at 2 mg/mL. Further investigations revealed that the binding of cell surface HS to virus is widespread within other serotypes of Human Enterovirus B (HEV-B) species (Goodfellow et al., 2001), whilst it had been shown that the HS binding to FMDV is likely to be an adaptation to cell culture (Jackson et al., 2000, Jackson et al., 1996; Neff et al., 1998).

Another study on receptors involving Coxsackievirus B3 PD (CVB3 PD) confirmed that this strain uses HS in addition to Coxsackievirus-Adenovirus receptors (CAR) (Zautner et al., 2003) as a receptor. This conclusion was based on evidence that Chinese hamster ovary cells treated with heparinase resist CVB3 PD infection. In addition, anionic compounds such as PPS, porcine intestinal HS, and

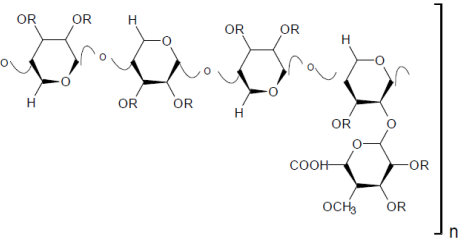


bovine pulmonary Hep strongly inhibited CVB3 PD infection at IC<sub>50</sub> of 18.92, 34.83 and 29.94 µg/mL, respectively.

Table 1.7. Characteristics of three important HS mimetics

Soluble compound	Abbreviation	Chemical structure	Molecular weight	Applications
Heparin sodium (Different sources)	Hep (Lamberg and Stoolmiller, 1974)	The major repeating disaccharide of Hep is IdoA(2S)-(1 4)-GlcNS(6S) depicted in Figure 1.8 (Rabenstein, 2002)	Varied, 15KDa on average (Nyberg et al., 2004)	<ul style="list-style-type: none"> <li>- Clinical uses: Relieving pain, inhibiting clotting, treatment of burns, restoring blood flow, and enhancing healing ( Saliba, 2001), Anti cancer (Coombe and kett, 2005)</li> <li>- Antiviral activity: (Zautner et al., 2003)</li> </ul>
Heparan sulphate (Different sources)	HS (Lamberg and Stoolmiller, 1974)	The domain structure of HS is comprised of blocks of repeating GlcA-(1 4)-GlcNAc disaccharides (NA domains) and blocks of highly sulphated, heparin-like IdoA-(1 4)-GlcNS disaccharides (NS domains), depicted in Figure 1.9 (Rabenstein, 2002)	Varied, 15KDa on average (Griffin et al., 1995)	<ul style="list-style-type: none"> <li>- Clinical uses: Relieving pain, inhibiting clotting, treatment of burns, restoring blood flow, and enhancing healing (Reviewed by Saliba, 2001), Anti cancer (Coombe and kett, 2005)</li> <li>- Antiviral activity: (Zautner et al., 2003)</li> </ul>

Table 1.7. Characteristics of three important HS mimetics (continued)

Soluble compound	Abbreviation	Chemical structure	Molecular weight	Applications
Pentosan Polysulphate	PPS (Dürüst and Meyerhoff, 2001)	 <p style="text-align: center;">R = SO<sub>3</sub><sup>-</sup></p> <p>PPS is a semi-synthetically Hep-like derivative, a hemicellulose isolated from the wood of the beech tree (<i>Fagus sylvatica</i>). It consists of repeating units of (1-4)-linked<sup>a</sup> β-D-xylanopyranoses (Dürüst and Meyerhoff, 2001)<sup>a</sup></p>	Varied, 5700 Da on average (Dürüst and Meyerhoff, 2001)	<p>Clinical use: Known as Elmiron<sup>®</sup> which is a drug for the relief of bladder pain or discomfort associated with interstitial cystitis (<a href="http://www.rxlist.com/elmiron-drug.htm">http://www.rxlist.com/elmiron-drug.htm</a>), anti cancer (Dürüst and Meyerhoff, 2001)</p> <p>Antiviral activity: (Baba et al., 1988b)</p>

<sup>a</sup>The molecular structure of PPS was drawn using ACD/ChemSketch 11.01, in accordance with (Dürüst and Meyerhoff, 2001)

### **1.7.8. The role of cell surface HS in mediating viral pathogenicity *in vivo***

It has been known that there is a correlation between *in vitro* interaction of cell surface HS with a virus and *in vivo* attenuation of that virus (Bernard et al., 2000). Bernard et al. (2000) showed that mutants of Venezuelan Equine Encephalitis virus (VEE) that interacted with cellular HS *in vitro*, showed a partial or complete attenuation in adult mice, even though the HS interaction was not assumed the only determinant of such *in vivo* attenuation. Similar results were obtained with Sindbis virus (SIN) where a reduced ability to bind to cellular HS allowed for greater viral production *in vivo*, resulting in more mortality (Byrnes and Griffin, 2000). Therefore, it might be speculated that the viral HS-binding may lower virus fitness *in vivo*.

However, these findings appear to contradict other papers reporting that interaction of viruses with cell surface HS contributed to increased level of neurovirulence (Zhu et al., 2011). In this respect, Ryman et al., (2007) reported a neuro-adapted Sindbis variant (NSV) of SIN laboratory strain that caused severe, often fatal encephalomyelitis in adult mice when the virus was inoculated intracranially. It was concluded that increased severity of encephalomyelitis caused by NSV is very likely associated with the ability of the virus to bind to cellular HS. These findings are also in line with *in vivo* and *in vitro* results of Tucker et al. (1993), Tanaka et al. (1998), Jinno-Oue et al. (2001), and Lee et al. (2002), where the capability of virus to use cellular HS led to more virulence.

The reason for this disagreement appears to lie in the route of virus inoculation, as once viruses were intracranially (i.c.) inoculated, the cellular HS-virus interaction contributed to more neurovirulence *in vivo*, while the other routes of virus inoculation resulted in more rapid clearance of virus from host animals. This fact may shed light on a significant role of HS as a co-receptor in mediating cellular tropism of viruses following i.c. inoculation (Reddi et al., 2004). Therefore, it can be concluded that viral derivatives with effective abilities to bind to cell surface HS show increased neurovirulence by changing cell tropism or improving viral replication within the host brain (Zhu et al., 2011). Table 1.8 has summarized

relationship between the cellular HS usage and *in vivo* pathogenesis in mutant viruses.

Table 1.8. Relationship between cellular HS usage and *in vivo* pathogenesis in mutant viruses, with modifications from Reddi et al. (2004)

Family/serotype <sup>1</sup>	Variant <sup>2</sup>	Region of mutation/mutant amino acid <sup>3</sup>	Charge change	HS use	<i>In vivo</i> route of virus inoculation <sup>5</sup>	<i>In vivo</i> virulence	Reference	
<i>Flaviviridae</i>	TBEV	BHK-21	Asp to Gly	Increasing the net positive charge	Yes	s.c.	Attenuated	Goto et al., 2003
	TBEV	BHK-21	Glu to Lys	Negative to positive	Yes	s.c.	Attenuated	Mandl et al., 2001
			Glu to Gly	Increasing the net positive charge				
	SFV	SK26	Ser to Arg	Neutral to positive	Yes	i.n.	No change	Hulst et al., 2001
	JEV	SW13	Glu to Lys	Negative to positive	Yes	f.p.	Attenuated	Lee and Lobgis, 2002
	MEV	SW13	ASP to Gly	Increasing the net positive charge	Yes	f.p.	Attenuated	Lee and Lobgis, 2000
<i>Togaviridae</i>	SIN	BHK-21	Ser to Arg	Neutral to positive	Yes	s.c.	Attenuated	Klimstra et al., 1998
	SIN	Recombinant	Gln to His	Neutral to positive	Yes	i.c.	More virulent	<i>In vitro</i> : Lee et al., 2002 <i>In vivo</i> : Tucker et al., 1993
	RRV	CEF	Asp to Lys	Negative to positive	Yes	n.d. <sup>6</sup>	Attenuated	<i>In vitro</i> : Heil et al., 2001 <i>In vivo</i> : Weir et al., (not published) cited by Heil et al., 2001
	VEE	BHK-21	Thr to Lys; Glu to Lys	Neutral to positive	Yes	f.p.	Attenuated	Bernard et al., 2000
	GDVII	Pgs-A745	n.d. <sup>4</sup>	Positive to negative	No	i.c.	Attenuated	Reddi et al., 2004

Table 1.8. Relationship between cellular HS usage and *in vivo* pathogenesis in mutant viruses (continued)

Family/serotype <sup>1</sup>	Variant <sup>2</sup>	Region of mutation/mutant amino acid <sup>3</sup>		Charge change	HS use	<i>In vivo</i> route of inoculation <sup>5</sup>	<i>In vivo</i> virulence	Reference	
<i>Retroviridae</i>	PVC-211 MuLV	Rat passaged	Envelope surface protein	Glu to Gly; Glu to Lys	Negative to positive	Yes	i.c.	More virulent	<i>In vitro</i> : Jinno-Oue et al., 2001 <i>In vivo</i> : Tanaka et al., 1998
	FMDV	BHK-21	Capsid	Glu to Lys	Negative to positive	Yes	i.d.	Attenuated	Zhao et al., 2003
FMDV	CHO-K1	His to Arg		Increasing the net positive charge	Yes	i.d.l.	Attenuated	Sa-Carvalho et al., 1997	
GDVII	Pgs-A745	n.d. <sup>4</sup>		Positive to negative	No	i.c.	Attenuated	Reddi et al., 2004	

1. Abbreviations of viruses: TBEV: tick-borne encephalitis virus; SFV: swine fever virus; JEV: Japanese encephalitis virus; MEV: Murray Valley encephalitis virus; SIN: Sindbis virus; RRV: Ross River virus; VEE: Venezuelan equine encephalitis virus; PVC-211 MuLV: murine leukemia virus strain PVC-211; FMDV: foot-and-mouth disease virus; GDVII: a high-neurovirulence strain of Theiler's m urine encephalomyelitis virus.

2. Cells which the viral mutants were passed in, unless otherwise indicated.

3. Three letter codes of amino acids; ASP: Aspartic acid; Gly: Glycine; Glu: Glutamic acid; Ser: Serine; Arg: Arginine; Gln: Glutamine; His: Histidine; Lys: Lysine; Thr: Threonine

4. While it has been stated that R3126L and N1051S were regions which displayed the mutations for the viral capsid, the amino acids substituted were not reported (Reddi et al., 2004).

5. *In vivo* routes of inoculation of virus: s.c.: subcutaneous; i.n.: intranasal; f.p.: footpad; i.c.: intracranial; i.d.: intradermal; i.d.l.: intradermal-lingual.

6. No information is given as to the route used for viral inoculation

## 1.8. DNA microarrays

### 1.8.1. Introduction

The global pattern of gene expression in a cell determines the structure and the function of that cell (Khan et al., 1999). In order to provide insight into global gene expression, a wide-genome analysis would be critically important. There are two major approaches for genome-wide expression analysis: serial analysis of gene expression (SAGE) and microarrays (Khan et al., 1999). SAGE is a technology that allows a rapid and thorough analysis of thousands of transcripts. In brief, short sequence tags (10-14bp) within each transcript of sample of interest are generated. These sequence tags contain adequate information to uniquely spot a transcript. Sequence tags will be linked together to form long serial molecules that will be cloned and sequenced. Then, by counting the number of times a particular tag is observed, the expression level of the corresponding transcript will be determined (Velculescu et al., 1995, 1997).

DNA microarray measures expression of a set of genes of interest in a biological sample at the transcriptional level (Khan et al., 1999). In a typical microarray experiment, the binding of a given cDNA molecule (obtained from total RNA of a sample of interest) to cDNA probes (corresponding to known genes) are examined. Then, by measuring the intensity of the binding, the expression levels of the relevant genes can be accurately determined. The basic aims of both SAGE and DNA microarray are similar. However, unlike SAGE, observations in microarray are based on hybridization, resulting in more quantitative, digital values. In addition, microarray experiments are cheaper to perform, so large-scale studies do not normally use SAGE. However, gene expression quantification is more precise in SAGE, as one can directly count the number of transcripts, whilst the binding intensities in microarrays drop in continuous gradients and are prone to background noise. In addition, the mRNA sequences in SAGE do not need to be already known, leading to discovery of gene variants that are not yet known ([ncbi.nlm.nih.gov/About/primer/microarrays.html](http://ncbi.nlm.nih.gov/About/primer/microarrays.html)).

Although microarray technology is not principally new, it has made significant improvements to the existing dot blot techniques where DNA is immobilised on membranes and usually probed using radioactively labelled DNA



probes. Firstly, microarray technology has enabled global analysis of the genome or transcriptome in one set of conditions so that expression of tens of thousands of different mRNA molecules or different single nucleotide polymorphisms (SNP) can be analysed on a 1-8 cm<sup>2</sup> glass. Thus, DNA microarray has made it feasible for scientists to look at the status of the whole pathways as they are affected by a variety of manipulations (Khan et al., 1999). At the present; however, all genes of the human genomes are not yet known. Therefore, microarray will generate results to which known genes, partially sequenced cDNAs, ESTs, and/or randomly chosen cDNAs from libraries of interest may correspond (Nguyen et al., 2002). The second critical advantage of DNA microarray over dot blot techniques lies in using fluorescence for detection, which has made it simple to use in many laboratories as opposed to traditional radioactivity. Thirdly, working with the rigid solid support (glass) of a microarray is much easier than the membranes used in dot blotting (Dufva, 2005).

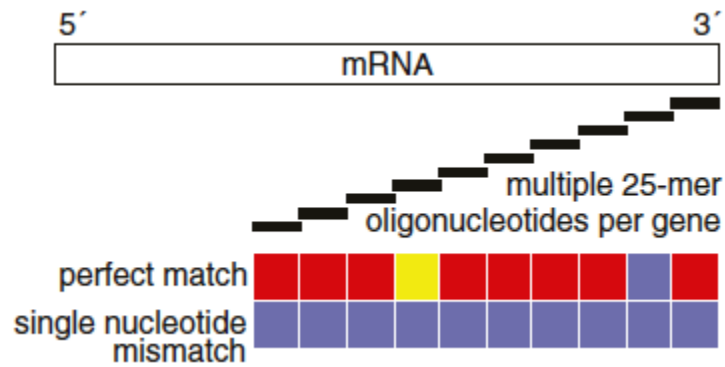
There are different ways to fabricate microarrays, resulting in having to design different numbers of probes and different probe characteristics, such as length, quality, etc (Dufva, 2009). In general, there are two major types of microarray fabrication: spotting pre-made cDNA probes and *in situ* synthesis of DNA arrays. The widely used spotted arrays are processed through a robotically controlled dispensing device that deposits the probes (either cDNAs or 70-80 mer oligonucleotides) onto the surface of microscope slides (Staal et al., 2003). *In situ* arrays, also known as oligo arrays or high-density oligo arrays, are made through synthesizing DNA probes directly on the surface of a chip, made of silicon, glass or polymeric material (Dufva, 2009). High-density oligo arrays are commercially made by Affymetrix, developed in the beginning of the 1990s and considered as the largest microarray manufacturer (Lockart et al., 1996). The reason that Affymetrix arrays are known as high-density oligo arrays lies in synthesizing tens of thousands of genes represented by hundreds of thousands of polynucleotide probes on small arrays in a minimum number of chemical steps (Lipshutz et al., 1998).

### **1.8.2. Design of a high density oligo microarray**

The general design of a high density oligo microarray is portrayed in Figure 1.13 (a,b). In brief, each gene is usually represented by a probe set, containing 11-20

unique (sometimes overlapping) oligonucleotides (each 25 mer), so that each oligonucleotide is a perfect match (PM) to a part of the gene. In addition to these PM oligonucleotides, there are 11-20 other oligonucleotides (each 25 mer) containing a mismatch (MM) at the central base (normally at position 13) of the nucleotide, which serves as a negative control oligonucleotide (Staal et al., 2003; Nguyen et al., 2002). Each PM or MM is synthesized in distinct features (or cells) on the array (also known as GeneChip) so that each two adjacent cells consist of a PM probe and its corresponding MM probe. In fact, such design ensures probe redundancy in high density oligo microarrays. Accordingly, it reduces the chances that fragments of an unrelated mRNA would randomly hybridize to the probe. (Lipshutz et al., 1998). Besides, the use of mismatch negative controls assure the researcher that the hybridization is not likely to occur by chance, because if hybridization would occur by chance (background noise, non-specific hybridization, or semi-specific hybridization), the target RNA molecule could bind to MM and produce a higher signal (Lipshutz et al., 1998).

a



b

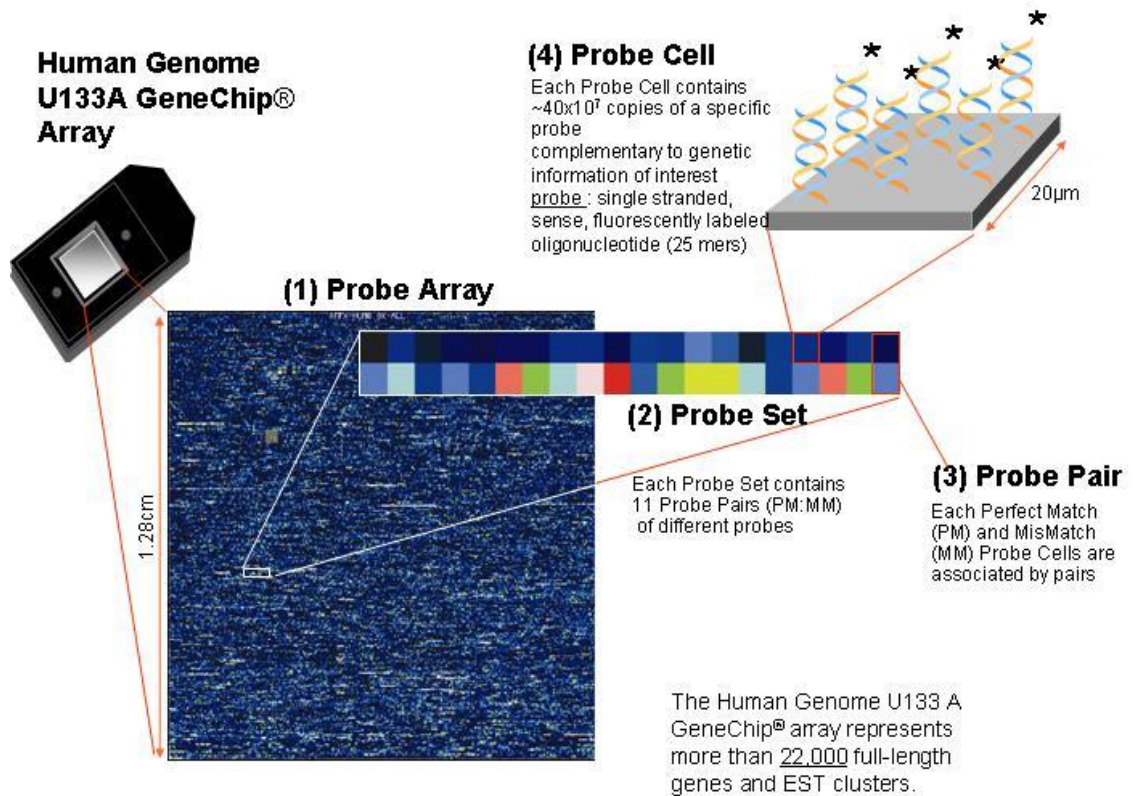


Figure 1.13. Schematic representation of the design of a GeneChip

a: A oligo microarray utilizes several different (and sometimes overlapping) 25-mer oligonucleotides which are perfect match to a specific gene. In addition, the array contains mismatch oligonucleotides that carry a mutation at position 13 of the oligonucleotide and serve as negative controls.

b: an example of a microarray expression chip composed of about 22,000 probe sets on a surface of about 1.2 cm<sup>2</sup>.

Ref. of panel a: Staal et al., (2003).

Ref of panel b: [http://www.weizmann.ac.il/home/ligivol/research\\_interests.html](http://www.weizmann.ac.il/home/ligivol/research_interests.html)

### 1.8.3. The general workflow for processing of a high density oligo microarray

In a high density oligo microarray analysis, a high quality RNA sample is crucial to ensure a successful microarray assay that, in turn, will ensure further clinical implications. The term RNA quality is defined by the composition of RNA purity and RNA integrity (Dumur et al., 2004). Then, one needs to ensure that every different mRNA (transcript) in a sample is amplified to the same degree, otherwise gene expression results will not be conclusive. As such, preparation of RNA samples for microarray requires linear amplification, not exponential.

The first step of microarray processing initiates with the synthesis of double stranded cDNA from RNA samples using reverse transcriptase, a T7 promoter-linked oligo (dT) primer and DNA polymerase. Then, the T7 linker in a cDNA template allows the linear amplification by T7 RNA polymerase which simultaneously incorporates labelled nucleotides in an *in vitro* transcription (IVT) reaction, leading to the generation of single stranded biotin-labelled antisense RNAs, also known as complementary RNAs (cRNAs) (Nguyen et al., 2002). Then, the fragmented, biotinylated cRNAs are added to the array hybridization chamber at 45°C for 18 hours in order to hybridise to the 25-mer oligonucleotides of each gene. At the end, the scanned image is processed using an appropriate software and an expression profile is produced (Staal et al., 2003; also see <http://www.affymetrix.com/support/index.affx>). Figure 1.15 illustrates a schematic experimental workflow for oligo microarray compared to cDNA microarray.

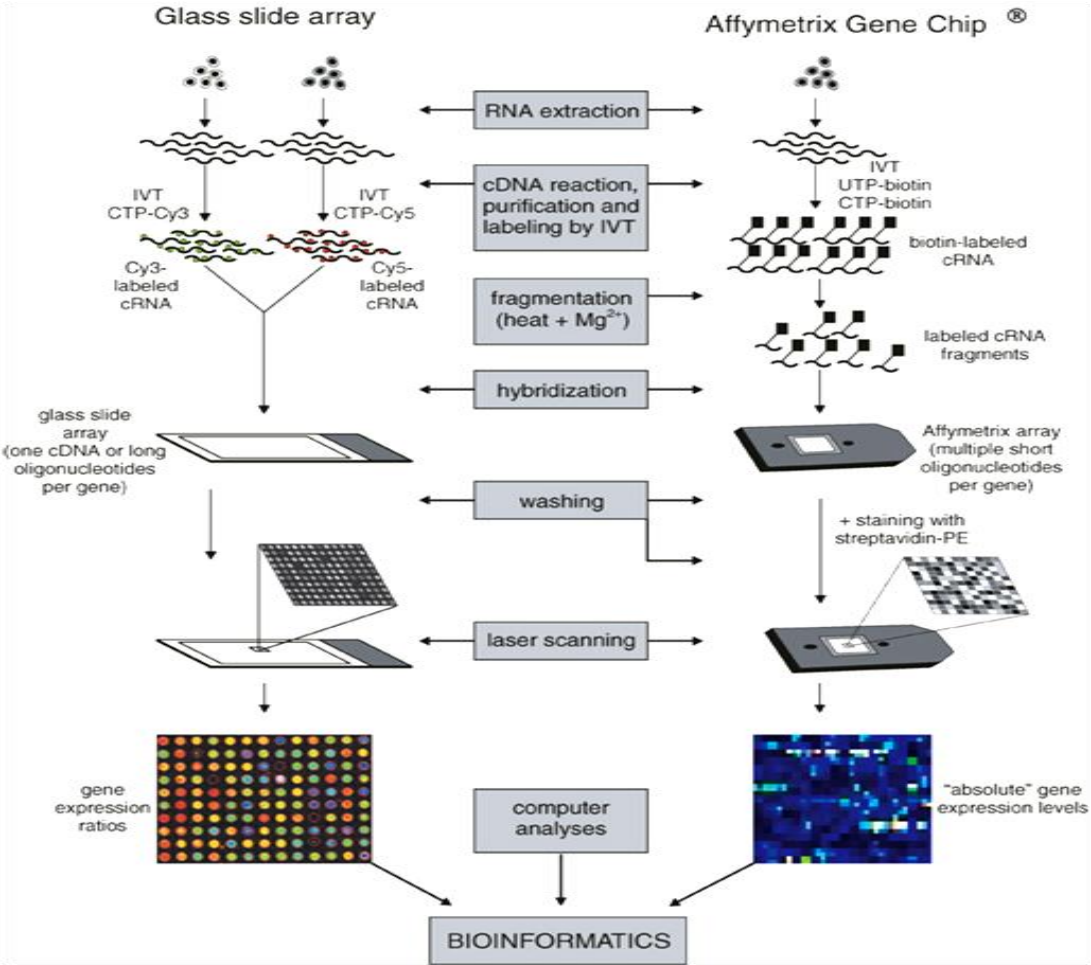


Figure 1.14. Illustration of an oligo microarray procedure compared to cDNA microarray

For cDNA microarray experiments, total RNA is obtained from two cell groups, for example infected and normal, from which cDNAs are generated and used for *in vitro* transcription (IVT) with Cy3 (green) or Cy5 (red) labeled nucleotides. Then, both types of labeled cRNA samples are mixed and hybridized on a glass slide. The next step is involved in generating an intensity image through a scanner with a laser followed by computer analysis of the image.

For an oligo microarray, starting material is one cell group from which RNA and then cDNA are made. The cDNAs are used in an IVT reaction to produce biotinylated cRNA followed by fragmentation. The fragmented cRNAs are hybridized to probes on the chip, washed and stained with PE-conjugated streptavidin. Then, the image intensity is obtained through a laser scanner followed by computer analysis of the image.

Ref.: Staal et al., (2003).

#### 1.8.4. Applications of DNA microarrays in clinical virology

As compared to conventional dot blotting approaches, DNA microarrays have made it feasible for researchers to measure expression of tens of thousands of genes simultaneously, with lower detection limits and improved binding kinetics. Microarray technology has evolved to be a powerful tool in the probing of gene activity and systems response to disease. As such, the impact of DNA microarray can be seen in a wide range of experimental and applied sciences (Campbell and Ghazal, 2004). There are at least three major roles for DNA microarrays in clinical virology, including diagnosis, molecular typing, and basic research (Clewley, 2004). Microarray technology can be used to simultaneously detect and type a range of viruses from a single sample. This is particularly imperative at the early stages of a viral outbreak or attack with an unknown infectious agent (Baxi et al., 2006). There are numerous instances of application of microarray in detection and typing viruses of various virus families.

Studies of microarrays in EV71 pathogenesis appear to be very limited. In order to explore cell tropism of EV71 at molecular level, Wen et al. (2003) used a limited microarray analysis of SK-N-SH cells in addition to immunofluorescent staining and transmission electron microscopy (TEM). The microarray analysis revealed that the neuron growth factor receptor (NGFR) and octamer-binding transcription factor 1 (Oct-1) genes were up regulated, whereas the human protein kinase C inhibitor-1 and epidermal growth factor receptor genes (ERBB-2) were down regulated. Consistent with microarray data, slot blot analysis showed that live EV71 induced over fourfold expression of NGFR gene as compared to heat-inactivated virus infection (Hi). It was then concluded that the receptor encoded by NGFR gene might be involved in cell tropism of EV71 (Wen et al., 2003).

Shih et al. (2004a) exploited a genome-wide cDNA microarray with EV71-infected human glioblastoma cells, SF268. Samples were taken at 13 different time points from two to 54 hours post infection using more than 10,000 human EST/cDNAs matching to known genes in GeneBank database. Overall more genes were up regulated than down regulated. The genes involved in host response to viral infection such as chemokine receptors, apoptosis related genes such as caspase-7 and caspase-3, a P53-responsive gene, and genes related to interferon or complement were up regulated following EV71 infection. Complement-related proteins are



involved in inflammation and play an important role in neuro-degenerative diseases as well as in innate immune response to microbial invasion. Shih et al. (2004a) concluded that complement might play a role in antiviral response against EV71 infection in CNS. It was also found that one of the components of the voltage-dependent calcium channel,  $L\alpha 1$ , was up regulated. This increase in calcium appears to be important in inducing cell death and release of viral progeny. A few genes were also down regulated throughout the period following infection, including genes encoding keratin 6A, cyclin G-associated kinase, transcription splicing, and translation factors.

Unlike previous studies that had shown an increase of IFN- $\gamma$  in the serum and depletion of lymphocytes in EV71-infected patients with pulmonary edema (Wang et al., 2003), no significant increases of IFN- $\alpha$ , - $\beta$ , - $\gamma$  or IFN-induced proteins RPKR, OAS1 were observed in the microarray analysis of EV71-infected cells (Shih et al., 2004a). It was concluded that this contradiction might be due to low sensitivity of the microarray analysis or that elevation of IFN- $\gamma$  does not happen in cells of CNS. The other possibility was postulated that EV71 has removed the host IFN response using a specific viral mechanism (Shih et al., 2004a), like some other viruses that have evolved a variety of mechanisms to inhibit the antiviral response of IFNs, such as HSV (Zimring et al., 1998), Influenza A (Talon et al., 2000) and Adenovirus (Gale and Katze, 1998). The identification and characterization of such mechanisms for EV71 will warrant further studies (Shih et al., 2004).

Further, Tsai et al. (2006) used the Shih et al.'s microarray data to illustrate possible pathways in SF268 cells following infection with EV71. Three pathways were determined: Jak-STAT signalling, cell cycle and apoptosis. They also demonstrated that some genes are associated with neural development and neural apoptosis (Tsai et al, 2006).

### 1.9. Aims of this PhD thesis

The literature review of this thesis showed that several natural and synthetic compounds have been reported to possess antiviral activities against EV71 infection *in vitro* and *in vivo*. However, no treatment for EV71 infection has been approved to date. Therefore, it is important to continue studies towards exploring compounds

with potential antiviral activity against EV71 infection. Besides, despite the recent discoveries of cellular receptors for strains of EV71 and CVA16, further studies are still warranted to investigate alternative cell surface receptors for different strains of these viruses in different cell lines. In this respect, the current literature review showed that no study has been undertaken to investigate the possible role of cellular HS, and the related HS mimetic compounds, in mediating or preventing infection of EV71 and CVA16, as two significant members of HEV-A.

Therefore, the research questions of this thesis were organized into four different experimental chapters. In Chapter 2, the main objective was to develop a colourimetric-based reliable and quantifiable method for EV71 titration. Then, Chapter 3 was designed to investigate potential antiviral activity of Hep, HS, and PPS as three major HS mimetic compounds against EV71 infection in Vero cells. Additionally, this Chapter was intended to determine the mode of anti-EV71 action of these compounds. Following Chapter 3, the project was expanded so that it aimed to generate a general picture of the use of HS as a cellular receptor by members of HEV-A and HEV-B, in addition to ones that have previously been reported in the literature. In line with the findings and conclusions of Chapter 4, Chapter 5 is directed towards gaining insight into the cellular and molecular mechanisms of action of Hep against clinical EV71 infection in neural cells, using a genome-wide microarray analysis. At the end, a final conclusion was drawn based on the results and observations of the four experimental chapters.

## 2. Chapter Two: Improvements in the Enterovirus 71 Titration

### 2.1. Introduction

Titration of viruses is a crucial step in any virological study, particularly where exact amounts of a virus need to be applied in experimental procedures such as testing efficacy of a potential antiviral drug (LaBarre and Lowy, 2001). There are a number of approaches to quantify a virus titre; however, the most common ones include finding the 50% endpoint where 50% of virus-infected subjects (cells or animals) die/survive (Reed and Muench, 1938), and directly counting plaques caused by viruses in infected cells (Dulbecco and Vogt, 1954). Other approaches may utilize polymerase chain reaction (PCR) (Baylis et al., 2004; Hunag et al., 2004), or reverse transcriptase (RT)-PCR (Prihod'ko et al., 2005). The use of each method may be justified by defined circumstances and aims, under the limitation of the virus and the cell type. For instance, while some viruses can produce cytopathic effect (CPE), which is an important indicator in determining the endpoint 50%, they might not easily form plaques; therefore a plaque assay would not be a suitable means of titrating such viruses (Heldt et al., 2006). In addition, PCR-based methods measure the total number of virus particles; however, the result might not directly represent the number of infectious particles present within a given sample (Heldt et al., 2006).

Historically, for titration of viruses or sera, an endpoint dilution in which a certain quantity of test animals reacted or died had been used. More accurately, Gaddum (1933) set the definition of a dilution by which half of the test animals are affected (Reed and Muench, 1938). In this respect, a large number of animals were treated with dilutions near the 50% point of reaction. This was, however, practically difficult when dealing with sensitive experiments such as immunological tests where the titre differences between samples can be very little. Therefore, Reed and Muench (1938) formulated a method to estimate the 50% endpoint. They used a murine model to measure the effect of titration of a protective serum at different  $\log_2$  dilutions. Surviving or dying mice treated with the protective serum were then counted cumulatively. This cumulative measurement was based on the assumption

that if a mouse has survived at a given dilution of the serum, it would have surely survived at a lower one. As such, numbers of surviving mice were added together in the direction in which dilution of the serum decreased. By contrast, a mouse dead at a given dilution of the serum would have died at any higher one. Thus, the dying mice were cumulatively counted in the direction in which dilution of the serum increased. The percentage of mortality at each dilution was calculated from the cumulative dead mice divided by the total number of “cumulative dead plus cumulative alive” mice at that dilution. This hypothesis was very important, as it became later the basis of the well-known 50% tissue culture infectious dose (TCID<sub>50</sub>) method for virus titration.

The algorithm used by Reed and Muench (1938) later became a reference for the TCID<sub>50</sub> method at which the calculated 50% endpoint is defined as a virus dilution at which 50% of the virus-infected cells die/survive. Despite the fact that many researchers attribute the TCID<sub>50</sub> calculations to Reed and Muench (1938), it appears there are conceptual and mathematical differences between the original work of Reed and Muench and typical current TCID<sub>50</sub> methods, which need to be taken into consideration. One important point is that Reed and Muench used a protective serum at log<sub>2</sub> dilutions in an animal model so that as the serum dilution increased, the mortality percentage increased too. On the contrary, TCID<sub>50</sub> is an *in vitro* method that determines the 50% endpoint of a virus at log<sub>10</sub> so that as the virus dilution increases, the dead cell percentage decreases. This difference causes further differences in the concepts and calculations of terms such as the proportionate distance (PD) the 50% endpoint, so that they represent the conditions of TCID<sub>50</sub> rather than the original Reed and Muench algorithm. The other significant point is that results of a classic TCID<sub>50</sub> assay are usually generated by microscopic observations of CPE, requiring an experienced eye, which is open to subjective errors. One significant subjective error arising from the classic method of TCID<sub>50</sub> is the possibility of misidentification of CPE within replications of a virus dilution and/or between different virus dilutions.

In addition, this method simply considers CPE a qualitative character of a well that is a unit of study in a microtiter plate. In reality, each well itself is composed of many seeded cells, requiring CPE to be considered a quantifiable character of virus-caused cell death. Therefore, the conventional TCID<sub>50</sub> method is

unable to measure viral CPE as a quantitative phenomenon contributed to cells or express it in relation to the different dilutions of the tested virus (LaBarre and Lowy, 2001). Furthermore, there are certain cells and viruses that do not show clear CPE, resulting in limited usefulness of conventional observation-based TCID<sub>50</sub> methods.

In order to improve reliability and reproducibility of the traditional TCID<sub>50</sub> method, a number of solutions have been suggested, including the use of colorimetric methods that can generate continuous data as well as eliminate the need for observation of CPE, resulting in reduced subjective errors. Among other examples, the reagent MTT [3-(4, 5-Dimethylthiazol-2-yl)-2, 5-diphenyltetrazolium bromide, a yellow tetrazole] has commonly been used for virus titration (Rubino and Nicholas 1992; Watanabe et al., 1994; Levi et al., 1995; and Anderson et al., 2005). As such, an MTT<sub>50</sub> term has been suggested as opposed to a TCID<sub>50</sub> value (Anderson et al., 2005; Heldt et al., 2006). The basis of MTT staining is that mitochondria of the living and healthy cells bio-reduce the tetrazolium salt of the MTT dye, producing colorful formazane crystals that can be dissolved in an appropriate solvent. The intensity of this color change is then correlated to the viable cell percentage (Cory et al., 1991; Barltrop et al., 1991; Riss and Moravec, 1993). Another such compound with a similar action is MTS [3-(4,5-dimethylthiazol-2-yl)-5-(3-carboxymethoxyphenyl)-2-(4-sulphophenyl)-2H-tetrazolium, inner salt; MTS(a)]. Although recently a number of studies have reported the use of MTS in antiviral experiments (Li et al., 2005; Selvam et al., 2008; Muhamad et al., 2010), its use for the estimation of virus titres appears to be limited (Distefano et al., 1995).

A number of viruses belonging to the *Picornaviridae* family have been titrated using an MTT-based colorimetric method (Anderson et al., 2005); however, there has been no study undertaken to evaluate colorimetric titration of EV71 or compare colorimetric-based and conventional methods of virus titration in EV71. As such, the aim of this study was to establish a rapid, quantifiable and accurate method of EV71 titration, using colorimetric methods and comparing the results obtained to those of the traditional TCID<sub>50</sub> assay. In this study, two strains of EV71 were titrated using the following approaches: the conventional method of TCID<sub>50</sub>, the conventional method of TCID<sub>50</sub> with modifications, the MTS and the MTT approaches. In addition, the relationship of the conditional and improved TCID<sub>50</sub> methods with viral plaque forming was investigated.

### 2.2. Materials and Methods

#### 2.2.1. Cell and virus

Two EV71 strains were used for this study: a cloned isolate of EV71 strain 6F/AUS/6/99 (GenBank Accession no DQ381846) kindly provided by Prof. Peter C. McMinn (Central Clinical School, University of Sydney, Australia), and a low passage clinical isolate of EV71 (Isolate number 99018233) supplied by Dr. Julian Druce of the Victorian Infectious Disease Reference Laboratories (VIDRL, Parkville VIC). African Green Monkey Kidney (Vero) cells (supplied by Prof. Peter C. McMinn) were maintained in Dulbecco's Modified Eagle's Medium with high glucose (DMEM, Invitrogen, Mulgrave, VIC, Australia) supplemented with 10% heat inactivated Fetal Bovine Serum (FBS, Invitrogen, Mulgrave, VIC, Australia). Passaging of the viruses was performed as follows: The 80% confluent Vero cells grown in 10 mL serum-free growth media were inoculated with 100-200  $\mu$ L of the initial stock virus. After 5 days, the supernatant was taken and subjected to centrifugation at 4000 rpm for 10 min. One mL of the supernatant was then mixed with 9 mL of the serum-free growth media to infect fresh 80% confluent Vero cells. This cycle was repeated until getting maximal CPE within 2-3 days. The last viral supernatant was then diluted with the serum-free growth media at the ratio of 1:100 up to 3 mL, which was further poured out into 7 mL of the serum-free growth media for the final CPE check within 2-3 days. Aliquots of the last viral suspensions were then stored at  $-80^{\circ}\text{C}$  until required. Cells were also stored cryogenically frozen in liquid nitrogen.

#### 2.2.2. Cell seeding and infection of cell cultures

Vero cells were seeded at  $3 \times 10^4$  cells (150  $\mu$ L/well) in 96-well plates or at  $3.6 \times 10^5$  cells (3 mL/well) in 6-well plates (Becton Dickinson, BD, North Ryde, NSW, Australia) followed by incubation at  $37^{\circ}\text{C}$  in a humidified atmosphere containing 5%  $\text{CO}_2$  until 80% confluency was reached. Before viral inoculation, or when quantifying the results, cell monolayers were thoroughly washed with phosphate buffered-saline (PBS, pH 7.4 at room temperature) three times. In all the experiments, the following controls were included: cell control (cells that were not infected with the virus) and undiluted virus control (cells that were infected with the

undiluted stock virus). The virus dilutions were made in DMEM+5% FBS and added to cells in a total volume of 50  $\mu$ L/well mixed with 100  $\mu$ L of the growth media (DMEM+5% FBS). Where stated, incubation was done at 37°C in a humidified atmosphere containing 5% CO<sub>2</sub>

### **2.2.3. Conventional TCID<sub>50</sub> titration assay**

The conventional endpoint titration assay has been reported previously (Reed and Muench, 1938). Briefly, the virus was diluted 1:10 from which a further eight log<sub>10</sub> dilutions were made and added to cells in six replicates. The plates were then incubated for 72 hours. After incubation, the wells were observed using an inverted microscope (Olympus Imaging Corp, China) and marked positive CPE, if cells had developed observable CPE in 30% or more of the surface of the well, as compared to both the undiluted virus control and cell control. Cells that did not show such conditions were marked negative CPE. Further calculations were conducted using the Reed-Muench formula (Reed and Muench, 1938). In brief, a proportionate distance (PD) was calculated and then added to the log of the dilution factor at which the infection (dead cell percentage) was just over 50%. The resulting value was considered as the TCID<sub>50</sub> log<sub>10</sub>. In addition to the Reed-Muench formula, the dead cell percentages were plotted against the virus dilutions on a log<sub>10</sub> scale. Then, the TCID<sub>50</sub> value was calculated using a regression analysis of the curve.

### **2.2.4. Modified traditional TCID<sub>50</sub> titration assay**

The method explained in 2.2.3 was modified as follows: Initially, a 1:10 dilution of the virus stock was prepared and a further thirteen dilutions were made based on log<sub>2</sub> and added to cells in six replicates. Following incubation for 72 hours, microscopic observations were performed as stated in 2.2.3 and the 50% endpoint was calculated using a regression analysis of the curve.

### **2.2.5. The MTS-based endpoint dilution assay**

Initially, a 1:10 dilution of the virus stock was prepared followed by a further eight log<sub>2</sub> dilutions, added to the cells in three replicates. Plates were incubated for 72 hours at which microscopic observations and virus quantification were performed. In order to quantify virus titration, the cell supernatant was aspirated and the monolayer was washed with PBS three times. Twenty microlitres of MTS

reagent (Promega, VIC, Australia) was mixed with 150  $\mu$ L of serum-free DMEM and was added to each well. After 90 minutes of incubation at 37°C with 5% CO<sub>2</sub>, the color change was measured using a Microplate Reader (BioRad, Japan) at 490 nm. The average absorbance of the cell control was considered as 100 % to which cell death percentages of each virus dilution were calculated (Schmidtke et al., 2001). The results were then graphed by plotting dead cell percentages against the virus dilutions. The 50% infectivity point was calculated through a linear regression analysis of the curve.

### 2.2.6. The MTT-based endpoint dilution assay

The method described in 2.2.5 was used; 1:10 and a further thirteen dilutions were prepared, however, instead of MTS, 20  $\mu$ l of MTT solution (Invitrogen, Mulgrave, VIC, Australia) (0.5% w/v in PBS) was dissolved in 150  $\mu$ L of serum-free DMEM and the mix was then added to each well (triplicate). The plates were then incubated for three hours after which the formazane was dissolved with DMSO (50  $\mu$ L/well) followed by another 8-minute incubation. Colour change was then recorded using the Microplate Reader at 540 nm from which the background absorption at 670 nm was subtracted. Results were analysed in the manner described in 2.2.5.

### 2.2.7. Virus titration via plaquing assay

The EV71 isolates were titrated through the typical plaquing assay (Dulbecco and Vogt, 1954, Shih et al., 2004b, Lin et al., 2002). Briefly, the virus dilutions were made based on the prediction of the number of plaque forming units (PFU), using a conversion formula:  $\text{PFU (mL)}/\text{TCID}_{50} \text{ (mL)} = 0.7$  (Davis et al., 1972). Briefly, Vero cells were seeded in 6-well plates at  $3.6 \times 10^5$  cells/well in 3 mL of the growth media and incubated until 80% cell confluency was reached. Cells were then washed three times with PBS followed by infection with 1 mL/well of various virus dilutions (Appendix 1) in DMEM+5% FBS and incubation at 37°C for one hour. This was followed by aspirating the viral inocula and washing cells three times with PBS. Three millilitres of overlay media containing the growth media mixed with 3% agarose gel (Ultrapure™ Agarose, Mulgrave, VIC, Australia, Invitrogen) at 1:4 (agarose gel: medium) ratio was then added to each well. The plates were incubated until the virus plaques were formed; they were then fixed by 10% formaldehyde for



1.5 hours and the agarose plugs were removed. The monolayer was stained with 1 mL/well of the staining solution (0.4% crystal violet, 1.67% ethanol in water) and incubated for eight minutes. The wells were then gently rinsed with water and air dried. The viral plaques were then counted and virus titre was measured in PFU/mL and multiplicity of infection (MOI), according to the following formula:

$$\text{PFU/mL} = \frac{\text{Average\# Plaques}}{V} \times D$$

Where D = dilution factor; V = volume of inoculum (per mL)

$$\text{MOI} = \frac{\text{PFU/mL} \times V}{N}$$

Where V = volume of viral inoculum (per mL); N = number of the cells seeded in the well

### 2.2.8. Statistical analysis

All the treatments were applied in triplicate, and each experiment was independently repeated two or three times. The curves were drawn using GraphPad Prism 5, while statistical analyses were performed using the unpaired independent two-sample *t*-Test (assuming equal variance).

## 2.3. Results

### 2.3.1. Traditional TCID<sub>50</sub>

The cloned EV71 strain was titrated based on the traditional TCID<sub>50</sub> method where visible cell shrinkage and rounding were considered signs of CPE by which further calculations were conducted (Appendix 2). A traditional algorithm of titration estimated the TCID<sub>50</sub> to be  $5.8 \times 10^6$  per mL (Table 2.1), whereas linear regression analysis of the curve (Figure. 2.1) generated a 50% endpoint value of  $5.3 \times 10^6$  per mL (Table 2.1). The results of both approaches were found not to be statistically different ( $p > 0.05$ ).

### 2.3.2. Modified traditional TCID<sub>50</sub>

In order to assess the impact of dilution factor on the accuracy of a conventional TCID<sub>50</sub>, a lower magnitude dilution factor (based on log<sub>2</sub> instead of log<sub>10</sub>) was used to carry out serial virus dilutions. The quantification of CPE was then done as described for the traditional TCID<sub>50</sub>, while the 50% endpoint was measured only using the regression analysis of the curve (Figures 2.2 and 2.3). The 50% endpoint value  $5.5 \times 10^4$  for the cloned EV71 showed a statistically significant difference ( $p < 0.01$ ) from that of traditional TCID<sub>50</sub> (Table 2.1). The modified traditional TCID<sub>50</sub> was then tested with clinical EV71. The calculated value of  $4.8 \times 10^4$  showed no statistical difference ( $p > 0.05$ ) from that of cloned EV71 (Table 2.1).

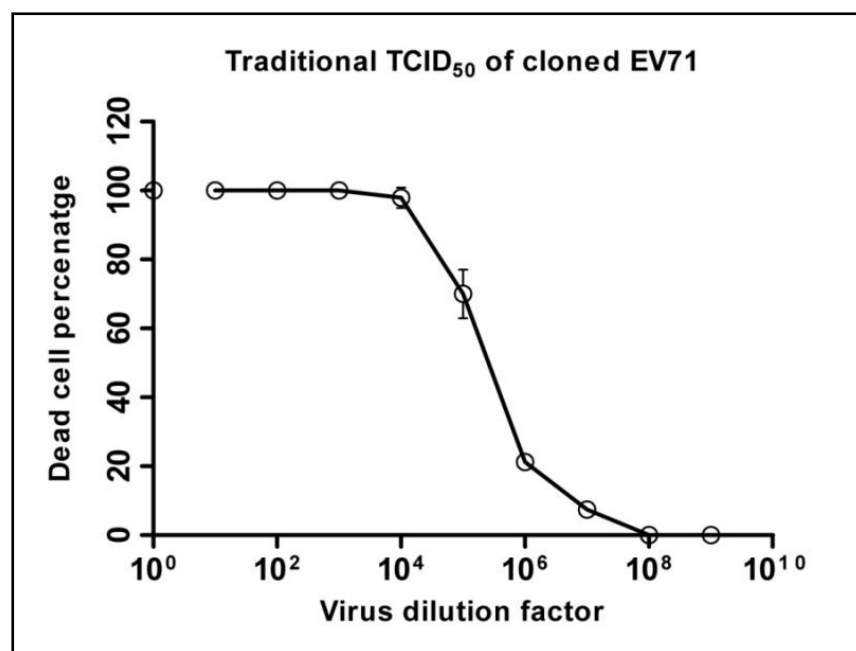


Figure 2.1. Depiction of the titre of the cloned EV71 virus using the conventional method of TCID<sub>50</sub>

## Chapter Two- Improvements in the Enterovirus 71 Titration

---

The dead cell percentages are plotted against virus dilutions on a  $\log_{10}$  scale. The dilution factor  $10^0$  represents undiluted virus control that was assumed to display 100% cell death. The values are means of three independent experiments from which standard deviations were calculated.

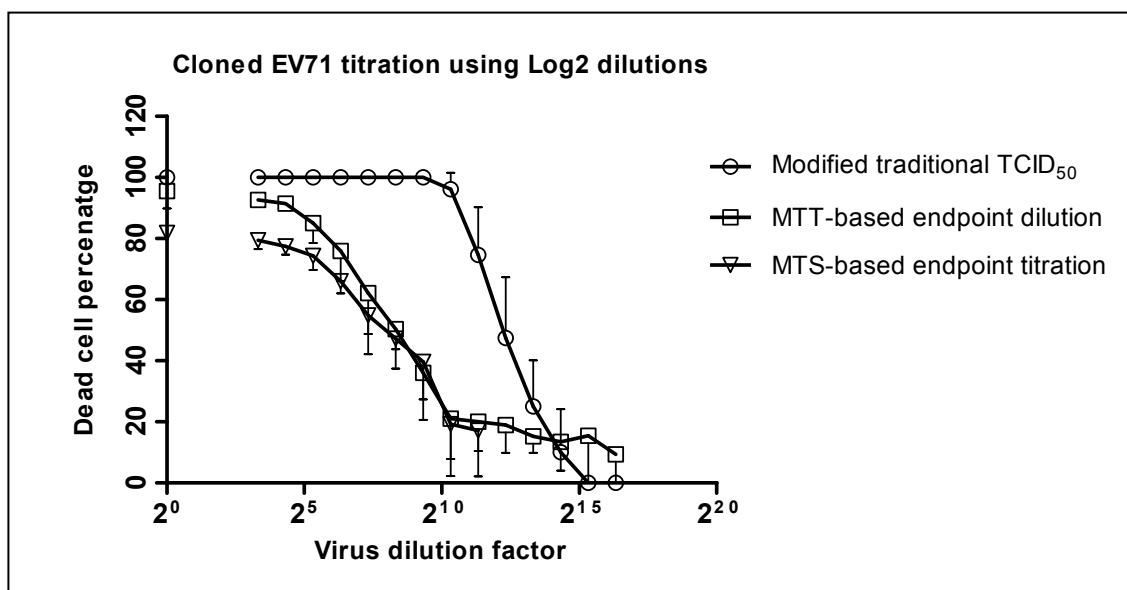
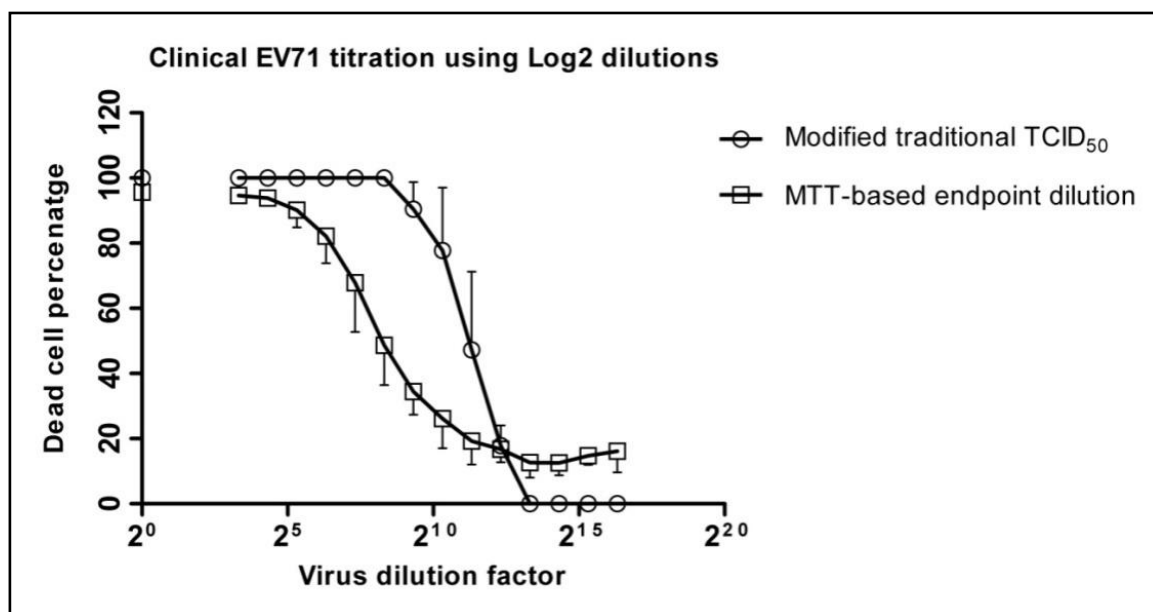


Figure 2.2. Depiction of the titre of the cloned EV71 virus using three methods based on log<sub>2</sub> dilution

The dead cell percentages are plotted against virus dilutions on a log<sub>2</sub> scale. The dilution factor 2<sup>0</sup> represents undiluted virus control, which was assumed to display 100% cell death in the modified traditional TCID<sub>50</sub> but was quantifiably calculated using MTT or MTS in the other methods. The values represent mean ± SD generated from three independent experiments.



**Figure 2.3. Depiction of the titre of the clinical EV71 virus using two methods based on log 2 dilution**

The dead cell percentages are plotted against virus dilutions on a log<sub>2</sub> scale. The dilution factor 2<sup>0</sup> represents undiluted virus control, which was assumed to display 100% cell death but was quantifiably calculated using MTT in the other method. The values are means of three independent experiments from which standard deviations were calculated.

### 2.3.3. The colorimetric-based virus titration

#### i. Analyzing microscopic observations

MTS and MTT reagents were used to generate continuous data of the virus titration. Before applying the MTS or MTT reagents, microscopic observations were performed both before removing supernatant (Figure 2.4a) and after removing supernatant followed by washing the monolayer with PBS (Figure 2.4b) to determine the amount of CPE in each well. For the observations prior to removing supernatant, indications of CPE such as cell rounding, shrinking or floating were seen in all the wells in a virus dilution-dependent manner. Cell controls appeared healthy, whereas the undiluted virus controls showed maximal CPE with few or no adhered cells. The microscopic analysis after removing the supernatant clearly showed the monolayer damage due to viral infection. Both sets of images (before/after removing the supernatant) indicated that the degree of CPE or monolayer damage that was associated with virus concentration. However, determination of the monolayer damage and associating it with virus dilution was obviously more practicable in the wells following removal of supernatant and washing with PBS (Figure 2.4 a,b). Therefore, we chose to remove supernatant and wash cells with PBS before adding either MTT or MTT into wells.

#### ii. Determination of the 50% endpoint

##### MTS-based titration

The colour change caused by the addition of MTS was proportional to the number of healthy living cells. It was assumed that the cell control maintained a viable cell percentage of 100%; this allowed a comparative calculation of the percentage of live cells in all other samples to be made. Using the quantifiable data generated by the MTS-TCID<sub>50</sub> assay, a graph was constructed by plotting the percentage of dead cells against the various virus dilutions (Figure 2.2). As expected, the undiluted virus controls showed the highest dead cell percentage (but not 100%); while the percentage was seen to decrease as the virus became more diluted up to dilution factor  $10 \times 2^7$ . These findings were also supported by microscopic observations. The MTS-generated results demonstrated a statistically significant difference ( $p < 0.01$ ) compared to those from both the conventional TCID<sub>50</sub> titration and the modified traditional TCID<sub>50</sub> assays (Table 2.1).

### MTT-based titration

Similar to MTS, the colour change caused by the addition of MTT was proportional to the number of healthy living cells. A graph was constructed by plotting the various virus dilutions against the percentage of dead cell (Figures 2.2 and 2.3). Using the regression analysis, the 50% infectivity point was calculated. These findings were compatible with the observations from microscopic observations (Figure 2.4). There was no significant difference ( $p>0.05$ ) between the TCID<sub>50</sub> values measured by either colourimetric method when investigating the cloned EV71 virus. Therefore, in all future tests only MTT was used to titrate the clinical EV71, as it was more cost effective and less time consuming when compared to MTS. Using the MTT method, the TCID<sub>50</sub> values calculated for the clinical isolate of EV71 were not significantly different ( $p>0.05$ ) from the cloned EV71 virus (Table 2.1).

### 2.3.4. Titration via plaquing assay

The EV71 plaques were extremely small yet detectable at day 2 post infection; in this test, all plaques were counted at day 3 post infection. Plaque formation was noted at an earlier time-point when cells were infected with the cloned EV71 compared to the clinical EV71 infection, but there was no obvious difference between the size and the shape of the plaques noted (Figure 2.5). In addition, there was no statistically significant difference ( $p>0.05$ ) between the total numbers of plaques counted when cells were infected with 100 TCID<sub>50</sub> of either virus strain (Table 2.2).

A conventional method was used to predict the plaque numbers using the known TCID<sub>50</sub> PFU/TCID<sub>50</sub> = 0.7, based on the MTT-TCID<sub>50</sub> results (Davis et al., 1972). The results showed that this conversion formula was not true for either the cloned or clinical EV71 virus strains, where the ratio of PFU/TCID<sub>50</sub> was found to be 0.04 for clinical EV71 and 0.07 for cloned EV71. In addition, these results revealed that there was an obvious difference in the predicted number of plaques between the MTT-TCID<sub>50</sub> assay and the traditional TCID<sub>50</sub> assay, with the MTS assay being more accurate (Table 2.2). The multiplicity of infection (MOI) values for both clinical and cloned EV71 were also calculated (Table 2.2) based on PFU

values and the conditions of each experiment (Table 2.2). There appeared to be no significant difference in the value calculated for either virus strain ( $p>0.05$ ).



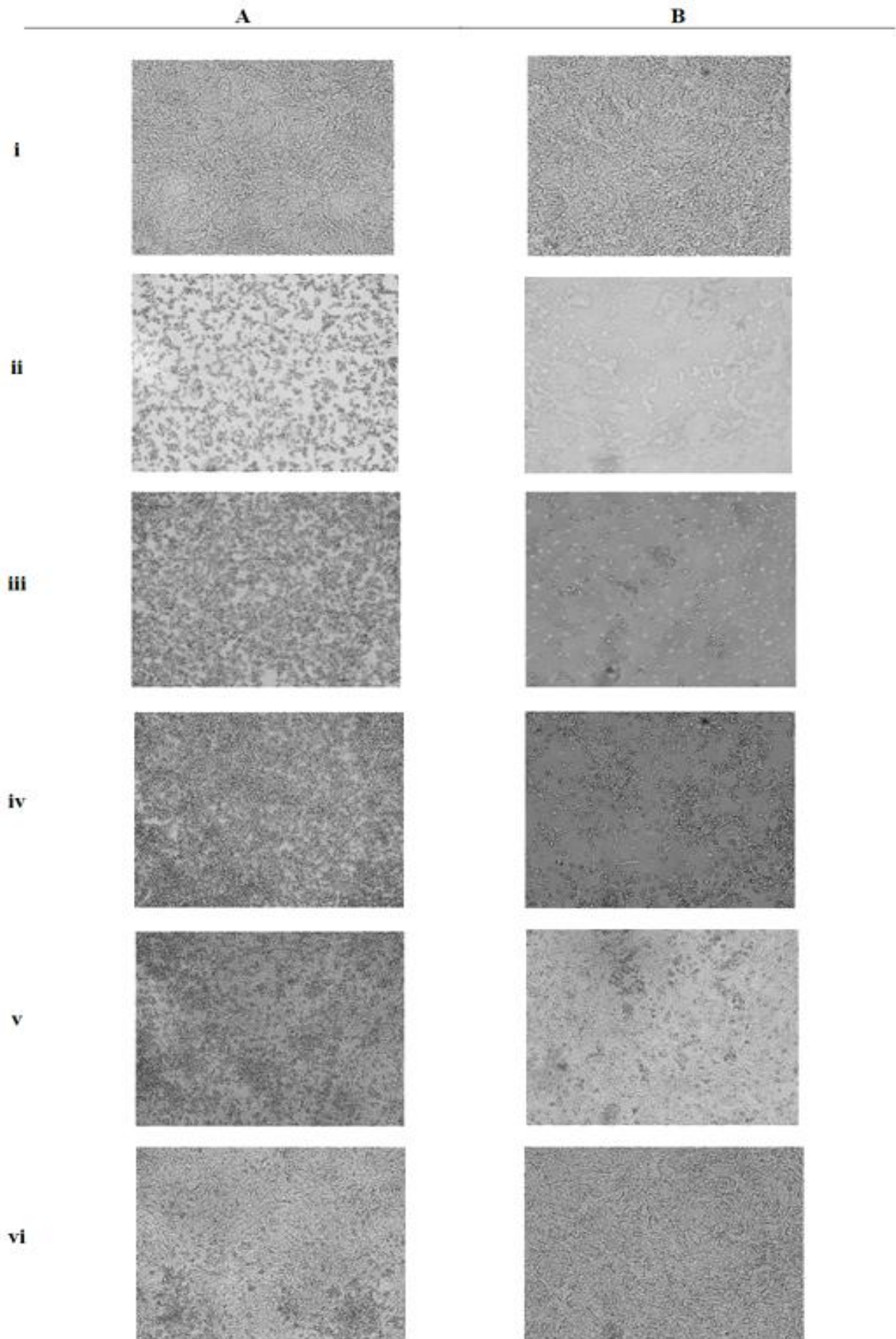


Figure 2.4. Micrographs of cell monolayer damages following EV71 infection

The photos in series A, show the wells before removing supernatant, while the photos in series B show the same wells after removing supernatant and washing with PBS. i: cell control; ii: undiluted virus control (1:1); iii: viral dilution 1:10<sup>1</sup>; iv: viral dilution 1:10 ×2<sup>3</sup>; v: viral dilution 1: 10 ×2<sup>7</sup>; vi: viral dilution 1: 10 ×2<sup>9</sup>. The photos are taken 72 hours post infection using inverted microscope (100 x magnifications, Olympus, CKX 41, Japan).

**Table 2.1. Comparison of TCID<sub>50</sub>/mL amounts resulted from different titration assays**

Virus	Method of titration				
	Traditional**		Modified traditional**	MTS**	MTT**
	Reed and Muench's formula	Regression analysis			
Cloned EV71	$5.8 \times 10^6 \pm 2,150,000$	$5.3 \times 10^6 \pm 970,000$	$5.5 \times 10^4 \pm 21000$	$6.5 \times 10^3 \pm 3400$	$8.1 \times 10^3 \pm 3700$
Clinically isolated EV71	-		$4.8 \times 10^4 \pm 14000$	-	$8.7 \times 10^3 \pm 3200$

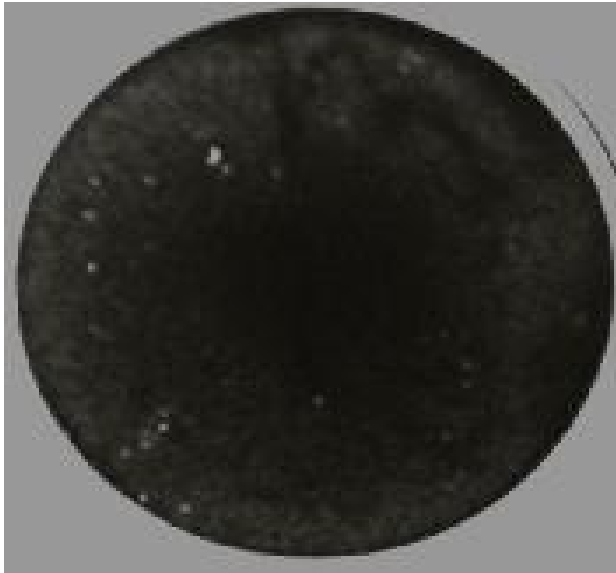
The values are expressed as mean  $\pm$  SD. The means are taken from three independent experiments from which standard deviations (SD) were calculated.

\*\*shows significant differences with a *p* level less than 0.01 between MTT or MTS-based TCID<sub>50</sub> and the traditional methods of TCID<sub>50</sub>. In addition, the modified traditional method significantly (*p*<0.01) differed from the traditional methods.

**Table 2.2. Comparison of TCID<sub>50</sub>, PFU and MOI amounts in the clinical and cloned strains of EV71**

Virus <sup>a</sup>	100 TCID <sub>50</sub> (per mL)	PFU (per mL)		MOI in the plaquing assay		MOI in the TCID <sub>50</sub> assay	
		Actual <sup>d</sup>	Predicted <sup>d</sup>	Actual <sup>d</sup>	Predicted <sup>d</sup>	Actual <sup>d</sup>	Predicted <sup>d</sup>
Cloned EV71	4.5×10 <sup>1</sup> <sup>b</sup> (5.5 × 10 <sup>2</sup> ) <sup>c</sup>	33,180 ± 4,728	315,000 (3,850,000) <sup>e</sup>	0.09 ± 0.01	0.9 (10.7) <sup>e</sup>	0.04 ± 0.01	0.4 (5.1) <sup>e</sup>
Clinically isolated EV71	8×10 <sup>1</sup> <sup>b</sup> (4.8 × 10 <sup>2</sup> ) <sup>c</sup>	30,856 ± 13,546	560,000 (3,360,000) <sup>e</sup>	0.09 ± 0.03	1.5 (9.3) <sup>e</sup>	0.04 ± 0.02	0.7 (4.4) <sup>e</sup>

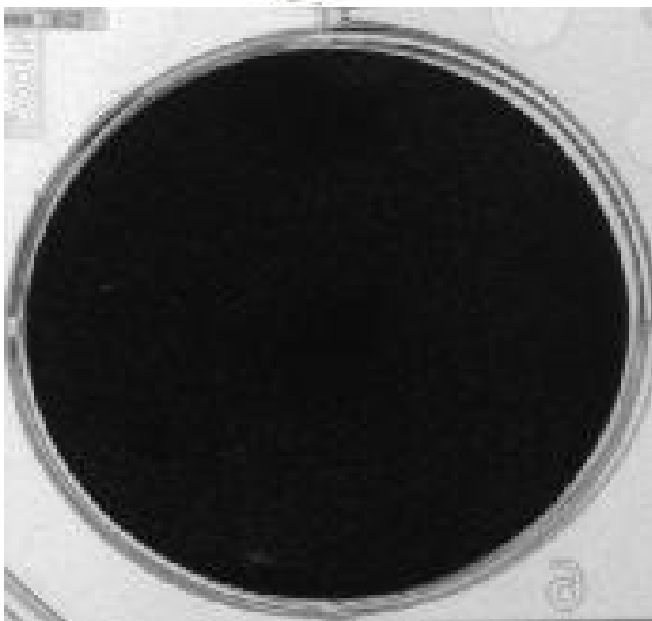
- a. There was no statistically significant difference in the results of PFU or MOI between the cloned EV71 and clinical EV71.
- b. The MTT-based virus titration was used to measure 100TCID<sub>50</sub> on samples of cloned EV71 and clinically isolated EV71. These virus suspensions were used in the plaquing assays mentioned in this table.
- c. Figures indicated in the brackets are the results of the modified traditional TCID<sub>50</sub>
- d. The actual values of PFU were generated from the actual results of plaquing assays (mean ± SD), while the predicted PFUs were calculated using the conversion factor 0.7. The actual and predicted values of MOI were calculated based on the actual and predicted values of PFUs, respectively.
- e. Figures indicated in the brackets are predicted PFUs or MOIs based on the modified traditional TCID<sub>50</sub>.



**Cloned virus isolate**



**Clinical virus isolate**



**Negative control**

**Figure 2.5. The plaque formation of both cloned and clinical EV71**

## Chapter Two- Improvements in the Enterovirus 71 Titration

---

The plaques were visualized with crystal violet 3 days post infection in Vero cells. The expected plaques were calculated based on the equation of  $\text{PFU/TCID}_{50} (\text{mL}) = 0.7$ , while the actual number of plaques was counted using the image taken by gel document device (BioRad). The negative control represents cells that were not infected with virus.

### 2.4. Discussion

In this study, an accurate colourimetric-based method was developed to quantify the titration of EV71 strains. There was a statistically significant difference ( $p < 0.01$ ) between the TCID<sub>50</sub> amounts calculated by the traditional method and that of the MTT or MTS methods. In addition, the described MTS or MTT-TCID<sub>50</sub> assay took only five days to reach completion. This allows for a more rapid analysis of large numbers of samples, as opposed to some of the previously described MTT methods, which took 7 days (Heldt et al., 2006) or 8-10 days (DiStefano et al., 1995) from seeding the plates to completion. There was no significant difference ( $p > 0.05$ ) in cloned EV71 titration between MTS and MTT methods or between the two strains of EV71 where titrated with MTT ( $p > 0.05$ ). This being said, MTS dye has the advantage in that the formazane does not require solubilization, making the analysis procedure quicker that may, in turn, reduce well-to-well and assay-to-assay variability. However, MTT is advantageous in that it is more cost effective product and more commonly used. Moreover, no significant difference was noticed in variability between MTS and MTT in cloned EV71 virus data and.

The improved methods of TCID<sub>50</sub> reported here also have the advantage of being more sensitive, compared to the conventional method of TCID<sub>50</sub>. Most of the conventional, and even some colourimetric-based viral titration assays utilize log<sub>10</sub>-based dilutions of virus. One pitfall can be that if the 50% endpoint of the virus occurs somewhere between two log<sub>10</sub> dilutions and not exactly at a dilution, the estimated 50% point on the curve trendline would be different from the actual value. This was well noted when comparing the conventional TCID<sub>50</sub> and modified conventional TCID<sub>50</sub>, which were different from each other only in virus dilutions used. While the TCID<sub>50</sub> values calculated using the conventional method was placed between virus dilution factors 10<sup>5</sup>-10<sup>6</sup>, this point was somewhere between 10×2<sup>8</sup>-10×2<sup>9</sup> using the log<sub>2</sub>-based traditional method. Thus, use of log<sub>2</sub> dilutions can increase sensitivity of the virus titration by generating more analyzable data. It also narrows the range of virus dilutions that surround the 50% endpoint that, in turn, would increase accuracy of calculation of the 50% endpoint. It is of note to point out that this increased sensitivity was not due to use of a regression analysis instead of

the usual method of Reed and Muench, as there was no significant difference ( $p>0.05$ ) between these two methods, which is in agreement with the results of Reed and Muench (1938). Therefore, it can be concluded that the accuracy of a virus titration assay could be significantly increased with lower magnitude dilution factors.

Another point with the traditional assay of TCID<sub>50</sub> is the use of six replicates at each virus dilution. This would not necessarily increase accuracy of the assay; instead, it might even generate additional undefined errors. The reason lies in the fact that the conventional TCID<sub>50</sub> relies on microscopic observations; and thus, the total subjective error due to wrong CPE scoring can increase as the number of individual wells increases per sample. The other problem is that virus dilution is based on log<sub>10</sub> in the conventional TCID<sub>50</sub>. This means that a very small portion of the virus suspension is taken from each dilution to make the following log<sub>10</sub> dilutions. Therefore, there might be a chance to decrease the precision of the assay so that differences in CPE intensity might not precisely correspond to different virus dilutions. In contrast, this is not the case with the MTT or MTS methods where the virus is diluted using a log<sub>2</sub> basis.

Previously, it was reported that the use of MTS in viral assays led to more variability in the results (DiStefano et al., 1995). This might be due to some cells being in the early stages of infection, where they are damaged and detached but not yet dead, which would lead to false positive results and a low specificity of MTS. In the current study, this was resolved by the aspiration of supernatant and thorough washing of the monolayer with PBS before addition of MTS reagent, as any unbound cells were removed, therefore eliminating this potential error. Thus, in the results presented here, MTS showed high specificity and produced results that were more consistent.

In this study, the relationship between PFU and TCID<sub>50</sub> was found to be different from the one commonly used by researchers (PFU/TCID<sub>50</sub> = 0.7), and this was different between two strains of EV71 as well. This would possibly suggest that there is no accurate, fixed conversion factor to estimate PFU based on a TCID<sub>50</sub> value of a virus sample. However, the plaquing assay demonstrated that the results of PFU or MOI were more compatible with the MTT/MTS-generated TCID<sub>50</sub> than the traditional methods. Therefore, the plaquing assay results supported the conclusion that MTT or MTS-based TCID<sub>50</sub> is more accurate and reliable compared



to traditional methods of TCID<sub>50</sub>. In order to titrate EV71 virus, one could use either plaquing assay or the improved TCID<sub>50</sub> assay, depending on the purpose of titration. However, when working with a sample of virus with an unknown titre, the results of this study suggest performing an MTT-based TCID<sub>50</sub> in order to attain a general picture of the virus infectivity strength and the extent to which the virus should be diluted. The TCID<sub>50</sub> information would then enable the researcher to predict the number of plaques for any infective dilution of the virus.

In conclusion, use of the log<sub>2</sub>-based MTS or MTT end-point dilution was found to increase sensitivity, specificity, reproducibility and reliability of the EV71 titration analysis and reduce the time involved compared to the conventional method. The MTT method established in this study has been incorporated into routine use in our laboratory for titration of viruses (data not shown). Therefore, the methods described in this study can be of use for the further antiviral assays, which require an accurate estimation of titration of the virus using TCID<sub>50</sub>-based titration and/or plaquing assay. Since CPE-based endpoint approaches are commonly used for virus titration, it is highly important to accurately quantify viral titration. Therefore, the improved virus titration described in this study would play an important role in any virus experimentation.

### 3. Chapter Three: Antiviral Activity of Heparan Sulphate Mimetic Compounds and Their Mechanism against Enterovirus 71

#### 3.1. Introduction

EV71 is considered a major etiological agent of diseases such as Hand Foot and Mouth Disease (HFMD), aseptic meningitis, herpangina and flaccid paralysis (McMinn, 2002). Despite these alarming statistics, there is currently no vaccine or approved antiviral drug for the prevention or treatment of EV71 infection (Weng et al., 2010). To date, several natural and synthetic compounds have been reported to possess antiviral activities against EV71 infection *in vitro* and/or *in vivo*. Naturally occurring compounds such as lactoferrin (Lin et al., 2002), allophycocyanin (Shih et al., 2003), ursolic acid (Chiang et al., 2005), danshen extracts (Wu et al., 2007), Sheng-Ma-Ge-Gen-Tang (Chang et al., 2008), Ge-Gen-Tang (Su et al., 2008) and aloe-emodin (Lin et al., 2008), have been shown to be effective antiviral agents against EV71. Similarly, synthetic molecules such as pyridylimidazolidinones (T.C. Chen et al., 2008a), small hairpin RNAs (Lu et al., 2004), short interfering RNAs (Sim et al., 2005; Tan et al., 2007) and ribavirin (Li et al., 2008), have also been reported to inhibit EV71 infection. However, none of these compounds has been clinically approved for the treatment of EV71 to date.

Glycosaminoglycans (GAGs) are frequently present in the extracellular matrix and cell membranes, involving in the regulation of several physiological and pathological processes, including mediating viral infections (Urbinati et al., 2008). Heparan sulphate (HS) proteoglycan (HSPG) is a GAG that serves as a cell receptor for many human viruses (Oloffson and Bergström, 2005). As such, many polysulphated compounds have been synthesized to mimic cell surface HS and to act as antiviral agents against a broad range of viruses (Urbinati et al., 2008). Despite the fact that these compounds were reported to demonstrate antiviral activities many years ago (Ginsberg et al., 1947; Green and Woolley, 1947; De Somer et al., 1968; Nahmias and Kibrick, 1964), investigation of the specific mechanisms underlying their activity has been more recent. At the forefront of this research were the studies

of Ito et al. (1987) and Ueno and Kuno (1987) who reported highly inhibitory effects for dextran sulphate and heparin in HIV infectivity assays. Further, Baba et al. (1988b) demonstrated broad-spectrum antiviral activities for several sulphated polysaccharides *in vitro*. Based on such findings, it has been proposed that because cell surface HS can be used as a receptor for many viruses, there is a possibility that HS mimetic compounds could be used as antiviral agents (Mandal et al., 2008).

The antiviral action of HS-like compounds against viruses from the *Enterovirus* genus have also been studied, suggesting HS as a possible surface receptor for members of this genus (Goodfellow et al., 2001; Zautner et al., 2003). Goodfellow et al. (2001) concluded that HS is the cell receptor for some isolates of echovirus as well as some other serotypes of Human Enterovirus B (HEV-B) species. They also observed that pretreatment of cells with heparinase I or heparin blocked the binding of the virus to the cell surface. Another study revealed that Coxsackievirus B3 variant PD (CVB3 PD) virus recognizes HS molecules as receptors in addition to the coxsackievirus-adenovirus receptors (CAR) (Zautner et al., 2001). This conclusion was based on evidence that the cells treated with heparinase became resistant to CVB3 PD infection. In addition, anionic HS mimetic compounds strongly inhibited CVB3 PD infection.

Despite the body of evidence that suggests HS mimetic compounds are effective antivirals against a number of viruses of different families, no research has been undertaken to examine the possible antiviral activity of HS mimetics against human Enterovirus A (HEV-A) and particularly EV71 infection. Thus, in this study, the potential antiviral activity of some HS mimetic compounds against EV71 was assessed. In addition, the mode of action of these compounds against EV71 infection was explored.

### 3.2. Materials and Methods

#### 3.2.1. Viruses and Cells

A cloned isolate of EV71 virus (GenBank Accession no DQ381846) and a Vero cell line were kindly supplied by Prof. Peter C. McMinn (Central Clinical School, University of Sydney, Australia). The virus and the cells were maintained in Dulbecco's Modified Eagle Medium (DMEM; Invitrogen, Mulgrave, VIC, Australia) supplemented with 10% (v/v) inactivated Fetal Bovine Serum (FBS) (Invitrogen, Mulgrave, VIC, Australia). Passaging of the virus was performed as described in Page 79, while titres of the virus were quantified on Vero cell monolayers using the 50% Tissue Culture Infective Dose (TCID<sub>50</sub>), according to a modified method of Reed and Muench's endpoint (Reed and Muench, 1938), previously described in Chapter 2. Aliquots of the virus were stored at -80°C until required. Cells were stored cryogenically frozen in liquid nitrogen.

#### 3.2.2. Compounds

Pentosan polysulphate sodium (NaPPS) was supplied by Dr. John McEwan of Sylvan Pharmaceuticals Pty Ltd, Bondi Junction, NSW, Australia. Heparan sulphate (HS) from porcine intestinal mucosa ( $\geq 90\%$  purity confirmed with SDS gel electrophoresis), heparin sodium salt (Hep) from bovine intestinal mucosa ( $\geq 140$  USP units/mg), and ribavirin (RBV) were all purchased from Sigma-Aldrich, Castle Hill, NSW, Australia. All the samples were dissolved in sterile distilled water (5 mg/mL) and stored at 4°C until use, as described previously (Zautner et al., 2003).

#### 3.2.3 Cell seeding and infection of cell cultures

Vero cells were seeded at  $3 \times 10^4$  cells/well in 96-well plates (Becton Dickinson, North Ryde, NSW, Australia) followed by incubation at 37°C/5% CO<sub>2</sub> until 80% confluency was reached. Before adding the compounds or the virus, or when quantifying the results, the monolayers were thoroughly washed with phosphate buffered-saline (PBS, pH 7.4 at room temperature) twice. In all the experiments, the following controls were included: cell control (cells that were not infected with the virus or treated with the compounds), virus control (cells that were infected only with the virus but not treated with the compounds in the antiviral assays), and the positive control (virus-infected cells treated with the clinically

licensed broad spectrum antiviral, Ribavirin).

### 3.2.4. Cytotoxicity assay

The toxicity of the compounds was determined using the method of Schmidtke et al. (2001) with modifications. Briefly, the media of the 80% confluent Vero cells was aspirated followed by addition of 100  $\mu$ L of each compound solution diluted in DMEM/10% FBS (at nine two-fold dilutions, ranging from 1000 to 3.9  $\mu$ g/mL). After incubation at 37°C/5% CO<sub>2</sub> for a further three days, the results were quantified using CellTiter 96<sup>®</sup> Aqueous One Solution (Promega, Alexandria NSW, Australia) (MTS), with absorbance set at 490 nm, according to the manufacturer's instructions. The cell viability percentages were measured based on the amount of living cells in compound-treated cells relative to cell controls (defined as 100% viability) (Schmidtke et al., 2001). The cytotoxicity curve was then generated by plotting cell viability percentages against compound concentrations. The 50% and 80% cytotoxic concentrations (CC<sub>50</sub> and CC<sub>80</sub> respectively) were estimated by linear regression analysis of the cytotoxicity curve.

### 3.2.5. Cytopathic effect inhibition assay

The medium of the 80% confluent Vero Cells (seeded at  $3 \times 10^4$  cells/well) was aspirated followed by infection with 50  $\mu$ L of EV71 (100 TCID<sub>50</sub>), and simultaneously treated with 100  $\mu$ L of each compound solution diluted in DMEM/10% FBS (at nine two-fold dilutions, in the range 1000 to 3.9  $\mu$ g/mL) to each well. After incubation for three days at 37°C/5% CO<sub>2</sub>, the results were quantified as described above. The virus inhibition percentages were measured using the following equation:  $T-V_c/C_c-V_c$ , where T= the optical density (OD) of compound-treated cells, V<sub>c</sub>= OD of virus control, C<sub>c</sub>=OD of cell control (Schmidtke et al., 2001). The antiviral activity curve was then generated by plotting virus inhibition percentages against compound concentrations. The IC<sub>50</sub> and IC<sub>80</sub> of the compounds were estimated using linear regression analysis of the antiviral activity curve.

### 3.2.6. Time of addition assay

The antiviral effect of the compounds was evaluated at different times of viral infection as originally described by Chiang et al. (2002). Briefly, 100  $\mu$ L/well

of each compound solution diluted in DMEM/10% FBS (at three different concentrations: 7.81, 250 and 1000  $\mu\text{g}/\text{mL}$ ) was added to 80% confluent Vero cells at either 1 hour or 2 hours prior to infection (-1 and -2, respectively), at the time of infection (0), or 1 hour or 2 hours after viral infection (+1 and +2, respectively). The infection was performed by adding 50  $\mu\text{L}/\text{well}$  of EV71 (100TCID<sub>50</sub>) and the time points (-1, -2, 0, +1, +2) were tested independently in separate plates. The plates were then incubated for three days at 37°C/5% CO<sub>2</sub> after which the virus inhibition was quantified as described in Section 3.2.4.

### 3.2.7. Attachment assay

To assess the ability of the compounds to inhibit viral binding, an attachment assay modified from De Logu et al. (2000) was performed. Briefly, 80% confluent cells were pre-chilled at 4°C for 1 hour followed by either: (i) infection with 50  $\mu\text{L}/\text{well}$  of EV71 (200TCID<sub>50</sub>) and simultaneously supplementation with 100  $\mu\text{L}/\text{well}$  of each compound at three concentrations (7.81, 250 and 1000  $\mu\text{g}/\text{mL}$ ); or (ii) infection with 50  $\mu\text{L}/\text{well}$  of EV71 (200TCID<sub>50</sub>) that had been mixed and pre-incubated with the 100  $\mu\text{L}/\text{well}$  of each compound at 4°C for half an hour. All the plates were held at 4°C for a further 3 hours, after which the monolayers were washed twice with PBS to remove the excess compounds as well as any unbound virus. The plates were then filled with 150  $\mu\text{L}/\text{well}$  of DMEM/10% FBS and incubated for a further three days at 37°C/5% CO<sub>2</sub>. The degree of the virus inhibition was recorded by microscopic observations over repeated experiments compared to the cell controls and the virus controls.

### 3.2.8. Penetration assay

The penetration assay developed by Albin et al., (1997) was used to evaluate the ability of the compounds to inhibit viral entry. Briefly, 80% confluent cells were pre-chilled and infected with EV71 at 200TCID<sub>50</sub> (50  $\mu\text{L}/\text{well}$ ) and incubated at 4°C for 3 hours to allow viral binding. After this step, cells were treated with 100  $\mu\text{L}/\text{well}$  of each compound at three concentrations (7.81, 250 and 1000  $\mu\text{g}/\text{mL}$ ) at room temperature, followed by incubation at 37°C/5% CO<sub>2</sub> for a further 20 minutes, 40 minutes or 60 minutes to allow the compound to interrupt virus penetration to the cells. Each time point was tested separately and independently. The supernatant was aspirated followed by washing cells with alkaline PBS (NaOH, pH 11) for 1

minute to inactivate un-penetrated viruses, after which acidic PBS (HCL, pH 3) was added to neutralize the pH. The neutralized PBS was then aspirated and cells were washed with normal PBS (pH 7.4) and overlaid with 150  $\mu$ L/well of DMEM/FBS10%. The plates were then incubated at 37°C/5% CO<sub>2</sub> for a further 72 hours. The results were quantified as described in Section 3.2.4.

### 3.2.9. Statistical analysis

All the treatments were applied in triplicate, and each experiment was independently repeated at least three times. The data were expressed as mean  $\pm$  standard deviation (SD). The results of the antiviral activity assays were analyzed using a one-way ANOVA test, compared to the cell control and virus control. The Tukey's honestly significant difference (HSD) test was then used to compare antiviral activity among concentrations of each compound, while unpaired independent two-sample *t*-Test was used to compare compounds with each other. A significance level (*p* value) of 5% or 1% was considered to compare the means.

## 3.3. Results

### 3.3.1. Cytotoxicity assay

Overall the cytotoxicity response of all the test compounds, apart from RBV, was linear and dose-dependent (Figure 3.1a). The concentration associated with 50% cytotoxicity (CC<sub>50</sub>), estimated using regression analysis, was more than the highest tested concentration (>1000  $\mu$ g/mL) for both Hep and PPS and 205  $\mu$ g/mL for HS (Table 3.1). The CC<sub>80</sub> of HS and all other HS-like compounds was above the highest tested concentration (>1000  $\mu$ g/mL), while CC<sub>50</sub> and CC<sub>80</sub> of RBV was considerably lower (Table 3.1). None of the HS mimetic compounds showed significant cytotoxicity at 3.9-31.25  $\mu$ g/mL at which they demonstrated effective antiviral activities (Figure 3.1b). The antiviral effect of RBV was clearly lower at its less toxic concentrations (3.9-7.81  $\mu$ g/mL) (Figure 3.1a,b).

### 3.3.2. Antiviral activity assay

Overall, all the HS-like compounds displayed some degree of inhibitory effect against EV71-caused CPE (*p*<0.01) compared to the cell control and virus control. In addition, antiviral activity of the HS-like compounds at nearly all the

concentrations less than 250 µg/ml was statistically significant ( $p < 0.05$ ), compared to those higher than 250 µg/ml as well as RBV ( $p < 0.05$ ). The anti-EV71 activity of the test compounds and RBV did not generate a linear dose-dependent response (Figure 3.1b). Instead, all the HS-like compounds exhibited low antiviral activity at the highest concentrations (1000, 500 and 250 µg/mL), higher activity in the range 125-7.81 µg/mL, and below which the antiviral activity fell sharply. The antiviral activity of RBV never rose above 60% and dropped at concentrations above or below 15.62 µg/mL (Figure 3.1b).

The  $IC_{50}$  of Hep, HS, PPS and RBV were calculated to be approximately 205, 290, 238 and 11.5 µg/mL, respectively. To determine the potencies of the tested compounds, the selectivity index (SI) of each the test compound was measured using both equations:  $SI_{50} = CC_{50}/IC_{50}$ ; and  $SI_{80} = CC_{80}/IC_{80}$ . Both  $SI_{50}$  and  $SI_{80}$  values demonstrated that Hep was ranked first followed by PPS (Table 3.1). Although the calculated  $SI_{50}$  value for HS was lower than for RBV, its  $SI_{80}$  values revealed a reverse trend. Despite having a low  $IC_{50}$ , RBV had a very high  $CC_{50}$  value, making its  $SI_{50}$  low and indicating that it was not the most effective antiviral investigated (Table 3.1).



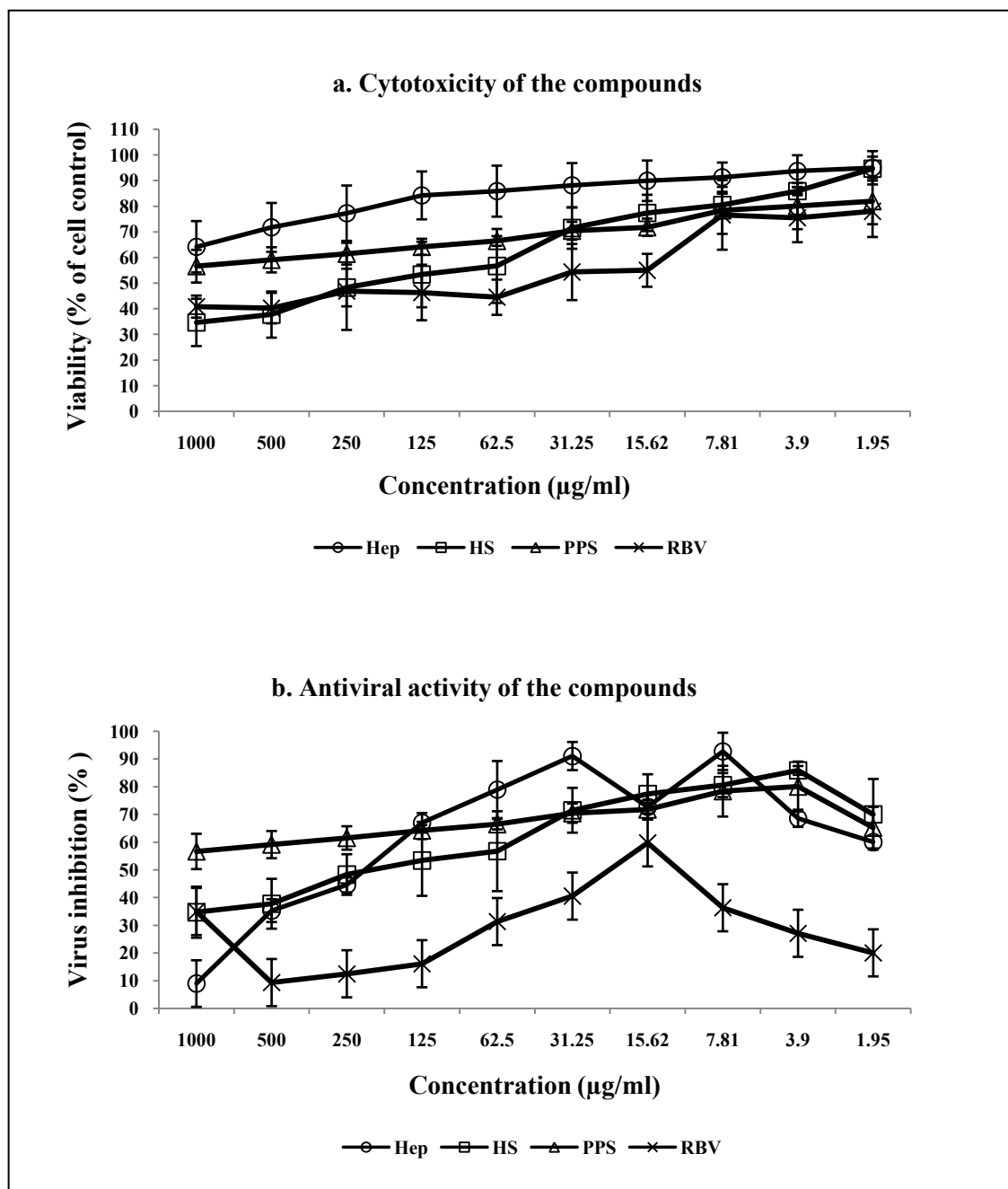


Figure 3.1. Cytotoxic effects and anti-Enterovirus 71 activities of the test compounds

## Chapter Three-Antiviral Activity of Heparan Sulphate Mimetic Compounds

---

a) Heparin sodium (Hep), heparan sulphate (HS), pentosan polysulphate (PPS) and ribavirin (RBV) at nine different concentrations were independently and individually added to 80% confluent Vero cells,. The results represent the mean  $\pm$  SD cell viability percentage of three independent experiments. The 50% and 80% cytotoxic concentration ( $CC_{50}$  and  $CC_{80}$ ),  $\mu\text{g/mL}$  for Hep, HS, PPS, and RBV were calculated using the linear regression analysis (Table 3.1).

b) Exposure of EV71 ( $100TCID_{50}$ ) to Hep, HS, PPS and RBV at nine different concentrations added to 80% confluent Vero cells. The values represent mean  $\pm$  SD virus inhibition percentage from at least three independent experiments. The 50% and 80% inhibitory concentration ( $IC_{50}$  and  $IC_{80}$ ),  $\mu\text{g/mL}$  for Hep, HS, PPS, and RBV were calculated using the linear regression analysis (Table 3.1).

**Table 3.1. Potency of antiviral activity of the compounds**

Compound	CC <sub>50</sub> <sup>a</sup> , μg/mL	IC <sub>50</sub> <sup>b</sup> , μg/mL	SI <sub>50</sub> <sup>c</sup>	CC <sub>80</sub> <sup>a</sup> , μg/mL	IC <sub>80</sub> <sup>b</sup> , μg/mL	SI <sub>80</sub> <sup>c</sup>
Hep	48430.2	205.00	236.24	Above <sup>d</sup>	5.00	Above <sup>d</sup>
HS	205.00	290.00	0.70	3914.17	22.50	173.97
PPS	10795.47	238.00	45.36	Above <sup>d</sup>	42.00	Above <sup>d</sup>
RBV	42.5	11.50	3.70	Below <sup>d</sup>	Above <sup>d</sup>	Below <sup>d</sup>

- CC is the concentration at which the compounds alone caused 50% and 80% cytotoxicity (when this was greater than the highest tested dose, the result was estimated by extrapolation of the results in Figure 3.1a).
- IC is the concentration at which the compounds caused 50% and 80% viral inhibitory
- The SI values represent the ratio of CC/IC for each compound.
- These values were outside (above or below) the range of concentrations tested in this study

In addition to SI, a novel index was also developed to compare potencies of the compounds at each concentration. This index was generated based on the ratio of the antiviral inhibition percentage (Figure 3.1b) to cytotoxicity percentage (Figure 3.1a) at each particular concentration (Appendix 3, Table 1). We feel that this index might be more accurate than the well-known antiviral drug index, SI, as SI ( $CC_{50}/IC_{50}$ ) is not always a true representation of how safe an antiviral drug would be. SI is generally used to compare two or more antiviral compounds only based on the 50% points of their antiviral and cytotoxicity curves. However, a compound may display a greater antiviral activity as well as low cytotoxicity at concentration(s) than its 50% points. Although the use of  $SI_{80}$  ( $CC_{50}/IC_{50}$ ) might in part solve this problem, it is still a representative of only one concentration (i.e. the 80% point). Thus, SI values may lack information as to concentrations of a compound that would be safer and more potent than the 50% or 80% point. Furthermore, a 50% or 80% point is normally estimated by regression analysis of the curve that may include concentrations out of the range being tested, as is true of Table 3.1. This would mean that SI values are not always generated using actual data, leading to a possible decrease in the accuracy of the results. As such, the new index enabled further comparisons between concentrations of a compound as well as between compounds (Appendix 3, Table 1). For example, one can state that RBV is safer than HS according to their  $SI_{50}$  values (Table 3.1), while RBV is more cytotoxic across most of the concentrations studied (Figure 3.1a). Using the new index, this problem is eliminated, as RBV was observed to be less potent in all of tested concentrations compared to HS.

### 3.3.3. Time of addition assay

A time of addition assay was carried out to examine whether the compounds exerted their antiviral activities before or after viral infection. The compounds were able to prevent CPE caused by EV71 at different time points of the viral infection. The study of the intensity of CPE inhibition, expressed as virus inhibition percentages compared to both the cell control and virus control (Figure 3.2), showed that Hep added one hour before infection at 250  $\mu\text{g}/\text{mL}$ , consistently inhibited virus-induced cell death by more than 80%. The degree of inhibition of Hep at 250  $\mu\text{g}/\text{mL}$  was significantly greater as compared to the other tested time points of Hep at 250

$\mu\text{g/mL}$  as well as the other compounds at the same time and the same concentration ( $p < 0.01$ ) (Figure 3.2). The results showed the time of addition of HS (at  $250 \mu\text{g/mL}$ ) affected the virus inhibition. Concurrently added HS ( $t=0$ ) had greater antiviral activity as compared to addition before or after infection ( $p < 0.01$ ). In contrast, PPS at  $250 \mu\text{g/mL}$  had no statistically significant effect on virus inhibition at any time point. RBV at  $250 \mu\text{g/mL}$  did not have antiviral activity before or after infection and displayed minimal antiviral activity at  $T=0$ . At a concentration  $7.81 \mu\text{g/mL}$ , Hep exerted significantly greater virus inhibition when added one hour before infection as compared when it was added two hours before or two hours after infection ( $p < 0.01$ ) (Figure 3.2). There was no significant difference between Hep and PPS when added at  $7.81 \mu\text{g/mL}$  one hour before infection ( $p > 0.05$ ). In addition, the degree of inhibition exerted by HS and RBV was low ( $p > 0.05$ ) at all the time points when tested at  $7.81 \mu\text{g/mL}$ . The HS-mimetic compounds at  $1000 \mu\text{g/mL}$  did not display statistically significant antiviral activity at any time point, whereas  $1000 \mu\text{g/mL}$  of RBV showed significant virus inhibition when applied one hour before infection ( $p < 0.01$ ) (Figure 3.2).

### 3.3.4. Virus binding assay

The tested compounds could inhibit EV71 attachment as determined by the virus binding assay. It was observed that all the HS-like compounds could obviously prevent EV71 attachment to Vero cells (Figure 3.3). The effect was most apparent with  $7.81 \mu\text{g/mL}$  of Hep (Figure 3.3c), HS (Figure 3.3e), and PPS (Figure 3.3g), whereas RBV did not significantly interfere with viral binding (Figure 3.3i).

Pre-incubation of the compounds with the virus for half an hour before the infection showed that Hep, HS, and PPS (Figure 3.3d,f,h) inhibited CPE caused by EV71 in a manner similar to that of the attachment assay stated above. Again, this was not observed with RBV (Figure 3.3j).

### 3.3.5. Penetration assay

The penetration assays were performed to examine whether the compounds were able to inhibit entry of virus into the host cells. The results revealed that RBV, but none of the test compounds, exerted some antiviral activities (Figure 3.4). Although the two-sample *t*-test analysis revealed no statistical difference among the compounds, the penetration assays demonstrated that RBV appeared to inhibit the

viral penetration to a greater extent than any of the HS mimetics. In addition, the antiviral activities were time interval-dependent, as the antiviral activity with 60 minutes of incubation was lower than those at 20-minute and 40-minute time intervals, at all the tested concentrations of the compounds.

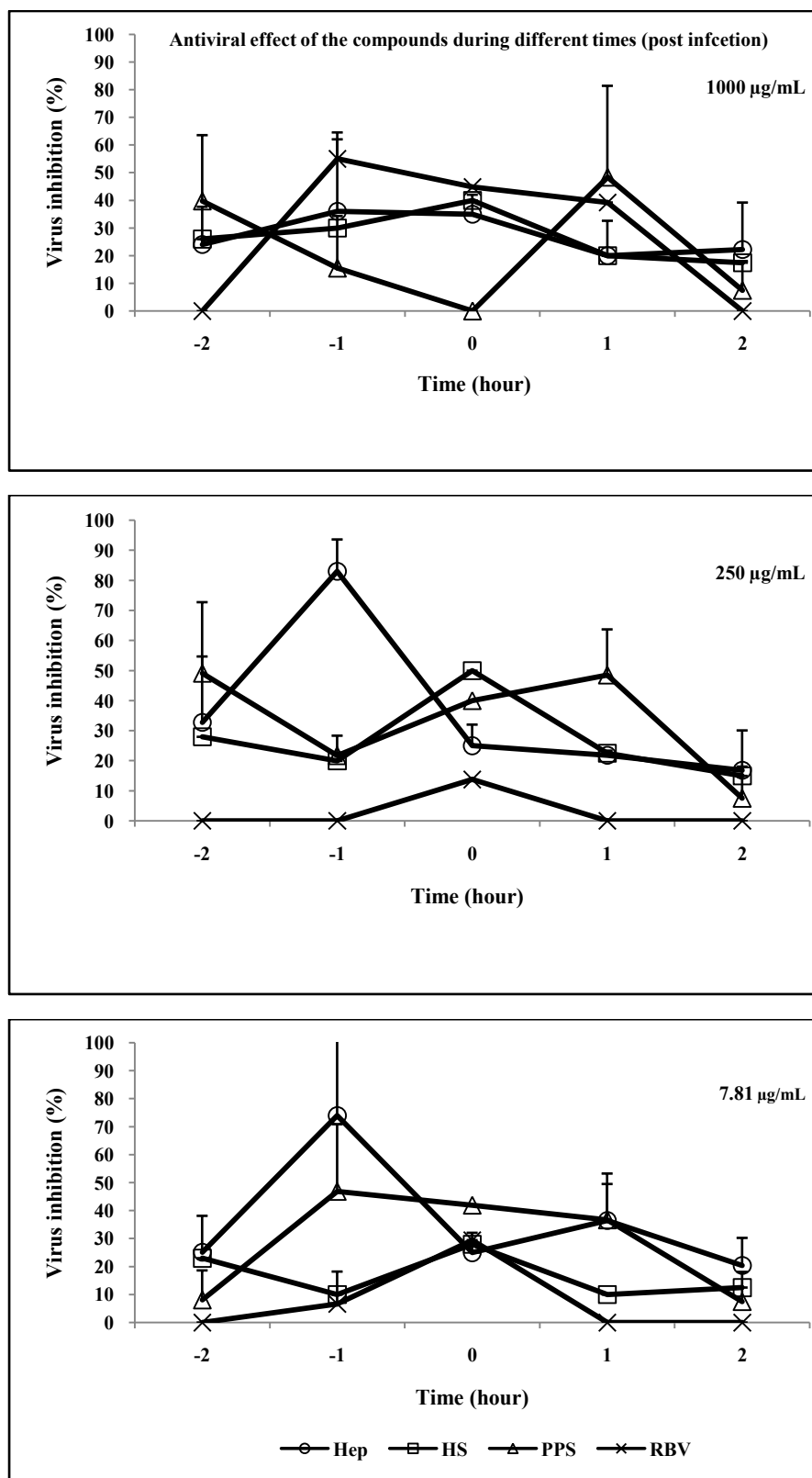


Figure 3.2. Antiviral effect of the compounds during different times of the virus infection

### **Chapter Three-Antiviral Activity of Heparan Sulphate Mimetic Compounds**

---

This experiment was essentially the same as that described in Figure 3.1,b, with the following modifications: the compounds Hep, HS, PPS, and RBV (at three concentrations 7.81, 250, and 1000,  $\mu\text{g/mL}$ ) were added to the cells prior ( $t=-1$  or  $-2$  hours), at ( $t=0$ ), or after ( $t=1$  or  $2$  hours) the time of infection. The values represent the mean  $\pm$  SD generated from at least three independent experiments.



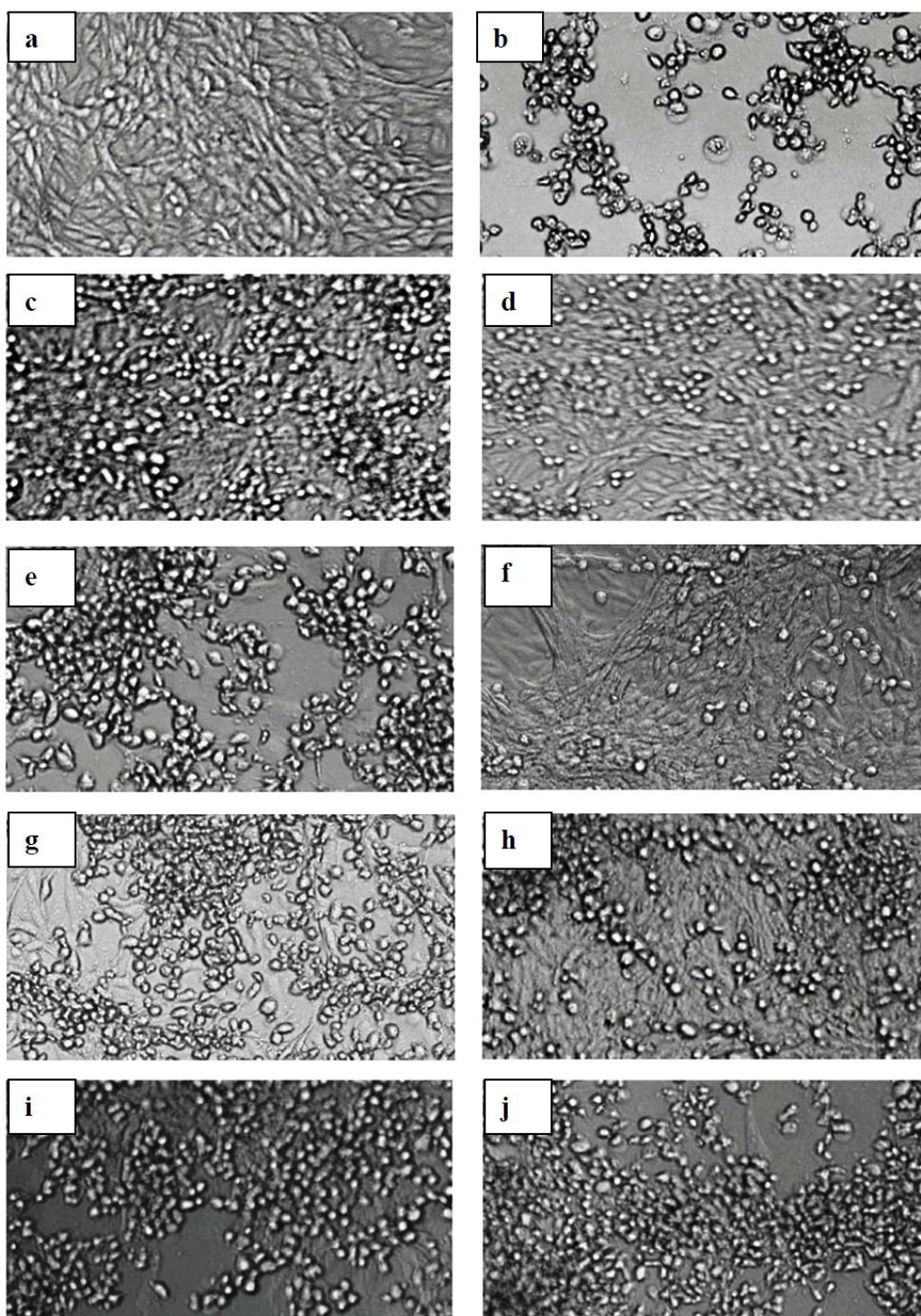
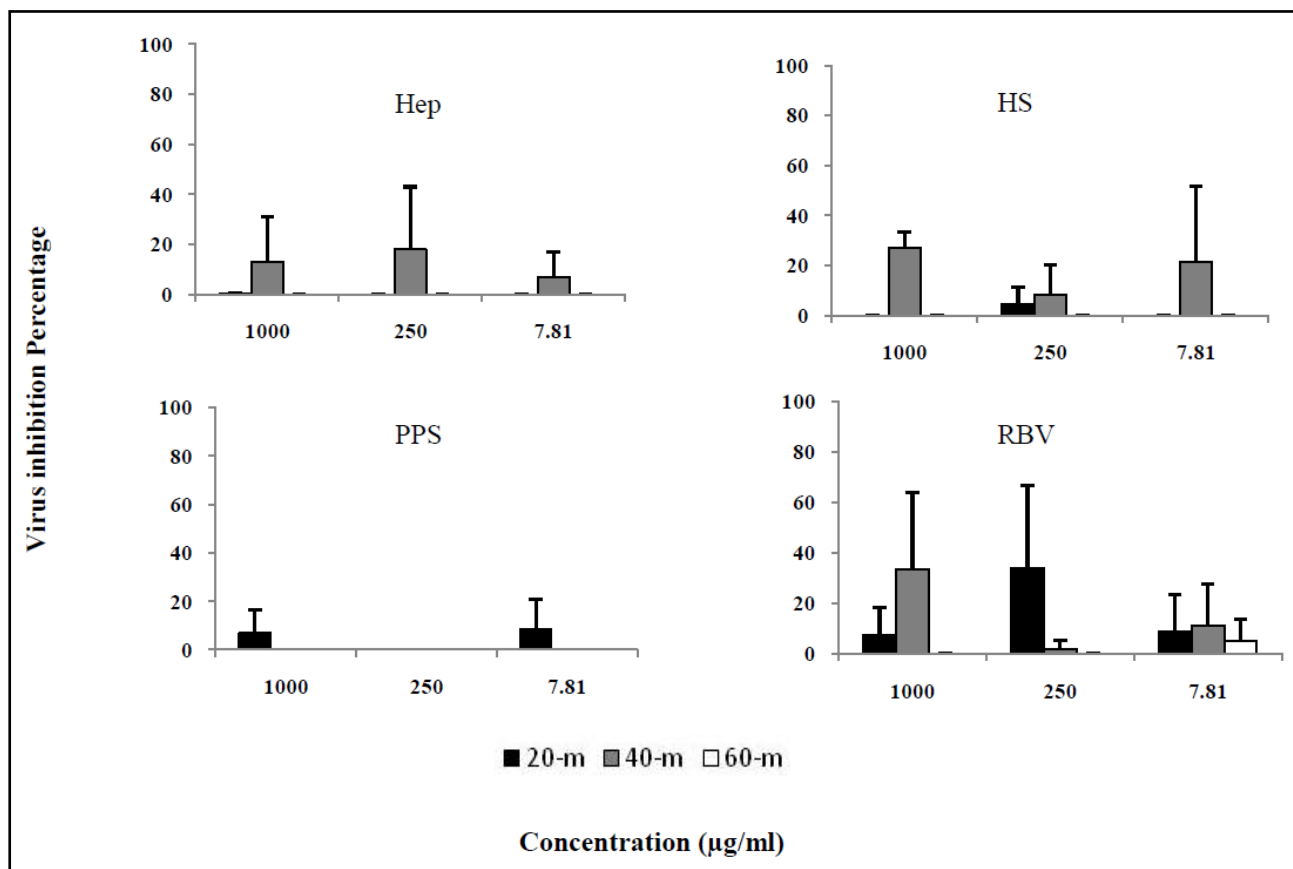


Figure 3.3. Inhibition of Enterovirus 71 binding to the Vero cells

## Chapter Three-Antiviral Activity of Heparan Sulphate Mimetic Compounds

---

Cells pre-chilled at 4°C were treated simultaneously with each compound and EV71 (at 200TCID<sub>50</sub>) and incubated at 4°C for three hours (panels c (Hep), e (HS), g (PPS), and i (RBV)). In the other assay, the pre-chilled cells were treated with the mix of each compound and the virus that had been pre-incubated at 4°C for half an hour (panels d (Hep), f (HS), h (PPS), and j (RBV)). Panel a shows cell control, while the panel b represents virus control. The assays were performed in triplicate and repeated at least three times independently. The photos (×100 magnification) were taken 72 hours post infection using an inverted microscope and represent the average of the observations for the compounds added at a concentration of 7.81, µg/mL.



**Figure 3.4. Effect of the test compounds on Enterovirus 71 entry into Vero cells**

The virus was added to the cells at 4°C followed by the addition of compounds to the cells and incubation at 37°C. The virus and the compounds were removed from the cells 20, 40 or 60 minutes later. The results are presented as percentage of virus inhibition and expressed as the mean ± SD generated from at least three independent experiments.

### 3.4. Discussion

The findings of this study revealed that HS, Hep and PPS all exhibited statistically significant antiviral activities ( $p < 0.01$ ) against EV71 in Vero cells within the first three days of infection. Their relative low cytotoxicity is in agreement with what was previously established for Coxsackievirus B3 (Zautner et al., 2003). However, in the present study, Hep exhibited the most effective and safe anti-EV71 activity at 7.81  $\mu\text{g/mL}$  ( $p < 0.05$ ), resulting in 92% viral inhibition, while PPS exhibited the best antiviral effect against Coxsackievirus B3 in CHO-K1 cells (Zautner et al., 2003). Hep has also been shown to have an antiviral effect against echovirus 7 and poliovirus 3 (Goodfellow et al., 2001).

RBV was used as a positive control, since it has previously been reported to exert anti-EV71 activity both *in vitro* and *in vivo* (Li et al., 2008), where RBV reduced the EV71 titre (with an  $\text{IC}_{50}$  of 65  $\mu\text{g/mL}$ ) in RD, SK-N-SH, and N18 cells. However, the results of this study revealed that the anti-EV71 activity of RBV was significantly lower ( $p < 0.05$ ) and its cytotoxicity was much higher when compared to those of the HS mimetics. The inhibition of EV71-caused CPE by RBV reached a maximum of 59.7% at 15.62  $\mu\text{g/mL}$  with 55.01% toxicity to the Vero cells over 72 hours post infection. Similarly, Scagliarini et al. (2006) reported a high cytotoxicity level for RBV in Vero cells where the  $\text{CC}_{50}$  of RBV was 31  $\pm$  6.2  $\mu\text{g/mL}$ . However, the low antiviral activity and high cytotoxicity of RBV observed here might be due to a cell-dependent effect of RBV (Scagliarini et al., 2006). Thus, it appears that further studies are warranted to test the usefulness of RBV as a positive control in different cell types.

In order to gain a more precise knowledge of the concentration of the tested compounds, molarities of the compounds at the tested concentrations were calculated (Appendix 3, Table 2). Then, the molarities were compared to the related physical concentrations (in  $\mu\text{g/mL}$ ) to find out how many moles of a physical concentration of the compound is required to exhibit some antiviral activity. The results supported the antiviral potencies of the compounds that were previously revealed using the physical concentrations. For example, while Hep at 7.81  $\mu\text{g/mL}$  was approximately 0.5  $\mu\text{M}$ , it exhibited more than 90% viral inhibition. On the contrary, RBV at the

same physical concentration was 31  $\mu\text{M}$ ; however, it showed only slight antiviral activity against EV71 infection.

The antiviral activity of the test compounds was affected by the time at which they were added to infected cells. However, only Hep at 250  $\mu\text{g}/\text{mL}$ , exerted a significant and more consistent virus inhibition, when added prior to infection as compared to post infection ( $p < 0.05$ ). There was no significant difference between Hep and PPS (at 7.81  $\mu\text{g}/\text{mL}$ ) when added one hour before infection ( $p > 0.05$ ); this could be attributed to the high variability that both compounds showed at one hour before infection with 7.81  $\mu\text{g}/\text{mL}$ . In general, the dose-dependent antiviral potency of HS-like compounds and RBV in time of addition assays matched that of the CPE-inhibition assay.

Although not statistically significant, RBV appeared to inhibit viral penetration to a greater extent than the HS-like compounds, suggesting that the test HS mimetics could not significantly prevent EV71 entering the host cells.

The potential for all the HS mimetics to inhibit EV71 attachment to Vero cells at concentrations of 7.81 and 250  $\mu\text{g}/\text{mL}$  was also demonstrated. This allows speculation that the hindrance of EV71 attachment could simply be caused by electrostatic associations between the virus and the negatively charged sulphate/carboxylate groups of the HS mimetics (Jenssen et al., 2006). However, the observed interference with EV71 attachment in this study might be beyond a simple electrostatic reaction between the HS mimetics and the virus (Schols et al., 1990). This may suggest that the soluble HS-like compounds could have hindered viral attachment through competition with cell surface HS, as the HS-like compounds are analogue forms of HSPG present on the cell receptor and can thus compete in binding to the virus. This may be supported with the fact that cellular HS is naturally present on mammalian cell surfaces, serving as the second largest group of carbohydrate-based receptors for human viruses of various families (Olofsson and Bergström, 2005). These conclusions, however, needs confirmation and could be tested by treatment with enzymes which cleave HS and/or Hep-like domains on HS chains from cell surface, such as heparinase enzymes I, II and III.

The results also showed no difference between the inhibitory effects of the compounds upon virus attachment in the two situations, pre-incubated with the virus or applied in the normal binding assay (as stated in Section 3.2.7). In the first

situation, one could speculate that the virus and the compounds are not attached to one another during pre-incubation, and their viral binding inhibitory effect would emerge only one they were added to the host cells. Clearly, this issue needs further confirmatory experiments.

The inhibitory effect of HS mimetics on viral attachment has been known for many years (Baba et al., 1988b). Heparin at 25  $\mu\text{g}/\text{mL}$  was shown to protect human T-cells against HIV-1 with an  $\text{IC}_{50}$  of 7  $\mu\text{g}/\text{mL}$  and without significant cytotoxicity, through inhibition of the virus attachment process. The hindrance of viral attachment was clearly captured using radiolabeled HIV-1 particles, where dextran sulphate and Hep prevented the adsorption of the virus to MT-4 cells. However, the antiviral activity of the tested compounds was independent of binding to CD4 as they did not interfere with the binding of monoclonal antibodies to the CD4 antigen receptor on MT-4 cells (Baba et al., 1988a). Later work demonstrated that Hep, PPS and some other HS mimetics prevented the binding of anti-gp120 monoclonal antibody to persistently HIV-1-infected HUT-78 cells in a dose-dependent manner, providing evidence for interaction of HS mimetics with HIV-1 gp120 (Schols et al., 1990). The capacity of Hep to prevent viral attachment was also shown for Dengue virus where Hep showed a potent antiviral activity (with an  $\text{IC}_{50}$  of 0.3  $\mu\text{g}/\text{mL}$ ) by inhibiting binding of recombinant surface glycoprotein of dengue virus-2 to Vero cells, while HS and other HS mimetics failed to display such effect. However, an unusual highly sulphated HS could inhibit the recombinant envelope protein binding with an  $\text{IC}_{50}$  of 4  $\mu\text{g}/\text{mL}$  (Chen et al., 1997).

There are limited reports of antiviral activity of HS mimetics and their interference with viral attachment in Enteroviruses. In the Enterovirus genus group B, it was reported that EV6 binding to RD cells was reduced by 95% in the presence of 1mg/mL of Hep (Goodfellow et al., 2001).

In the current study, RBV was not seen to significantly interfere with viral binding, which is expected as the mode of action of RBV in poliovirus has previously been proved to correlate directly with its mutagenic activity on viral RNA polymerase, leading to lethal mutagenesis. The proven mechanisms of action of RBV against other viruses include a decrease in intracellular guanosine triphosphate pools and/or immunomodulatory activities (Crotty et al., 2000). Therefore, the mode

of action of RBV against EV71 infection would more than likely be intracellular and would not involve the virus attachment.

Hep in combination with aspirin is effective for prophylaxis and treatment of venous thromboembolism, coronary heart disease, and short-term treatment of unstable angina (Datasheets of heparin sodium injection). Although a safe dosage of Hep administered by injection depends on age, weight, clinical application and the route of injection, it is usually initiated with 50 units/kg bodyweight for children (Datasheets of heparin sodium injection). Therefore, the effective antiviral doses of Hep observed in this work (7.81-62.5  $\mu\text{g/mL}$ ) would be equivalent to 3.9-31.25 Howell units/mL that is less than the initial clinical dose of Hep. Nevertheless, these findings should be evaluated *in vivo*.

Despite the fact that poly anionic compounds have long been studied for their antiviral properties, no previous research has investigated the potential antiviral activity of Hep and its derivatives against human Enterovirus A viruses, including EV71. In this study, the antiviral activities of HS mimetic compounds against EV71 were demonstrated. Thus, they may have potential as therapeutic compounds for the treatment of EV71 infection. In addition, a possible role for Hep and other HS mimetics in the hindrance of EV71 attachment to host cells was proposed. However, these findings will require further investigations in order to confirm this and explore the molecular mechanisms underlying the antiviral action of HS-like compounds. This work in turn will lead to the design and testing of antiviral drugs that are more effective against enteroviral infection.

## 4. Chapter Four: Contributions of Heparan Sulphate as a Candidate Receptor for Enteroviruses

### 4.1. Introduction

Cell surface heparan sulphate (HS) is increasingly receiving attention due to having the capability to interact with many viruses of diverse families, and thus, to play key roles in mediating viral infection for these viruses (Zhu et al., 2011). For many viruses, however, virus-HS interaction originates from multiple passages of the virus in cell culture. Examples include Foot and Mouth Disease Virus (FMDV) (Sa-Carvalho et al., 1997; Baranowski et al., 1998; Escarmis et al., 1998; Neff et al., 1998), Sindbis virus (SIN) (Klimstra et al., 1998), and Venezuelan Equine Encephalitis virus (VEE) (Bernard et al., 2000). One mechanism that confers this capacity for a virus to bind to cellular HS in cell culture lies in amino acid changes in the viral glycoprotein. For instance, Bernard et al., (2000) stated that the mutant VEE isolates that bound to HS *in vitro* had acquired a positively charged lysine in their E2 glycoprotein, which could interact with the negatively charged HS. This was coupled with the observation of antiviral activities of heparin (Hep), dextran sulphate and chondroitin sulphate B against VEE infection in Baby Hamster Kidney (BHK) cells.

Unlike viruses such as FMDV, the use of cellular HS by some other viruses might not be attained through adaptation to cell culture. This difference can often be confirmed by using low passage clinical isolates of viruses followed by further confirmatory experiments. For example, it was shown that HS-mediated infection of GDVII, a high-neurovirulence isolate of Theiler's murine encephalomyelitis virus (TMEV), is not established through adaptation to cell culture (Reddi and Lipton, 2002). This was in part confirmed by antiviral activity of 1 mg/mL of soluble HS against suckling mouse brains stocks of GDVII in Chinese hamster ovary (CHO) cells. In addition, this mouse-derived virus did not cause cytopathic effect (CPE) in glycosaminoglycan (GAG)-deficient CHO mutant cells (Reddi and Lipton, 2002). As a further confirmatory experiment, a isolate of GDVII, designated as GD-A745, was adapted to grow in GAG-deficient CHO cells. Genome sequence analysis



revealed two point mutations in the viral capsid of this virus: N1051S and R3126L, as compared to the strain GDVII. These mutations were speculated to be responsible for the loss of a positive charge needed to interact with cell surface HS. As it was expected, soluble HS could only slightly inhibit GD-A745 infection. Moreover, HS-deficient murine MI-D macrophages and murine neuro 2A neuroblastoma cells displayed higher levels of GD-A745-mediated CPE as compared to the parental GDVII. Taken together, these findings suggested that the use of cellular HS by GDVII is not an artifact of cell culture adaptation of the virus.

As the official International Committee on Taxonomy of Viruses (ICTV) 2011 states, the *Enterovirus* genus consists of 10 species including human Enteroviruses (HEV)-A, B, C, and D (<http://ictvonline.org>). HEVs are ubiquitous pathogens that can infect people of all ages, causing a broad spectrum of clinical manifestations including acute respiratory illness, aseptic meningitis, myocarditis, hand-foot-and-mouth disease, neonatal multi-organ failure and acute flaccid paralysis (Caro et al., 2001; Stalkup and Chilukuri, 2002). There are many serotypes within the HEVs species, including Coxsackievirus A16 and Enterovirus 71 (HEV-A), Echovirus serotypes, swine vesicular disease virus and all the Coxsackievirus B serotypes (HEV-B), some Coxsackievirus A serotypes and polioviruses (HEV-C), and Enterovirus 68, and 70 (HEV-D) (<http://ictvonline.org>). To date, several Enteroviral receptors have been identified and characterized at the molecular level (Table 4.1). The most common Enteroviral receptors include glycoproteins like decay- accelerating factor (DAF; DC55) (Bergelson et al., 1993, 1994, 1995; Ward et al., 1994; Shafren et al., 1995) and the coxsackievirus and adenovirus receptor (CAR) (Bergelson et al., 1997, 1998; Tomoko et al., 1997; Martino et al., 2000).

While there is concrete evidence of non-HS viral receptors, discovery of the possible role of cell surface HS in mediating infection of Enteroviruses does not have a long history. Thus far, the role of HS in mediating infection of Enteroviruses has only been reported for serotypes of HEV-B (Table 4.1). Goodfellow et al. (2001) showed that a low-passage clinical isolate of Echovirus 6 bound to HS in a DAF-independent manner. They also showed that Hep could block RD cell infection of some other members of HEV-B, including Echovirus serotypes 2, 3, 5, 6, 9, 15, 16, 19, 25, 26, 30. In addition, cell surface HS was shown to mediate entry of Coxsackievirus B3 (CVB3) variant PD into DAF- and CAR-negative cell lines.

Amino acid substitutions in VP1 were identified as the molecular basis of this extended cell tropism for CVB3 PD (Zautner et al., 2003). However, since the CVB3 variant PD was a laboratory strain, it remains unknown whether the binding of CVB3 to HS is only a cell culture phenomenon or a characteristic of the wild virus in nature.

In accordance with the above-mentioned findings, Escribano-Romero et al. (2004) demonstrated that a low-passage clinical isolate of swine vesicular disease virus (SVDV) (belonging to HEV-B) utilized cellular HS for binding to IB-RS-2 (a porcine kidney cell line) cells. This was concluded from significant antiviral activity of 100 µg/mL of Hep towards the SVDV infection in IB-RS-2 cells. In addition, the viral binding was blocked in the absence of cell surface HS through removing it with the enzyme heparinase III. Since the mode of action of Hep as a HS mimetic compound was shown to be through inhibiting viral attachment and not penetration, it was hypothesized that the binding of SVDV to cellular HS mediates an early move of the virus-cell interaction. This event would then aid the further recognition of other receptors such as CAR that have previously been found to serve as a common receptor for all of CVB serotypes (Martino et al., 2000).

To the best of our knowledge, no study has been undertaken to investigate the possibility that Enterovirus 71 (EV71) and Coxsackievirus A16 (CVA16), two significant members of HEV-A, utilize HS as an attachment co-receptor. Therefore, the aim of this study was to investigate the possible role of HS in mediating infection of low-passage clinical isolates of HEV-A in both African Green Monkey kidney cells and a human neuroblastoma cell line. In addition to EV71 and CVA16, the possibility of use of cellular HS by a clinical isolate of CVB4, which has not yet been reported to utilize HS as a receptor, was investigated. In summary, this study aimed to generate a general picture of the use of HS as a co-receptor by representatives of HEV-A and HEV-B, in addition to ones that have previously been reported in literature.

Table 4.1. Cell receptors of members of Human Enteroviruses

Species	Non-HS receptors					HS receptors				
	Serotype <sup>1</sup>	Source	Receptor <sup>2</sup>	Cell <sup>3</sup>	Ref.	Serotype <sup>1</sup>	Source	Receptor <sup>2</sup>	Cell <sup>3</sup>	Ref.
<i>Human Enterovirus A</i>	EV71	clinical isolates from all genogroups of EV71	SCARB2	RD, HeLa, Hep-2, 293T, HepG2	Yamayoshi et al., 2009	-	-	-	-	-
	EV71	clinical isolates from genogroups B3, B4, C1, C2, and C4	PSGL-1 (CD162)	Jurkat T cells	Nishimura et al., 2009	-	-	-	-	-
	CVA16	n.d.	SCARB2	RD	Yamayoshi et al., 2009	-	-	-	-	-
	CVA16	G10 (a reference strain)	PSGL-1 (CD162)	L-PSGL-1.1	Nishimura et al., 2009	-	-	-	-	-
<i>Human Enterovirus B</i>	Echovirus 6, 7, 11, 12, 13, 20, 21, 29, and 33	Old clinical isolates adapted to cell culture	DAF (CD55)	HeLa, RD	Bergelson et al., 1994; Ward et al., 1994	Echovirus 6	Several low clinical isolates	HS	RD	Goodfellow et al., 2001
	Echovirus 1 and 8	Prototype strains adapted to cell culture	VLA-2	HeLa	Bergelson et al., 1992 and 1993	Echovirus 2, 3, 5, 6, 9, 15, 25	n.d.	Possibly HS	RD	Goodfellow et al., 2001
	CVB3	CVB3-RD (adapted to cell culture)	DAF (CD55)	RD	Bergelson et al., 1995	CVB3	PD, a cloned isolate	HS	CHO-K1	Zautner et al., 2003
	CVB1 and 5	CVB1: conn-5 (a reference strain); CVB5: Faulkner (a reference strain)	DAF (CD55)	HeLa, Hep-2	Shafren et al., 1995	-	-	-	-	-

Table 4.1. Cell receptors of members of Human Enteroviruses (continued)

Species	Non-HS receptors					HS receptors				
	Serotype <sup>1</sup>	Source	Receptor <sup>2</sup>	Cell <sup>3</sup>	Ref.	Serotype <sup>1</sup>	Source	Receptor <sup>2</sup>	Cell <sup>3</sup>	Ref.
<i>Human Enterovirus B</i>	CVB1, 2, 3, 4, 5, and 6	Either reference strains or low passaged clinical isolates	CAR	CHO-CAR, NIH 3T3, murine CHO cells	Bergelson et al., 1997; Tomko et al., 1997, Bergelson et al., 1998; Martino et al., 2000	-	-	-	-	-
	SVDV	UK/27/72	CAR; DAF	CHO-CAR; HeLa	Martino et al., 2000	SVDV	SPA/2/93 (a low passaged clinical isolate)	HS	IB-RS-2	Escribano-Romero et al., 2004
	CVA9	Griggs (adapted to cell culture)	$\alpha_5\beta_1$ integrin	GMK	Roivainen et al., 1994	-	-	-	-	-
	CVA9	n.d.	GRP78-MHC-I	GMK	Triantafyllou et al., 2002	-	-	-	-	-
	Echovirus 22	A reference strain	$\alpha_5\beta_1$ integrin	GMK	Roivainen et al., 1994	-	-	-	-	-
<i>Human Enterovirus C</i>	CVA13, 15, 18, and 20	Prototype strains	ICAM-1	CHO-ICAM-1; RD-ICAM-1	Newcombe et al., 2003	-	-	-	-	-
	CVA21	KuyKendall	ICAM-1; DAF	CHO-ICAM-1; CHO-DAF; HeLa	Shafren et al., 1997	-	-	-	-	-
	CVA24	110390 (clinical)	Sialic acid	Human ocular; CHO	Nilsson et al., 2008					

## Chapter Four-Contributions of HS as a Candidate Receptor for Enteroviruses

---

1. Abbreviations of viruses: EV71: Enterovirus 71; CVA16: Coxsackievirus A16; CVB (1-6): Coxsackievirus B (1-6); SVDV: swine vesicular disease virus; CVA9: Coxsackievirus A 9; CVA14, 15, 18, 20, 21, 24: Coxsackievirus A14, 15, 18, 20, 21, 24.

2. Abbreviations of receptors: SCARB2: the human scavenger receptor class B member 2; PSGL (CD162): a sialomucin membrane protein; DAF (CD155): Decay accelerating factor; VLA-2: an integrin molecule; CAR: the coxsackievirus and adenovirus receptor; GRP78: a 70 kDa-member of the heat shock protein 70 family of stress proteins; MHC-I: major histocompatibility complex class I [CVA9 utilizes the  $\alpha_v\beta_6$  integrin and GRP78 as attachment receptors, then MHC-I is used by the virus as a means of penetration (Triantafilou et al., 2002)]; ICAM-1: intercellular adhesion molecule-1; HS: heparan sulphate.

3. Abbreviations of cells: RD: Rhabdomyosarcoma; HeLa: a line derived from cervical cancer cells; Hep-2: a cell line established from human laryngeal carcinoma; 293T: a Human Embryonic Kidney cell line; HepG2: a Human hepatocellular liver carcinoma *cell* line; Jurkat T cells: a T lymphocyte cell line established from T cell leukemia; L-PSGL-1.1: an L929 (a murine aneuploid fibrosarcoma cell line) cell clone that stably expresses high amounts of human PSGL-1; CHO-CAR, -DAF, -ICAM-1: Chinese hamster ovary (CHO) transfected to express CAR, DAF or ICAM-1 receptors; CHO-K1: a Chinese hamster ovary cell line; RD-ICAM-1: RD cells transfected to express ICAM-1 receptor; GMK: Green Monkey Kidney cell line; IB-RS-2: a Porcine Kidney Cell line.

### 4.2. Materials and Methods

#### 4.2.1. Cell lines and viruses

An African Green Monkey kidney cell line (Vero) was kindly provided by Prof. Peter C. McMinn (Central Clinical School, University of Sydney, Australia). A human neuroblastoma cell line, SK-N-SH, from the European Collection of Cell Cultures (Catalogue number 86012802) was purchased from CellBank Australia (Westmead, NSW, Australia). The cells were maintained in Dulbecco's Modified Eagle's Medium (DMEM, Invitrogen, Mulgrave, VIC, Australia) with high glucose supplemented with 10% heat inactivated Fetal Bovine Serum (FBS, Invitrogen, Mulgrave, VIC, Australia). The cells were not passaged more than 20 times after reviving from the original stocks.

A cloned isolate of EV71 strain 6F/AUS/6/99 (GenBank Accession number DQ381846) was kindly provided by Prof. Peter C. McMinn (Central Clinical School, University of Sydney, Australia). Low passage clinical isolates of the following human Enteroviruses were used: EV71 (isolate number 99018233); Coxsackievirus A16 (isolate number CAIG 9902-2745-4PMEK); and Coxsackievirus B4 (isolate number 99039838); all supplied by Dr. Jullian Druce of the Victorian Infectious Disease Reference Laboratories (North Melbourne, VIC, Australia). The viruses were propagated in 80% confluent monolayers of Vero cells using serum-free DMEM as described in Page 79. The virus titres were determined in Vero cells using an MTT-based TCID<sub>50</sub> method as described in Chapter 2 (Page 81). These low passage viral isolates were further passaged not more than ten times in order to eliminate the possibility of developing HS binding virus mutants through adaptation to cell culture. The final viral supernatants were aliquoted and stored at -80°C until use.

#### 4.2.2. Reagents

Pentosan polysulphate sodium salt (provided by Dr. John McEwan, Sylvan Pharmaceuticals Pty Ltd, Bondi Junction, NSW, Australia) and heparin sodium salt (Hep) from bovine intestinal mucosa ( $\geq 140$  USP units/mg, catalogue number H0777) purchased from Sigma-Aldrich (Castle Hill, NSW, Australia) were dissolved in sterile distilled water (10 mg/mL) and stored at 4°C until use, as described elsewhere

(Zautner et al., 2003). Heparinase enzymes I (Catalogue number H2519) and III (Catalogue number H8891) were obtained from Sigma-Aldrich and stored at  $-20^{\circ}\text{C}$  until use.

### 4.2.3. Cell seeding and infection of cell cultures

Vero and SK-N-SH cells were seeded at  $1.5 \times 10^4$  and  $1.35 \times 10^4$  cells/well, respectively, in 96-well plates (Becton Dickinson, North Ryde, NSW, Australia) followed by incubation at  $37^{\circ}\text{C}/5\% \text{CO}_2$  until 80% confluent. The virus (before adding the compounds) or the monolayers (when quantifying results) were thoroughly washed with phosphate buffered-saline (PBS, pH 7.4 at room temperature) two or three times. In all of the experiments, the following controls were included: cell control (cells that were not infected with virus or treated with compounds or enzymes) and virus control (cells that were infected only with virus but not treated with compounds or enzymes).

### 4.2.4. Cytotoxicity assay

The toxicity effect of Hep and PBS on Vero cells was previously described in Chapter 3 (Figure 3.1, Page 104). In order to determine whether the compounds had any toxicity effect on neural SK-N-SH cells, a cytotoxicity assay was performed using the method of Schmidtke et al. (2001), as described previously (Chapter 3, Page 100) with slight modifications. In brief, the media of the 80% confluent cells was aspirated followed by addition of 100  $\mu\text{L}$  of each compound solution diluted in DMEM/10% FBS (at nine two-fold dilutions, ranging from 3.9 to 1000  $\mu\text{g}/\text{mL}$ ). After incubation at  $37^{\circ}\text{C}/5\% \text{CO}_2$  for a further two days, the results were quantified using 20  $\mu\text{L}/\text{well}$  of MTT reagent (Invitrogen, Mulgrave, VIC, Australia) dissolved in PBS (0.5% w/v) (Anderson et al., 2005). The plates were then incubated in a humidified  $37^{\circ}\text{C}$  incubator with 5%  $\text{CO}_2$  for 2-3 hours after which the formazon was dissolved with DMSO (50  $\mu\text{L}/\text{well}$ ) followed by another 10-minute incubation. The colour change was then recorded using a microplate reader at 540 nm. The cell viability percentages were measured based on the amount of living cells in compound-treated cells relative to cell controls (defined as 100% viability) (Schmidtke et al., 2001). The cytotoxicity curve was then generated by plotting cell viability percentages against compound concentrations. The 50% and 80% cytotoxic

concentrations (CC<sub>50</sub> and CC<sub>80</sub> respectively) were estimated by linear regression analysis of the cytotoxicity curve.

### 4.2.5. Infectivity assay with soluble glycosaminoglycans

80% confluent cells were infected with 50  $\mu$ L/well of virus at 100TCID<sub>50</sub>, followed by the addition of 100  $\mu$ L/well of Hep or PPS at various concentrations (ranging from 3.9 to 1000  $\mu$ g/mL) in triplicates. Following incubation for 48 hours at 37°C in the presence of 5% CO<sub>2</sub>, the degree of inhibition of CPE was quantified as described above. The virus inhibition percentages were measured using the following equation:  $T - V_c / C_c - V_c$ , where T= the optical density (OD) of compound-treated cells, V<sub>c</sub>= OD of virus control, C<sub>c</sub>=OD of cell control (Pauwels et al., 1988). The antiviral activity curve was then generated by plotting virus inhibition percentages against compound concentrations. The 50% and 80% inhibitory concentrations (IC<sub>50</sub> and IC<sub>80</sub>) of the compounds were estimated using linear regression analysis of the antiviral activity curve.

### 4.2.6. Virus binding assay

The effect of the compound on virus attachment was assessed by a virus binding assay, modified from De Logu et al. (2000), as described in Chapter 3 (Page 101) with minor changes. Briefly, 80% confluent cells were pre-chilled at 4°C for 1.5 hours followed by infection with a mixture of the virus (at 100TCID<sub>50</sub>) and the compound at 125  $\mu$ g/mL (unless otherwise stated in Results) that had been pre-incubated together at 4°C for 45 minutes (Bernard et al., 2000). The glycosaminoglycans were given an opportunity to inhibit viral binding at 4°C for another 1.5 hours (for CVB4) or 2 hours (for the other viruses); afterward the monolayers were washed three times with PBS to wash out the excess compounds and any unbound viruses. The plates were then filled with 150  $\mu$ L/well of DMEM/5% FBS and incubated for a further 2 days at 37°C/5% CO<sub>2</sub>. Quantification of results was performed as described in 4.2.5.

### 4.2.7. GAG-lytic enzyme treatment

Heparinase enzymes I and III were reconstituted at a heparinase buffer at 295 Sigma U/mL and 300 Sigma U/mL, respectively. The heparinase buffer was either Tris-based (20 mM Tris-HCl with 50-mM NaCl, 4-mM CaCl<sub>2</sub>, and 0.01% (W/V)



BSA (Volpi and Lindhardt, 2010)) or PBS-based (PBS with 4 mM CaCl<sub>2</sub>, 0.5 mM MgCl<sub>2</sub>, 0.1 % (W/V) glucose, 1% (V/V) FBS, and 0.5% (W/V) BSA (Zautner et al., 2003)). The pH in both buffers was adjusted to 7 (Ma et al., 2006). The buffers were aliquoted and stored at 4°C before use within one week of preparation (Volpi and Lindhardt, 2010; Vera-Bravo et al., 2003). The enzyme solutions were aliquoted and stored at -20°C until use.

Following washing the 80% confluent monolayer three times with PBS, the cells were treated with 10 U (35 µL/well) (unless otherwise stated in results) of heparinase I, heparinase III, and a mixture of the both. Wells overlaid only with 35 µL/well of the buffer were allocated to virus control and cell control (Leong et al., 1998). The plates were incubated at 37°C/5% CO<sub>2</sub> for 60 minutes, followed by removing supernatant and washing the monolayers three times with warm PBS (Zautner et al., 2003). The wells were then filled with 50 µL of DMEM/5% FBS and pre-chilled at 4°C for 90 minutes, afterward 100 TCID<sub>50</sub> of virus was inoculated into both enzyme-treated and virus control wells in 35 µL/well followed by incubation at 4°C for 1.5 hours (for CVB4) or 2 hours (for the other viruses) (Flynn et al., 1993; Vrublevskaia et al., 2002). After washing 3 times with PBS to eliminate un-bound viruses, the wells were overlaid with 150 µL of the growth medium (DMEM + 5% FBS) followed by incubation at 37°C/5% CO<sub>2</sub> for 48 hours. The effect of GAG-lytic enzymes on virus attachment was determined using MTT staining as described in 4.2.5.

### 4.2.8. Statistical analysis

All the treatments were applied in triplicate, and each experiment was independently repeated at least two times. The curves were drawn using GraphPad Prism 5 in which the data were expressed as mean ± standard deviation (SD). An unpaired independent two-sample *t*-Test was used to compare means with each other, with a significance level (*p* value) of 5% or 1%.

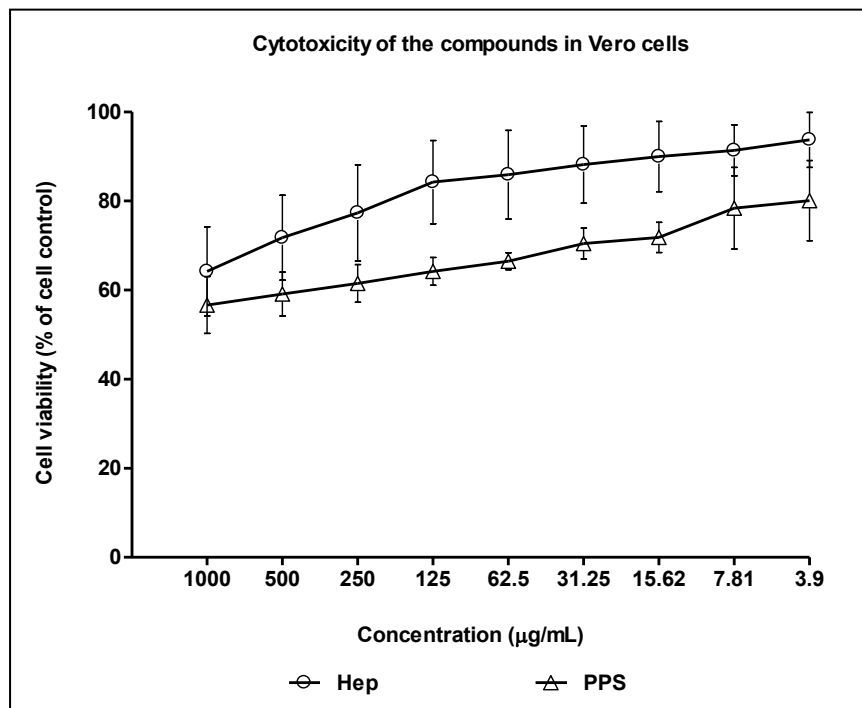
### 4.3. Results

#### 4.3.1. Cytotoxicity assay

The toxicity of Hep and PPS on Vero cells has previously been tested (Figure 4.1.a). While the cytotoxicity response of both Hep and PPS was linear and dose-dependent in Vero cells, the compounds displayed a different trend in neural cells with more fluctuations (Figure 4.1.b). However, statistical analyses revealed no significant difference in cytotoxicity of Hep between Vero and neural cells, except at the concentration 1000  $\mu\text{g}/\text{mL}$  at which Hep was less toxic in neural cells ( $p < 0.05$ ). This was different with PPS in that the observed cytotoxicity response in Vero cells was lower at 500  $\mu\text{g}/\text{mL}$  ( $p < 0.05$ ) and 125  $\mu\text{g}/\text{mL}$  ( $p < 0.01$ ), and greater at 3.9  $\mu\text{g}/\text{mL}$  ( $p < 0.05$ ) in comparison with those in SK-N-SH cells. Overall, Hep exerted less toxicity in both Vero and neural cells compared with PPS at most of the concentrations ( $p < 0.05$ ).

The concentration associated with 50% cytotoxicity ( $CC_{50}$ ), estimated using regression analysis, was greater than the highest tested concentration ( $> 1000 \mu\text{g}/\text{mL}$ ) for Hep in both Vero and neural cells, whereas the  $CC_{50}$  of PPS was 383  $\mu\text{g}/\text{mL}$  in SK-N-SH cells, which was much lower compared with that in Vero cells. The 80% cytotoxicity concentrations were all greater than the highest tested doses of Hep and PPS in both Vero and neural cells.

a



b

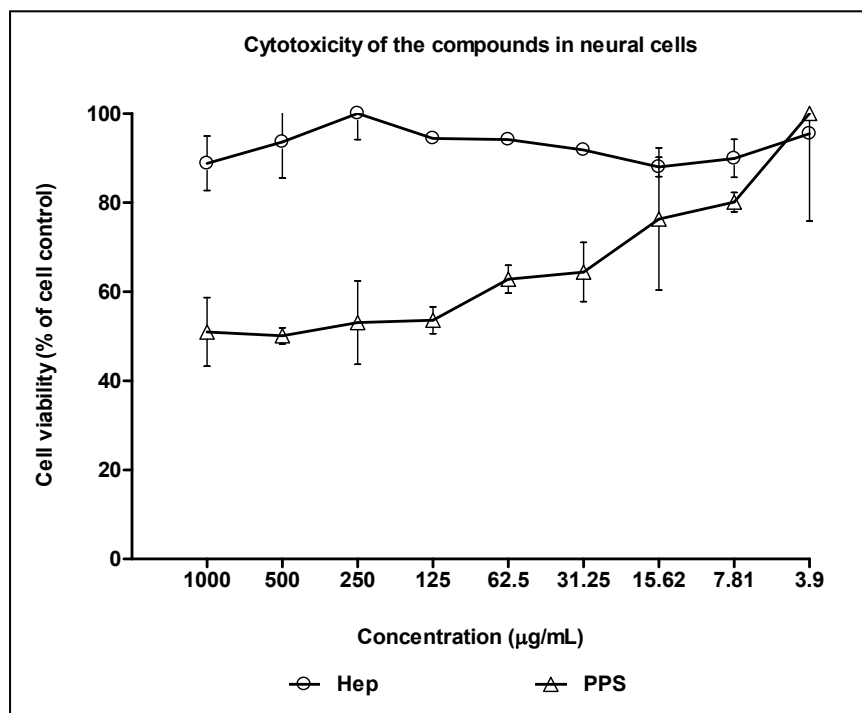


Figure 4.1. Comparison of the cytotoxic effects of Hep and PPS in Vero and neural cells.

Hep and PPS were independently and individually added to 80% confluent Vero cells (a) or neural cells (b). The results represent the mean  $\pm$  SD cell viability percentage of three independent experiments. The 50% and 80% cytotoxic concentrations ( $CC_{50}$  and  $CC_{80}$ ),  $\mu\text{g/mL}$  were calculated using the linear regression analysis.

### 4.3.2. Anti-Enteroviral activity of Hep and PPS

Both HS-like compounds Hep and PPS exhibited low antiviral activities towards the cloned EV71 strain at the highest concentrations (1000, 500 and 250  $\mu\text{g}/\text{mL}$ ), whereas they showed higher activities in the range of 125-7.81  $\mu\text{g}/\text{mL}$  (Figure 4.2 a,b). This trend was not seen with the clinical isolates of EV71 and CVA16, where Hep and PPS exhibited a dose-dependent antiviral activity against these viruses in Vero cells (Figure 4.2 a,b). The antiviral responses of Hep and PPS against CVB4 were quite different by comparison with the other viruses in Vero cells (Figure 4.2 a,b).

Statistical analyses revealed that Hep and PPS exhibited significant antiviral actions ( $p < 0.05$ ) against the cloned EV71 strain at concentrations less than 250  $\mu\text{g}/\text{mL}$ , as compared with cell control and virus control in Vero cells (Chapter 3). Hep at 7.81  $\mu\text{g}/\text{mL}$  showed more potent antiviral activity so that it prevented infection by more than 90% ( $p < 0.05$ ), in comparison with PPS. In this study, it was seen that the antiviral activities of Hep or PPS against the cloned EV71 strain at most of the concentrations were greater than those against both the clinical isolates of EV71 and CAV16 ( $p < 0.05$ ). However, PPS at 1000  $\mu\text{g}/\text{mL}$  displayed more potent antiviral action against the both clinical isolates of EV71 and CVA16 than the cloned EV71 strain ( $p < 0.01$ ). The antiviral response curve of Hep did not reach 50% against the clinical isolates of EV71 or CVA16 in Vero cells, while PPS displayed a virus inhibition over 50% against the clinical isolate of EV71 at both 1000  $\mu\text{g}/\text{mL}$  and 125  $\mu\text{g}/\text{mL}$  (Figure 4.2a,b). Also, it exhibited greater than 50% virus inhibition against the clinical isolate of CVA16 at 1000  $\mu\text{g}/\text{mL}$ .

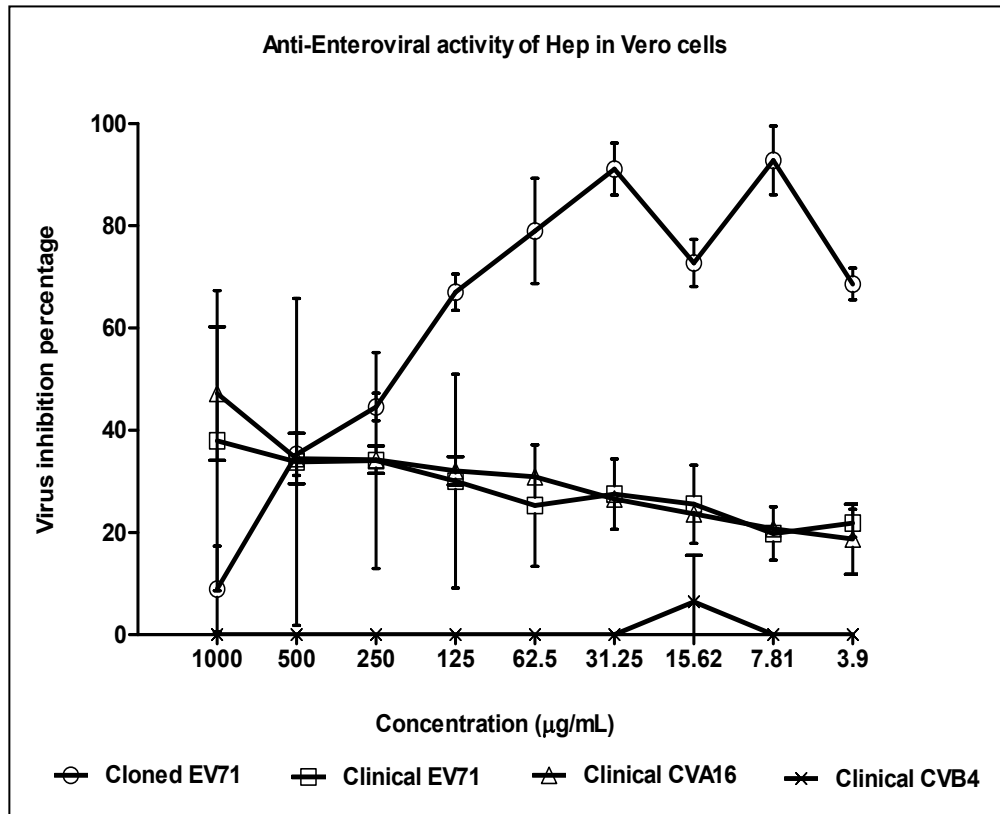
Overall, there was no statistically significant difference in virus inhibition between Hep and PPS against the clinical isolate of EV71 or CVA16 ( $p > 0.05$ ). Also, the antiviral response curves of Hep and PPS against the clinical isolate of EV71 did not significantly differ from those against the clinical isolate of CVA16 in Vero cells ( $p > 0.05$ ).

Hep and PPS showed an obviously different antiviral trend in CVB4 than the other viruses (Figure 4.2 a,b) in Vero cells, which was statistically meaningful for most of the concentrations ( $p < 0.05$ ). None of the tested concentrations of Hep or PPS could inhibit viral infection of the clinical isolate of CVB4 in Vero cells, aside from concentration 15.62  $\mu\text{g}/\text{mL}$  at which PPS exerted a moderate anti-CVB4

activity of 45% that was significantly different from most of the concentrations of PPS ( $p<0.05$ ). At this concentration, no significant difference was observed among the clinical isolates of EV71, CVA16, and CVB4 ( $p>0.05$ ).

In accordance with MTT-quantified antiviral responses, amount of viral CPE inhibition at any concentration of Hep or PPS was visualized and recorded for all the viruses (along with cell and virus controls) using an inverted microscope. As an example, Figure 4.3 demonstrates micrographs of inhibition of clinical EV71-caused CPE by various concentrations of PPS in Vero cells.

a



b

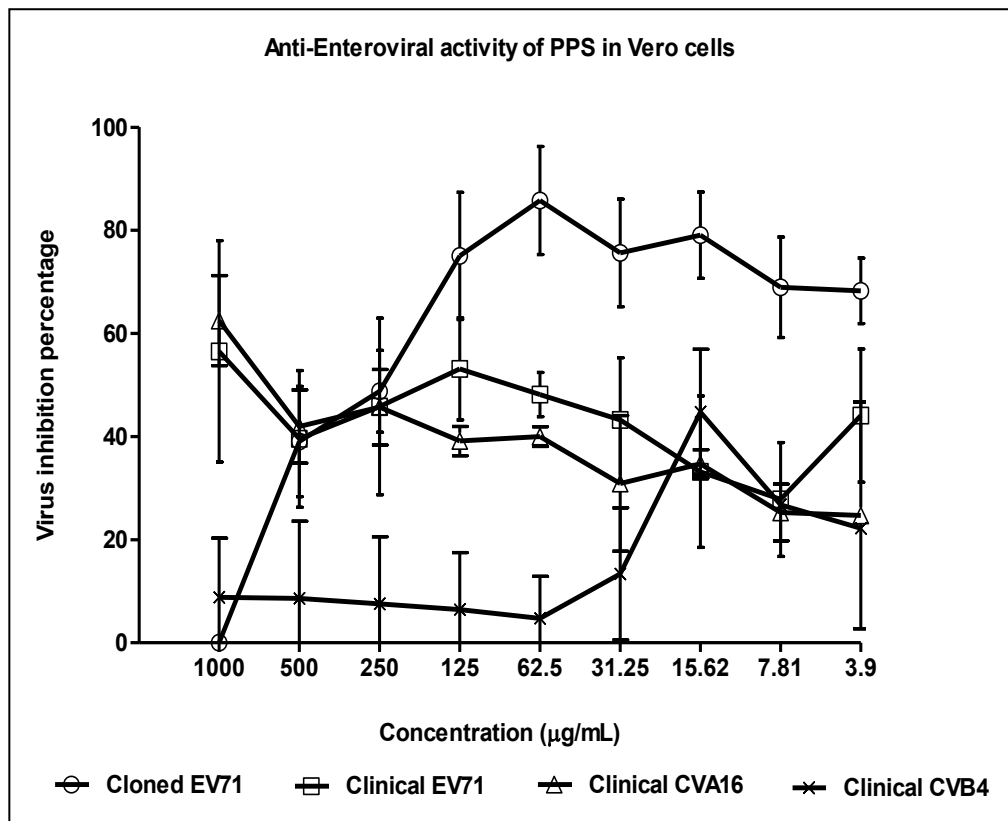


Figure 4.2. Anti-Enteroviral activities of Hep and PPS in Vero cells.

## Chapter Four-Contributions of HS as a Candidate Receptor for Enteroviruses

---

Exposure of 100 TCID<sub>50</sub> of cloned Enterovirus 71, clinical Enterovirus 71, clinical Coxsackievirus A16, and clinical Coxsackievirus B4 to Hep (a) or PPS (b) at nine different concentrations added to 80% confluent Vero cells. The values represent mean  $\pm$  SD virus inhibition percentage collected at 48 hours post infection from at least two independent experiments. The antiviral actions of Hep and PPS against cloned EV71 in Vero cells have been taken from the previous results (Chapter 3, Page 104).

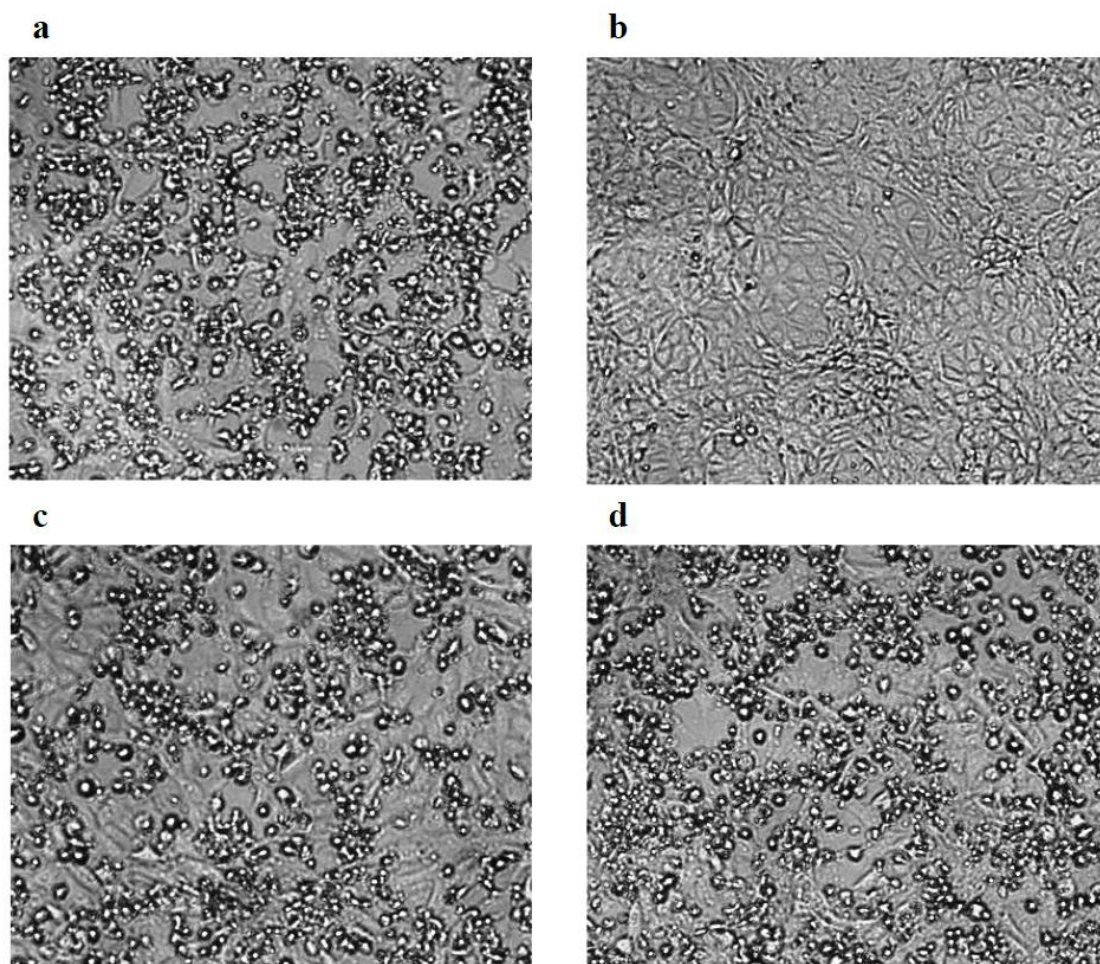


Figure 4.3. Micrographs of clinical EV71 CPE inhibition by PPS in Vero cells



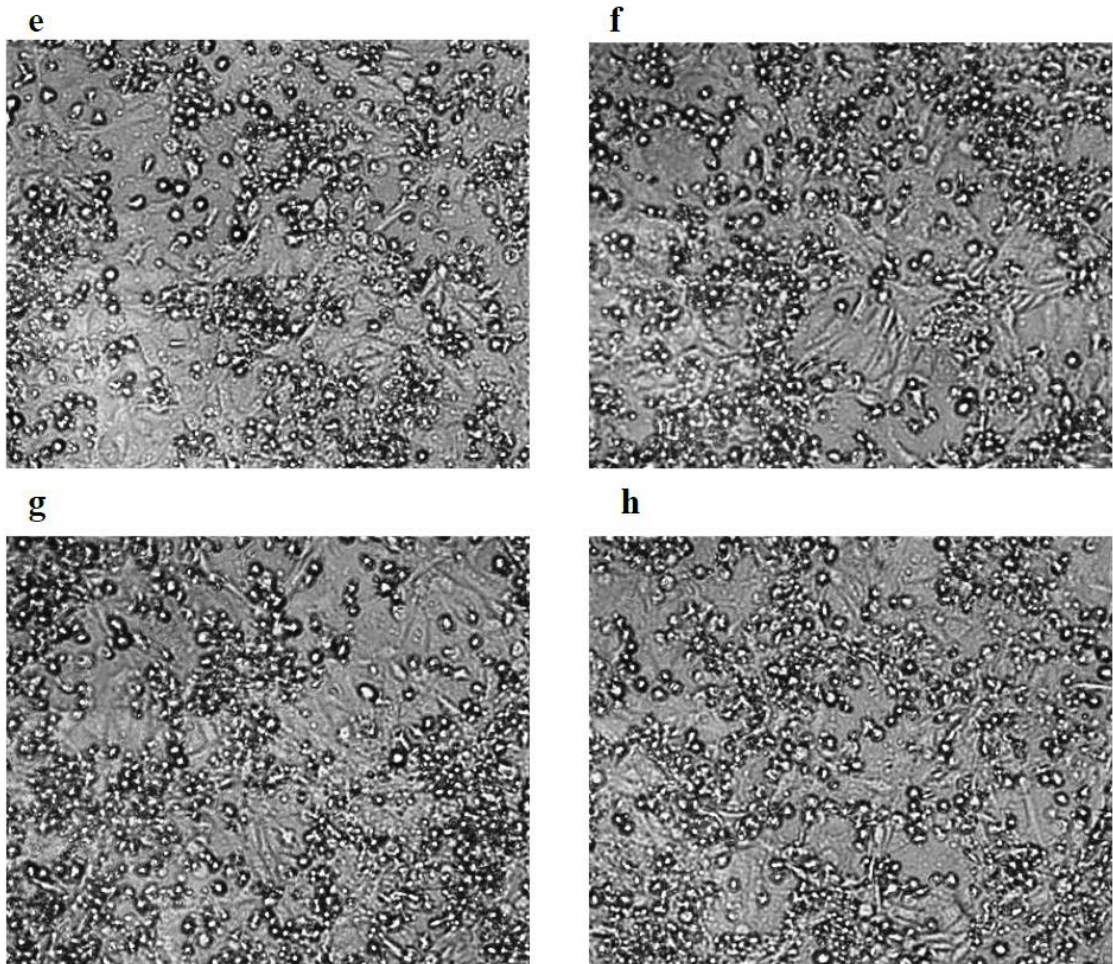


Figure 4.3. Micrographs of clinical EV71 CPE inhibition by PPS in Vero cells (Continued)

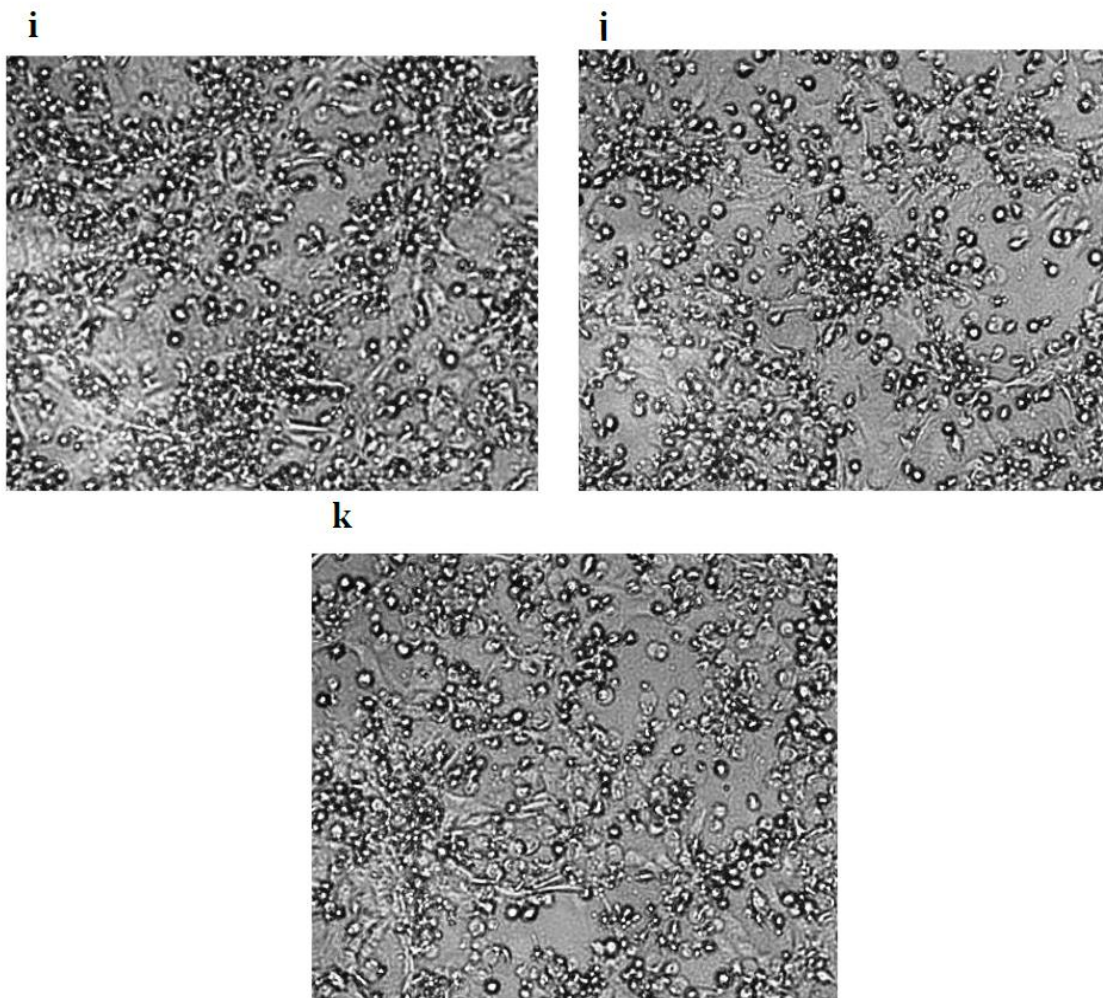


Figure 4.3. Micrographs of clinical EV71 CPE inhibition by PPS in Vero cells (Continued)

## Chapter Four-Contributions of HS as a Candidate Receptor for Enteroviruses

---

Exposure of 100 TCID<sub>50</sub> of clinical Enterovirus 71 to PPS at nine different concentrations added to 80% confluent Vero. Panel a shows virus control, while the panel b represents cell control. Panels c, d, e, f, g, h, i, j, k show clinical EV71-infected cells treated with 3.9, 7.8, 15.62, 31.25, 62.5, 125, 250, 500, and 1000 µg/mL PPS, respectively. The photos (×100 magnification) were taken 48 hours post infection using an inverted microscope (Olympus, CKX 41, Japan) before washing cells with PBS.

In neural cells, no obvious Enteroviral CPE in infected cells was detected, except for the cloned EV71 strain. In addition, the tested Enteroviruses did not efficiently infect neural cells passaged more than 10 times (started from the purchased stock). Therefore, all the assays performed in neural cells essentially needed to be independently repeated several times, which led to an increase in experimental variations. Overall, the quantification assays revealed different antiviral responses for all the viruses as compared with those in Vero cells (Figure 4.4 a,b). Unlike Vero cells, the trend of the antiviral activity curve of Hep against cloned EV71 in neural cells was dose-dependent and did not reach 50% virus inhibition. As a result, antiviral activity of Hep against cloned EV71 in Vero cells was significantly greater than that in neural cells at all the concentrations below 250  $\mu\text{g}/\text{mL}$  ( $p < 0.01$ ). Similarly, PPS behaved differently in neural cells as compared to Vero cells so that its antiviral activity in neural cells was significantly weaker at concentrations 500-7.81  $\mu\text{g}/\text{mL}$  ( $p < 0.01$ ). In neural cells, the antiviral response of PPS against cloned EV71 was different from Hep so that it showed a relatively steady trend from 1000 to 7.8  $\mu\text{g}/\text{mL}$  after which a viral inhibition greater than 50% at 3.9  $\mu\text{g}/\text{mL}$  was seen. However, there was no statistically significant difference in antiviral activities of Hep and PPS against cloned EV71 in neural cells ( $p > 0.05$ ).

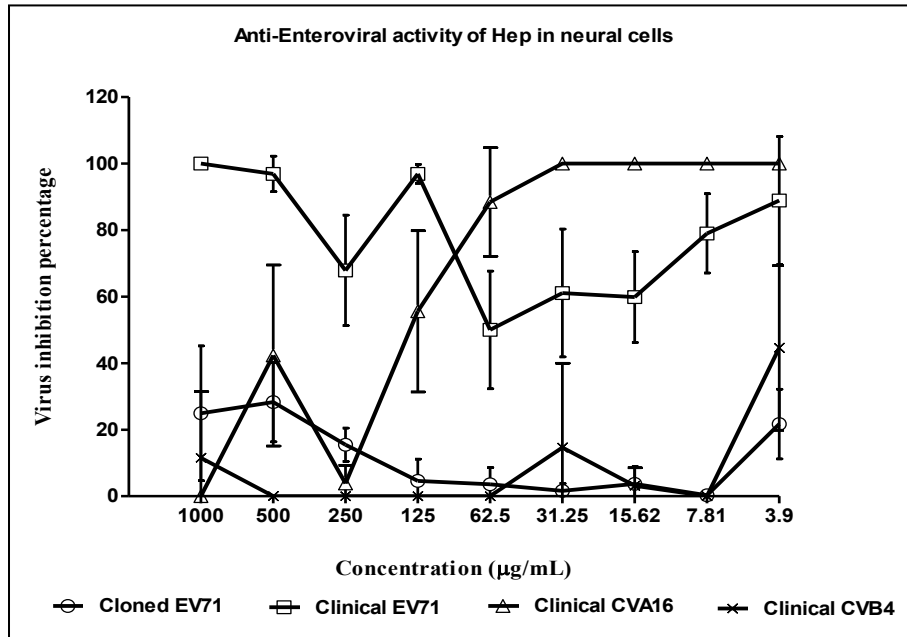
Unlike the cloned EV71, the antiviral activities of both Hep and PPS against clinical EV71 were substantial in neural cells as compared to Vero cells ( $p < 0.05$ ). In neural cells, while PPS completely abolished the virus at all of the tested concentrations, Hep displayed a strong and dose-dependent antiviral action between 1000-250  $\mu\text{g}/\text{mL}$ , followed by a significant fall at 62.5  $\mu\text{g}/\text{mL}$  after which the activity gradually increased by about 88%, even though this increase was not statistically significant ( $p > 0.05$ ) (Figure 4.4 a,b). However, there was no statistically significant difference in antiviral activity between Hep and PPS against clinical EV71 in neural cells ( $p > 0.05$ ).

Similarly, CVA16 infection was considerably inhibited by Hep in neural cells. For the concentrations 62.5-3.9  $\mu\text{g}/\text{mL}$ , Hep displayed a significantly greater antiviral action against CVA16 in neural cells as compared to that in Vero cells ( $p < 0.05$ ). The figures for PPS were more variable so that there was no statistical difference at 62.5 and 3.9  $\mu\text{g}/\text{mL}$  ( $p > 0.05$ ); that is, the viral inhibition was greater in

Vero cells at the concentrations 1000-250  $\mu\text{g}/\text{mL}$ , and greater in neural cells at the rest of the concentrations ( $p < 0.05$ ). In addition, antiviral activities of Hep and PPS did not significantly differ from each other against CVA16 in neural cells ( $p > 0.05$ ), except for 62.5  $\mu\text{g}/\text{mL}$  at which Hep exerted greater antiviral activity than PPS ( $p < 0.05$ ).

The antiviral response of Hep towards CVB4 was noticeably different from the other viruses (Figure 4.2c). Hep failed to prevent CVB4 infection at most of the concentrations, except at 3.9  $\mu\text{g}/\text{mL}$  at which a moderate virus inhibition was observed, whereas the PPS antiviral activity was inconclusive. Overall, CVB4 could not efficiently infect neural cells.

a



b

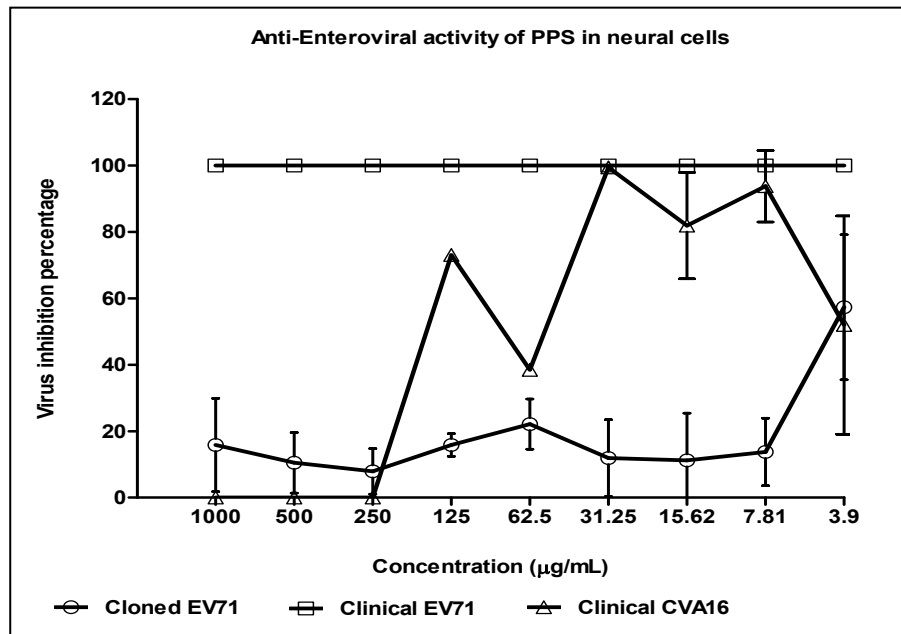


Figure 4.4. Anti-Enteroviral activities of Hep and PPS in neural cells.

100 TCID<sub>50</sub> of clinical isolates of cloned EV71, clinical EV71, clinical CVA16, and clinical CVB4 were exposed to Hep (a) or PPS (b) at nine different concentrations added to 80% confluent SK-N-SH cells. The values represent mean ± SD virus inhibition percentage collected at 48 hours post infection from at least three independent experiments. The antiviral activity of PPS against CVB4 in neural cells is not shown, as the virus did not grow in neural cells efficiently, and thus, the results were inconclusive

### 4.3.3. Enteroviral attachment in the presence of GAGs compounds

In order to assess the possible role of cell surface HS in Enteroviral binding to host cells, the effect of soluble HS mimetics (Hep and PPS) on inhibiting the Enteroviral attachment to Vero and neural cells was evaluated. Chilled cell monolayers were infected with a mix of the virus and the compound (at 125 µg/mL) that had been incubated together at 4°C for 45 minutes, and viral attachment was allowed to occur at 4°C. The microscopic observations and the quantification results revealed that the cloned EV71, clinical EV71 and clinical CVA16 isolates were all significantly prevented from binding to Vero cells by Hep and PPS. In addition, there was no significant difference in preventing Enteroviral attachment between Hep and PPS ( $p>0.05$ ). While Hep could prevent attachment of the clinical isolate of EV71 by more than 68%, the figures were over 56% for the cloned EV71 and 43% for the clinical CVA16. However, there was no statistically significant difference in virus binding inhibition by Hep between the three viruses ( $p>0.05$ ).

In line with Hep, PPS greatly inhibited the binding of the cloned EV71 and clinical EV71 isolate by about 60% and 65%, respectively. Nevertheless, it exerted a moderate inhibition (42%) for attachment of CVA16 to Vero cells, making a statistical difference in preventing virus attachment by PPS between clinical EV71 and clinical CVA16 ( $p<0.05$ ). As expected from the antiviral assay results, CVB4 attachment was not prevented by Hep or PPS (Figure 4.5. a). In addition, it was also observed that CVB4 needed just 45 minutes to bind to Vero cells, whereas it took at least 2 hours for the other viruses to do so.

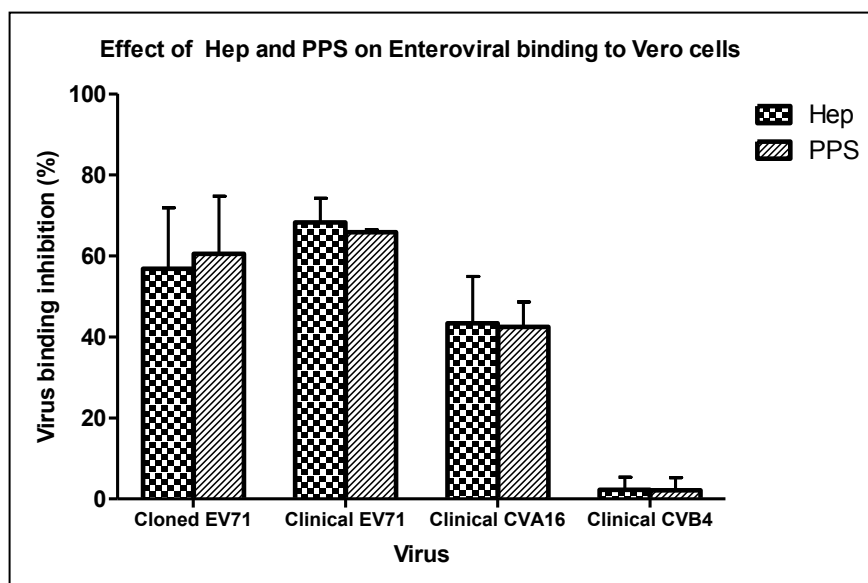
The Attachment assays for all the viruses were performed with Hep and PPS at 125 µg/mL, based on the results seen in the antiviral assays. Apart from this concentration, the effect of Hep and PPS on CVB4 binding was also assessed at 15.62 µg/mL. The reason was that in the antiviral assays both Hep and PPS unexpectedly had demonstrated slight antiviral activities against CVB4 in Vero cells only at 15.62 µg/mL (Figure 4.2a,b). The results showed that virus inhibitions by Hep and PPS at 15.62 µg/mL were around 15% and 12%, respectively (Appendix 4). Therefore, there was no statistically significance difference in CVB4 attachment inhibition between different concentrations of Hep or PPS as well as between Hep and PPS ( $p>0.05$ ).

In neural cells, the effects of Hep and PPS on Enteroviral binding were much more pronounced than those in Vero cells. PPS completely blocked viral attachment to neural cells for all the three viruses, cloned EV71, clinical EV71, and clinical CVA16 (Figure 4.5. b). While Hep significantly prevented binding of clinical EV71 to neural cells, it failed to inhibit cloned EV71 attachment and exerted only 26% viral attachment inhibition for clinical CVA16. Consequently, there was a noticeable significant difference between Hep and PPS in the CVA16 as well as cloned EV71 attachment inhibition ( $p<0.01$ ). Since CVB4 could not efficiently infect neural cells, the attachment assay results for this virus were inconclusive.

Microscopic controlled, repeated observations were also carried out to monitor whether observed viral CPE inhibited by Hep or PPS are in accordance with the MTT-quantified attachment assay (Figure 4.6).



a



b

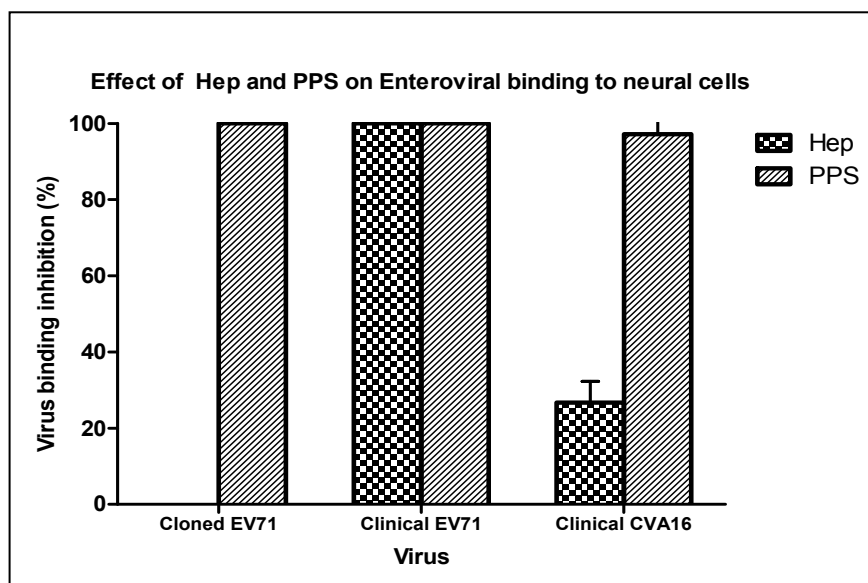


Figure 4.5. The effect of GAGs on Enteroviral binding to Vero and neural cells.

Pre-chilled cells were treated with the mix of each compound and the virus that had been pre-incubated at 4°C for 45 minutes. Viral attachment was then allowed to occur at 4°C. The values represent mean ± SD virus binding inhibition percentage collected at 48 hours post infection from at least two independent experiments. The viral inhibition activities of Hep and PPS against CVB4 in neural cells are not shown, as the virus did not get into neural cells efficiently, and thus, the results were inconclusive.

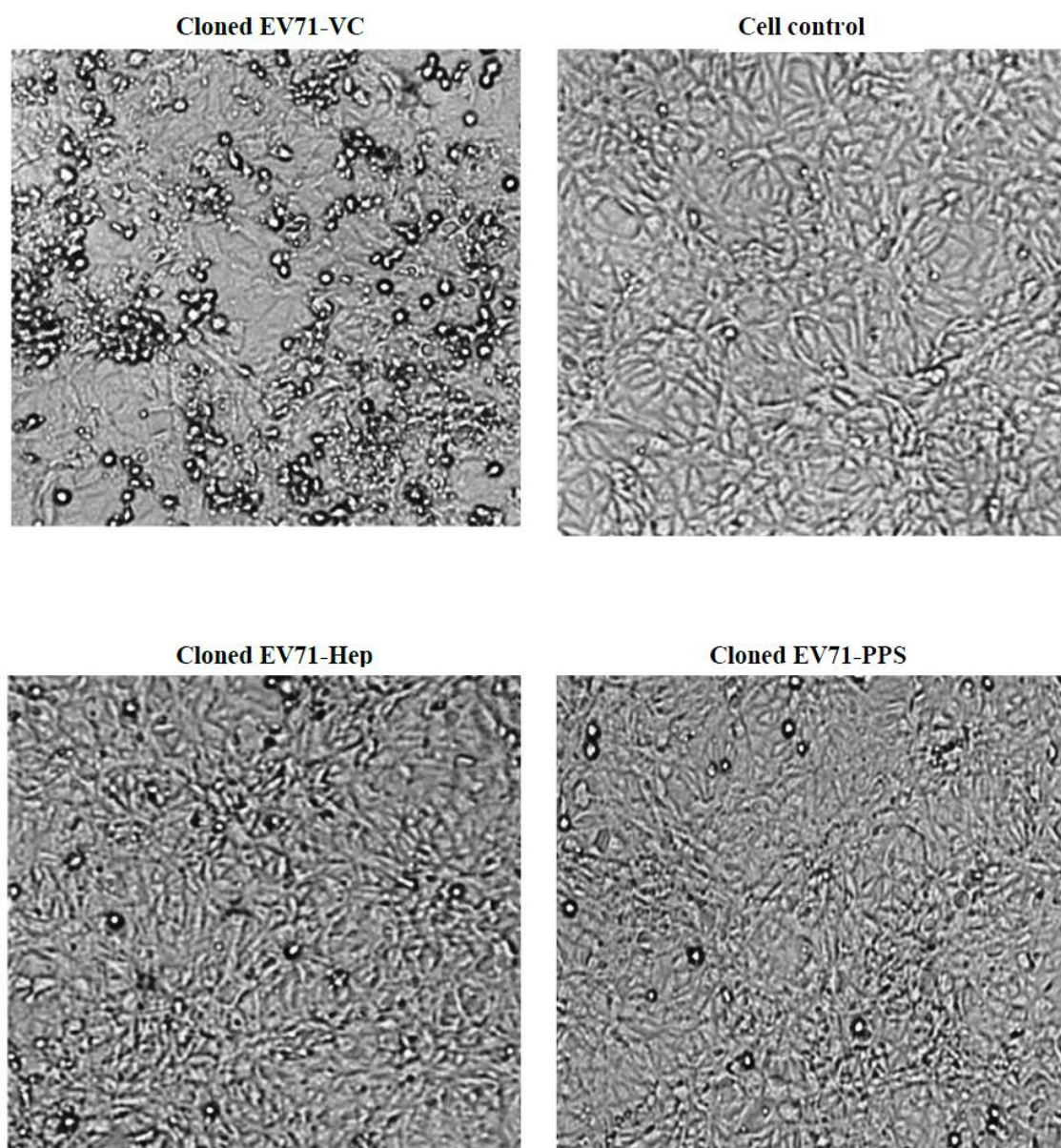


Figure 4.6. Micrographs of inhibition of Enteroviral binding to Vero cells

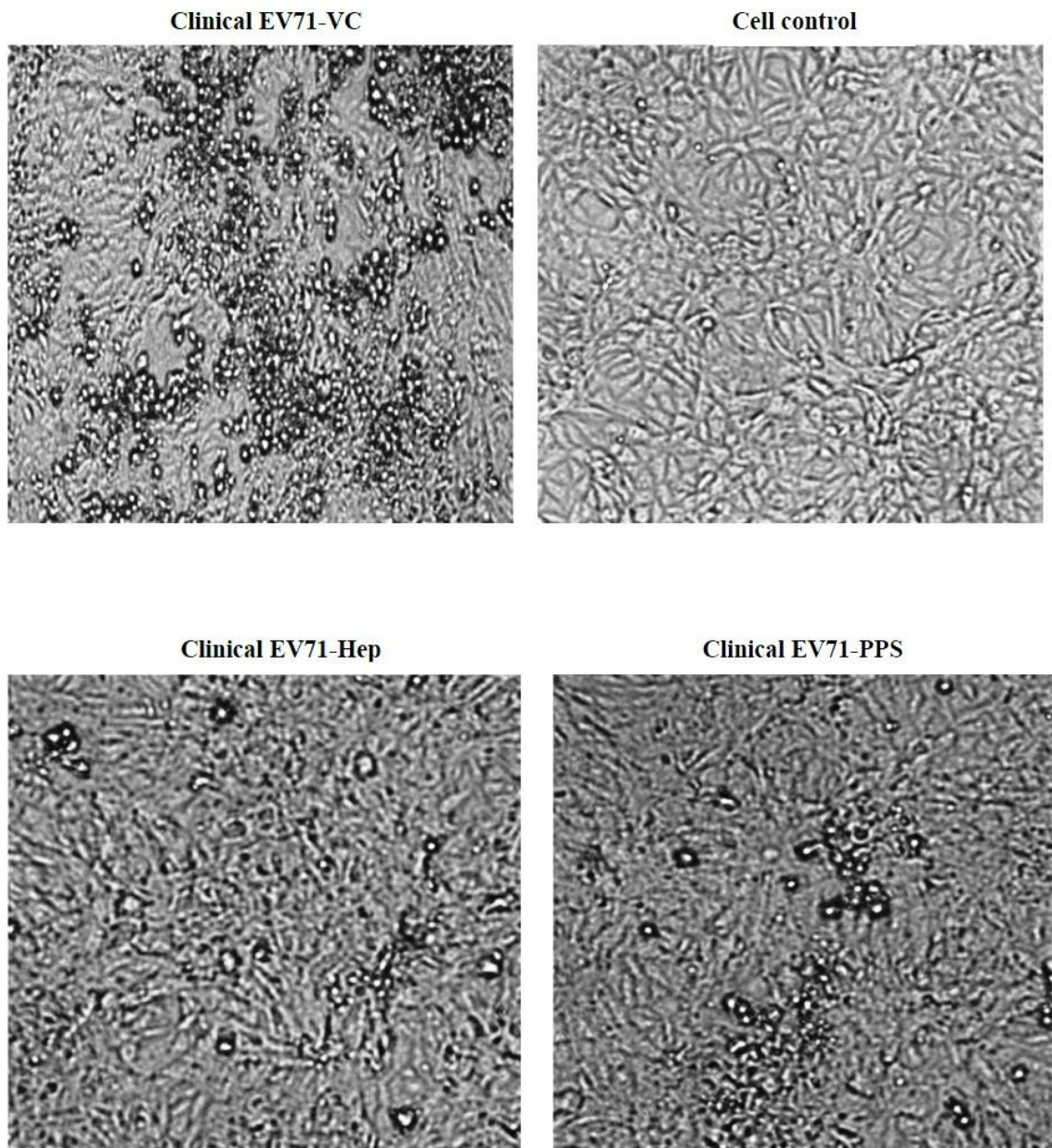


Figure 4.6. Micrographs of inhibition of Enteroviral binding to Vero cells (continued)

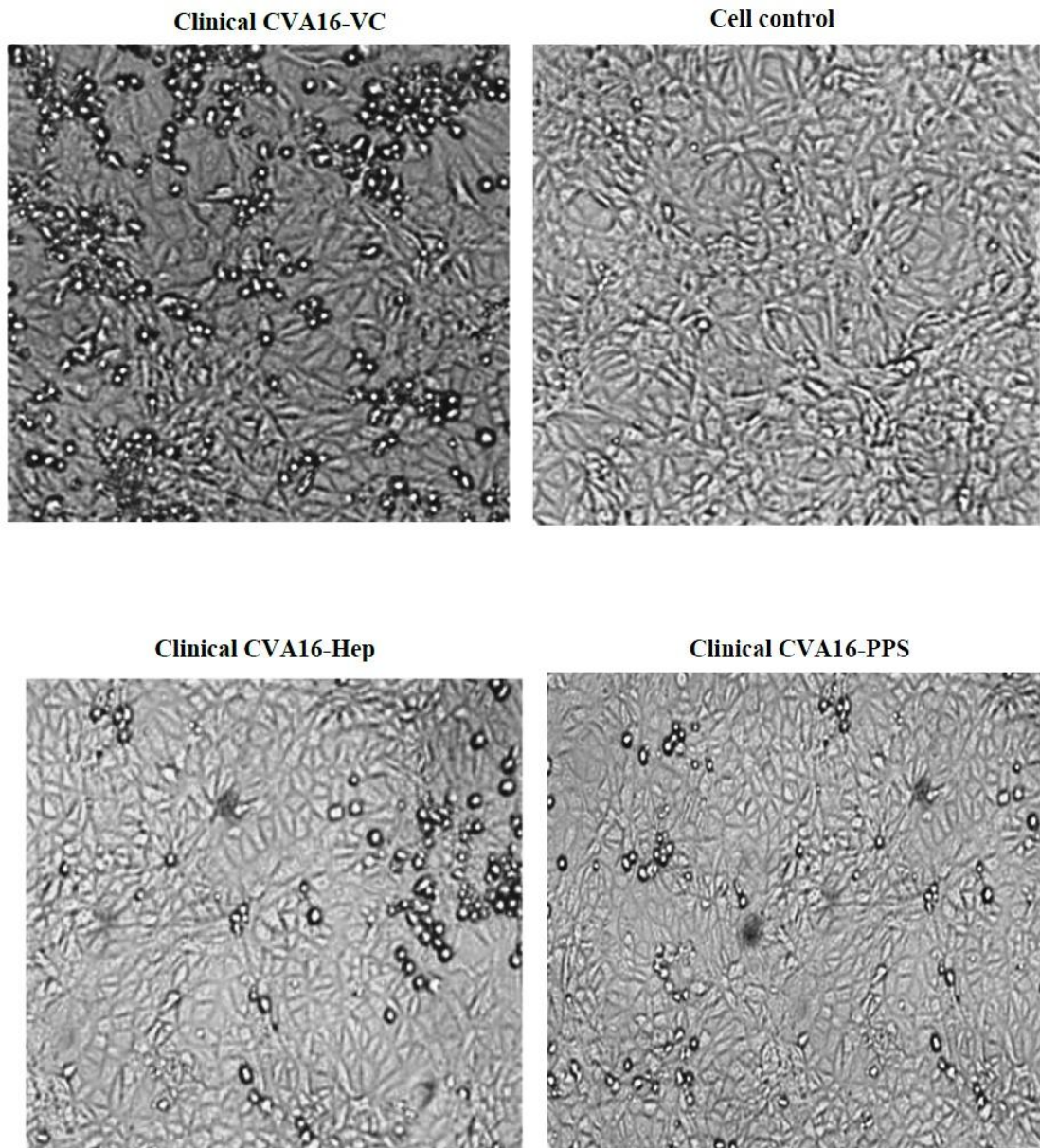


Figure 4.6. Micrographs of inhibition of Enteroviral binding to Vero cells (continued)

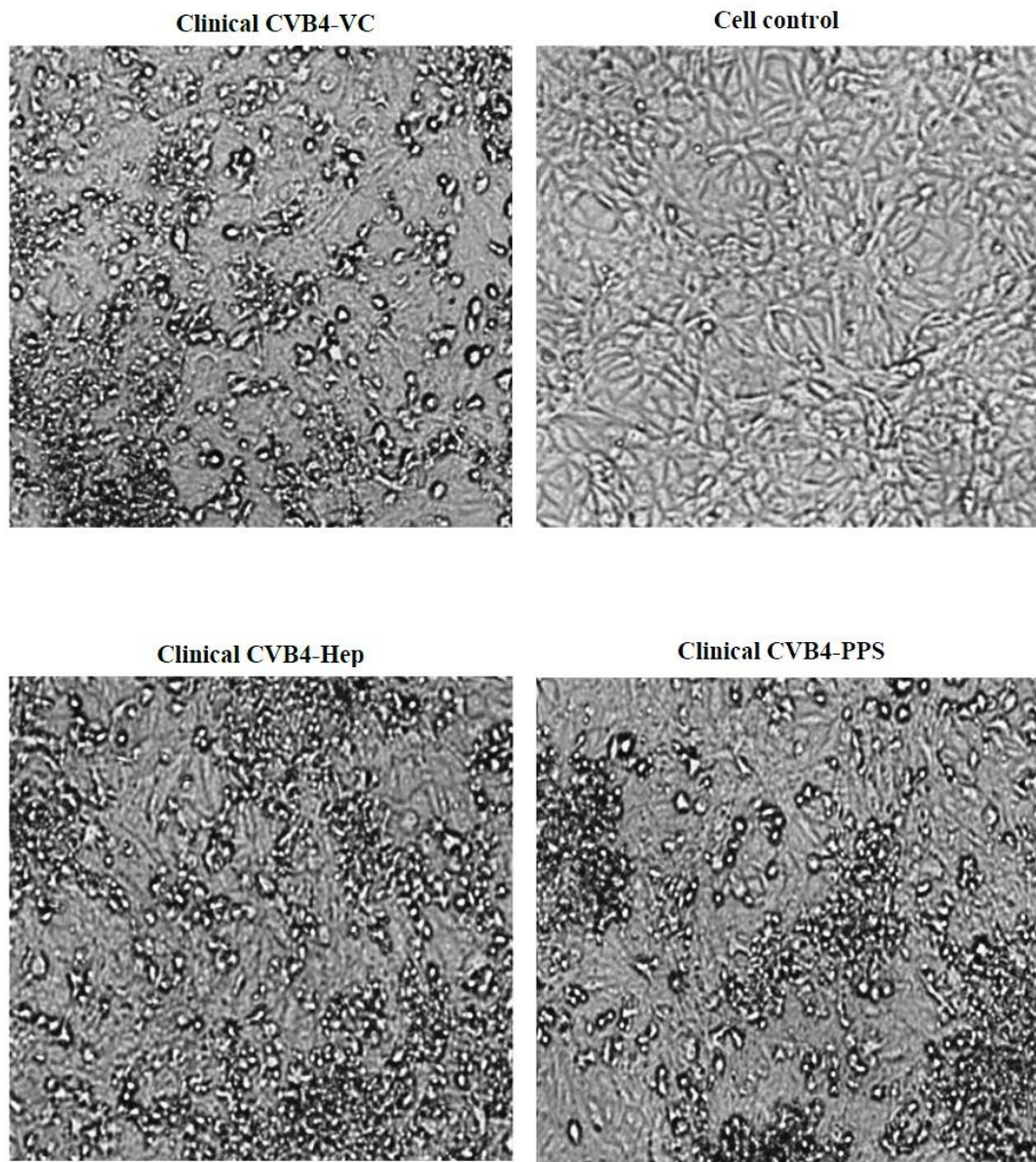


Figure 4.6. Micrographs of inhibition of Enteroviral binding to Vero cells (continued)

## Chapter Four-Contributions of HS as a Candidate Receptor for Enteroviruses

---

Pre-chilled cells were treated with a mix of each compound and the virus that had been pre-incubated at 4°C for 45 minutes. Viral attachment was allowed to occur at 4°C. Panels show virus-infected cells treated with either Hep or PPS at 125 µg/mL, in comparison to cell control (not infected or treated) and virus control (Enteroviral-infected cells not treated with the compounds). The assays were performed in triplicate and repeated at least three times independently. The photos (×100 magnification) were taken 48 hours post infection using an inverted microscope (Olympus, CKX 41, Japan) before washing the cells with PBS.

### 4.3.4. Enteroviral attachment in the absence of cell surface HS

To confirm direct interaction of the Enteroviruses and cell surface GAGs, Enteroviral attachment to heparinase-treated cells was investigated. Vero and neural cells were treated with heparinase I, heparinase III or a mix of both enzymes after which attachment was performed at 4°C as described for virus binding assay. While treatment with heparinase I inhibited the cloned EV71 attachment to Vero cells by about 24%, it demonstrated viral attachment inhibition of over 52% for the clinical EV71. Treatment with heparinase III or a mix of heparinase I and III did not demonstrate significant viral inhibition for the cloned EV71 or clinical EV71 isolates. In addition, no inhibition was observed with enzyme-treated cells infected with CVA16 and CVB4 (Figure 4.7). Instead, the CVB4 infection was significantly higher in heparinase-treated Vero cells as compared to non-treated ones ( $p < 0.01$ ). The cloned EV71 binding to neural cells was not prevented by the heparinase enzymes. In addition, the heparinase results were inconclusive for clinical EV71, clinical CVA16, and CVB4 in neural cells.

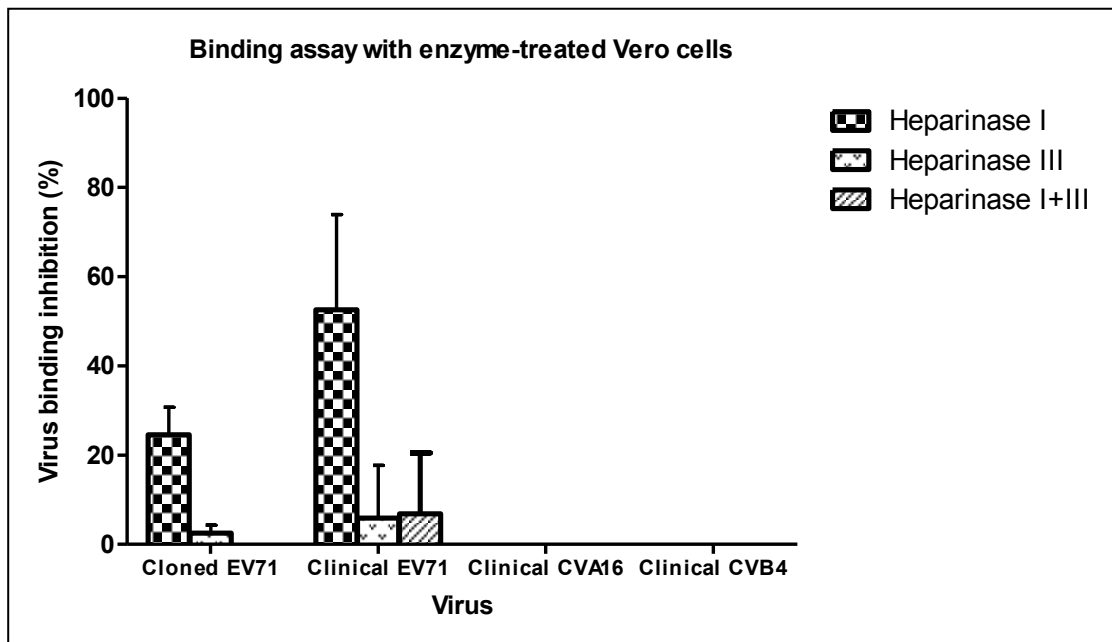


**Figure 4.7. Relative effect of heparinase enzymes on Enteroviral binding to Vero cells.**

Vero cells were treated with heparinase enzymes. Then, the cells were pre-chilled at 4°C followed by infection with virus. Viral attachment was allowed to occur at 4°C. The values represent mean  $\pm$  SD virus binding inhibition percentage collected at 48 hours post infection from at least two independent experiments.



### 4.4. Discussion

Enteroviruses use a wide range of cell surface receptors, including SCARB2, CD162, VLA-2, CAR, CD55,  $\alpha_v\beta_6$  integrin, GRP78- MHC-I, ICAM-1, sialic acid, and HS (Table 4.1). While there are limited reports that show members of HEV-B may utilize HS as a capture co-receptor (Goodfellow et al, 2001; Zautner et al, 2003; Escribano-Romero et al, 2004), no study has been undertaken to examine HS usage by HEV-A or HEV-C. Previous studies have shown that several glycosaminoglycan mimetic compounds, including HS, Hep and PPS exhibited significant antiviral activities ( $p < 0.05$ ) against the infection of a cloned strain of EV71 at concentrations less than their toxic dose as compared with ribavirin (as a positive control) in Vero cells (Chapter 2). The tested compounds also showed a potential to inhibit the viral binding to Vero cells, suggesting a possible role for cellular HS to mediate the early infection of EV71 in Vero cells; albeit the results were not quantified. In this study, therefore, the possible roles of cell surface HS in mediating viral infection and attachment for members of HEV-A and HEV-B were assessed.

Enzymatic cleavage of cell surface HS of Vero cells by heparinase I had a moderate effect on the attachment of the cloned EV71 strain, while treatments with heparinase III or a mix of heparinases I and III did not prevent the viral attachment. Heparinase I primarily cleaves highly sulphated heparin-like domains of the cell surface HS, while heparinase III acts exclusively on less sulphated domains of the cell surface HS (Ernst et al., 1995). In addition, abolition of the entire cell surface HS can be achieved through treatment of cells with heparinase I and III together. These observations appear to be in accordance with the previous results where Hep (as a highly sulphated compound) exhibited significantly higher antiviral activity as well as viral attachment inhibition against the cloned EV71 strain in Vero cells, in comparison with those of less sulphated compounds, i.e. HS or PPS (Chapter 2).

However, the extent of the viral attachment inhibition by enzymatic treatment was not well compatible with the previous antiviral potencies of Hep or PPS and the current virus binding assays, particularly if it be taken into account that the same batch of the virus was used for both heparinase treatment and virus binding assays. One possibility might be that the cloned EV71 attachment is not merely dependent on cell surface HS in Vero cells. Therefore, it could be postulated that the

virus alternatively uses one of the three suggested candidates for cell receptors of EV71; SCARB2 (Yamayoshi et al., 2009), PSGL (Nishimura et al., 2009) or sialic acid-linked glycans (Yang et al., 2009), in the absence of cell surface HS in Vero cells. Another possibility is that the antiviral potencies of Hep or PPS toward the infection/attachment of the cloned EV71 strain might be unspecific and more related to electrostatic nature of interaction between these soluble GAGs and the virus (Escribano-Romero et al, 2004).

In addition, it cannot be ruled out that the cloned EV71 strain has likely attained its capability to interact with HS through adaptation to cell culture, like viruses such as FMDV (Sa-Carvalho et al., 1997; Baranowski et al., 1998; Escarmis et al., 1998; Neff et al., 1998), SIN (Klimstra et al., 1998), and VEE (Bernard et al., 2000). This hypothesis might be supported with the fact that RNA viruses have a high mutation rate that allows them to adapt quickly to environmental changes (Escribano-Romero et al, 2004) and the cloned EV71 strain has been passaged for a relatively long period in our study. Therefore, amino acid changes would possibly occur in the virus capsid during succeeding cultures, giving the virus the capability to use cell surface HS. This warrants further studies by genome analysis in order to determine point mutations in the viral capsid that are responsible for interaction with HS. Overall, the results suggest that cell surface HS may not be essential for the cloned EV71 infection or attachment in Vero cells.

In this study, neither Hep nor PPS showed significant potencies against the cloned EV71 infection in neural cells. Moreover, while PPS showed a substantial effect on viral attachment in neural cells, Hep failed to inhibit the cloned EV71 attachment. As expected, the cloned EV71 binding to SK-N-SH cells was not prevented by the heparinase enzymes. Thus, overall it can be speculated that the cell surface HS may not play an important role in the cloned EV71 infection or attachment in neural cells.

In order to diminish the possibility of cell culture adaptation for HS use, the clinical isolates of Enteroviruses were maintained at a very low passage number. Inhibition of viral infection by soluble GAGs is conventionally considered an approach to determine the viral capability to bind to cell surface HS (Escribano-Romero et al, 2004). As such, in this study, the antiviral activities of soluble Hep and PPS at various concentrations were investigated against the tested clinical

Enteroviruses in Vero cells as well as SK-N-SH cells. The moderate antiviral activity of Hep and PPS against the clinical isolate of EV71 initially suggested a difference between laboratory strains of EV71 and clinical isolates in cell HS usage. However, further tests demonstrated that both Hep and PPS could significantly interfere with viral binding to Vero cells for clinical EV71. Besides, removing the cell surface HS by heparinase I obviously prevented clinical EV71 attachment to Vero cells, whereas treatment with heparinase III or a mix of heparinases I and III could not offer a significant prevention of viral attachment. One possibility might be that the addition of the both enzymes at the tested concentration could have damaged the cells. Thus, the role of heparinase in removing cellular HS and preventing viral attachment could have been masked by a negative impact of the mixture of the enzymes on the host cells.

It is thus concluded that clinical EV71 may utilize highly sulphated (Hep-like) domains of the cell surface HS during infection or attachment in Vero cells. This conclusion appears to be compatible with the antiviral action of Hep against viral attachment. Thus, unlike cloned EV71, heparin-like domains of cell surface HS are specific and necessary for at least one clinical isolate of EV71 infection or binding to Vero cells.

Hep and PPS blocked clinical EV71 infection and attachment in neural cells. However, it should not be ignored that the inconsistent pattern of inhibition of clinical EV71 by Hep might in part reflect issues related to technical optimization. In addition, heparinase assays with clinical EV71 did not generate convincing results in neural cells. Therefore, no conclusions could be made as to HS usage by clinical EV71 in neural cells. This might suggest the presence and the action of other cell receptors for clinical EV71 in these cells. Unlike poliovirus, for which a neural specific factor has been determined, there is still no report of a neural specific factor that mediates EV71 neural pathogenesis (Weng et al, 2010). The other possibility might be that the role of Hep or PPS in the viral infection and attachment is not demonstrated through interference with virus binding to HS but via other unknown mechanism(s) of action, which warrants further investigations. Since EV71 is well known for causing severe neurological complications, the strong antiviral actions of Hep and PPS against clinical EV71 infection in neural cells would be imperative, particularly as Hep did not exert toxicity at any concentration in neural cells.

While Hep or PPS exhibited a relatively significant antiviral activity against CVA16 infection and attachment in Vero cells, no viral inhibition for this virus was observed in cells treated with heparinase enzymes. Therefore, the viral use of cell surface HS as a binding co-receptor in Vero cells cannot be confirmed. It has recently been discovered that SCRAB2 can serve as an attachment receptor for CVA16 (Yamayoshi et al., 2009). Thus, one could propose that CVA16 might alternatively use either HS or SCRAB2, or another yet to be identified cell receptor to bind to Vero cells. Yet, the role of HS in mediating infection or binding of CVA16 in Vero cells cannot be ruled out, as interaction of this low passage clinical isolate with Hep (in the attachment assay) is less likely to be gained only through adaptation to cell culture. Therefore, further genome sequencing and other confirmatory experiments would be useful to detect motifs in the viral capsid that confer the capability to bind to cell surface HS in addition to other potential cell receptors. Both Hep and PPS at non-toxic concentrations could considerably prevent the clinical CVA16 infection in neural cells, but only PPS demonstrated strong antiviral activity against the viral attachment. Like clinical EV71, the results of heparinase assays against clinical CVA16 were not conclusive.

Infection by CVB4, a member of HEV-B, was considerably different when compared to the other viruses of HEV-A. Overall, no significant inhibition was observed in CVB4 infection or attachment in Vero cells or neural cells. Strangely, PPS only at 15.62 µg/mL demonstrated considerable antiviral action in Vero cells at which it failed to inhibit the viral binding. In addition, not only did heparinase treatment fail to prevent CVB4 binding to Vero cells, but the heparinase-treated cells showed a greater degree of the viral infection as compared to untreated cells infected with CVB4. In a similar way, Reddi and Lipton (2002) reported that removal of sialic acid from the cell surface could significantly increase the viral binding and infection of a high-neurovirulence strain (GDVII) of Theiler's murine encephalomyelitis virus, suggesting that the virus can possibly bind to both HS and an unknown protein receptor to which direct access is hampered by sialic acid. Also, it has previously been demonstrated that CVB4 binds to the coxsackievirus and adenovirus receptor (CAR, a 46 kDa transmembrane glycoprotein) in Chinese hamster ovary (CHO) cells (Bergelson et al, 1997; Tomoko et al, 1997; Bergelson et al, 1998). Therefore, it can be suggested that eliminating the HS cell surface could

possibly eliminate the influence of HS on CAR or another unknown cell surface receptor, leading to an increased viral infection. In addition, CVB4 bound to Vero cells much quicker than the other viruses in the presence of Hep or PPS during attachment assays; this might be because Hep or PPS delayed binding CVA16, cloned EV71, and clinical EV71 to Vero cells, in contrast to CVB4.

This study is the first to clarify that CVB4 does not likely use HS for infection and attachment to Vero cells. These findings appear to be also in agreement with the previous study, where it was concluded that Hep failed to inhibit infection of strains of Coxsackievirus B2 and B3 in RD cells (Goodfellow et al, 2001). By contrast, in the other only report it was shown that a laboratory strain of CVB3 utilized HS for binding (Zautner et al., 2003). Thus, it can be speculated that the binding of CVB3 to HS might be a cell culture phenomenon and not a characteristic of the cell receptors of Coxsackieviruses in nature. Of note was that in the current study, CVB4 did not efficiently grow in neural cells, leading to a low level of infection or binding. This could be attributed to the fact that this virus was a low passage clinical isolate of CVB4 and has not been adapted to grow in neural cell culture. Yet, it can be speculated that cell surface HS does not appear to play an important role in the CVB4 infection or attachment in neural cells, as Hep (as a HS-like compound) failed to prevent viral infection of CVB4 in neural cells.

In this research, various experiments were employed to confirm the role of cell surface HS in viral infection and binding for members of Enteroviruses. Nevertheless, it would also be valuable to use other approaches to validate or extend the attained results. In this regard, direct binding of Enteroviruses to heparin could be assessed by affinity chromatography on heparin-Sepharose columns (Escribano-Romero et al, 2004). In addition, the use of a GAG-deficient cell line and/or mutant virus strain that lacks the HS usage character could prove the role of HS in virus pathogenesis and infection (Reddi and Lipton, 2002). Along with GAGs and heparinase enzymes, the use of sialic acid and neuraminidase could demonstrate if the virus also utilizes sialic acid as an attachment receptor (Yang et al., 2009). The structural protein genes of the clinical EV71 isolate needs to be sequenced to confirm if there are motifs in the viral capsid proteins that have conferred the HS usage capability to the virus, in comparison with cloned EV71 and CVA16. In addition, it would be worthy to investigate the effect of GAGs against clinical

isolates of EV71 infection in a murine model to examine the role of HS in virulence or neurovirulence *in vivo*.

In conclusion, the findings presented here provide evidence for differences between the two main groups of non-polio Enteroviruses in binding to cell surface HS. While cellular HS was shown to be involved in mediating infection/attachment for clinical isolates of HEV-A, clinical CVB4 as a member of Coxsackieviruses most likely does not use HS for infection/attachment. These findings might suggest directions for further studies on pathogenesis or designing antiviral drugs for HEV groups A and B. However, according to the flexibility in picornavirus receptor usage (Baranowski et al., 1998; Zautner et al., 2003), it cannot be ruled out that the viruses may easily adapt to bind to different receptor(s) even in the same cell type (Escribano-Romero et al, 2004). In neural cells, although the involvement of cellular HS in mediating Enteroviral infection could not be confirmed, strong antiviral potencies of Hep and PPS against the clinical EV71 and clinical CVA16 isolates would be of importance. More specifically, because EV71 is well known for causing severe neurological complications, it is of interest to follow these findings *in vivo*. In addition, the mechanism underlying antiviral activities of Hep and PPS against clinical EV71 in neural cells warrants further investigation.

## 5. Chapter Five: Microarray Analysis of Antiviral Activity of Heparin against Enterovirus 71

### 5.1. Introduction

In the field of antiviral research, a close interaction and association between chemists and biomedical scientists has led to many successful studies recorded in the literature as to the antiviral activities of natural, semi-synthetic, or synthetic compounds (De Clercq, 2005). Whilst discovering or confirming antiviral activity of a compound *in vitro* or *in vivo* is essential, it is of vital importance to attain a deeper understanding of the mechanisms underlying antiviral actions of the compound. This will assist scientists to continue improving current therapeutic strategies as well as designing new therapies (Feld and Hoofnagle, 2005).

There are many different approaches to identify the mechanisms of action of antiviral drugs. One of the most successful approaches to date is global gene-expression analysis using DNA microarrays (Früh et al., 2001). Having the capability to measure expression of thousands of genes simultaneously with low detection limits, DNA microarray has had a great impact on a wide range of experimental and applied sciences (Campbell and Ghazal, 2004), including antiviral drug design. There are numerous reports of the use of microarray technology to determine changes in cellular gene expression induced directly by virus and/or cellular defence system following viral infection (Früh et al., 2001). Information revealed by such cellular arrays can be merged with those of viral arrays, leading to determination of changes in the transcriptome of a host cell following viral infection. This is very useful for antiviral drug discovery, as, it is, for example, possible to target host cell proteins that are necessary for virus propagation and pathogenesis (Früh et al., 2001).

In addition to microarray analysis of virus-infected cells, microarray technology can be used to directly assess expression profiles of host genes treated by antiviral drugs. One of the better known examples of this is discovering the mode of action of the antiviral activity of interferons (IFNs). It was known that IFNs exert their antiviral activity through inducing the following proteins: 1) RNA-dependent

protein kinase (PKR); 2) 2',5'-oligoadenylate synthetase-1 (OAS1); 3) 2-5A-dependent RNase (RNaseL) enzyme; and 4) proteins belonging to Mx family, all of which have been shown to inhibit the growth of certain viruses (Stark et al., 1998). The OAS enzymes synthesize a complex mixture of 5'-triphosphorylated oligoadenylic acid that further activates RNaseL, a ubiquitous endoribonuclease (Dong and Silverman, 1995; Marie et al., 1999; Rebouillat and Hovanessian, 1999). High levels of RNaseL can then suppress viral replication of a number of different viruses, such as encephalomyocarditis virus, vesicular stomatitis virus, human parainfluenza virus-3, and vaccinia virus (Diaz-Guerra et al., 1997b; Zhou et al., 1998; Ghosh et al., 2000). However, the antiviral activity of IFNs was shown to be only partially dependent on the aforementioned IFN-induced proteins, as mice triply deficient for RPK, RNaseL, and Mx genes remained partially responsive to the antiviral effects of IFNs (Zhou et al., 1999). These results suggested that there are additional IFN-stimulated genes (ISGs) that act as potent antiviral effectors.

Thus, in order to identify interferon-stimulated genes (ISGs) and elucidate new functions for IFN, an early oligonucleotide microarray was undertaken with RNA samples collected from human and murine cell lines treated with IFN- $\alpha$ , IFN- $\beta$ , and IFN- $\gamma$ . The results identified 122 ISGs induced by IFN and it was elucidated that IFNs exert miscellaneous functions such as cell proliferation and differentiation, immune response modulation, and virus inhibition through inducing different genes (Der et al., 1998). Further microarray analyses were conducted with HeLa cells infected with vaccinia virus recombinants co-expressing OAS-RNaseL enzymes (Domingo-Gil et al., 2010). The aim was to obtain a universal view of transcriptional changes following activation of OAS1 and RNaseL when the two enzymes are produced simultaneously. The results demonstrated up regulation and down regulation of several genes.

In comparison to the above-mentioned types of microarray analysis, there has been minimal investigation into use of microarray to explore the mode of action of an antiviral drug or a purported antiviral compound following viral infection. In this respect, Lam et al. (2006) reported the use of microarray analysis to reveal the gene expression pattern of Alexander cells that were treated with an ethanolic extract of *Phyllanthus nanus* (*P. nanus*). Alexander cells are human epithelial-like hepatoma cells, which contained an integrated HBV genome so that the cells constantly secrete



HBV surface antigen (HBsAg) into the culture medium. A limited microarray analysis with 800 human cDNA clones (obtained from an HBV integrated hepatocellular carcinoma (HCC) subtracted cDNA library) revealed several genes with up regulation or down regulation. Among these, the Annexin 7 (Axn7) gene was highlighted with a threefold up regulation, which was further confirmed by semi-quantitative RT PCR with Axn7 gene specific primers. It was suggested that Axn7 might play a possible role in  $\text{Ca}^{2+}$ -mediated exocytosis and endocytosis. The experimental results also showed that the level of HBsAg in the medium of Axn7 over-expressed Alexander cells was reduced. This may be due to two possibilities: (1) increased endocytosis capability of Axn7 would help eliminate HBsAg from the medium; or (2) the over-expressed Axn7 would bind to the intracellular HBsAg and prevent their secretion (Lam et al., 2006).

The use of microarray technology in the field of Enterovirus 71 (EV71) pathogenesis appears to be very limited, in that the only large-scale microarray analysis of EV71 infection was performed by Shih et al. (2004a). These microarray-based studies may shed light on the possible mechanisms of the host response to EV71 infection as well as contribute to both the prevention and treatment of this disease in the future. To this effect, there has been no study reported in literature that assesses the mechanisms of action of antivirals against EV71 infection. In addition, the relationship between profile of host transcripts and EV71 replication cycle remains unclear (Shih et al., 2004a). In other words, the cellular proteins that are necessary for viral propagation of EV71, which could be targets in antiviral drug discovery, are currently unknown.

It was previously shown that Heparin (Hep) significantly inhibited EV71 infection and binding in both Vero and a human neural cell line, SK-N-SH, *in vitro* (Chapter 4). However, unlike Vero cells, the possible role of cell surface heparan sulphate (HS) in mediating EV71 infection of the neural cells could not be confirmed. In addition, because EV71 is well known for causing severe neurological complications, the observed strong antiviral potencies of Hep against EV71 infection of the neural cells would warrant further investigations. Thus, the aim of this study was to gain insight into the cellular and molecular mechanisms of action of Hep against clinical EV71 infection in SK-N-SH cells. Changes in the expression profiles of the host cells were comparatively assessed under four conditions:

negative control (cells lacking both infection and treatment), cells treated only with Hep, EV71-infected cells treated with Hep, and cells infected with EV71 without treatment with Hep.

## 5.2. Materials and Methods

### 5.2.1. Cell lines and viruses

Vero cells and a human neural cell line, SK-N-SH, were prepared as described in Chapter 4 (Page 126). Cells were not passaged more than 20 times after reviving the original stocks.

A low passage clinical isolate of EV71 (isolate number 99018233, supplied from Victorian Infectious Disease Reference Laboratories, North Melbourne, VIC, Australia) and the cloned EV71 strain (kindly provided by Prof. Peter C. McMinn, Central Clinical School, University of Sydney, Australia) were passaged as described in 4.2.1 (Page 125). The viruses were propagated in 80% confluent monolayers of Vero cells using serum-free DMEM. The virus titres were determined in Vero cells using a MTT-based TCID<sub>50</sub> method as described in Chapter 2 (Page 81). The clinical isolate of EV71 was maintained at low passage in order to minimize the possibility of gaining susceptibility to Hep through adaptation to cell culture. The final viral supernatants were aliquoted and stored at -80 °C until use.

### 5.2.2. Reagents

Heparin sodium salt (Hep) from bovine intestinal mucosa ( $\geq 140$  USP units/mg, catalogue number H0777) purchased from Sigma-Aldrich (Castle Hill, NSW, Australia) was dissolved in sterile distilled water (10 mg/ml) and stored at 4 °C until use, as described elsewhere (Zautner et al., 2003).

### 5.2.3. Cell seeding and infection of cell cultures

SK-N-SH cells were seeded at  $1.35 \times 10^4$  cells/150  $\mu$ L/well or  $1.3 \times 10^5$  cells/1600  $\mu$ L/well in 96-well plates or 12-well plates, respectively (Becton Dickinson, North Ryde, NSW, Australia) followed by incubation at 37 °C/5% CO<sub>2</sub> until 80% confluent. Before adding Hep or the virus, or when quantifying the results, the monolayers were thoroughly washed with phosphate buffered-saline (PBS, pH 7.4 at room temperature) two or three times. In all the experiments, the

following four conditions were included: cell control (cells that were not infected with the virus or treated with Hep, abbreviated as CC), virus control (cells that were infected with EV71 at 100 TCID<sub>50</sub> but not treated with Hep, abbreviated as VC), compound control (cells that were treated by Hep at 125 µg/mL but not infected with the virus, abbreviated as Cyto), and treatment (cells treated with 125 µg/mL of Hep and simultaneously infected with 100 TCID<sub>50</sub> of EV71, abbreviated as Hep).

### 5.2.4. Cytotoxicity and antiviral activity assays

Initial cytotoxicity and antiviral activity assessments were carried out in 96-well plates as described in 4.2.4 and 4.2.5 (Pages 126 and 127), respectively. Based on these initial results, the clinical EV71 isolate was selected as the target virus and Hep at 125 µg/mL as the treatment. Then, anti-EV71 activity and cytotoxicity of Hep and total RNA isolation were simultaneously carried out in 12-well plates. Each condition described in 5.2.3 was repeated in triplicate; two wells for MTT-based assessments and one well for RNA isolation. Thus, the total RNAs were extracted at the same time as anti-EV71 activity and cytotoxicity of Hep were evaluated; using replicates of the same conditions. Each experiment was independently replicated three times. After reaching 80% cell confluency, the media was aspirated followed by addition of 1600 µL of DMEM/10% FBS alone (cell control) or containing one of the treatments (stated in 5.2.3). Following incubation at 37°C/5% CO<sub>2</sub> for a further 48 hours, antiviral and cytotoxicity assays were quantified by adding 200 µL of MTT reagent (Invitrogen, Mulgrave, VIC, Australia, dissolved in PBS, 0.5% w/v) (Anderson et al., 2005) mixed with 1600 µL of serum-free DMEM per well. The plates were then incubated in a humidified 37°C/5% CO<sub>2</sub> for 2-3 hours after which the formazon was dissolved with DMSO (500 µL/well) followed by another 10-minute incubation. Then, 50 µL of the solution in each well was transferred into each well of a 96-well plate. The colour change was recorded using a microplate reader at 540 nm. The cell viability percentages were measured based on the amount of living cells in compound-treated cells relative to cell controls (defined as 100% viability) (Schmidtke et al., 2001). The percentage of virus inhibition was measured using the following equation:  $T - V_c / C_c - V_c$ , where T= the optical density (OD) of compound-treated cells, V<sub>c</sub>= OD of virus control, C<sub>c</sub>=OD of cell control (Pauwels et al., 1988).

### **5.2.5. Total RNA isolation and purification**

Using the RNeasy Mini Kit of Qiagen (QIAGEN Pty Ltd, VIC, Australia, catalogue number 74104), total RNA was isolated and purified from cells treated under the conditions described in 5.2.3 at 48 hours post infection. For each condition, three independent replicates were prepared so that twelve samples were tested in hybridization assays. For RNA extraction, trypsinized cells were centrifuged at 1000 rpm at 4°C for 5 minutes followed by the addition of 400 µL of the lysis buffer (trade name: RLT, containing guanidine thiocyanate). An equal volume of ethanol (70%) was then added to the homogenized lysate followed by transferring 700 µL of the solution to an RNeasy spin column and centrifugation at 11,000 x g for 15 seconds. The consecutive washing and drying steps were performed using centrifugation at 11000 x g according to the manufacturer's instructions. Finally, the total RNA was eluted using 60 µL of RNase-free water. This step was repeated to increase the yield of total RNA isolated.

### **5.2.6. RNA qualification and quantification**

In order to obtain an estimate of RNA purity and integrity, the RNA samples were initially monitored by agarose (1%) gel electrophoresis stained with 2.5 µL of 10 mg/mL ethidium bromide stock on the same day as total RNA was extracted. The absence of DNA contamination and the presence of sharp 18S and 28S ribosomal bands, where the intensity of the 28S rRNA band was approximately twice that of 18S rRNA, indicated RNA samples that were suitable for further analysis (Skrypina et al., 2003). Then, the accurate quality (purity and integrity) and quantity of the total RNA samples were measured using the Eukaryote Total RNA Nano assay version 2.6 (Agilent 2100 Bioanalyzer, Agilent Technologies, Inc.), carried out at the Peter MacCallum Cancer Centre (East Melbourne, VIC, Australia). Electropherograms of total RNA samples with an integrity number (RIN) over 8.5 were analysed and the following criteria were taken into account: at least 20% of fragmented RNA was located between 28S and 18S rRNA, the 28S and 18S peaks account for at least, 5% and 10% of the overall RNA, respectively, and there was no more than 60% of RNA with fragment sizes smaller than 18S rRNA (Schoor et al., 2003). The total RNA samples that passed these criteria were selected for antisense RNA synthesis and labelling.

### 5.2.7. Arrays

For twelve RNA samples (four conditions at three replications), twelve GeneChip<sup>®</sup> Human Gene 1.0 ST arrays offering whole-transcript coverage ([www.affymetrix.com](http://www.affymetrix.com)) were purchased from Affymetrix (catalogue number 901086) and processed at the Peter MacCallum Cancer Centre. Each microarray chip used in this study contained 33,297 distinct probe sets (transcript cluster IDs), each represented by approximately 26 probes (25-mer) spread across the full lengths of the gene. The Gene 1.0 ST arrays have greater than 99% coverage of sequences present in the Reference Sequence (RefSeq) collection and require sense orientation of labeled cDNA targets. Further information about the array can be found at [www.affymetrix.com](http://www.affymetrix.com).

### 5.2.8. Target preparation and hybridization process

The target preparation and hybridization process was performed as a commercial service at the Peter MacCallum Cancer Centre. The Ambion<sup>®</sup> WT Expression Kit was used to generate sense-strand cDNA targets, while the Affymetrix GeneChip<sup>®</sup> WT Terminal Labeling Kit (internal abridged protocol) was used to fragment, label and hybridize to the arrays. In brief, 3  $\mu\text{L}$  of starting total RNA (300 ng) was mixed with 2  $\mu\text{L}$  of the mix of T7-(N)6 Primers/Poly-A RNA control solution followed by incubation at 70°C for 5 minutes and 4°C for a minimum of 2 minutes. These Poly-A RNA controls served as exogenous positive controls that were amplified and labelled together with the total RNA samples to check the entire target labelling process, independently from the quality of the starting RNA samples. The first strand of cDNA was then synthesized under the following thermal program: 25°C for 10 minutes, 42°C for 60 minutes, 70°C for 10 minutes, and 4°C for minimum 2 minutes. DNA polymerase then synthesized the second strand, and thus, a double stranded cDNA was produced that served as a template for further *in vitro* transcription (IVT). Anti-sense cRNA was synthesized during the IVT process using T7 RNA polymerase under the following conditions: 37°C for 16 hours and 4°C overnight. Following cleanup of cRNA, second cycle cDNA (sense stand) was synthesized using 10  $\mu\text{g}$  of cRNA and 1.5  $\mu\text{L}$  of random primers (3  $\mu\text{g}/\mu\text{L}$ ) for each sample, incubated at 70°C for 5 minutes, 25°C for 5 minutes, and 4°C for a minimum of 2 minutes. Following hydrolysis of cRNA and

cleanup of sense-stranded cDNA, fragmentation and labeling sense-stranded cDNA was performed using the Affymetrix GeneChip<sup>®</sup> WT Terminal Labeling Kit. Hybridization was performed in a hybridization oven at 45°C, 60 rpm for 17 ± 1 hours followed by washing and scanning of the arrays.

### 5.2.9. Statistical analysis

All of the cytotoxicity and antiviral activity experiments were applied in triplicate, and each experiment was independently repeated at least three times. Curves were drawn using GraphPad Prism 5 in which the data were expressed as mean ± standard deviation (SD).

Since Affymetrix does not add mismatch probes in the newer arrays such as GeneChip<sup>®</sup> Human Gene 1.0 ST array, background noise was handled by a background-correction step during the normalization. Partek Genomics Suite version 6.5 was utilized to import and analyze raw data from the array cells. Using one-step Tukey's bi-weight, normalized values of multiple probes for the same gene (at each replication) were summarized into a single value representing consensus level of expression for that gene. Then, the following five contrasts were made: Hep vs. CC; VC vs. CC; Cyto vs. CC; Hep vs. VC; and Hep vs. Cyto (the abbreviations are described in 5.2.3).

For each contrast, only samples from the two target groups were included. A single factor ANOVA inside Partek was applied to generate *P* values for each gene. These *P* values were then adjusted by Benjamini and Hochberg's Multiple testing correction to reduce false discovery rate (FDR) (Benjamini and Hochberg, 1995).

## 5.3. Results

### 5.3.1. Cytotoxicity and antiviral activity

Cytotoxicity of Hep and its antiviral potency at 125 µg/mL against the clinical EV71 isolate in the neural cells, SK-N-SH, were assessed at the same time as extraction of total RNA using the replicates of the same conditions. MTT-based quantification of data revealed that Hep at 125 µg/mL significantly inhibited clinical EV71 infection with no cytotoxicity on SK-N-SH cells. These results were in agreement with the previous findings, demonstrated in Figures 4.1b and 4.4a (Pages 130 and 141, respectively).

### **5.3.2. Assessment of total RNA samples**

Most of the RNA samples monitored by agarose (1%) gel electrophoresis showed two sharp bands of 18S rRNA and 28S rRNA with no significant degraded RNA or DNA contamination. The total RNA samples were further assessed with an Agilent 2100 Bioanalyzer, using an RNA 6000 Nano Kit including a ladder with the following RNA fragments: 25, 200, 500, 1000, 2000, and 4000 bp. The results are displayed as both gel-like images (Figure 5.1) and electropherograms for each sample (Figure 5.2), showing that all samples were acceptable with RIN values above the threshold required (RIN=8.5). In addition, RNA sample concentrations compared to the ladder were all acceptable for the further microarray analysis that would require an input of minimum 100 ng (Appendix 5). Ribosomal bands of the samples contributed to total RNA by more than 28%. All specifications of total RNA samples revealed by the Bioanalyzer are included in Table 1 of Appendix 5. In addition, electropherograms of the RNA samples are depicted in Figure 1 of Appendix 5.

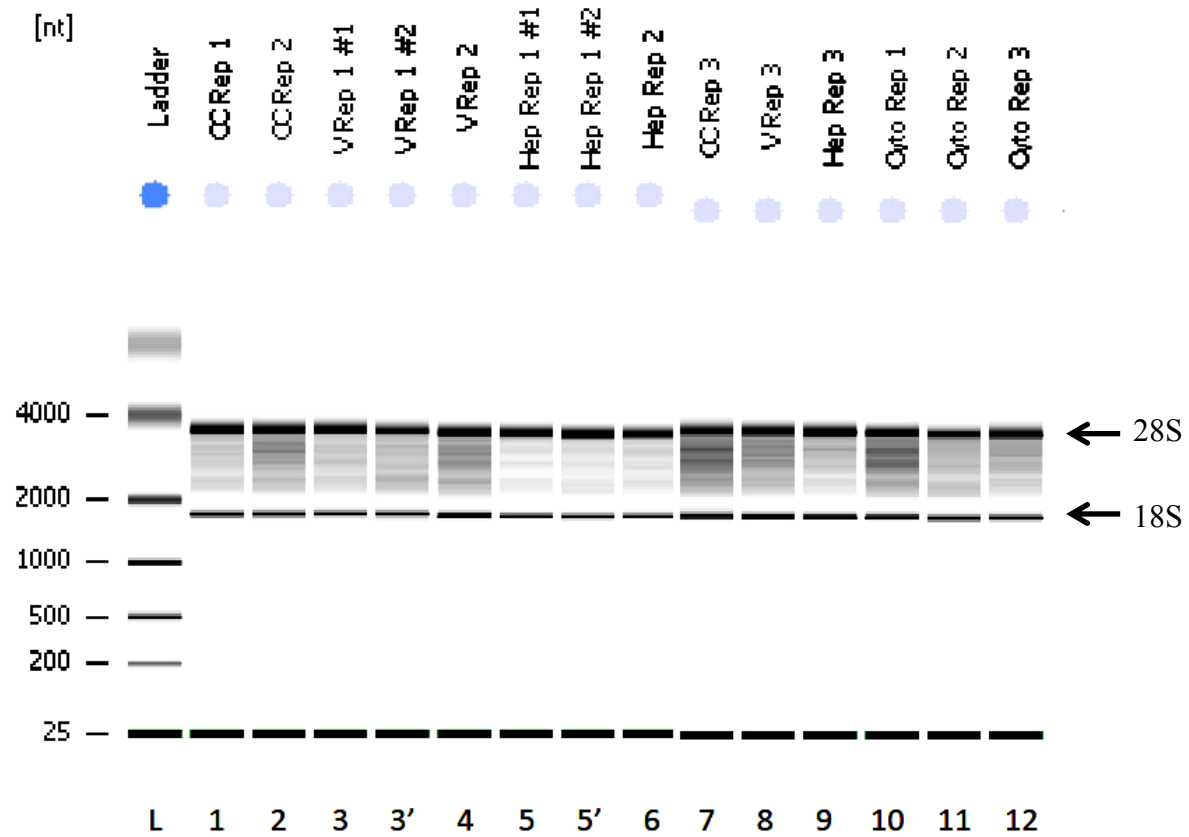


Figure 5.1. Gel-like images of RNA Nano assay



## Chapter Five-Microarray Analysis of Antiviral Activity of Hep against EV71

---

The images show electrophoresis file run summary generated by Agilent 2100 Bioanalyzer (Agilent Technologies, Inc.). Sharp bands of 18S rRNA and 28S rRNA of the RNA samples are evident. Lanes 1-12 represent CC Rep 1; CC Rep 2; V Rep 1; V Rep2; Hep Rep1; Hep Rep2; CC Rep3; V Rep3; Hep Rep3; Cyto Rep1; Cyto Rep2; and Cyto Rep3, respectively. Lanes 3 and 5 represent the same replications of the lanes 3 and 5, respectively. The markers indicate the locations of 18S rRNA and 28S rRNA.

Abbreviations: CC (cell control; cells not infected or treated); V (virus control; cells infected with EV71 but not treated with Hep); Hep (treatment; EV71-infected cells treated with Hep); Cyto (compound control; cells treated with Hep but not infected with EV71); Rep: replication.

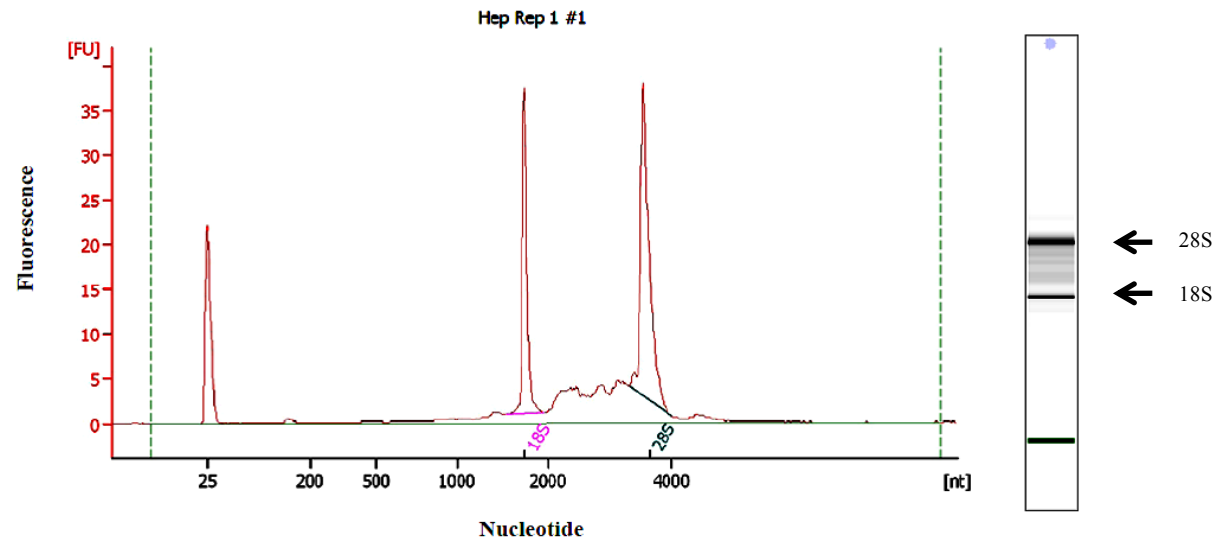


**Figure 5.2. The electropherogram of an RNA sample, generated by the Bioanalyzer**

The picture on the left shows an electropherogram of total RNA of EV71-infected cells treated with Hep generated by Agilent 2100 Bioanalyzer (Agilent Technologies, Inc.). Bioanalyzer measures the amount of fluorescence as RNA samples are pulsed through a microchannel over time. Separation channels pulse smaller molecules quicker than larger ones so that smaller-sized molecules (less than 18S rRNA) appear on the left side of electropherogram. The system then creates a graph called an electropherogram. Depicted on the right is a gel-like image of the same sample. This is an example of one sample (Hep Rep1) and electropherograms of all RNA samples are depicted in Figure 1 of Appendix 5. The markers indicate the locations of 18S rRNA and 28S rRNA.

### **5.3.3. Gene expression profiling of SK-N-SH cells**

Changes in gene expression profiling of the twelve RNA samples of SK-N-SH cells (described in 5.2.3) were independently normalized. Overall, results showed that the histograms of gene expression values of the samples followed the same trend, suggesting arrays were technically acceptable (Figure 5.3). In addition, despite principal component analysis (PCA) showing that the third replication of VC (VC-R3) appeared to be an outlier (Figure 2, Appendix 5), the conditions clustered together appropriately suggested they could be separated by arbitrary hyperplanes (Figure 3, Appendix 5).

The microarray data of this study have been deposited in NCBI's Gene Expression Omnibus (Edgar et al., 2002) and are accessible through GEO Series accession number GSE34234; online at:

<http://www.ncbi.nlm.nih.gov/geo/query/acc.cgi?acc=GSE34234>.

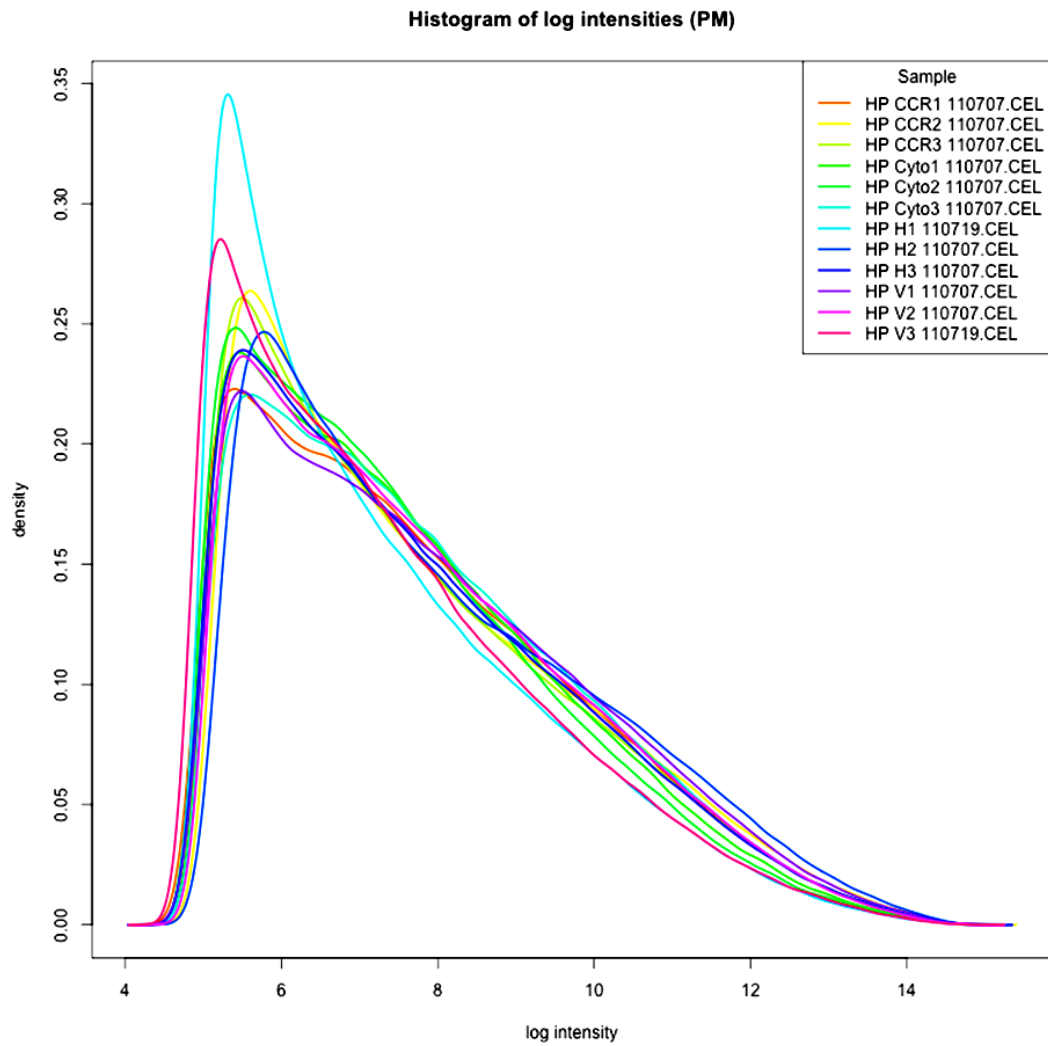


**Figure 5.3. Frequency of gene-level intensities**

The histogram depicts frequencies of normalized intensities of perfect match (PM) for all of the twelve samples. The gene-level values were summarized from probe-set level intensities by one-step Tukey’s biweight. Each coloured line represents one of the 12 samples as follows:

CCR1-CCR3: cell control (replications 1-3); Cyto1-Cyto3: compound control (replications 1-3); H1-H3: EV-infected cells treated with Hep (replications 1-3); and V1-V3: virus control (replications 1-3). HP stands for Hamid Pourianfar.

#### 5.3.4. Pattern of gene expression induced by antiviral activity of Hep

The statistical parameters of ANOVA,  $p$  value, multiple test correction, and fold change were calculated within each contrast (stated in 5.2.9). Then, a multi-level selection and analysis procedure was employed in order to attribute changes in the gene transcription level to the antiviral activity of Hep. In order to simplify the analysis, we began with statistical analysis of differences between the conditions of treatment (i.e. Hep-treated cells infected with EV71) and virus control (i.e. cells infected with EV71 only), at a  $p$  value less than 0.05. Consequently, 1849 genes were selected which of 144 genes displayed expression fold changes equal or more than 1.5 (up-regulation or down-regulation). These 144 differentially expressed genes were further monitored in the condition of virus control to select for those genes that fulfilled the following conditions: being significantly induced by the EV71 infection of SK-N-SH cells at a  $p$  value less than 0.05 and FDR-adjusted  $p$  value lower than 0.48 with a fold change of at least 1.5 (up regulation or down regulation). As a result, 14 genes were selected that were further monitored in the condition of treatment. Table 5.1 summarizes this information and illustrates how the treatment (Hep+EV71) changed expression intensities of genes that had been significantly induced by EV71. These Hep-caused changes in gene expression profiles were either significant or not significant as compared to cell control; however, more importantly, they were statistically significant in comparison with the condition of EV71 only ( $p < 0.05$  with a fold change of at least  $\pm 1.5$ ).

In addition to 14 well-annotated genes listed in Table 5.1, 14 un-annotated genes were also selected based on the above-mentioned selection procedure (Table 5.2). No annotation was given to these 14 genes using the NetAffx annotation pipeline in the new search conducted on the 14<sup>th</sup> of November 2011.

Table 5.1. Effect of interaction between Hep and EV71 on genes of neural cells (well annotated genes)

RefSeq//Gene symbol	Gene description	VC vs. CC <sup>a</sup>		Hep vs. CC <sup>a</sup>		Hep vs. VC <sup>a</sup>	
		Fold change <sup>b</sup>	P value	Fold change <sup>b</sup>	P value <sup>c</sup>	Fold change <sup>b</sup>	P value
NM_024094 // DSCC1	Defective in sister chromatid cohesion 1 homolog ( <i>S. cerevisiae</i> )	-1.52	0.03	+1.48	0.044	+2.26	3.1×10 <sup>-3</sup>
NM_001001522 // TAGLN	Transgelin	-2.17	0.042	-1.01	n.s.	+2.14	0.024
NM_004541 // NDUFA1	NADH dehydrogenase (ubiquinone) 1 alpha subcomplex, 1, 7	-1.96	0.038	+1.06	n.s.	+2.08	0.046
NM_006520 // DYNLT3	Dynein, light chain, Tctex-type 3	-2.08	7.8×10 <sup>-3</sup>	-1.02	n.s.	+2.03	0.01
NM_181786 // HKR1	HKR1, GLI-Kruppel zinc finger family member	-2.19	2.06×10 <sup>-3</sup>	-1.1	n.s.	+2.00	4.49×10 <sup>-3</sup>
NM_020200 // PRTFDC1	Phosphoribosyltransferase domain containing 1	-2.12	9.22×10 <sup>-4</sup>	-1.34	6.77×10 <sup>-3</sup>	+1.57	3.73×10 <sup>-3</sup>
NM_016328 // GTF2IRD1	GTF2I repeat domain containing 1	-1.55	0.043	-1.01	n.s.	+1.53	0.026
NM_014729 // TOX	Thymocyte selection-associated high mobility group box	-5.81	4.68×10 <sup>-5</sup>	-3.86	1.15×10 <sup>-3</sup>	+1.50	0.038
NM_030968//C1QTNF1	C1q and tumor necrosis factor related protein 1	+3.35	4.87×10 <sup>-4</sup>	+2.22	7.44×10 <sup>-5</sup>	-1.510	0.02
NM_007170 // TESK2	Testis-specific kinase 2	+1.71	5.71×10 <sup>-3</sup>	+1.06	n.s.	-1.62	4.16×10 <sup>-3</sup>
NM_006399 // BATF	Basic leucine zipper transcription factor, ATF-like	+1.67	0.02	+1.03	n.s.	-1.62	0.03
NM_052862 // RCSD1	RCSD domain containing 1	+1.55	4.92×10 <sup>-3</sup>	-1.05	n.s.	-1.63	3.22×10 <sup>-3</sup>
NM_001008540 // CXCR4	Chemokine (C-X-C motif) receptor 4	+1.55	0.019	-1.06	n.s.	-1.63	0.028
NM_175617 // MT1E	Metallothionein 1E	+2.49	0.012	-1.17	n.s.	-2.92	7.18×10 <sup>-3</sup>

<sup>a</sup>Abbreviations: VC vs. CC: virus control contrasted against cell control; Hep vs. CC: EV71-infected cells treated with Hep contrasted against cell control; Hep vs. VC: EV71-infected cells treated with Hep contrasted against virus control.

<sup>b</sup>+ and – symbols indicate up regulation and down regulation of the genes, respectively. For each contrast, the direction of fold change (+ or –) is toward the left hand condition. The fold change values in Hep vs. VC are sorted in descending order.

<sup>c</sup>n.s. resembles not significant values ( $p > 0.05$ ).

Table 5.2. Effect of Hep on genes of EV71-infected of neural cells (un-annotated genes)<sup>a</sup>

Cluster transcript ID	VC vs. CC		Hep vs. CC		Hep vs. VC	
	Fold change	<i>P</i> value	Fold change	<i>P</i> value	Fold change	<i>P</i> value <sup>a</sup>
7892904	-2.12	7.93×10 <sup>-3</sup>	+1.1	n.s.	+2.34	5.27×10 <sup>-3</sup>
7893771	-2.15	8.49×10 <sup>-3</sup>	-1.16	n.s.	+1.86	0.039
7895000	-1.84	0.031	-1.02	n.s.	+1.81	0.033
7892628	-2.29	2.45×10 <sup>-3</sup>	-1.33	n.s.	+1.72	0.037
7896113	-1.75	0.019	-1.05	n.s.	+1.67	2.87×10 <sup>-3</sup>
7894973	-1.64	0.034	1	n.s.	+1.64	2.98×10 <sup>-3</sup>
7896426	-2.02	0.018	-1.29	n.s.	+1.57	0.039
7895836	-1.50	0.041	+1.04	n.s.	+1.56	0.025
7893253	+1.55	0.019	1.02	n.s.	-1.51	0.031
7894742	+1.65	7.56×10 <sup>-3</sup>	1.02	n.s.	-1.61	0.019
7896256	+1.65	0.025	1.02	n.s.	-1.62	0.037
7894614	+1.78	0.015	1	n.s.	-1.76	8.48×10 <sup>-3</sup>
7893967	+2.18	7.73×10 <sup>-3</sup>	+1.22	n.s.	-1.8	7.85×10 <sup>-3</sup>
7893180	+1.82	0.011	-1.56	0.044	-2.83	2.02×10 <sup>-3</sup>

<sup>a</sup>Abbreviations, symbols and notes of this table are the same as Table 5.1.

In the next step, the effect of Hep on genes of EV71-infected neural cells was compared with the effect of Hep on genes of normal (not infected) neural cells (Table 5.3). The results of this comparative analysis revealed that no significant change was observed in expression of thirteen genes of the fourteen genes listed in Table 5.1 when Hep was applied alone ( $p > 0.05$  and/or a fold change less than 1.5). The only significant difference was observed for gene of Basic Leucine Zipper Transcription Factor, ATF-Like (BATF) where addition of Hep to non-infected neural cells caused this gene to be up regulated 1.54 times at a  $p$  value less than 0.05. While treatment of EV71-infected cell did not significantly change the expression of BATF, the difference in the fold change between EV71-infected cells treated with Hep and normal cells treated with Hep was just less than 1.5 with a  $p$  value less than 0.05.

The afore-mentioned comparisons were also accomplished for the un-annotated genes (Table 5.4). The results showed that Hep significantly induced gene of cluster transcript ID #7893967 in non-infected neural cells ( $p < 0.05$  with a fold change more than 1.5). In addition, the difference between EV71-infected cells treated with Hep and normal cells treated with Hep was statistically significant ( $p < 0.05$  with a fold change more than 1.5). No significant change was observed in expression of the rest of unknown genes ( $p > 0.05$  and/or a fold change less than 1.5) (Table 5.4).



Table 5.3. Comparison of effects of Hep on genes of normal and EV71-infected neural cells (well annotated genes)

RefSeq//Gene symbol	Gene description	Cyto vs. CC <sup>a</sup>		Hep vs. CC <sup>a</sup>		Hep vs. Cyto <sup>a</sup>	
		Fold change <sup>b</sup>	P value	Fold change <sup>b</sup>	P value <sup>c</sup>	Fold change <sup>b</sup>	P value
NM_024094 // DSCC1	Defective in sister chromatid cohesion 1 homolog ( <i>S. cerevisiae</i> )	+1.01	n.s.	+1.48	0.044	+1.46	n.s.
NM_001001522 // TAGLN	Transgelin	-1.46	n.s.	+1.2	n.s.	-1.03	n.s.
NM_004541 // NDUFA1	NADH dehydrogenase (ubiquinone) 1 alpha subcomplex, 1, 7	+1.41	n.s.	+1.06	n.s.	-1.33	n.s.
NM_006520 // DYNLT3	Dynein, light chain, Tctex-type 3	-1.90	n.s.	-1.02	n.s.	+1.85	n.s.
NM_181786 // HKR1	HKR1, GLI-Kruppel zinc finger family member	-1.21	n.s.	-1.1	n.s.	+1.11	n.s.
NM_020200 // PRTFDC1	Phosphoribosyltransferase domain containing 1	-1.10	n.s.	-1.34	6.77×10 <sup>-3</sup>	-1.22	n.s.
NM_016328 // GTF2IRD1	GTF2I repeat domain containing 1	+1.04	n.s.	-1.01	n.s.	-1.06	n.s.
NM_014729 // TOX	Thymocyte selection-associated high mobility group box	+1.08	n.s.	-3.86	1.15×10 <sup>-3</sup>	-4.17	8.07×10 <sup>-4</sup>
NM_030968//C1QTNF1	C1q and tumor necrosis factor related protein 1	-1.17	n.s.	+2.22	7.44×10 <sup>-5</sup>	+2.60	5.1×10 <sup>-4</sup>
NM_007170 // TESK2	Testis-specific kinase 2	-1.24	n.s.	+1.06	n.s.	+1.32	0.015
NM_006399 // BATF	Basic leucine zipper transcription factor, ATF-like	+1.54	0.026	+1.03	n.s.	-1.49	0.04
NM_052862 // RCSD1	RCSD domain containing 1	+1.22	9.44×10 <sup>-3</sup>	-1.05	n.s.	-1.28	3.58×10 <sup>-3</sup>
NM_001008540 // CXCR4	Chemokine (C-X-C motif) receptor 4	+1.14	n.s.	-1.06	n.s.	-1.20	n.s.
NM_175617 // MT1E	Metallothionein 1E	+1.19	n.s.	-1.17	n.s.	-1.40	n.s.

<sup>a</sup>Abbreviations: Cyto vs. CC: neural cells treated with Hep only (compound control); Hep vs. CC: EV71-infected cells treated with Hep contrasted against cell control; Hep vs. Cyto: EV71-infected cells treated with Hep contrasted against compound control.

<sup>b</sup>+ and – symbols indicate up regulation and down regulation of the genes, respectively. For each contrast, the direction of fold change (+ or –) is toward the left hand condition.

<sup>c</sup>n.s. resembles not significant values ( $p > 0.05$ ).

Table 5.4. Comparison of effects of Hep on genes of normal and EV71-infected neural cells (un-annotated genes)<sup>a</sup>

Cluster transcript ID	Cyto vs. CC		Hep vs. CC		Hep vs. Cyto	
	Fold change	<i>P</i> value	Fold change	<i>P</i> value	Fold change	<i>P</i> value <sup>a</sup>
7892904	+1.26	n.s.	+1.1	n.s.	-1.14	n.s.
7893771	-1.03	n.s.	-1.16	n.s.	-1.12	n.s.
7895000	-1.09	n.s.	-1.02	n.s.	+1.07	n.s.
7892628	-1.29	n.s.	-1.33	n.s.	-1.03	n.s.
7896113	-1.35	n.s.	-1.05	n.s.	+1.29	n.s.
7894973	+1.48	n.s.	1	n.s.	-1.48	0.01
7896426	-1.30	n.s.	-1.29	n.s.	+1.01	n.s.
7895836	+1.24	n.s.	+1.04	n.s.	-1.19	n.s.
7893253	+1.40	5.88×10 <sup>-3</sup>	1.02	n.s.	-1.37	0.019
7894742	+1.37	n.s.	1.02	n.s.	-1.34	n.s.
7896256	+1.26	n.s.	1.02	n.s.	-1.23	n.s.
7894614	+1.16	n.s.	1	n.s.	-1.15	n.s.
7893967	+2.08	0.013	+1.22	n.s.	-1.71	0.017
7893180	-1.05	n.s.	-1.56	0.044	-1.48	n.s.

<sup>a</sup>Abbreviations, symbols and notes of this table are the same as Table 5.3.

As it was stated in the first paragraph of this section, 14 well-annotated genes were selected based on the criterion that the EV71 infection significantly changed expression of them, and then, Hep affected the expression profiles significantly, as compared to virus control (Table 5.1). Apart from this selection, 8 other well-annotated genes were found in this study that demonstrated a significance difference between EV71-infected cells and EV71-infected cells treated with Hep ( $p < 0.05$  with a fold change more than 1.5) (Table 5.5). However, EV71 infection did not significantly induce the expression of these genes ( $p > 0.05$ ), in comparison to cell control. In addition, further investigations revealed that none of these genes were induced by Hep when added to normal neural cells. As a result, there was significant differences in expression of 5 genes of these 8 genes between the conditions of Hep only and EV71-infected cells treated with Hep ( $p < 0.05$  with a fold change more than 1.5) (Table 5.6). Thus, these 5 genes were also considered important for further bioinformatics characterization, in addition to the previous 14 genes.

The results of this study also revealed that there were more than 1000 other genes induced by EV71 infection with expression fold changes ranged from +46.5 to -10.7 at significance levels lower than 0.015 and FDR-adjusted  $p$  value lower than 0.33. However, since these changes were not related to the antiviral activity of Hep, they were not further analyzed in the current study but will be investigated in future studies.

In addition to the above-mentioned quantifiable comparisons, Figure 5.4 graphically compares the four conditions (Hep, VC, Cyto, and CC) together. These comparisons have been made for one replication of each condition at the same positions (features) on the chips.

Table 5.5. Hep-induced genes that were not induced significantly by EV71 infection of neural cells (well annotated genes)<sup>a</sup>

RefSeq//Gene symbol	Gene description	VC vs. CC		Hep vs. CC		Hep vs. VC	
		Fold change	P value	Fold change	P value	Fold change	P value
NM_016090 // RBM7	RNA binding motif protein 7	-1.15	n.s.	+1.63	0.047	+1.87	0.047
NM_024329 // EFHD2	EF-hand domain family, member D2	1	n.s.	+1.88	1.67×10 <sup>-3</sup>	+1.87	0.036
NM_018039 // KDM4D	Lysine (K)-specific demethylase 4D	-1.22	n.s.	+1.52	0.027	+1.85	0.01
NM_024580 // EFTUD1	Elongation factor Tu GTP binding domain containing 1	+1.24	n.s.	+1.68	0.015	+1.68	0.012
NM_001005340 // GPNMB	Glycoprotein (transmembrane) nmb	-1.45	n.s.	-2.27	4.6×10 <sup>-3</sup>	-1.57	0.01
NM_006287 // TFPI	Tissue factor pathway inhibitor (lipoprotein-associated coagulation inhibitor)	-1.06	n.s.	-1.68	0.048	-1.58	0.033
NM_080865 // GPR62	G protein-coupled receptor 62	+1.02	n.s.	-1.76	0.043	-1.80	0.012
NM_145665 // SPANXE	SPANX family, member E	+1.11	n.s.	-1.98	0.026	-2.19	0.04

Table 5.6. Comparison of effects of Hep on genes of normal and EV71-infected cells that were not induced significantly by EV71 infection<sup>a</sup>

RefSeq//Gene symbol	Gene description	Cyto vs. CC		Hep vs. CC		Hep vs. Cyto	
		Fold change <sup>b</sup>	P value	Fold change	P value	Fold change	P value
NM_016090 // RBM7	RNA binding motif protein 7	-1.17	n.s.	+1.63	0.047	+1.96	0.03
NM_024329 // EFHD2	EF-hand domain family, member D2	-1.05	n.s.	+1.88	1.67×10 <sup>-3</sup>	+1.98	1.25×10 <sup>-3</sup>
NM_018039 // KDM4D	Lysine (K)-specific demethylase 4D	-1.29	n.s.	+1.52	0.027	+1.95	7.39×10 <sup>-3</sup>
NM_001005340 // GPNMB	Glycoprotein (transmembrane) nmb	-1.38	n.s.	-2.27	4.6×10 <sup>-3</sup>	-1.65	0.013
NM_006287 // TFPI	Tissue factor pathway inhibitor (lipoprotein-associated coagulation inhibitor)	1	n.s.	-1.68	0.048	-1.69	0.019

<sup>a</sup>Abbreviations, symbols and notes of this table are the same as the previous Tables.

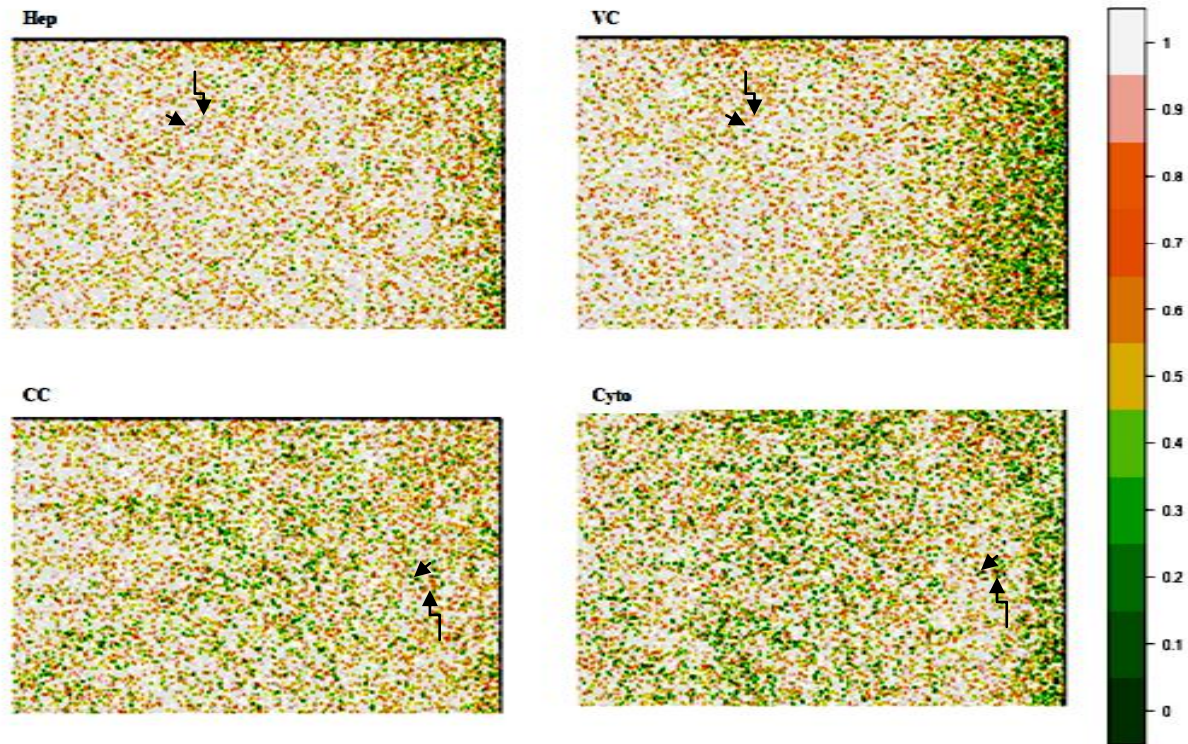


### Figure 5.4. Scanned images of microarray analysis of four conditions

The images are small parts of each chip that represent how genes are differentially expressed across different conditions. The colour intensity (right) shows different colours for gene expression values so that dark green colour represents up-regulated genes and white represents down-regulated genes. The pictures are aligned so that differentially expressed genes could be visualized. To make comparisons simpler, examples of the same features are compared between Hep and VC, and examples of the other same features are compared between CC and Cyto. The same expression intensity is indicated with straight arrows, while differentially expressed features are indicated with elbow arrows. CC: cell control (cells not infected or treated); V: virus control (cells infected with EV71 but not treated with Hep); Hep: EV71-infected cells treated with Hep; Cyto: cells treated with Hep but not infected with EV71.

### 5.4. Discussion

Significant antiviral activities of Hep against clinical EV71 infection in the human neuroblastoma cell line, SK-N-SH, was previously demonstrated and presented in Chapter 4 of this thesis. The data described in this Chapter followed up this work by investigating changes that Hep might provoke in gene expression profiles of EV71-infected neural cells. In order to increase the reliability and accuracy of this assessment, a genome-wide microarray analysis of Hep was performed using total transcripts taken directly from host cells treated with Hep following EV71 infection. A multi-level selection procedure was applied to select for genes for which expression was changed due to antiviral activity of Hep, in comparison to the virus, cell, and compound controls. Therefore, the work reported here has the advantage of using a multi-level comparison with several controls. Additionally, these microarray data can directly be compared to MTT-based antiviral activity and cytotoxicity analyses in cell culture.

For most of the genes that will be described below, it was observed that while EV71 infection down or up regulated expression of them significantly, treatment with Hep imposed significant changes in expression profiles of these genes with comparison to virus control. By contrast, addition of Hep alone to uninfected cells did not induce these genes, as compared to cell control. Thus, it is speculated that the inductive effect of Hep on these genes is more likely associated to its antiviral activity in the presence of EV71 than its general effect on normal, uninfected cells. In order to achieve a meaningful and effective interpretation, the following discussion has been condensed to the more important gene classes.

In this study, while EV71 infection significantly down regulated the expression of DSCC1 by 1.52 ( $p<0.05$ ), treatment with Hep up regulated it significantly ( $p<0.05$ ), leading to a substantial difference of fold change (+2.26) between the conditions of treatment and virus control ( $p<0.05$ ). In eukaryotes, DSCC1 along with chromosome transmission fidelity factor 18 homolog (*S. cerevisiae*) (CHTF18) and chromosome transmission fidelity factor 8 homolog (*S. cerevisiae*) (CHTF8) is involved in sister chromatid cohesion establishment, the control of eukaryotic DNA replication and fidelity of chromosome transmission. In

addition, sister chromatid cohesion1 (SCC1)/RAD21, SCC3, structural maintenance of chromosomes 1 (SMC1), and SMC3 form the cohesin complex that firmly holds sister chromatid DNAs together physically from S phase until their separation in Anaphase (Uhlmann et al., 1999; Bermudez et al., 2003). It is thought that DSCC1, CHTF18 and CHTF8 may play a role in the establishment of cohesion by interacting directly with the cohesin complex (i.e. SCC1/RAD21, SCC3, SMC1 and SMC3). Being ubiquitous among different species, the afore-mentioned genes involved in cohesion play an essential role in cell proliferation (Bermudez et al., 2003). As such, mutations in any one of these subunits result in arresting the growth and decreasing the number of cells and ultimately lead to cell death (Atienza et al., 2005; Ghiselli, 2006; Gluenz et al., 2008).

The Search Tool for the Retrieval of Interacting Genes/Proteins (STRING) 9.0 showed that DSCC1 binds to proliferating cell nuclear antigen (PCNA), CHTF18 and CHTF8 (STRING 9.0, entry ID Q9BVC3). Interestingly, our results showed that treatment of EV71-infected neural cells up regulated PCNA and CHTF18 by 1.35 and 1.31 at  $p$  values of 0.015 and  $5.75 \times 10^{-3}$ , respectively; whereas the EV71 infection did not change expression of these genes. This effect of Hep caused a comparative difference in fold change (+1.47 times at a  $p$  value  $3.87 \times 10^{-3}$ ) between the conditions of treatment and virus control in the expression of PCNA. As a control, addition of Hep to uninfected neural cells did not change expression of any of the afore-mentioned genes, suggesting a role for Hep when it is applied in the presence of EV71. Therefore, it could be suggested that down regulation of DSCC1 by EV71 infection might be, at least partially, associated to suppressing cell cycle of neural cells *in vitro* that in turn would increase apoptosis. Then, Hep might act against the EV71-mediated apoptosis associated with down regulation of DSCC1 through up regulation of this gene and other related genes such as PCNA.

EV71 infection repressed expression of TAGLN (TAGLN1) significantly by 2.17-fold, while treatment with Hep changed the expression profile of this gene in comparison with virus control, with a fold change of +2.14 ( $p < 0.05$ ). Provided by RefSeq collection (accession number NM\_001001522), it has been stated that the protein encoded by TAGLN, Transgelin1, is a transformation and shape-change sensitive actin cross-linking/gelling protein that can be found in smooth muscle and non-smooth muscle cells (particularly neural cells), localized to the cell membrane



and cytoplasm. Thus far, a functional role of this protein has been unclear, although Transgelin1 is best characterized compared to other isoforms Transgelins 2 and 3.

Similar to the findings of this study, Chang and Laimins (2000) reported that infection of human keratinocytes cells by high-risk human papillomavirus (HPV) type 31 down regulated TAGLN by 3.2-fold. It was concluded that down regulation of TAGLN may contribute to loss of contact inhibition and enhanced motility characteristic of HPV-transformed cells. Consistent with these findings, a substantial down regulation (more than 21-fold) was observed with human cytomegalovirus (CMV)-infected primary human foreskin fibroblasts (Hertel and Mocarski, 2004). It was speculated that this change is part of changes caused by the virus infection to disrupt the organization of the cytoplasmic microfilaments and to cause significant damage to the formation of stress fibers, filopodia, and lamellipodia, leading to the rounded, enlarged cell CPE observed at late times of the infection. Therefore, it might be suggested that CPE observed in the virus control condition of this study is partially related to a negative impact of EV71 on expression of Transgelin1. Then, Hep changed this pattern significantly, resulting in control of the infection of neural cells *in vitro*.

NDUFA1, encoding NADH dehydrogenase (ubiquinone) 1 alpha subcomplex, 1, 7, was significant down regulated (1.96-fold) by EV71 infection of neural cells. The protein encoded by NDUFA1 is an essential component of complex I of the mitochondrial membrane respiratory chain (RC), which transfers electrons from NADH to ubiquinone (RefSeq, accession number NM\_004541).

Very recently, Ebermann et al. (2012) provided evidence for the role of NDUFA1 and other genes of complexes of RC in regulating Coxsackievirus B3 (CVB3)-mediated myocarditis (MC) *in vivo*. Elevated amount of complex 1 and 3 of RC in mice promoted further events such as exhaustion of the antioxidative system and induction of a sustainable oxidative stress and mitochondrion-related apoptosis, reflecting an antiviral intracellular against the acute MC. By contrast, decreased complexes of RC led to suppression in both oxidative stress and mitochondrial apoptosis, letting the virus replicate greatly in the heart. In our study, the results revealed that EV71-mediated down regulation of NDUFA1 was neutralized by Hep (+2.08-fold,  $p < 0.05$ ) in comparison to virus control. The impact of Hep on either virus-infected cells or uninfected cells was not significant as compared to cell

control, indicating change in the profile of NDUFA1 only occurred in EV71 infection followed by interference by Hep. In addition, other subunits of complex 1 or other complexes of mitochondrial RC were not induced by EV71. Therefore, in the context of cell culture, it could be suggested that repression of NDUFA1 by EV71 would benefit progression of the viral infection through suppression of both oxidative stress and mitochondrial apoptosis that the latter is an effective host response to minimize damage of early viral infection. Then, Hep generated a mitochondrial intracellular antiviral state by neutralization of EV71-caused down regulation of NDUFA1. In addition, because infection of some clinical isolates of EV71 have been reported to lead to myocarditis (S.C. Chen et al., 2007; K.T. Chen et al., 2008), these findings could possibly have one *in vivo* implication in that NDUFA1 might be considered a therapeutic target for patients with EV71-induced MC.

In our investigation, while the EV71 infection significantly down regulated expression of TOX by 5.81-fold, treatment of the cells with Hep significantly changed the fold change (-3.86), resulting in a significant difference of fold change (+1.50) between the two conditions ( $p < 0.05$ ). TOX is now known as a protein that plays multiple roles in the immune system (Aliahmad et al., 2011). In the thymus, pre-T cell receptor (pre-TCR)-mediated signaling and then TCR-mediated signaling induce changes in gene expression, resulting in the maturation of CD4 and CD8 lineage T cells from common precursors. Besides, TOX expression has been shown to be highly up regulated by both pre-TCR and TCR activation of immature thymocytes (Wilkinson et al., 2002), suggesting a role for TOX in differentiation of T cells (Yun et al., 2011). These findings may have *in vivo* implications in that EV71 has been reported to infect lymphoid organs, including the spleen and thymus (Wang et al., 2004). In addition, in one fatal case of EV71 infection, the virus was detected in the intestinal lymph nodes, cerebrospinal fluid, spleen, thymus, kidney, brain, heart and lung (The WHO office in China, 2008, online at <http://www.wpro.who.int/NR/rdonlyres/591D6A7B-FB15-4E94-A1E9-1D3381847D60/0/HFMDCCDC20080515ENG.pdf>). Taken together, it could be hypothesized that down regulation of TOX by EV71 might be related to what has been reported as a decrease in T cells following EV71 infection (Wang et al., 2003). While this proposition warrants further *in vivo* and *in vitro* investigations, it appears

that these findings are not sufficient to make a direct link between EV71-mediated suppressed TOX in neural cells and why Hep has targeted up regulating of TOX relative to virus control.

In this study, while the EV71 infection of neural cells increased C1QTNF1 expression +3.35 times, the down regulating impact of Hep caused a significant difference in the fold change by -1.51-fold between the conditions of treatment and virus control. C1QTNF1 encodes complement C1q tumor necrosis factor-related protein 1, also known as G protein-coupled receptor (GPCR)-interacting protein (GIP). GIPs interact with GPCRs, and thus, are involved in control of the targeting, trafficking and signalling of these molecules. GPCRs themselves are involved in many physiological processes such as the visual and smell senses, regulation of immune system activity and inflammation, automatic nervous system transmission, and in many diseases (Bockaert et al., 2004).

GPCRs are considered the largest receptor superfamily in the human genome. In the virology context, perhaps one of the most physiologically important examples of GPCRs is chemokine (C-C motif) receptor 5 (CCR5) that along with more than 10 other GPCRs have been shown to act as co-receptors for infection of HIV-1, HIV-2, and simian immunodeficiency virus (SIV) (Shimizu et al., 2000). Thus, it is not surprising that expression of receptors such as CCR5 and/or CXCR4 in target cells particularly CD4<sup>+</sup> T cells is elevated following HIV infection (Juffermans et al., 2000). Interestingly, chemokine (C-X-C motif) receptor 4 (CXCR4), as a GPCR, was observed to be up regulated in our microarray experiments that will be further discussed. In addition, it was also seen that two other GPCRs were significantly up regulated by EV71 infection of neural cells, including G protein-coupled receptor kinase 5 (+1.66-fold) and G protein-coupled receptor 176 (+1.78-fold) ( $p < 0.01$ ). As it was recently shown that GIPs are involved in GPCR functions in neurons (Bockaert et al., 2010), our findings might suggest that EV71 would induce an increase in expression of C1QTNF1 that may in turn assist a GPCR(s) (which remains to be identified) to function. As a result, EV71 would be able to divert putative GPCR(s) in neural cells to a state in which the viral replication could succeed and manifest its pathogenesis. On the contrary, Hep was seen to modulate this effect of EV71 through a significant decline in EV71-mediated up regulation of C1QTNF1, in comparison with virus control.

In this study, testis-specific kinase 2 encoded by TESK2 was seen up regulated by EV71 infection (+1.71-fold) followed by a significant interference by Hep, resulting in -1.62 times of difference of fold change between the two conditions. Testis-specific kinase 2 is a serine/threonine protein kinase for which a role in inducing apoptosis has been suggested (Toshima et al., 2001). It was demonstrated that expression of TESK2 in HeLa cells was involved in actin cytoskeletal re-organization by phosphorylating and regulating cofilin/ADF. In addition, a TESK2 mutant with an excess phosphorylation activity caused condensation and fragmentation of nuclei, followed by apoptosis in HeLa cells (Toshima et al., 2001). Thus, these findings may have an implication in the current investigation in that the EV71-mediated increase of TESk2 would ultimately lead to death of neural cells. Again, Hep might have likely modulated these events through a decrease in the extent of up regulation of the protein.

As a GPCR, CXCR4 was elevated by EV71 infection (+1.55-fold,  $p < 0.05$ ) in neural cells. In addition, Hep was observed to suppress the expression of this gene, making a difference of fold change between the conditions of treatment and virus control (-1.63-fold,  $p < 0.05$ ). CXCR4 receptors generally serve to modulate cellular functions such as cell migration, differentiation, and proliferation. Particularly, CXCR4 is one of the seven known CXC chemokine receptors in mammals and together with CCR5 are utilized by HIV-1 to gain entry into target cells (Juffermans et al., 2000). This receptor has a wide cellular distribution, from neutrophils, monocytes, T and B cells to vascular endothelial cells and neuronal cells (Bajetto et al., 1999). To the best of our knowledge, use of CXCR4 receptor by Enteroviruses has not been reported to date. However, Shih et al. (2004a) reported an up regulation for CCR5 following EV71 infection in glioblastoma cells, SF268. Taken together, it could be proposed that EV71 entry to neural cells might be partially mediated by CXCR4. The addition of Hep could have interfered with EV71 penetration by suppressing expression of CXCR4 in comparison to virus control. This postulation needs further confirmatory experiments and investigations.

In addition to CXCR4, we found that heparan sulfate 2-O-sulfotransferase 1 (HS2ST1) was significantly up regulated by EV71 infection of neural cells (+1.81-fold). This protein is responsible for the biosynthesis of cell surface HS. Addition of soluble Hep, as treatment, to EV71-infected neural cells did not significantly

change expression of HS2ST1 compared to virus control. This initially means soluble Hep does not do anything with direct induction of HS2ST1 and thus cell surface HS. However, these findings provide evidence that clinical EV71 needs cell surface HS to infect or bind neural cells, in accordance with the results of cell culture (Chapter 4). Considering this, it would then be reasonable to think soluble Hep (as a HS mimetic compound) can compete with cell surface HS as a candidate attachment co-receptor of EV71. Taken together, it might be concluded that increasing the level of HS2ST1 by EV71 is masked by competitive electrostatic interaction between soluble Hep and EV71 capsid that ultimately leads to preventing the viral infection or attachment.

In Chapter 4, it was also shown that while Hep greatly blocked infection and attachment of EV71 in neural cells, no conclusive results were generated with heparinase assays. In that Chapter, we concluded that those findings might suggest other cell receptors for clinical EV71 in neural cells in the absence of HS. Thus far, no neural specific receptor has been reported for EV71 neural pathogenesis (Weng et al, 2010). Based on the microarray findings of this Chapter, we might be able to conclude that in the absence of cell surface HS; neural cells might use neural-specific receptors such as CXCR4 and/or likely other CXC chemokine cell receptors. Other possibility might be that because soluble Hep (or other soluble GAGs) is not used in a heparinase assay, EV71 induction of HS2ST1 would lead to biosynthesizing cell surface HS without being impeded by Hep. Thus, this would mean there is sufficient cell surface HS for EV71 to bind and then infect host cells. It should be noted that the afore-mentioned conclusions needs further confirmation by Western blot, Real Time RT PCR and further confirmatory experiments.

Metallothionein 1E encoded by MT1E was highly elevated by EV71 infection (+2.49-fold,  $p<0.05$ ). Treatment of EV71-infected cells with Hep then significantly changed this profile by -2.92 times ( $p<0.01$ ) as compared to virus control. Having a high content of cystein residues, metallothioneins (MTs) can bind various heavy metals and are transcriptionally regulated by both heavy metals and glucocorticoids (UniProtKB, entry ID P04732). In fact, MTs are mainly known to play a role in detoxifying heavy metals. These proteins are also highly induced in response to pathological conditions such as inflammation, viral infection, anticancer drugs, and agents that generate reactive oxygen (Ghoshal et al., 2001). There are at

least ten known closely related metallothionein proteins expressed in the human body of which MT-I and II are present in all cells throughout the body (Thirumoorthy et al., 2011).

As part of cellular antioxidant mechanism, MTs protect the host cells from cytopathic effect of free radicals generated upon viral infection. Induction of MT following viral infection has been reported for few viruses, including influenza *in vitro* (Geiss et al., 2001) and *in vivo* (Ghoshal et al., 2001). Geiss et al. (2001) showed that expression of MT1 isoforms B, G, H, and L and MT2 in HeLa cells was elevated by influenza infection, but MT1E was not mentioned in their report. They concluded that MT induction might correspond to a host response to viral attachment-induced oxidative stress.

We searched for further isoforms of MT and interestingly found that in addition to MT1E, MT1 isoforms G and H and MT2 were also significantly up regulated following EV71 infection (virus control) at fold changes that were very similar to what Geiss et al. (2001) reported. However, unlike MT1E, Hep was not seen to change gene expression pattern of other MT isoforms than MT1E upon EV71 infection. MT1E in EV71-infected cells treated with Hep was not changed as compared to cell control but it was substantially down regulated (-2.92-fold at p value of  $7.18 \times 10^{-3}$ ) as compared to virus control. Thus, if we accept that up regulation of MTs benefit host cells to modulate viral attachment-induced oxidative stress, then the impact of Hep on EV71-infected cells would appear to be harmful for cells. However, this postulation may not be the only possible one, as Hep did not change gene expression patterns of other isoforms of MT in infected cells, as did not in the condition of compound control when applied alone. As such, another possibility might be that EV71-induced up regulation of MT1E likely would cause or induce other harmful pathways for cells leading to cytopathic effect, as opposite to other isoforms of MT. Thus, in this respect Hep could have assisted the host cells against EV71 infection; this issue would appear to worth further investigations.

The second group of genes induced by Hep was those that were not significantly induced by EV71 infection but were seen changed in the treatment condition. Further investigations revealed that some of these genes were not induced by Hep alone. Thus, we proposed that Hep in EV71-infected cells changed expression pattern of these genes in order to inhibit viral infection. These genes

included RBM7, EFHD2, KDM4D, GPNMB, and TFPI. There is no adequate information on genes RBM7, EFHD2, KDM4D, and TFPI in the literature to make relevant conclusions. Thus, we limited our analysis to GPNMB.

GPNMB encodes Glycoprotein (transmembrane) nmb that is induced in macrophages by IFN-gamma and lipopolysaccharide and serves as a feedback regulator of pro-inflammatory responses (Ripoll et al., 2007). In an attempt to gain deeper understanding of stage-specific patterns of gene expression during HIV-1 infection, a lymphatic tissue microarray analysis was performed (Li et al., 2009). Among the induced genes, there was an increase in several immunosuppressive genes including GPNMB. Similarly, Lee et al. (2010) reported that expression of GPNMB as an immunosuppressive gene was increased 3.861-fold following infection of pigs by Porcine circovirus type 2 (PCV2). Although these microarray analyses were accomplished on lymph nodes that were taken from infected humans or animals, still they might bear implications for our microarray study. GPNMB is an immunosuppressor gene and is shown to be up regulated following viral infection. However, in our microarray analysis, no induction of this gene was observed in the virus control. Instead, treatment of EV71-infected neural cells with Hep suppressed expression of this gene by 2.27-fold ( $p$  value of  $4.6 \times 10^{-3}$ ), causing a significant difference between the treatment condition and virus control or compound control. This might reflect a possible molecular target for antiviral activity of Hep *in vivo*, if neural cells would be lymph nodes infected with EV71. Thus, GPNMB induction in neural cells appears to be worthy to warrant further investigations.

Our microarray results also revealed 76 well-annotated genes that were exclusively induced (up or down) by Hep when it was added to uninfected neural cells. However, these were not in the scope of the current study, as Hep is not currently approved as an antiviral drug (like RBV or interferon). Therefore, in order to assess molecular basis of antiviral activity of Hep against EV71, fundamentally we should explore effect of Hep on gene expression patterns of EV71-infected cells, as compared to cell, virus, and compound controls.

In this study, we tried to determine global impact of Hep on EV71 infection of neural cells using a large-scale microarray analysis. To the best of our knowledge, this was the first microarray analysis of anti-EV71 compounds. In addition, this study could potentially be considered as a systematic approach for

screening and characterization of genes that are target for antiviral activity of a compound. Instead of stating a long list of gene functions and pathways, we tried to select for EV71-induced genes that were exclusively affected by antiviral activity of Hep in a real situation of viral infection of the cells, through a multi-level comparison and characterization.

Overall, the findings of this study suggest several molecular targets by which Hep might exert its profound antiviral activity against clinical EV71 infection in neural cells. Mostly, Hep appeared to modulate induction effect of EV71 on several genes in a way that may benefit the host cell and inhibit the viral infection. The most important genes where expression patterns were significantly changed by Hep include genes related to; (i) cell growth, (ii) DNA repair and replication, (iii) cytoplasmic microfilaments and related apoptosis, (iv) regulation of energy metabolism and mitochondrion-related apoptosis, (v) cytoplasmic viral transport, (vi) transmembrane proteins and the related signaling pathways, (vii) phosphoribosyltransferase, (viii) transcription factors, (ix) G protein-coupled receptors and G protein-coupled receptor-interacting proteins, (x) remodeling actin filament assembly, (xi) chemokine receptors, and (xii) immunosuppression. In addition, Hep sometimes appeared to be harmful for cells, like the case in that Hep likely suppresses regulation of Metallothionein 1E.

One of the possibilities suggested by the findings of Chapter 4 was that the role of Hep (or PPS) in preventing viral infection/attachment in neural cells might not be through interference with virus binding to cellular HS but via other unknown mechanism(s) of action. However, electrostatic interaction between the negatively charged Hep and the positively charged viral capsid could still be the case and interfere with EV71 attachment/entry. Hence, it should not be ruled out that the Hep-related effects seen in this microarray analysis might partially be attributed to a significant inhibitory effect of Hep on EV71 entry into the cells.

In conclusion, we propose that our microarray findings may suggest new directions for further studies on molecular targets of anti-EV71 activity of Hep. EV71 is a neurotropic virus that can cause severe and fatal CNS complications in infected patients. There is no approved drug for prophylaxis of EV71-caused disease and discovering a molecular drug target(s) for EV71 infection would be beneficial. The microarray analysis reported here was a large-scale microarray pilot study and



thus further confirmatory experiments such as real time RT PCR and Western blotting would be warranted in order to confirm the mode of action of Hep implied here.

## 6. Chapter Six: Final Conclusions

### 6.1. Establishment of a method for improving accuracy of EV71 titration

At the present time, the 50% tissue culture infectious dose (TCID<sub>50</sub>) is the most common approach for the titration of viruses that produce a cytopathic effect (CPE) in cell culture. Nevertheless, the conventional method of the TCID<sub>50</sub> (Reed and Muench, 1938) is mostly based on microscopic observations and scoring of viral CPE that in turn gives rise to subjective errors. For this reason, this method is unable to generate a quantifiable picture of how the virus titre is changed upon various dilutions. The findings of this study revealed that use of the log<sub>2</sub>-based MTS or MTT end-point dilution increased accuracy, reproducibility and reliability of the Enterovirus 71 (EV71) titration analysis. Additionally, the log<sub>2</sub>-based improved method of TCID<sub>50</sub> reported here has the advantage of being more sensitive, compared to common colourimetric-based viral titration assays that utilize 10-based logarithmic dilutions of virus. Coupled with the improved method TCID<sub>50</sub>, the plaquing assay results demonstrated that both plaque forming units (PFUs) and multiplicity of infection (MOI) amounts were more compatible and predictable with the log<sub>2</sub>-based MTT TCID<sub>50</sub>.

Although established for titration of EV71, the improved method of TCID<sub>50</sub> can also be used for other viruses to solve the common conceptual and mathematical problems of the traditional TCID<sub>50</sub> and improve upon the colourimetric-based titration methods currently in use. Thus, it could play a key role in any viral experimentation that needs accurate, quick, and cost-effective titration of CPE-generating viruses. Notably, this improved method would be useful for viruses for which antiviral compounds are increasingly sought after, including EV71, as it is a requisite for researchers to ensure that a consistently accurate and quantified titre of the virus is used in any step of their research.

## 6.2. Antiviral activities of heparan sulphate mimetics against EV71

This study was the first attempt to examine the possible potencies of soluble heparan sulphate (HS) mimetics against EV71 infection *in vitro*. Many polysulphated compounds have been synthesized to mimic cell surface HS and to serve as antiviral agents against a broad range of viruses. However, no research has been undertaken to examine the possible antiviral activity of HS mimetics against human Enterovirus A (HEV-A) and particularly EV71 infection. HS, heparin sodium salt (Hep) and pentosan polysulphate (PPS) all exhibited statistically significant antiviral activities towards a cloned EV71 strain in Vero cells, when compared to Ribavirin (RBV) ( $p < 0.05$ ). A potential for all of the HS mimetics to prevent EV71 attachment to Vero cells at low toxic concentrations was also demonstrated. Although conclusions as to the direct interaction between the HS mimetics and the virus were unable to be made, these findings initially suggested that the HS-like compounds are soluble, analogue forms of cell surface HS and can thus compete in binding to the virus. On the contrary, in this study RBV was not seen to significantly prevent EV71 binding, despite having previously been reported to exert anti-EV71 activity both *in vitro* and *in vivo* in RD, SK-N-SH, and N18 cells (Li et al., 2008). Hence, it is speculated that this difference might be attributed to RBV affecting a different part of the viral life cycle than attachment, such as viral replication.

Thus, these findings may have potential for further studies on the treatment of EV71 infection. In conclusion, the results of this study warranted further investigation of the role that cell surface HS may play in mediating EV71 infection and attachment.

## 6.3. Contributions of HS as a candidate receptor for Enteroviruses

Based on the observations and findings of Chapter 3, the involvement of HS in viral infection for low passage clinical representatives of HEV-A and HEV-B was examined. In short, Hep and PPS significantly inhibited infection and attachment of Coxsackievirus A16 (CVA16) and both cloned and clinical isolates of EV71 but showed no affect on Coxsackievirus B4 (CVB4) ( $p < 0.05$ ) in Vero cells. While enzymatic removal of HS by heparinases I prevented the binding of a clinical isolate

of EV71 by 52%, removal of the HS by heparinases I or III did not inhibit CVA16 or CVB4 binding. Unexpectedly, enzymatic cleavage of HS by heparinase I only had a moderate effect on the attachment of the cloned EV71 strain. These findings suggest that cell surface HS may not be essential for the attachment of the cloned EV71 strain.

Therefore, to explain the observations reported in Chapter 3, it was postulated that the cloned EV71 strain has possibly attained its capability to interact with cell surface HS through a reversible adaptation to tissue culture. Such adaptation has been reported for several viruses such as Foot-and-mouth disease (FMDV) (Sa-Carvalho et al., 1997; Baranowski et al., 1998; Escarmis et al., 1998; Neff et al., 1998), Sindbis virus (SIN) (Klimstra et al., 1998), and Venezuelan equine encephalitis virus (VEE) (Bernard et al., 2000). It could also be hypothesized that the cloned EV71 strain uses one or more of the following EV71 cell receptor candidates: the human scavenger receptor class B member 2 (SCARB2) (Yamayoshi et al., 2009); the human P-selectin glycoprotein ligand-1 (PSGL; also called CD162) (Nishimura et al., 2009); or sialic acid-linked glycans (Yang et al., 2009). This may warrant further investigations, aiming at examination of the effects of SCARB2 or PSGL monoclonal antibodies against the cloned EV71 infection/attachment. In addition, since the *Picornaviridae* family (like many other viruses) use several alternative cell receptors for attachment, it cannot be ruled out that cloned EV71 strain may still use HS as an alternative attachment co-receptor in Vero cells. The antiviral activity of Hep and PPS against the cloned EV71 isolate in Vero cells (Chapter 3) could also be explained by the electrostatic nature of the interaction between the soluble negatively charged HS mimetics and the positively charged capsid proteins of EV71. Thus, in general, exploiting the antiviral activity of HS mimetics compounds against EV71 may be an effective strategy that warrants further investigations.

Unlike the cloned EV71 strain, it was concluded that clinical EV71 utilizes highly sulphated domains of the cell surface HS during infection/attachment in Vero cells. Thus, it could be suggested that the heparin-like domains of cell surface HS are specific and necessary for infection/binding of at least one natural, clinical isolate of EV71 to Vero cells. Like the cloned isolate of EV71, it is also possible that the clinical isolate of EV71 might use other known or unknown cell surface attachment

receptors. Thus, the data presented here suggest that cell surface HS could be added as a candidate to the list of known attachment cell receptors for EV71.

Despite Hep and PPS demonstrating significant antiviral activity towards CVA16 attachment in Vero cells, heparinase assays led to the conclusion that CVA16 is not dependent on cell surface HS for binding. For example, this virus might use SCARB2 (Yamayoshi et al., 2009) or any other yet to be identified cell receptor to bind to Vero cells.

With regard to CVB4, it appears that cell surface HS does not play a key role in CVB4 infection/attachment. The virus might utilize the coxsackievirus and adenovirus receptor (CAR) to bind to Vero cells, as was previously reported in Chinese hamster ovary (*CHO*) cells (Bergelson et al, 1997; Tomoko et al, 1997; Bergelson et al, 1998).

Cell surface HS may not play an important role in the infection/attachment of the cloned EV71 strain and CVB4 to the neural cell line. In addition, although infection and attachment of clinical EV71 and clinical CVA16 were significantly prevented by Hep and PPS, the heparinase treatment of SK-N-SH cells did not generate conclusive results for these viruses. This might suggest the presence of other cell receptors for clinical EV71 in neural cells. One possibility might be that the role of Hep or PPS in viral infection and attachment is not through interference with virus binding to HS but via other unknown mechanism(s) of action. Therefore, further studies will be required in order to determine usage of alternative attachment receptor(s) other than HS by clinical EV71 and CVA16 in SK-N-SH cells.

In conclusion, HEV groups A and B can be divided according to their HS usage. Thus, it could be suggested that while CVB4 most likely does not use HS for infection/attachment, the role of HS as an attachment co-receptor for HEV-A could not be ruled out. Specifically, the findings of this study suggested that cell surface HS plays an important role in binding of clinical EV71 to Vero cells. The observed strong antiviral actions of Hep and PPS against the clinical isolate of EV71 in the neural cells are also important, as EV71 is known to cause severe neurological complications, suggesting further studies *in vivo*. Although it could not be confirmed whether HS mimetics exert their effect through viral attachment in neural cells, it might suggest the involvement of neural receptors or other mechanisms by

which Hep or PPS exert their antiviral activity. This warranted further investigations to assess the effects of the virus and HS mimetics on the genome of the cells.

#### **6.4. Microarray analysis of anti-EV71 activity of Hep**

It was established that Hep exhibited considerable antiviral activity towards a clinical EV71 isolate in the human neuroblastoma cell line, SK-N-SH (Chapter 4). Thus, the gene expression profiling of the EV71-infected neural cells treated by Hep was worthy of further investigation using a human genome-wide microarray expression analysis. This study was of importance because discovery or confirmation of antiviral activity of a compound *in vitro* or *in vivo* requires further investigations to gain a better understanding of the mechanisms underlying the actions of these compounds.

There has been minimal study undertaken to directly investigate the mode of action of an antiviral drug during viral infection. The microarray analysis reported here had the advantage of being performed using total transcripts taken from host cells treated with Hep following EV71 infection, in comparison to cell control, virus control and compound control. The microarray data were also coupled with cell culture results under the same conditions. Then, a strict multi-level selection procedure was applied to select for genes whose expression profile was changed by the antiviral activity of Hep. Overall, of more than 30,000 genes studied, 14 well-known annotated genes were selected that could possibly be targets for the antiviral activity of Hep against the EV71 infection in neural cells. Moreover, many unknown transcripts were also found that passed all of the selection process criteria for antiviral activity of Hep. Once a physiological function is assigned to any of these genes, it will likely become an appropriate research subject in future.

For most of the selected genes, Hep appeared to modulate the impact of EV71 infection on expression pattern of genes so that it may benefit the host cell and prevent consequent cell death. In addition, it should not be ruled out that at least part of the Hep-caused changes in gene profiling of EV71-infected cells could be due to inhibition of the virus entry by Hep. Both of these possibilities might shed light on molecular targets of EV71 infection of neural cells, which could be of importance for developing antiviral drugs against the virus infection.

In summary, gene classes whose expression profiling was changed by antiviral activity Hep were related to:

- Cell growth, DNA repair and replication
- Cytoplasmic microfilaments and related apoptosis
- Regulation of energy metabolism and mitochondrion-related apoptosis
- Cytoplasmic viral transport
- Transmembrane proteins and the related signaling pathways
- Phosphoribosyltransferase,
- Transcription factors
- G protein-coupled receptors and G protein-coupled receptor-interacting proteins
- Remodeling actin filament assembly
- Chemokine receptors,
- Immunosuppression

Different from these modes of actions, Hep also appeared to be harmful for cells in that it suppressed/increased regulation of genes that were induced by the cells as part of cellular defence system.

This was the first microarray analysis of anti-EV71 compounds and the first study of gene-level antiviral activity of Hep. Furthermore, this study could potentially be considered as a systematic approach for screening and characterization of genes involved in antiviral activity of a compound. In conclusion, the microarray findings of this study may suggest new directions for designing protein-level drug targets against EV71 infection. Although microarray analysis reported here was a large-scale microarray pilot study analyzed using a multi-level selection procedure, further confirmatory experiments such as real time RT PCR and Western blotting will be essentially warranted. In addition to mode of action of Hep, the findings revealed that there were more than 1000 other genes induced by EV71 infection with expression fold changes ranged from +46.5 to -10.7 at very high significance levels. These findings will be used for gaining a better understanding of neurovirulence of EV71 in another study.

## 6.5. Final statement

Thus far, no approved drug for prophylaxis of EV71-caused disease has been reported. Therefore, research studies should continue to explore potential compounds that exhibit excellent potencies against the infection. In conclusion, the findings of this PhD project provide evidence that the role of cell surface HS, and consequently HS mimetics, in mediating or preventing infection of HEV-A is considerable. This will facilitate further research to evaluate these compounds as antiviral drugs against infection of HEV-A and particularly EV71 *in vitro* followed by *in vivo* bio-assays. In addition, several cellular targets and pathways were determined to be possible targets for drugs against EV71 infection that can be considered directions for further investigations.



## Appendices

### Appendix 1

#### Use of TCID<sub>50</sub> to determine viral dilutions for plaquing assay

In the plaquing assay, initially a 2-mL suspension of EV71 containing 100 TCID<sub>50</sub> of the virus was made using the MTT-based approach (as described in Chapter 2, Page 81). This suspension was considered a reference so that further viral dilution factors were made based on that. The criterion was based on numbers of plaques that each 1-mL viral dilution was predicted to form in each well of a 6-well plate so that plaques could be distinguishable and countable. The following equation was used to predict viral plaques:  $\text{PFU (mL)} = 0.7 \times \text{TCID}_{50} \text{ (mL)}$  (Davis et al., 1972).

For example, one mL of 100 TCID<sub>50</sub> cloned strain of EV71 was estimated to generate 315,000 plaques per well. Based on this calculation, further 4 viral dilutions were determined: 1:315 (to generate 1000 plaques), 1:630 (to generate 500 plaques), 1:1260 (to generate 250 plaques), 1:3150 (to generate 100 plaques). In addition to these 4 viral dilutions, a negative control (uninfected cells) and positive control (the suspension of 100 TCID<sub>50</sub> cloned strain of EV71 that was predicted to generate 315,000 plaques).

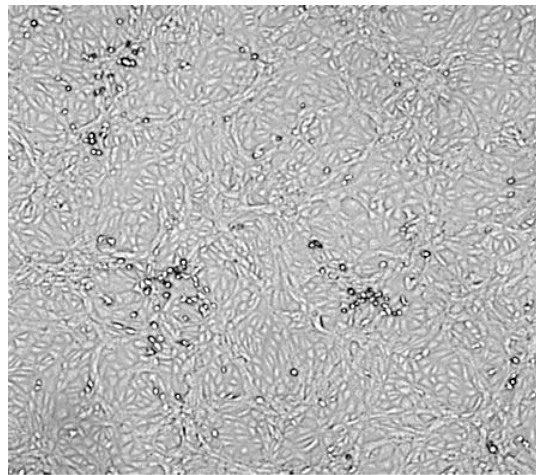
However, the observed viral plaques per any viral dilution were less than the predicted ones and did not follow the equation of  $\text{PFU (mL)}/\text{TCID}_{50} \text{ (mL)} = 0.7$ . Yet, it was an initial, reasonable estimation for making viral dilutions so that there was a reasonable relationship between TCID<sub>50</sub>-based viral dilutions and numbers of observed viral plaques.

## Appendix 2

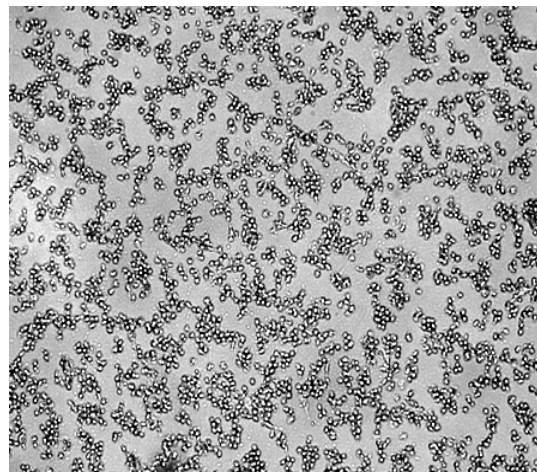
### Observation and scoring of viral CPE in the traditional TCID<sub>50</sub>:

1. Check the wells under the microscope. Once CPE is 100% in the undiluted virus control (as the following pictures shows), go to the step 2.
2. Mark each well as “CPE positive” or “CPE negative”. Calculate the TCID<sub>50</sub> as following table illustrates.

**a**



**b**



The pictures depict symptoms of EV71 cytopathic effect in Vero cells. Cytopathic effect is result of lysis of the host cell by the virus. Cell shrinkage and rounding (a) appears in the first a few hours or first day of viral infection followed by floating and detaching dead cells (b) at 72 hours post infection. The photos are taken with the invert microscope, 100 times magnification.

The conventional algorithm for determination of TCID<sub>50</sub> based on manually scored CPE

Dilution factor	No. of wells showing CPE	No. of wells not showing CPE	Cumulative No. of wells infected	Cumulative no. of wells not infected	Calculated infectivity ratio	Calculated infectivity percentage
10 <sup>1</sup>	6	0	30	0	30/30	100
10 <sup>2</sup>	6	0	24	0	24/24	100
10 <sup>3</sup>	6	0	18	0	18/18	100
10 <sup>4</sup>	6	0	12	0	12/12	100
10 <sup>5</sup>	4	2	6	2	6/8	75
10 <sup>6</sup>	1	5	2	7	2/9	22.222
10 <sup>7</sup>	1	5	1	12	1/13	7.692
10 <sup>8</sup>	0	6	0	18	0/18	0
10 <sup>9</sup>	0	6	0	24	0/24	0

The values represent one of the two independent experiments carried out from which the 50% point was calculated using the Reed-Muench's formula.

$$PD = \frac{\text{closest infectivity above 50\%} - 50\%}{\text{closest infectivity above 50\%} - \text{closest infectivity below 50\%}}$$

Dilution factor (DF) = (PD) + (dilution factor of the closest dilution above 50% CPE ratio);

PD = 0.334; DF = 5 + 0.474 = 5.334; 10<sup>5.474</sup>/40 μL; TCID<sub>50</sub> would be ≈ 7.4 × 10<sup>6</sup> per mL

### Appendix 3

#### Drug safety index

**Table 1. Drug safety index of the antiviral concentrations for the tested compounds**

		Effective range of antiviral concentrations (µg/mL)					
		125	62.5	31.25	15.62	7.81	3.9
Compounds	Hep	4.247	5.598	7.698	7.231	10.705	10.904
	HS	1.434	1.769	2.390	4.202	4.352	5.894
	PPS	2.097	2.557	2.681	2.804	3.190	3.423

Each value is generated by dividing of the antiviral inhibition percentage by cytotoxicity percentage at the relevant concentration. As can be seen in the table, the greater the drug safety value, the less toxic it is and the more effective it is. Thus, for example, the concentrations 7.81 and 3.9 µg/mL appears to be most effective ones within Hep concentrations and between the compounds, which is in compatible with the actual observations and results

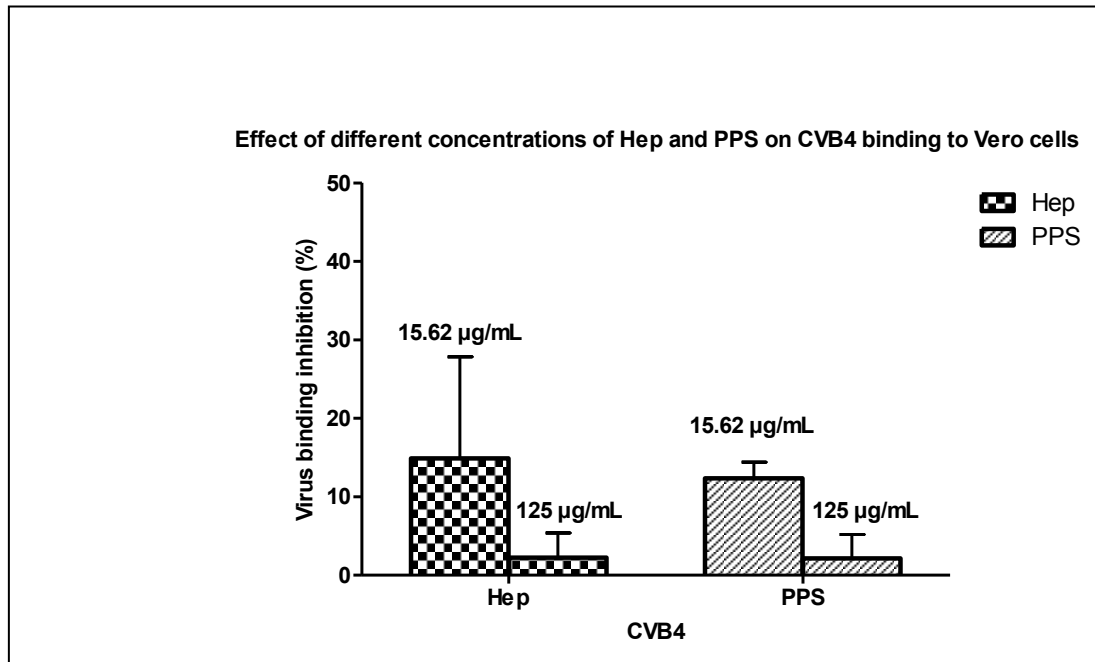
**Table2. Estimated molarities (µM) of the tested compounds**

		Concentration (µg/ml)								
		1000	500	250	125	62.5	31.25	15.62	7.81	3.9
Compound	Hep	66	33	16	8	4	2	1	0.5	0.3
	HS	66	33	16	8	4	2	1	0.5	0.3
	PPS	222	111	55	27	13	6	3	1	0.9
	RBV	4095	2047	1023	511	255	127	63	31	15

- Hep: ~15000 Da (15000 g/mol) (Dietrich et al., 1999; Nyberg et al., 2004)
- HS (from porcine intestinal mucosa): ~ 15000 Da (15000 g/mol) on average (Griffin et al., 1995)
- PPS: (NaPPS) 4000-5000; 4500 Da (4500 g/mol) on average (Material Safety Data Sheet, Biopharm Australia Pty Ltd)
- RBV: 244.20 Da (244.20 g/mol) (Sigma-Aldrich)

Appendix 4

Testing different concentrations of Hep and PPS against CVB4



## Appendix 5

### Some of microarray results

**Table 1. Quality control specifications of total RNA samples**

Sample <sup>a</sup>	RIN <sup>b</sup>	RNA concentration (ng/ $\mu$ L)	A28S/A18S	RNA area	rRNA % <sup>c</sup>
CC <sub>1</sub>	9.2	168	1.5	170.1	43.1
CC <sub>2</sub>	8.5	179	1	181.2	29.4
CC <sub>3</sub>	8.5	81	1.3	143.1	27.9
VC <sub>1</sub>	9.2	129	1.3	130.1	41
VC <sub>2</sub>	8.8	157	1.2	158.3	32.7
VC <sub>3</sub>	8.8	84	1.3	149.0	32.3
Hep <sub>1</sub>	9.4	151	1.5	152.1	48.4
Hep <sub>2</sub>	9.1	82.2	1.4	82.2	40.7
Hep <sub>3</sub>	9.2	97	1.5	171.6	41.6
Cyto <sub>1</sub>	8.5	92	1.1	162.4	28.5
Cyto <sub>2</sub>	8.6	89	1.1	156.9	33.7
Cyto <sub>3</sub>	8.9	66	1.4	116.2	37.7

- CC: cell control (cells not infected or treated); VC: virus control (cells infected with EV71 but not treated with Hep); Hep: EV71-infected cells treated with Hep; Cyto: cells treated with Hep but not infected with EV71; the subscript digit numbers indicate replications.
- RIN: RNA integrity number (out of 10)
- Percentage of ribosomal RNA (28S+18S) (of total RNA area)

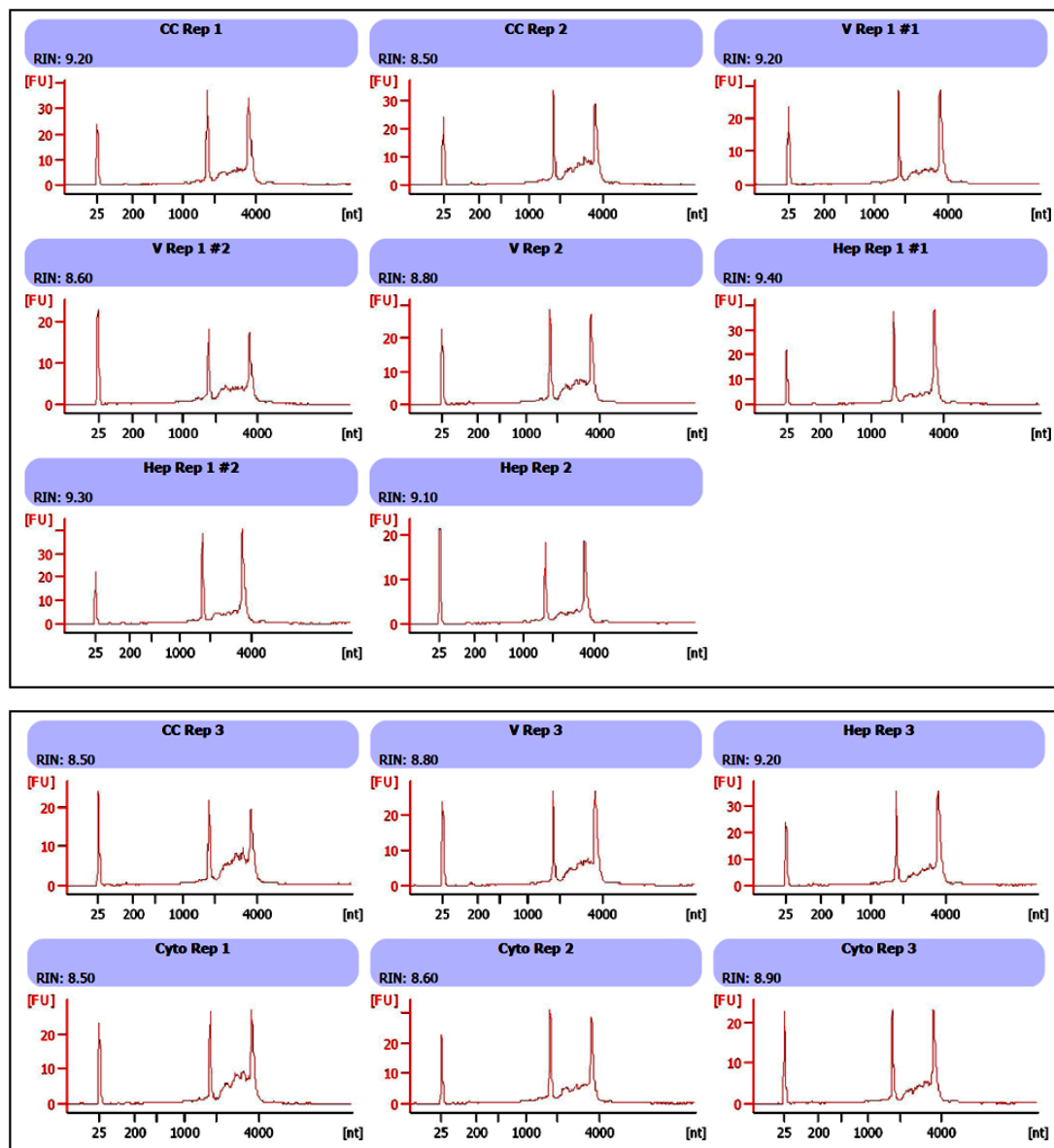


**Figure 1. All electropherograms of RNA samples analyzed by Bioanalyzer**

The images show electropherogram summary generated by Agilent 2100 Bioanalyzer (© Copyright 2003 - 2009 Agilent Technologies, Inc.). CC: cell control (cells not infected or treated); V: virus control (cells infected with EV71 but not treated with Hep); Hep: EV71-infected cells treated with Hep; Cyto: cells treated with Hep but not infected with EV71; the subscript digit numbers indicate replications. There are two samples for some of replications.

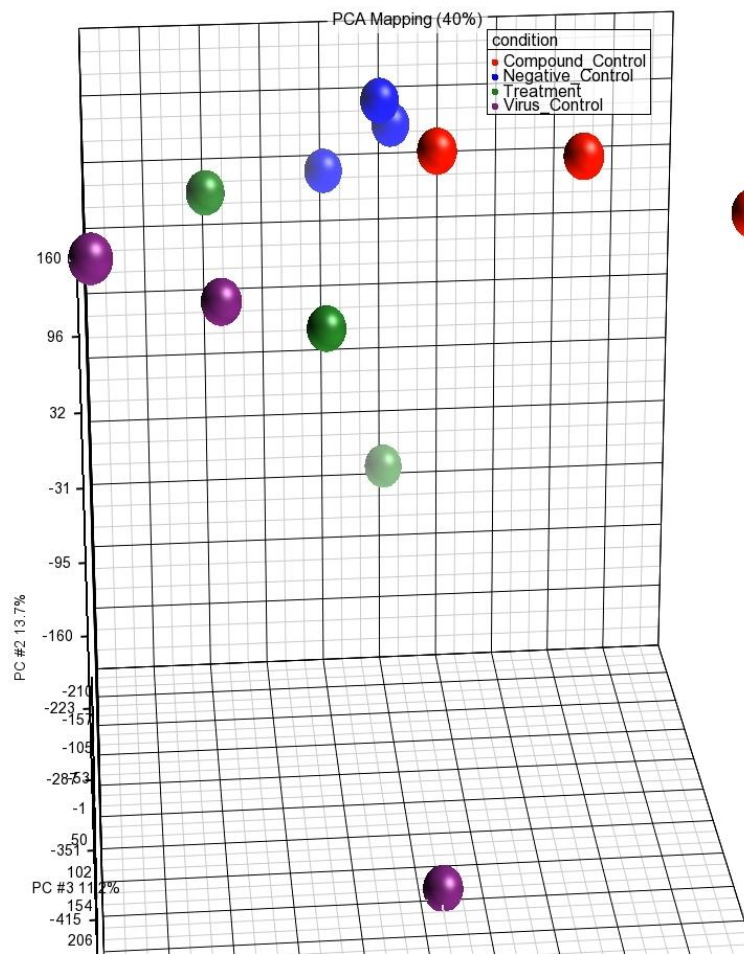


**Figure 2. Principle component analysis (PCA) of the twelve samples**

Conditions (each at three replications) included: cell control (in blue), virus control (in purple), treatment (in green), and compound control (in red).



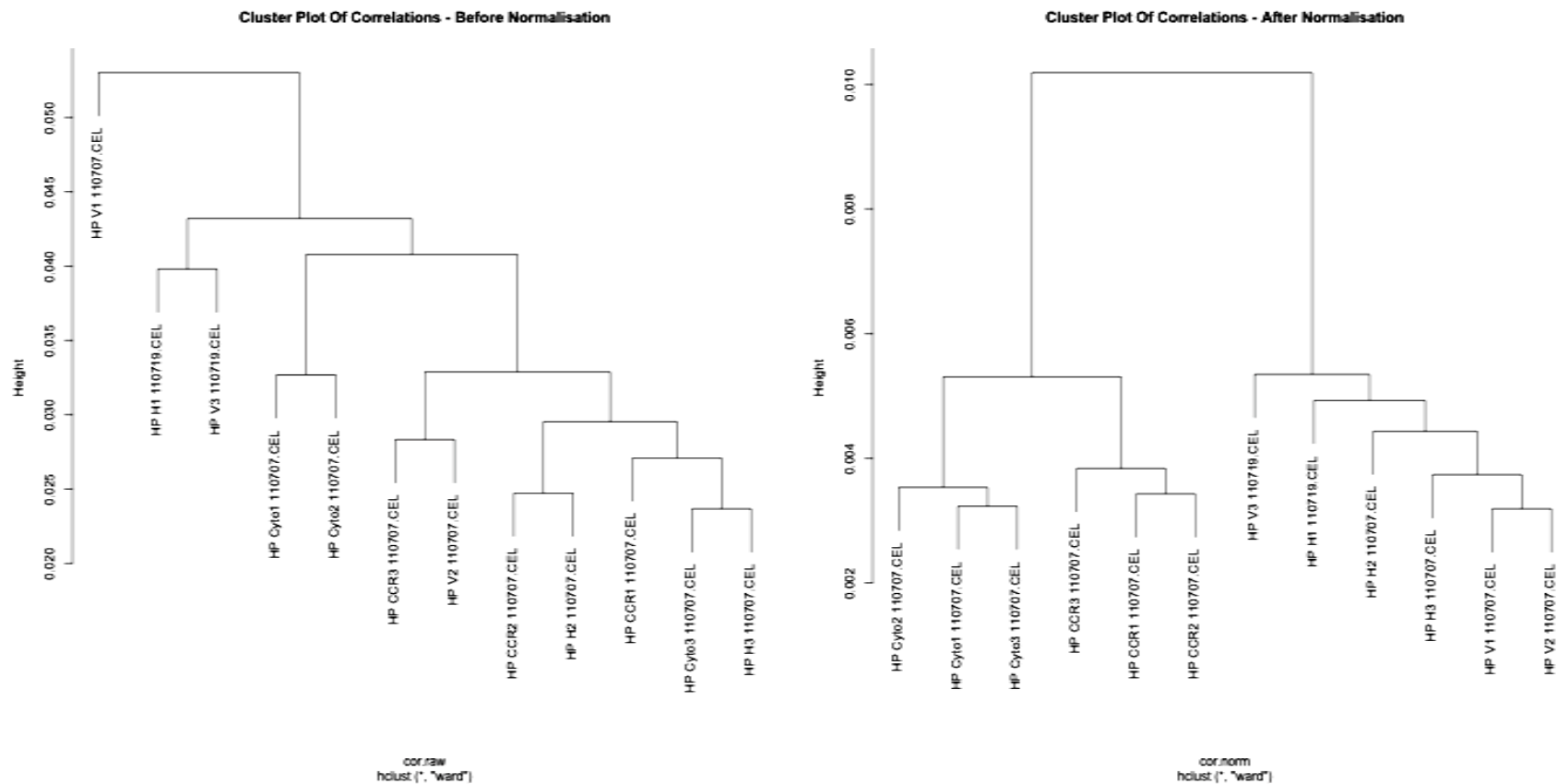


**Figure 3. Cluster plots of correlations, before and after normalization**

CC: cell control (cells not infected or treated); V: virus control (cells infected with EV71 but not treated with Hep); H: EV71-infeted cells treated with Hep; Cyto: cells treated with Hep but not infected with EV71; the subscript digit numbers indicate replications. HP stands for HR Pourianfar.

## **Bibliography**

- Aboudy, Y., Mendelson, E., Shalit, I., Bessalle, R., Fridkin, M., 1994. Activity of two synthetic amphiphilic peptides and magainin-2 against herpes simplex virus types 1 and 2. *Int. J. Pept. Protein Res.* 43, 573–582.
- Adamiak, B., Ekblad, M., Bergstrom, T., Ferro, V., Trybala, E., 2007. Herpes simplex virus type 2 glycoprotein G is targeted by the sulfated oligo- and polysaccharide inhibitors of the virus attachment to cells. *J. Virol.* 81, 13424-13434.
- Airaksinen, A., Pariente, N., Menéndez-Arias, L., Domingo, E., 2003. Curing of foot-and-mouth disease virus from persistently infected cells by ribavirin involves enhanced mutagenesis. *Virology* 311, 339-349.
- Albin, R., Chase, R., Risano, C., Lieberman, M., Ferrari, E., Skelton, A., Buontempo, P., Cox, S., DeMartino, J., Wright-Minogue, J., Jirau-Lucca, G., Kelly, J., Afonso, A., Kwong, A.D., Rozthon, E., O'Connell, J.F., 1997. SCH 43478 and analogs: in vitro activity and in vivo efficacy of novel agents for herpesvirus type 2. *Antiviral Res.* 35, 139-146.
- Albiol-Matanić, V.C., Castilla, V., 2004. Antiviral activity of antimicrobial cationic peptides against Junin virus and herpes simplex virus. *Int. J. Antimicrob. Agents* 23, 382-389.
- Aliahmad P, Seksenyan A, Kaye J. 2011. The many roles of TOX in the immune system. *Curr. Opin. Immunol.* 24, 1-5.
- Andersen, J.H., Jenssen, H., Gutteberg, T.J., 2003. Lactoferrin and lactoferricin inhibit Herpes simplex 1 and 2 infection and exhibit synergy when combined with acyclovir. *Antiviral Res.* 58, 209-215.

- Andersen, J.H., Osbakk, S.A., Vorland, L.H., Traavik, T., Gutteberg, T.J., 2001. Lactoferrin and cyclic lactoferricin inhibit the entry of human cytomegalovirus into human fibroblasts. *Antiviral Res.* 51, 141-149.
- Anderson, P., Alm, S., Edman, K., Lindberg, A.M., 2005. A novel and rapid method to quantify cytolitic replication of Picornaviruses in cell culture. *J. Virol. Methods* 130, 117-123.
- Andino, R., Bøddeker, N., Silvera, D., Gamarnik, A.V., 1999. Intracellular determinants of picornavirus replication. *Trends Microbiol.* 7, 76-81.
- Andries, K., Dewindt, B., Snoeks, J., Willebrords, R., Van Eemeren, K., Stokbroekx, R., Janssen, P.A., 1992. In vitro activity of pirodavir (R 77975), a substituted phenoxy-pyridazinamine with broad-spectrum antipicornaviral activity. *Antimicrob. Agents Chemother.* 36, 100-107.
- Asahina, Y., Izumi, N., Enomoto, N., Uchihara, M., Kurosaki, M., Onuki, Y., Nishimura, Y., Ueda, K., Tsuchiya, K., Nakanishi, H., Kitamura, T., Miyake, S., 2005. Mutagenic effects of ribavirin and response to interferon/ribavirin combination therapy in chronic hepatitis C. *J. Hepatol.* 43, 623-629.
- Atienza, J.M., Roth, R.B., Rosette, C., Smylie, K.J., Kammerer, S., Rehbock, J., Ekblom, J., Denissenko, M.F., 2005. Suppression of RAD21 gene expression decreases cell growth and enhances cytotoxicity of etoposide and bleomycin in human breast cancer cells. *Mol. Cancer Ther.* 4, 361-8.
- Baba, M., Pauwels, R., Balzarini, J., Arnout, J., Desmyter, J., De Clercq, E., 1988a. Mechanism of inhibitory effect of dextran sulfate and heparin on replication of human immunodeficiency virus in vitro. *Proc. Natl. Acad. Sci. USA.* 85, 6132-6136.
- Baba, M., Snoeck, R., Pauwels, R., De Clercq, E., 1988b. Sulfated polysaccharides are potent and selective inhibitors of various enveloped viruses, including herpes

- simplex virus, cytomegalovirus, vesicular stomatitis virus, and human immunodeficiency virus. *Antimicrob. Agents Chemother.* 32, 1742-1745.
- Bajetto, A., Bonavia, R., Barbero, S., Piccioli, P., Costa A, Florio T, Schettini, G., 1999. Glial and neuronal cells express functional chemokine receptor CXCR4 and its natural ligand stromal cell-derived factor 1. *J. Neurochem.* 73, 2348-2357.
- Baranowski, E., Sevilla, N., Verdaguer, N., Ruiz-Jarabo, C.M., Beck, E., Domingo, E., 1998. Multiple virulence determinants of foot-and-mouth disease virus in cell culture. *J. Virol.* 72, 6362-6372.
- Bartrop, J.A., Owen, T.C., Cory, A.H., Cory, J.G., 1991. 5-(3-carboxymethoxyphenyl)-2-(4,5-dimethylthiazolyl)-3-(4-sulfophenyl)tetrazolium, inner salt (MTS) and related analogs of 3-(4,5-dimethylthiazolyl)-2,5-diphenyltetrazolium bromide (MTT) reducing to purple water-soluble formazans as cell-viability indicators. *Bioorg. Med. Chem. Lett.* 1, 611-614.
- Barnard, D.L., Huffman, J.H., Morris, J.L., Wood, S.G., Hughes, B.G., Sidwell, R.W., 1992. Evaluation of the antiviral activity of anthraquinones, anthrones and anthraquinone derivatives against human cytomegalovirus. *Antiviral Res.* 17, 63-77.
- Barth, H., Schäfer, C., Adah, M.I., Zhang, F., Linhardt, R.J., Toyoda, H., Kinoshita-Toyoda, A., Toida, T., Van Kuppevelt, T.H., Depla, E., Von Weizsäcker, F., Blum, H.E., Baumert, T.F., 2003. Cellular binding of hepatitis C virus envelope glycoprotein E2 requires cell surface heparan sulfate. *J. Biol. Chem.* 278, 41003-41012.
- Baxi, M.K., Baxi, S., Clavijo, A., Burton, K.M., Deregt, D., 2006. Microarray-based detection and typing of foot-and-mouth disease virus. *Vet. J.* 172, 473-481.

- Baylis, A.S., Shah, N., Minor, D.P., 2004. Evaluation of different assays for the detection of parvovirus B19 DNA in human plasma. *J. Virol. Methods* 121, 7-16.
- Benjamini, Y., Hochberg, Y., 1995. Controlling the false discovery rate: a practical and powerful approach to multiple testing. *J. Roy. Statistical Society B*, 57, 289 - 300.
- Bergelson, J.M., Chan, M., Solomon, K.R., St John, N.F., Lin, H., Finberg, R.W., 1994. Decay-accelerating factor (CD55), a glycosylphosphatidylinositol-anchored complement regulatory protein, is a receptor for several echoviruses. *Proc. Natl. Acad. Sci.* 91, 6245-6248.
- Bergelson, J.M., Cunningham, J., Droguett, G., Kurt-Jones, E., Krithivas, A., Hong, J., Horwitz, M., Crowell, R., Finberg, R., 1997. Isolation of a common receptor for Coxsackie B viruses and adenoviruses 2 and 5. *Science* 275, 1320 - 1323.
- Bergelson, J.M., Krithivas, A., Celi, L., Droguett, G., Horwitz, M.S., Wickham, T., Crowell, R.L., Finberg, R.W., 1998. The murine CAR homolog is a receptor for coxsackie B viruses and adenoviruses. *J. Virol.* 72, 415-419.
- Bergelson, J.M., Mohanty, J., Crowell, R., St. John, N., Lublin, D., Finberg, R., 1995. Coxsackievirus B3 adapted to growth in RD cells binds to decay- accelerating factor (CD55). *J. Virol.* 69, 1903-1906.
- Bergelson, J.M., Shepley, M., Chan, B., Hemler, M., Finberg, R., 1992. Identification of the integrin VLA-2 as a receptor for Echovirus 1. *Science* 255, 1718-1720.
- Bergelson, J.M., St John, N., Kawaguchi, S., Chan, M., Stubdal, H., Modlin, J., Finberg, R.W., 1993. Infection by Echoviruses 1 and 8 depends on the alpha 2 subunit of human VLA-2. *J. Virol.* 67, 6847-6852.

- Bermudez, V.P., Maniwa, Y., Tappin, I., Ozato, K., Yokomori, K., Hurwitz, J., 2003. The alternative Ctf18-Dcc1-Ctf8-replication factor C complex required for sister chromatid cohesion loads proliferating cell nuclear antigen onto DNA. *Proc. Natl. Acad. Sci. U.S.A.* 100, 10237-10242.
- Bernard, K.A., Klimstra, W.B., Johnston, R.E., 2000. Mutations in the E2 glycoprotein of Venezuelan Equine encephalitis virus confer heparan sulfate interaction, low morbidity, and rapid clearance from blood of mice. *Virology* 276, 93-103.
- Bernfield, M., Götte, M., Park, P.W., Reizes, O., Fitzgerald, M.L., Lincecum, J., Zako, M., 1999. Functions of cell surface heparan sulfate proteoglycans. *Annu. Rev. Biochem.* 68, 729-777.
- Bernstein, E., Caudy, A.A., Hammond, S.M., Hannon, G.J., 2001. Role for a bidentate ribonuclease in the initiation step of RNA interference. *Nature* 409, 363-366.
- Binford, S.L., Maldonado, F., Brothers, M.A., Brothers, Weady, P.T., Zalman, L.S., Meador III, J.W., Matthews, D.A., Patick, A.K., 2005. Conservation of amino acids in human rhinovirus 3C protease correlates with broad-spectrum antiviral activity of rupintrivir, a novel human rhinovirus 3C protease inhibitor. *Antimicrob. Agents Chemother.* 49, 619-626.
- Bitko, V., Musiyenko, A., Shulyayeva, O., Barik, S., 2005. Inhibition of respiratory viruses by nasally administered siRNA. *Nat. Med.* 11, 50-55.
- Bockaert, J., Perroy, J., Becamel, C., Marin, P., Fagni, L., 2010. GPCR interacting proteins (GIPs) in the nervous system: Roles in physiology and pathologies. *Annu. Rev. Pharmacol. Toxicol.* 50, 89-109.
- Bockaert, J., Roussignol, G., Becamel, C., Gavarini, S., Joubert, L., Dumuis, A., Fagni, L., Marin, P., 2004. GPCR-interacting proteins (GIPs): nature and functions. *Biochem. Soc. Trans.* 32, 851-855.

- Brown, B.A., Oberste, M.S., James, P., Alexander, J.R., A., Kennett, M.L., Pallansch, M.A., 1999. Molecular epidemiology and evolution of Enterovirus 71 strains isolated from 1970 to 1998. *J. Virol.* 73, 9969-9975.
- Brown, B.A., Pallansch, M.A., 1995. Complete nucleotide sequence of Enterovirus 71 is distinct from poliovirus. *Virus Res.* 39, 195-205.
- Byrnes, A.P., Griffin, D.E., 2000. Large-plaque mutants of Sindbis virus show reduced binding to heparan sulfate, heightened viremia, and slower clearance from the circulation. *J. Virol.* 74, 644-651.
- Cabezas, J., 1991. Some questions and suggestions on the type references of the official nomenclature (IUB) for sialidase(s) and endosialidase. *Biochem. J.* 278, 311-312.
- Campbell, C.J., Ghazal, P., 2004. Molecular signatures for diagnosis of infection: application of microarray technology. *J. Appl. Bacteriol.* 96, 18-23.
- Caro, V., Guillot, S., Delpeyroux, F., Crainic, R., 2001. Molecular strategy for serotyping of human enteroviruses. *J. Gen. Virol.* 82, 79-91.
- Chang, C.S., Lin, Y.T., Shih, S.R., Lee, C.C., Lee, Y.C., Tai, C.L., Tseng, S.N., Chern, J.H., 2005. Design, synthesis, and anticoronavirus activity of 1-[5-(4-arylphenoxy)alkyl]-3-pyridin-4-ylimidazolidin-2-one derivatives. *J. Med. Pharm. Chem.* 48, 3522-3535.
- Chang, J.S., Wang, K.C., Chiang, L.C., 2008. Sheng-Ma-Ge-Gen-Tang inhibited Enterovirus 71 infection in human foreskin fibroblast cell line. *J. Ethnopharmacol.* 119, 104-108.
- Chang, Y.E., Laimins, L.A., 2000. Microarray analysis identifies interferon-inducible genes and Stat-1 as major transcriptional targets of human papillomavirus type 31. *J. Virol.* 74, 4174-4182.

- Chen, C.S., Yao, Y.C., Lin, S.C., Lee, Y.P., Wang, Y.F., Wang, J.R., Liu, C.C., Lei, H.Y., Yu, C.K., 2007. Retrograde axonal transport: a major transmission route of enterovirus 71 in mice. *J. Virol.* 81, 8996-9003.
- Chen, K.T., Lee, T.C., Chang, H.L., Yu, M.C., Tang, L.H., 2008. Human Enterovirus 71 disease: clinical features, epidemiology, virology, and management. *Open Epidemiol. J.*, 1, 10-16.
- Chen, S.C., Chang, H.L., Yan, T.R., Cheng, Y.T., Chen, K.T., 2007. An eight-year study of epidemiologic features of Enterovirus 71 infection in Taiwan. *AM. J. Trop. Med. Hyg.* 77, 188-191.
- Chen, T.C., Liu, S.C., Huang, P.N., Chang, H.Y., Chern, J.H., Shih, S.R., 2008a. Antiviral activity of pyridyl imidazolidinones against Enterovirus 71 variants. *J. Biomed. Sci.* 15, 291-300.
- Chen, T.C., Weng, K.F., Chang, S.C., Lin, J.Y., Huang, P.N., Shih, S.R., 2008b. Development of antiviral agents for Enteroviruses. *J. Antimicrob. Chemother.* 62, 1169-1173.
- Chen, Y., Maguire, T., Hileman, R.E., Fromm, J.R., Esko, J.D., Linhardt, R.J., Marks, R.M., 1997. Dengue virus infectivity depends on envelope protein binding to target cell heparan sulphate. *Nat. Med.* 3, 866-871.
- Chern, J.H., Lee, C.C., Chang, C.S., Lee, Y.C., Tai, C.L., Lin, Y.T., Shia, K.S., Lee, C.Y., Shih, S.R., 2004. Synthesis and antienteroviral activity of a series of novel, oxime ether-containing pyridyl imidazolidinones. *Bioorg. Med. Chem. Lett.* 14, 5051-5056.
- Chiang, L.C., Chiang, W., Chang, M.Y., Ng, L.T., Lin, C.C., 2002. Antiviral activity of *Plantago major* extracts and related compounds in vitro. *Antiviral Res.* 55, 53-62.



- Chiang, L.C., Ng, L.T., Cheng, P.W., Chiang, W., Lin, C.C., 2005. Antiviral activities of extracts and selected pure constituents of *Ocimum basilicum*. *Clin. Exp. Pharmacol. Physiol.* 32, 811-816.
- Chung, Y.C., Huang, J.H., Lai, C.W., Sheng, H.C., Shih, S.R., Ho, M.S., Hu, Y.C., 2006. Expression, purification and characterization of Enterovirus-71 virus-like particles. *World J. Gastroenterol.* 12, 921-927.
- Clewley, J.P., 2004. A role for arrays in clinical virology: fact or fiction? *J. Clin. Virol.* 29, 2-12.
- Contreras, A.M., Hiasa, Y., He, W., Terella, A., Schmidt, E.V., Chung, R.T., 2002. Viral RNA mutations are region specific and increased by ribavirin in a full-length hepatitis C virus replication system. *J. Virol.* 76, 8505–8517.
- Coombe, D.R., Kett, W.C., 2005. Heparan sulfate-protein interactions: therapeutic potential through structure-function insights. *Cell. Mol. Life Sci.* 62, 410-424.
- Cory, A.H., Owen, T.C., Barltrop, J.A., Cory, J.G., 1991. Use of an aqueous soluble tetrazolium/formazan assay for cell growth assays in culture. *Cancer Commun.* 3, 207-212.
- Crotty, S., Cameron, C.E., Andino, R., 2001. RNA virus error catastrophe: direct molecular test by using ribavirin. *Proc. Natl. Acad. Sci. U.S.A.* 98, 6895–6900.
- Crotty, S., Maag, D., Arnold, J.J., Zhong, W., Lau, J.Y.N., Hong, Z., Andino, R., Cameron, C.E., 2000. The broad-spectrum antiviral ribonucleoside ribavirin is an RNA virus mutagen. *Nat. Med.* 6, 1375-1379.
- Crublet, E., Andrieu, J.P., Vivès, R.R., Lortat-Jacob, H., 2008. The HIV-1 envelope glycoprotein gp120 features four heparan sulfate binding domains, including the co-receptor binding site. *J. Biol. Chem.* 283, 15193-15200.

- Da Silva, E.E., Winkler, M.T., Pallansch, M.A., 1996. Role of Enterovirus 71 in Acute Flaccid Paralysis after the Eradication of Poliovirus in Brazil. *Emerging Infect. Dis.* 2, 231-233.
- Davis, B.D., Dulbecco, R., Eisen, H.N., Ginsberg, H.S., Wood, W.B., 1972. Nature of viruses, in: *Microbiology*. Harper and Row, New York, pp. 1044-1053.
- De Clercq, E., 2005. Antiviral drug discovery and development: Where chemistry meets with biomedicine. *Antiviral Res.* 67, 56-75.
- De Jesus, N., 2007. Epidemics to eradication: the modern history of poliomyelitis. *Virology J.* 4, 70.
- De Logu, A., Loy, G., Pellerano, M.L., Bonsignore, L., Schivo, M.L., 2000. Inactivation of HSV-1 and HSV-2 and prevention of cell-to-cell virus spread by Santolina insularis essential oil. *Antiviral Res.* 48, 177-185.
- De Somer, P., De Clercq, E., Billiau, A., Schonke, E., Claesen, M., 1968. Antiviral activity of polyacrylic and polymethacrylic acids: I. mode of action in vitro. *J. Virol.* 2, 878-885.
- Der, S.D., Zhou, A., Williams, B.R., Silverman, R.H., 1998. Identification of genes differentially regulated by interferon alpha, beta, or gamma using oligonucleotide arrays. *Proc. Natl. Acad. Sci. U.S.A.* 95, 15623–15628.
- Desmond, R.A., Accortt, N.A., Talley, L., Villano, S.A., Soong, S.J., Whitley, R.J., 2006. Enteroviral meningitis: natural history and outcome of pleconaril therapy. *Antimicrob. Agents Chemother.* 50, 2409-2414.
- DeVincenzo, J.P., 2008. RNA interference strategies as therapy for respiratory viral infections. *Pediatr. Infect. Dis. J.* 27, S118-122.

- Diaz-Guerra, M., Rivas, C., Esteban, M., 1997. Inducible expression of the 2-5A synthetase/RNase L system results in inhibition of vaccinia virus replication. *Virology* 227, 220–228.
- Dietrich, C.P., Paiva, J.F., Castro, R.A.B., Chavante, S.F., Jeske, W., Fareed, J., Gorin, P.A.J., Mendes, A., Nader, H.B., 1999. Structural features and anticoagulant activities of a novel natural low molecular weight heparin from the shrimp *Penaeus brasiliensis*. *Biochim. Biophys. Acta, Gen. Subj.* 1428, 273-283.
- Distefano, D.J., Gould, S.L., Munshi, S., Robinson, D.K., 1995. Titration of human-bovine rotavirus reassortants using a tetrazolium-based colorimetric end-point dilution assay. *J. Virol. Methods* 55, 199-208.
- Domingo-Gil, E., González, J.M., Esteban, M., 2010. Identification of cellular genes induced in human cells after activation of the OAS/RNaseL pathway by vaccinia virus recombinants expressing these antiviral enzymes. *J. Interferon Cytokine Res.* 30, 171-188.
- Dong, B., Silverman, R.H., 1995. 2-5A-dependent RNase molecules dimerize during activation by 2-5A. *J. Biol. Chem.* 270, 4133–4137.
- Dufva, M., 2005. Fabrication of high quality microarrays. *Biomol. Eng.* 22, 173-184.
- Dufva, M., 2009. Fabrication of DNA microarray, in: Dufva, M., (Ed.), *DNA Microarrays for Biomedical Research*. Humana Press 529, 63-79.
- Dulbecco, R., Vogt, M., 1954. Plaque formation and isolation of pure lines with poliomyelitis viruses. *J. Exp. Med.* 99, 167-182.
- Dumur, C.I., Nasim, S., Best, A.M., Archer, K.J., Ladd, A.C., Mas, V.R., Wilkinson, D.S., Garrett, C.T., Ferreira-Gonzalez, A., 2004. Evaluation of quality-control criteria for microarray gene expression analysis. *Clin. Chem.* 50, 1994-2002.

- Dürüst, N., Meyerhoff, M.E., 2001. Determination of pentosan polysulfate and its binding to polycationic species using polyion-sensitive membrane electrodes. *Analytica Chimica Acta* 432, 253-260.
- Ebermann, L., Wika, S., Klumpe, I., Hammer, E., Klingel, K., Lassner, D., Völker, U., Erben, U., Zeichhardt, H., Schultheiss, H.P., Dörner, A., 2012. The mitochondrial respiratory chain has a critical role in the antiviral process in Coxsackievirus B3-induced myocarditis. *Lab. Invest.* 92, 125-134.
- Edgar, R., Domrachev, M., Lash, A.E., 2002. Gene Expression Omnibus: NCBI gene expression and hybridization array data repository. *Nucleic Acids Res.* 30, 207-10.
- Elbashir, S.M., Harborth, J., Lendeckel, W., Yalcin, A., Weber, K., Tuschl, T., 2001a. Duplexes of 21-nucleotide RNAs mediate RNA interference in cultured mammalian cells. *Nature* 411, 494-498.
- Elbashir, S.M., Lendeckel, W., Tuschl, T., 2001b. RNA interference is mediated by 21- and 22-nucleotide RNAs. *Genes Dev.* 15, 188-200.
- Ernst, S., Langer, R., Cooney, C.L., Sasisekharan, R., 1995. Enzymatic degradation of glycosaminoglycans. *Crit. Rev. Biochem. Mol. Biol.* 30, 387-444.
- Escarmis, C., Carrillo, E.C., Ferrer, M., Arriaza, J.F.G., Lopez, N., Tami, C., Verdaguer, N., Domingo, E., Franze-Fernandez, M.T., 1998. Rapid selection in modified BHK-21 cells of a foot-and-mouth disease virus variant showing alterations in cell tropism. *J. Virol.* 72, 10171-10179.
- Escribano-Romero, E., Jimenez-Clavero, M.A., Gomes, P., Garcia-Ranea, J.A., Ley, V., 2004. Heparan sulphate mediates swine vesicular disease virus attachment to the host cell. *J. Gen. Virol.* 85, 653-663.

- Feld, J.J., Hoofnagle, J.H., 2005. Mechanism of action of interferon and ribavirin in treatment of hepatitis C. *Nature* 436, 967-972.
- Fire, A., Xu, S., Montgomery, M.K., Kostas, S.A., Driver, S.E., Mello, C.C., 1998. Potent and specific genetic interference by double-stranded RNA in *Caenorhabditis elegans*. *Nature* 391, 806-811.
- Flynn, S.J., Burgett, B.L., Stein, D.S., Wilkinson, K.S., Ryan, P., 1993. The amino-terminal one-third of pseudorabies virus glycoprotein gIII contains a functional attachment domain, but this domain is not required for the efficient penetration of Vero cells. *J. Virol.* 67, 2646-2654.
- Früh, K., Simmen, K., Mattias Luukkonen, B.G., Bell, Y.C., Ghazal, P., 2001. Virogenomics: a novel approach to antiviral drug discovery. *Drug Discovery Today* 6, 621-627.
- Fry, K.M., 1996. Endogenous glycoconjugates are not associated with filter feeding in mosquito larvae (Diptera: Culicidae). *Can. J. Zool.* 74, 413-422.
- Gaddum, J.H., 1933. Reports of biological standards, III. Methods of biological assay depending on a quantal response. Med. Res. Council, London; Special Report Series, No. 183.
- Gale, M., J. R., Katze, M.G., 1998. Molecular mechanisms of interferon resistance mediated by viral-directed inhibition of PKR, the interferon-induced protein kinase. *Pharmacol. Ther.* 78, 29-46.
- Gallagher, J.T., Walker, A., 1985. Molecular distinctions between heparan sulphate and heparin. Analysis of sulphation patterns indicates that heparan sulphate and heparin are separate families of N-sulphated polysaccharides. *Biochem. J.* 230, 665-674.

- Geiss, G.K., An M.C., Bumgarner, R.E., Hammersmark, E., Cunningham, D., Katze, M.G., 2001. Global impact of influenza virus on cellular pathways is mediated by both replication-dependent and-independent events. *J. Virol.* 75, 4321-4331.
- Germi, R., Crance, J.M., Garin, D., Guimet, J., Lortat-Jacob, H., Ruigrok, R.W.H., Zarski, J.P., Drouet, E., 2002. Heparan sulfate-mediated binding of infectious dengue virus type 2 and yellow fever virus. *Virology* 292, 162-168.
- Ghiselli, G. 2006. SMC3 knockdown triggers genomic instability and p53-dependent apoptosis in human and zebrafish cells. *Mol. Cancer* 5, 52-64.
- Ghosh, A., Sarkar, S.N., Sen, G.C., 2000. Cell growth regulatory and antiviral effects of the P69 isozyme of 2-5 (A) synthetase. *Virology* 266, 319–328.
- Ghoshal, K., Majumder, S., Zhu, Q., Hunzeker, J., Datta, J., Shah, M., Sheridan, J.F., Jacob, S.T., 2001. Influenza virus infection induces metallothionein gene expression in the mouse liver and lung by overlapping but distinct molecular mechanisms. *Mol. Cell. Biol.* 21, 8301-8317.
- Ginsberg, H.S., Goebel, W.F., Horsfall, F.L., 1947. Inhibition of mumps virus multiplication by a polysaccharide. *Proc. Soc Exp. Biol. Med.* 66, 99-100.
- Gluezn, E., Sharma, R., Carrington, M., Gull, K., 2008. Functional characterization of cohesin subunit SCC1 in *Trypanosoma brucei* and dissection of mutant phenotypes in two life cycle stages. *Mol. Microbiol.* 69, 666-680.
- Goodfellow, I.G., Sioofy, A.B., Powell, R.M., Evans, D.J., 2001. Echoviruses bind heparan sulfate at the cell surface. *J. Virol.* 75, 4918-4921.
- Goto, A., Hayasaka, D., Yoshii, K., Mizutani, T., Kariwa, H., Takashima, I., 2003. A BHK-21 cell culture-adapted tick-borne encephalitis virus mutant is attenuated for neuroinvasiveness. *Vaccine* 21, 4043-4051.

- Green, R.H., Woolley, D.W., 1947. Inhibition by certain polysaccharides of hemagglutination and of multiplication of influenza virus. *J. Exp. Med.* 86, 55-64.
- Greve, J.M., Davis, G., Meyer, A.M., Forte, C.P., Yost, S.C., Marlor, C.W., Kamarck, M.E., McClelland, A., 1989. The major human rhinovirus receptor is ICAM-1. *Cell* 56, 839-847.
- Griffin, C.C., Linhardt, R.J., Van Gorp, C.L., Toida, T., Hileman, R.E., Schubert, R.L., Brown, S.E., 1995. Isolation and characterization of heparan sulfate from crude porcine intestinal mucosal peptidoglycan heparin. *Carbohydr. Res.* 276, 183-197.
- Haasnoot, J., Westerhout, E.M., Berkhout, B., 2007. RNA interference against viruses: strike and counterstrike. *Nat. Biotech.* 25, 1435-1443.
- Hammond, S.M., Bernstein, E., Beach, D., Hannon, G.J., 2000. An RNA-directed nuclease mediates post-transcriptional gene silencing in *Drosophila* cells. *Nature* 404, 293-296.
- Harris, K. S., Hellen, C.U.T., Wimmer, E., 1990. Proteolytic processing in the replication of picornaviruses. *Semin. Virol.* 1, 323–333.
- Heil, M.L., Albee, A., Strauss, J.H., Kuhn, R.J., 2001. An amino acid substitution in the coding region of the E2 glycoprotein adapts Ross River virus to utilize heparan sulfate as an attachment moiety. *J. Virol.* 75, 6303-6309.
- Heldt, C.L., Hernandez, R., Mudiganti, U., Gurgel, P.V., Brown, D.T., Carbonell, R.G., 2006. A colorimetric assay for viral agents that produce cytopathic effects. *J. Virol. Methods* 135, 56-65.
- Hertel, L., Mocarski, E.S., 2004. Global analysis of host cell gene expression late during cytomegalovirus infection reveals extensive dysregulation of cell cycle

- gene expression and induction of pseudomitosis independent of US28 function. *J. Virol.* 78, 11988-12011.
- Ho, M., 2000. Enterovirus 71: The virus, its infections and outbreaks. *J. Microbiol., Immunol. Infect.* 33, 205-216.
- Ho, M., Chen, E.R., Hsu, K.H., Twu, S.J., Chen, K.T., Tsai, S.F., Wang, J.R., Shih, S.R., 1999. An Epidemic of Enterovirus 71 Infection in Taiwan. *N. Engl. J. Med.* 341, 929-935.
- Hokaiwado, N., Takeshita, F., Banas, A., Ochiya, T., 2008. RNAi-based drug discovery and its application to therapeutics. *IDrugs* 11, 274-278.
- Huang, C., Hung, J.J., Wu, C.Y., Chien, M.S., 2004. Multiplex PCR for rapid detection of pseudorabies virus, porcine parvovirus and porcine circoviruses. *Vet. Microbiol.* 101, 209-214.
- Huang, D.D., 2008. The potential of RNA interference-based therapies for viral infections. *Curr. HIV/AIDS Rep.* 5, 33-39.
- Huang, S.C., Hsu, Y.W., Wang, H.C., Huang, S.W., Kiang, D., Tsai, H.P., Wang, S.M., Liu, C.C., Lin, K.H., Su, I.J., Wang, J.R., 2008. Appearance of intratypic recombination of Enterovirus 71 in Taiwan from 2002 to 2005. *Virus Res.* 131, 250-259.
- Hulst, M.M., Van Gennip, H.G.P., Vlot, A.C., Schooten, E., De Smit, A.J., Moormann, R.J.M., 2001. Interaction of classical swine fever virus with membrane-associated heparan sulfate: role for virus replication in vivo and virulence. *J. Virol.* 75, 9585-9595.
- Hüther, A., Dietrich, U., 2007. The emergence of peptides as therapeutic drugs for the inhibition of HIV-1. *AIDS Rev.* 9, 208-217.



- Ito, M., Baba, M., Sato, A., Pauwels, R., De Clercq, E., Shigeta, S., 1987. Inhibitory effect of dextran sulfate and heparin on the replication of human immunodeficiency virus (HIV) in vitro. *Antiviral Res.* 7, 361-367.
- Jackson, T., Blakemore, W., Newman, J.W.I., Knowles, N.J., Mould, A.P., Humphries, M.J., King, A.M.Q., 2000. Foot-and-mouth disease virus is a ligand for the high-affinity binding conformation of integrin  $\alpha_5\beta_1$ : influence of the leucine residue within the RGD motif on selectivity of integrin binding. *J. Gen. Virol.* 81, 1383-1391.
- Jackson, T., Ellard, F., Ghazaleh, R., Brookes, S., Blakemore, W., Corteyn, A., Stuart, D., Newman, J., King, A., 1996. Efficient infection of cells in culture by type O foot-and-mouth disease virus requires binding to cell surface heparan sulfate. *J. Virol.* 70, 5282-5287.
- Jang, S., Krausslich, H., Nicklin, M.J., Duke, G.M., Palmenberg, A.C., Wimmer, E., 1988. A segment of the 5' nontranslated region of encephalomyocarditis virus RNA directs internal entry of ribosomes during in vitro translation. *J. Virol.* 62, 2636 - 2643.
- Jenssen, H., Andersen, J.H., Uhlin-Hansen, L., Gutteberg, T.J., Rekdal, O., 2004. Anti-HSV activity of lactoferricin analogues is only partly related to their affinity for heparan sulfate. *Antiviral Res.* 61, 101–109.
- Jenssen, H., Hamill, P., Hancock, R.E.W., 2006. Peptide antimicrobial agents. *Clin. Microbiol. Rev.* 19, 491-511.
- Jinno-Oue, A., Oue, M., Ruscetti, S.K., 2001. A unique heparin-binding domain in the envelope protein of the neuropathogenic PVC-211 murine leukemia virus may contribute to its brain capillary endothelial cell tropism. *J. Virol.* 75, 12439-12445.
- Juffermans, N.P., Paxton, W.A., Dekkers, P.E.P., Verbon, A., De Jonge, E., Speelman, P., Van Deventer, S.J.H., Van Der Poll, T., 2000. Up-regulation of HIV

- coreceptors CXCR4 and CCR5 on CD4+ T cells during human endotoxemia and after stimulation with (myco) bacterial antigens: the role of cytokines. *Blood* 96, 2649-2654.
- Ketzinel-Gilad, M., Shaul, Y., Galun, E., 2006. RNA interference for antiviral therapy. *J. Gene Med.* 8, 933-950.
- Keyaerts, E., Vijgen, L., Chen, L., Maes, P., Hedenstierna, G., Van Ranst, M., 2004. Inhibition of SARS-coronavirus infection in vitro by *S*-nitrosoacetylpenicillamine, a nitric oxide donor compound. *Int. J. Infect. Dis.* 8, 223–6.
- Khan, J., Saal, L.H., Bittner, M.L., Chen, Y., Trent, J.M., Meltzer, P.S., 1999. Expression profiling in cancer using cDNA microarrays. *Electrophoresis* 20, 223-229.
- King, A.M.Q., Brown, F., Christian, P., Hovi, T., Hyypia, T., Knowles, N.J., Lemon, S.M., Minor, P.D., Palmenberg, A.C., Skern, T., Stanway, G., 2000. Family *Picornaviridae*, in: Van Regenmortel, M.H.V., Fauquet, C.M., Bishop, D.H.L., Calisher, C.H., (Eds.), *Virus Taxonomy: classification and nomenclature of viruses* (Seventh report of the International Committee on Taxonomy of Viruses). California: Academic Press, San Diego, pp. 657-683.
- Kleene, R., Schachner, M., 2004. Glycans and neural cell interactions. *Nat. Rev. Neurosci.* 5, 195-208.
- Klimstra, W.B., Ryman, K.D., Johnston, R.E., 1998. Adaptation of Sindbis virus to BHK cells selects for use of heparan sulfate as an attachment receptor. *J. Virol.* 72, 7357-7366.
- Konig, H., Rosenwirth, B., 1988. Purification and partial characterization of poliovirus protease 2A by means of a functional assay. *J. Virol.* 62, 1243-1250.
- Kreuger, J., Spillmann, D., Li, J.P., Lindahl, U., 2006. Interactions between heparan sulfate and proteins: the concept of specificity. *J. Cell Biol.* 174, 323-327.

- LaBarre, D.D., Lowy, R.J., 2001. Improvements in methods for calculating virus titer estimates from TCID<sub>50</sub> and plaque assays. *J. Virol. Methods* 96, 107-126.
- Lam, W.Y., Leung, K.T., Law, P.T.W., Lee, S.M.Y., Chan, H.L.Y., Fung, K.P., Ooi, V.E.C., Waye, M.M.Y., 2006. Antiviral effect of *Phyllanthus nanus* ethanolic extract against hepatitis B virus (HBV) by expression microarray analysis. *J. Cell. Biochem.* 97, 795-812.
- Lamberg, S.I., Stoolmiller, A.C., 1974. Glycosaminoglycans, a biochemical and clinical review. *J. Investig. Dermatol.* 63, 433-449.
- Lanford, R.E., Chavez, D., Guerra, B., Lau, J.Y., Hong, Z., Brasky, K.M., Beames, B., 2001. Ribavirin induces error-prone replication of GB virus b in primary tamarin hepatocytes. *J. Virol.* 75, 8074–8081.
- Lee, E., Lobigs, M., 2002. Mechanism of virulence attenuation of glycosaminoglycan-binding variants of Japanese encephalitis virus and Murray Valley encephalitis virus. *J. Virol.* 76, 4901-4911.
- Lee, E., Pavy, M., Young, N., Freeman, C., Lobigs, M., 2006. Antiviral effect of the heparan sulfate mimetic, PI-88, against dengue and encephalitic flaviviruses. *Antiviral Res.* 69, 31-38.
- Lee, G., Han, D., Song, J.Y., Lee, Y.S., Kang, K.S., Yoon, S., 2010. Genomic expression profiling in lymph nodes with lymphoid depletion from porcine circovirus 2-infected pigs. *J. Gen. Virol.* 91, 2585-2591.
- Lee, P., Knight, R., Smit, J.M., Wilschut, J., Griffin, D.E., 2002. A single mutation in the E2 glycoprotein important for neurovirulence influences binding of Sindbis virus to neuroblastoma cells. *J. Virol.* 76, 6302-6310.
- Leong, J.M., Wang, H., Magoun, L., Field, J.A., Morrissey P.E., Robbins, D., Tatro, J.B., Coburn, J., Parveen, N., 1998. Different classes of proteoglycans contribute

- to the attachment of *Borrelia burgdorferi* to cultured endothelial and brain cells. *Infect. Immun.* 66, 994-999.
- Levi, R., Beeor-Tzahar, T., Arnon, R., 1995. Microculture virus titration-a simple colourimetric assay for influenza virus titration. *J. Virol. Methods* 52, 55-64.
- Li, Q., Smith, A.J., Schacker, T.W., Carlis, J.V., Duan, L., Reilly, C.S., Haase, A.T., 2009. Microarray analysis of lymphatic tissue reveals stage-specific, gene expression signatures in HIV-1 infection. *J. Immunol.* 183, 1975-1982.
- Li, S.Y., Chen, C., Zhang, H.Q., Guo, H.Y., Wang, H., Wang, L., Zhang, X., Hua, S.N., Yu, J., Xiao, P.G., Li, R.S., Tan, X., 2005. Identification of natural compounds with antiviral activities against SARS-associated coronavirus. *Antiviral Res.* 67, 18-23.
- Li, Z.H.L.C., Ling, P., Shen, F.H., Chen, S.H., Liu, C.C., Yu, C.K., Chen, S.H., 2008. Ribavirin Reduces Mortality in Enterovirus 71-Infected Mice by Decreasing Viral Replication. *J. Infect. Dis.* 197, 854-857.
- Lin, C.W., Wu, C.F., Hsiao, N.W., Chang, C.Y., Li, S.W., Wan, L., Lin, Y.J., Lin, W.Y., 2008. Aloe-emodin is an interferon-inducing agent with antiviral activity against Japanese encephalitis virus and Enterovirus 71. *Int. J. Antimicrob. Agents.* 32, 355-359.
- Lin, T.Y., Chu, C., Chiu, C.H., 2002. Lactoferrin inhibits Enterovirus 71 infection of human embryonal rhabdomyosarcoma cells in vitro. *J. Infect. Dis.* 186, 1161-1164.
- Lin, T.Y., Liu, Y.C., Jheng, J.R., Tsai, H.P., Jan, J.T., Wong, W.R., Horng, J.T., 2009. Anti-Enterovirus 71 activity screening of Chinese herbs with anti-infection and inflammation activities. *Am. J. Chin. Med.* 37, 143-158.
- Lin, T.Y., Twu, S.J., Ho, M.S., Chang, L.Y., Lee, C.Y., 2003. Enterovirus 71 Outbreaks, Taiwan: Occurrence and Recognition. *Emerg. Infect. Dis.* 9, 291.

- Lin, Y.C., Wu, C.N., Shih, S.R., Ho, M.S., 2002. Characterization of a Vero cell-adapted virulent strain of Enterovirus 71 suitable for use as a vaccine candidate. *Vaccine* 20, 2485-2493.
- Lin, Y.L., Huang, Y.L., Ma, S.H., 1997. Inhibition of Japanese encephalitis virus infection by nitric oxide: antiviral effect of nitric oxide on RNA virus replication. *J. Virol.* 71, 5227–35.
- Lipshutz, R.J., Fodor, S.P.A., Gingeras, T.R., Lockhart, D.J., 1998. High density synthetic oligonucleotide arrays. *Nat. Genet.* 21, 20-24.
- Liu, M.Y., Liu, W., Luo, J., Liu, Y., Zhu, Y., Berman, H., Wu, J., 2011. Characterization of an outbreak of hand, foot, and mouth disease in Nanchang, China in 2010. *PLoS ONE* 6, art. no. e25287.
- Lockhart, D.J., et al. 1996. Expression monitoring by hybridization to high-density oligonucleotide arrays. *Nat. Biotechnol.* 14, 1675–1680.
- Lu, W.W., Hsu, Y.Y., Yang, J.Y., Kung, S.H., 2004. Selective inhibition of Enterovirus 71 replication by short hairpin RNAs. *Biochem. Biophys. Res. Commun.* 325, 494-499.
- Lum, L.C.S., Wong, K.T., Lam, S.K., Chua, K.B., Goh, A.Y.T., 1998. Neurogenic pulmonary oedema and Enterovirus 71 encephalomyelitis. *Lancet* 352, 1391-1391.
- Ma, X., Wang, Z., Li, S., Shen, Q., Yuan, Q., 2006. Effect of CaCl<sub>2</sub> as activity stabilizer on purification of heparinase I from *Flavobacterium heparinum*. *J. Chromatogr. B* 843, 209-215.
- Maag, D., Castro, C., Hong, Z., Cameron, C.E., 2001. Hepatitis C virus RNA-dependent RNA polymerase (NS5B) as a mediator of the antiviral activity of ribavirin. *J. Biol. Chem.* 276, 46094–46098.

- Malik, D.K., Baboota, S., Ahuja, A., Hasan, S.I., Ali J., 2007. Recent advances in protein and peptide drug delivery systems. *Curr. Drug Delivery* 4, 141-151.
- Mandal, P., Pujol, C.A., Carlucci, M.J., Chattopadhyay, K., Damonte, E.B., Ray, B., 2008. Anti-herpetic activity of a sulfated xylomannan from *Scinaia hatei*. *Phytochemistry* 69, 2193-2199.
- Mandl, C.W., Kroschewski, H., Allison, S.L., Kofler, R., Holzmann, H., Meixner, T., Heinz, F.X., 2001. Adaptation of tick-borne encephalitis virus to BHK-21 cells results in the formation of multiple heparan sulfate binding sites in the envelope protein and attenuation in vivo. *J. Virol.* 75, 5627-5637.
- Marchetti, M., Longhi, C., Conte, M.P., Pisani, S., Valenti, P., Seganti, L., 1996. Lactoferrin inhibits herpes simplex virus type 1 adsorption to Vero cells. *Antiviral Res.* 29, 221-231.
- Marie, I., Rebouillat, D., Hovanessian, A.G., 1999. The expression of both domains of the 69/71 kDa 2',5' oligoadenylate synthetase generates a catalytically active enzyme and mediates an anti-viral response. *Eur. J. Biochem.* 262, 155-165.
- Martino, T.A., Petric, M., Weingartl, H., Bergelson, J.M., Opavsky, M.A., Richardson, C.D., Modlin, J.F., Finberg, R.W., Kain, K.C., Willis, N. Gauntt, C.J., Liu, P.P., 2000. The Coxsackie-Adenovirus Receptor (CAR) is used by reference strains and clinical isolates representing all six serotypes of Coxsackievirus group B and by swine vesicular disease virus. *Virology* 271, 99-108.
- Maurer, M., Theoharides, T., Granstein, R.D., Bischoff, S.C., Bienenstock, J., Henz, B., Kovanen, P., Piliponsky, A.M., Kambe, N., Vliagoftis, H., Levi-Schaffer, F., Metz, M., Miyachi, Y., Befus, D., Forsythe, P., Kitamura, Y., Galli, S., 2003. What is the physiological function of mast cells? *Exp. Dermatol.* 12, 886-886.
- McMinn, P.C., 2002. An overview of the evolution of Enterovirus 71 and its clinical and public health significance. *FEMS Microbiol. Rev.* 26, 91-107.

- McNicholl, I., McNicholl, J., 2001. Neuraminidase inhibitors: zanamivir and oseltamivir. *Ann. Pharmacother.* 35, 57-70.
- Mendelsohn, C., Wimmer, E., Racaniello, V., 1989. Cellular receptor for poliovirus: Molecular cloning, nucleotide sequence, and expression of a new member of the immunoglobulin superfamily. *Cell* 56, 855-855.
- Mettenleiter, T.C., 2001. Brief overview on cellular virus receptors. *Virus Res.* 82, 3-8.
- Mizuta, K., Abiko, C., Murata, T., Matsuzaki, Y., Itagaki, T., Sanjoh, K., Sakamoto, M., Kongo, S., Murayama, S., Hayasaka, K., 2005. Frequent importation of enterovirus 71 from surrounding countries into the local community of Yamagata, Japan, between 1998 and 2003. *J. Clin. Microbiol.* 43, 6171-6175.
- Molla, A., Hellen, C.U., Wimmer, E., 1993. Inhibition of proteolytic activity of poliovirus and rhinovirus 2A proteinases by elastase-specific inhibitors. *J. Virol.* 67, 4688-4695.
- Moscufo, N., Yafal, A.G., Rogove, A., Hogle, J., Chow, M., 1993. A mutation in VP4 defines a new step in the late stages of cell entry by poliovirus. *J. Virol.* 67, 5075-5078.
- Muhamad, M., KeeL, Y., Rahman, N.A., Yusof, R., 2010. Antiviral actions of flavanoid-derived compounds on dengue virus type-2. *Int. J. Biol. Sci.* 6, 294-302.
- Nahmias, A.J., Kibrick, S., 1964. Inhibitory effect of heparin on herpes simplex virus. *J. Bacteriol.* 87, 1060-1066.
- Neff, S., Sá-Carvalho, D., Rieder, E., Mason, P., Blystone, S., Brown, E., Baxt, B., 1998. Foot-and-mouth disease virus virulent for cattle utilizes the integrin  $\alpha(v)\beta_3$  as its receptor. *J. Virol.* 72, 3587-3594.

- Newcombe, N.G., Andersson, P., Johansson, E.S., Au, G.G, Lindberg, A.M., Barry, R.D., Shafren, D.R., 2003. Cellular receptor interactions of C-cluster human group A coxsackieviruses. *J. Gen. Virol.* 84, 3041-3050.
- Nguyen, D.V., Arpat, A.B., Wang, N., Carroll, R.J., 2002. DNA microarray experiments: biological and technological aspects. *Biometrics* 58, 701-717.
- Nilsson, E.C., Jamshidi, F., Johansson, S.M., Oberste, M.S., Arnberg, N., 2008. Sialic acid is a cellular receptor for Coxsackievirus A24 variant, an emerging virus with pandemic potential. *J. Virol.* 82, 3061-3068.
- Nishimura, Y., Shimojima, M., Tano, Y., Miyamura, T., Wakita, T., Shimizu, H., 2009. Human P-selectin glycoprotein ligand-1 is a functional receptor for Enterovirus 71. *Nat. Med.* 15, 794-797.
- Norkin, L., 1995. Virus receptors: implications for pathogenesis and the design of antiviral agents. *Clin. Microbiol. Rev.* 8, 293-315.
- Nyberg, K., Ekblad, M., Bergström, T., Freeman, C., Parish, C.R., Ferro, V., Trybala, E., 2004. The low molecular weight heparan sulfate-mimetic, PI-88, inhibits cell-to-cell spread of herpes simplex virus. *Antiviral Res.* 63, 15-24.
- Olofsson, S., Bergström, T., 2005. Glycoconjugate glycans as viral receptors. *Ann. Med.* 37, 154-172.
- Palliser, D., Chowdhury, D., Wang, Q.Y., Lee, S.J., Bronson, R.T., Knipe, D.M., Lieberman, J., 2006. An siRNA-based microbicide protects mice from lethal herpes simplex virus 2 infection. *Nature* 439, 89-94.
- Palmenberg, A.C., 1990. Proteolytic Processing of Picornaviral Polyprotein. *Annu. Rev. Microbiol.* 44, 603-623.



- Papy-Garcia, D., Barbier-Chassefière, V., Rouet, V., Kerros, M.E., Klochendler, C., Tournaire, M.C., Barritault, D., Caruelle, J.P., Petit, E., 2005. Nondegradative Sulfation of Polysaccharides. Synthesis and Structure Characterization of Biologically Active Heparan Sulfate Mimetics. *Macromolecules* 38, 4647-4654.
- Parker W.B., 2005. Metabolism and antiviral activity of ribavirin. *Virus Res.* 107, 165-171.
- Patel, K.P., Bergelson, J.M., 2009. Receptors identified for hand, foot and mouth virus. *Nat. Med.* 15, 728-729.
- Paul, A., 2002. Possible unifying mechanism of picornavirus genome replication, in Semler, B.L., Wimmer, E., (Eds.), *Molecular Biology of Picornaviruses*. ASM Press, Washington, D.C. p. 227-246.
- Pauwels, R., Balzarini, J., Baba, M., Snoeck, R., Schols, D., Herdewijn, P., Desmyter, J., De Clercq, E., 1988. Rapid and automated tetrazolium-based colorimetric assay for the detection of anti-HIV compounds. *J. Virol. Methods* 20, 309-321.
- Pérez-Vélez, C.M., Anderson, M.S., Robinson, C.C., McFarland, E.J., Nix W.A., Pallansch, M.A., Oberste, M.S., Glodé, M.P., 2007. Outbreak of Neurologic Enterovirus Type 71 Disease: A Diagnostic Challenge. *Clin. Infect. Dis.* 45, 950-957.
- Pevear, D.C., Fancher, M.J., Felock, P.J., Rossmann, M.G., Miller, M.S., Diana, G., Treasurywala, A.M., McKinlay, M.A., Dutko, F.J., 1989. Conformational change in the floor of the human rhinovirus canyon blocks adsorption to HeLa cell receptors. *J. Virol.* 63, 2002-2007.
- Prikhod'ko, G.G., Vasilyeva, I., Reyes, H., Wong, S., Brown, K.E., Jameson, T., Busby, T.F., 2005. Evaluation of a new LightCycler reverse transcription-polymerase chain reaction infectivity assay for detection of human parvovirus B19 in dry-heat inactivation studies. *Transfusion* 45, 1011-1019.

- Putnak, J.R., Phillips, B.A., 1981. Picornaviral structure and assembly. *Microbiol. Rev.* 45, 287-315.
- Qu, Z., Liebler, J.M., Powers, M.R., Galey, T., Ahmadi, P., Huang, X.N., Ansel, J.C., Butterfield, J.H., Planck, S.R., Rosenbaum, J.T., 1995. Mast cells are a major source of basic fibroblast growth factor in chronic inflammation and cutaneous hemangioma. *Am. J. Pathol.* 147, 564-573.
- Rabenstein, D.L., 2002. Heparin and heparan sulfate: structure and function. *Nat. Prod. Rep.* 19, 312-331.
- Ramírez-Salazar, E., Centeno, F., Nieto, K., Valencia-Hernández, A., Salcedo, M., Garrido, E., 2011. HPV16 E2 could act as down-regulator in cellular genes implicated in apoptosis, proliferation and cell differentiation. *Virol. J.* 8, art. no. 247.
- Rebouillat, D., Hovanessian, A.G., 1999. The human 2',5'-oligoadenylate synthetase family: interferon-induced proteins with unique enzymatic properties. *J. Interferon Cytokine Res.* 19, 295–308.
- Reddi, H.V., Kumar, A.S.M., Kung, A.Y., Kallio, P.D., Schlitt, B.P., Lipton, H.L., 2004. Heparan sulfate-independent infection attenuates high-neurovirulence GDVII virus-induced encephalitis. *J. Virol.* 78, 8909-8916.
- Reddi, H.V., Lipton, H.L., 2002. Heparan sulfate mediates infection of high-neurovirulence Theiler's viruses. *J. Virol.* 76, 8400-8407.
- Reed, L.J., Muench, H., 1938. A simple method of estimating fifty percent endpoints. *Am. J. Epidemiol.* 27, 4931-4937.
- Ripoll, V.M., Irvine, K.M., Ravasi, T., Sweet, M.J., Hume, D.A., 2007. Gpnmb is induced in macrophages by IFN- $\gamma$  and lipopolysaccharide and acts as a feedback regulator of proinflammatory responses. *J. Immunol.* 178, 6557–6566.

- Riss, T.L., Moravec, R.A., 1992. Comparison of MTT, XTT and a novel tetrazolium compound MTS for in vitro proliferation and chemosensitivity assays. *Mol. Biol. Cell.* 3, 184a.
- Rogers, J.M., Diana, G.D., McKinlay, M.A., 1999. Pleconaril: A broad spectrum antipicornaviral agent. *Adv Exp Med Biol.* 458, 69-76.
- Roivainen, M., Piirainen, L., Hovi, T., Virtanen, I., Riikonen, T., Heino, J., Hyypiä, T., 1994. Entry of Coxsackievirus A9 into host cells: specific interactions with  $[\alpha]v[\beta]3$  integrin, the vitronectin receptor. *Virology* 203, 357-365.
- Rotbart, H.A., 2000. Antiviral therapy for Enteroviruses and rhinoviruses. *Antiviral Chem. Chemother.* 11, 261-271.
- Rubino, K.L., Nicholas, J.A., 1992. A novel, spectrophotometric microneutralization assay for respiratory syncytial virus. *J. Virol. Methods* 39, 55-67.
- Rueckert, R., 1990. Picornaviruses and their replication, in: Fields, B.N., Knipe, D.M., (Eds.), *Virology*. New York, Lippincott-Raven, 507-548.
- Rusnati, M., Urbinati, C., Caputo, A., Possati, L., Lortat-Jacob, H., Giacca, M., Ribatti, D., Presta, M., 2001. Pentosan polysulfate as an inhibitor of extracellular HIV-1 Tat. *J. Biol. Chem.* 276, 22420-22425.
- Rutz, S., Scheffold, A., 2004. Towards in vivo application of RNA interference - New toys, old problems. *Arthritis Res. Ther.* 6, 78-85.
- Ryman, K.D., Gardner, C.L., Burke, C.W., Meier, K.C., Thompson, J.M., Klimstra, W.B., 2007. Heparan sulfate binding can contribute to the neurovirulence of neuroadapted and nonneuroadapted Sindbis viruses. *J. Virol.* 81, 3563-3573.
- Ryu, S.Y., Lee, C.K., Lee, C.O., Kim, H.S., Zee, O.P., 1992. Antiviral triterpenes from *Prunella vulgaris*. *Arch. Pharmacol Res.* 15, 242-245.

- Sa-Carvalho, D., Rieder, E., Baxt, B., Rodarte, R., Tanuri, A., Mason, P., 1997. Tissue culture adaptation of foot-and-mouth disease virus selects viruses that bind to heparin and are attenuated in cattle. *J. Virol.* 71, 5115-5123.
- Saliba Jr, M.J., 2001. Heparin in the treatment of burns: A review. *Burns* 27, 349-358.
- Sasisekharan, R., Venkataraman, G., 2000. Heparin and heparan sulfate: biosynthesis, structure and function. *Curr. Opin. Chem. Biol.* 4, 626-631.
- Scagliarini, A., Vaccari, F., Gallina, L., Pozzo, F., Prosperi, S., 2006. In vitro evaluation of antiviral activity of ribavirin against canine distemper virus. *Vet. Res. Commun.* 30, 269-272.
- Schauer, R., 1985. Sialic acids and their role as biological masks. *Trends Biochem. Sci.* 10, 357-360.
- Schmid, M., Wimmer, E., 1994. IRES-controlled protein synthesis and genome replication of poliovirus. *Arch. Virol. Suppl.* 9, 279-289.
- Schmidt, N., EH, L., Ho, H., 1974. An apparently new Enterovirus isolated from patients with disease of the central nervous system. *J. Infect. Dis.* 129, 304-309.
- Schmidtke, M., Schnittler, U., Jahn, B., Dahse, H.M., Stelzner, A., 2001. A rapid assay for evaluation of antiviral activity against Coxsackievirus B3, influenza virus A, and herpes simplex virus type 1. *J. Virol. Methods* 95, 133-143.
- Schols, D., Pauwels, R., Desmyter, J., De Clercq, E., 1990. Dextran sulfate and other polyanionic anti-HIV compounds specifically interact with the viral gp120 glycoprotein expressed by T-cells persistently infected with HIV-1. *Virology* 175, 556-561.

- Schoor, O., Weinschenk, T., Hennenlotter, J., Corvin, S., Stenzl, A., Rammensee, H.G., Stevanović, S., 2003. Moderate degradation does not preclude microarray analysis of small amounts of RNA. *BioTechniques* 35, 1192-1201.
- Sebbage, V., 2009. Cell-penetrating peptides and their therapeutic applications. *Biosci. Horiz.* 2, 64-72.
- Selvam, P., Murgesh, N., Chandramohan, M., De Clercq, E., Keyaerts, E., Vijgen, L., Maes, P., Neyts, J., Ranst, M.V., 2008. *In Vitro* antiviral activity of some novel isatin derivatives against HCV and SARS-CoV viruses. *Indian J. Pharm. Sci.* 70, 91-94.
- Severson, W.E., Schmaljohn, C.S., Javadian, A., Jonsson, C.B., 2003. Ribavirin Causes Error Catastrophe during Hantaan Virus Replication. *J. Virol.* 77, 481-488.
- Shafren, D., Bates, R., Agrez, M., Herd, R., Burns, G., Barry, R., 1995. Coxsackieviruses B1, B3, and B5 use decay accelerating factor as a receptor for cell attachment. *J. Virol.* 69, 3873-3877.
- Shafren, D., Dorahy, D., Ingham, R., Burns, G., Barry, R., 1997. Coxsackievirus A21 binds to decay-accelerating factor but requires intercellular adhesion molecule 1 for cell entry. *J. Virol.* 71, 4736-4743.
- Shen, W.C., Chiu, H.H., Chow, K.C., Tsai, C.H., 1999. MR imaging findings of Enteroviral encephalomyelitis: an outbreak in Taiwan. *AJNR Am. J. Neuroradiol.* 20, 1889-1895.
- Shia, K.S., Li, W.T., Chang, C.M., Hsu, M.C., Chern, J.H., Leong, M.K., Tseng, S.N., Lee, C.C., Lee, Y.C., Chen, S.J., Peng, K.C., Tseng, H.Y., Chang, Y.L., Tai, C.L., Shih, S.R., 2002. Design, synthesis, and structure-activity relationship of Pyridyl Imidazolidinones: a novel class of potent and selective Human Enterovirus 71 inhibitors. *J. Med. Chem.* 45, 1644-1655.

- Shih, S.R., Ho, M.S., Lin, K.H., Wu, S.L., Chen, Y.T., Wu, C.N., Lin, T.Y., Chang, L.Y., Tsao, K.C., Ning, H.C., Chang, P.Y., Jung, S.M., Hsueh, C., Chang, K.S., 2000. Genetic analysis of Enterovirus 71 isolated from fatal and non-fatal cases of hand, foot and mouth disease during an epidemic in Taiwan, 1998. *Virus Res.* 68, 127-136.
- Shih, S.R., Stollar, V., Lin, J.Y., Chang, S.C., Chen, G.W., Li, M.L., 2004a. Identification of genes involved in the host response to Enterovirus 71 infection. *J. NeuroVirol.* 10, 293-304.
- Shih, S.R., Tsai, K.N., Li, Y.S., Chueh, C.C., Chan, E.C., 2003. Inhibition of Enterovirus 71-induced apoptosis by allophycocyanin isolated from a blue-green alga. *J. Med. Virol.* 70, 119-125.
- Shih, S.R., Tsai, M.C., Tseng, S.N., Won, K.F., Shia, K.S., Li, W.T., Chern, J.H., Chen, G.W., Lee, C.C., Lee, Y.C., Peng, K.C., Chao, Y.S., 2004b. Mutation in Enterovirus 71 capsid protein VP1 confers resistance to the inhibitory effects of pyridylimidazolidinone. *Antimicrob. Agents Chemother.* 48, 3523-3529.
- Shimizu, N., Soda, Y., Kanbe, K., Liu, H.Y., Mukai, R., Kitamura, T., Hoshino, H., 2000. A putative G protein-coupled receptor, RDC1, is a novel coreceptor for human and simian immunodeficiency viruses. *J. Virol.* 74, 619-626.
- Sidwell, R.W., Huffman, J.H., Khare, G.P., Allen, L.B., Witkowski, J.T., Robins, R.K., 1972. Broad-spectrum antiviral activity of Virazole: 1-beta-D-ribofuranosyl-1,2,4-triazole-3-carboxamide. *Science* 177, 705-706.
- Sim, A.C.N., Luhur, A., Tan, T.M.C., Chow, V.T.K., Poh, C.L., 2005. RNA interference against Enterovirus 71 infection. *Virology* 341, 72-79.
- Skrypina, N.A., Timofeeva, A.V., Khaspekov, G.L., Savochkina, L.P., Beabealashvili, R.S., 2003. Total RNA suitable for molecular biology analysis. *J. Biotechnol.* 105, 1-9.

- Staal, F.J.T., Van Der Burg, M., Wessels, L.F.A., Barendregt, B.H., Baert, M.R.M., Van Den Burg, C.M.M., Van Huffel, C., Langerak, A.W., Van Der Velden, V.H.J., Reinders, M.J.T., Van Dongen, J.J.M., 2003. DNA microarrays for comparison of gene expression profiles between diagnosis and relapse in precursor-B acute lymphoblastic leukemia: choice of technique and purification influence the identification of potential diagnostic markers. *Leukemia* 17, 1324-1332.
- Stalkup, J.R., Chilukuri, S., 2002. Enterovirus infections: A review of clinical presentation, diagnosis, and treatment. *Dermatol. Clin.* 20, 217-223.
- Stanway, G., Hovi, T., Knowles, N.J., Hyypia, T., 2002. Molecular and biological basis of Picornavirus taxonomy, in: Semler, B.L., Wimmer, E., (Eds.), *Molecular Biology of Picornaviruses*. Washington DC: ASM Press, 17-24.
- Stark, G.R., Kerr, I.M., Williams, B.R., Silverman, R.H., Schreiber, R.D., 1998. How cells respond to interferons. *Annu. Rev. Biochem.* 67, 227–264.
- Streeter, D.G., Witkowski, J.T., Khare, G.P., Sidwell, R.W., Bauer, R.J., Robins, R.K., Simon, L.N., 1973. Mechanism of action of 1-Dribofuranosyl-1,2,4-triazole-3-carboxamide (Virazole), a new broadspectrum antiviral agent. *Proc. Natl. Acad. Sci. U.S.A.* 70, 1174–1178.
- Su, F.M., Chang, J.S., Wang, K.C., Tsai, J.J., Chiang, L.C., 2008. A Water Extract of *Pueraria Lobata* Inhibited Cytotoxicity of Enterovirus 71 in a Human Foreskin Fibroblast Cell Line. *Kaohsiung J. Med. Sci.* 24, 523-530.
- Sydiskis, R.J., Owen, D.G., Lohr, J.L., Rosler, K.H., Blomster, R.N., 1991. Inactivation of enveloped viruses by anthraquinones extracted from plants. *Antimicrob. Agents Chemother.* 35, 2463–6.
- Takemoto, K.K., Fabisch, P., 1964. Inhibition of herpes simplex virus by natural and synthetic acid polysaccharides. *Proc. Soc. Exp. Biol. Med.* 116, 140–144.

- Talon, J., Horvath, C.M., Polley, R., Basler, C.F., Muster, T., Palese, P., Garcia-Sastre, A., 2000. Activation of interferon regulatory factor 3 is inhibited by the influenza A virus NS1 protein. *J. Virol.* 74, 7989-7996.
- Tan, E.L., Tan, T.M.C., Chow, V.T.K., Poh, C.L., 2007a. Enhanced potency and efficacy of 29-mer shRNAs in inhibition of Enterovirus 71. *Antiviral Res.* 74, 9-15.
- Tan, E.L., Tan, T.M.C., Chow, V.T.K., Poh, C.L., 2007b. Inhibition of Enterovirus 71 in virus-infected mice by RNA interference. *Mol. Ther.* 15, 1931-1938.
- Tanaka, A., Oka, K., Tanaka, K., Jinno, A., Ruscetti, S.K., Kai, K., 1998. The entire nucleotide sequence of friend-related and paralysis-inducing PVC-441 murine leukemia virus (MuLV) and its comparison with those of PVC-211 MuLV and Friend MuLV. *J. Virol.* 72, 3423-3426.
- Thao, N.T.T., Ngoc, N.T.K., Tú, P.V., Thúy, T.T., Cardoso, M.J., McMinn, P.C., Phuektes, P., 2010. Development of a multiplex polymerase chain reaction assay for simultaneous identification of human Enterovirus 71 and Coxsackievirus A16. *J. Virol. Methods* 170, 134-139.
- Thirumorthy, N., Shyam Sunder, A., Manisenthil Kumar, K.T., Senthil kumar, M., Ganesh, G.N.K., Chatterjee, M., 2011. A review of metallothionein isoforms and their role in pathophysiology. *World J. Surg. Oncol.* 9, art no 9.
- Tomko, R.P., Xu, R., Philipson, L., 1997. HCAR and MCAR: The human and mouse cellular receptors for subgroup C adenoviruses and group B coxsackieviruses. *Proc. Natl. Acad. Sci. U.S.A.* 94, 3352-3356.
- Toshima, J., Toshima, J.Y., Takeuchi, K., Mori, R., Mizuno, K., 2001. Cofilin Phosphorylation and Actin Reorganization Activities of Testicular Protein Kinase 2 and Its Predominant Expression in Testicular Sertoli Cells. *J. Biol. Chem.* 276, 31449-31458.



- Toyoda, H., Nicklin, M.J., Murray, M.G., Anderson, C.W., Dunn, J.J., Studier, F.W., Wimmer, E., 1986. A second virus-encoded proteinase involved in proteolytic processing of poliovirus polyprotein. *Cell* 45, 761-770.
- Triantafilou, K., Fradelizi, D., Wilson, K., Triantafilou, M., 2002. GRP78, a coreceptor for Coxsackievirus A9, interacts with major histocompatibility complex class I molecules which mediate virus internalization. *J. Virol.* 76, 633-643.
- Tsai, K.N., Tsai, T.Y., Chen, C.M., 2006. A new approach to deciphering pathways of Enterovirus 71-infected cells. *Biomed. Eng.: Appl. Basis Commun.* 18, 337-342.
- Tucker, P.C., Strauss, E.G., Kuhn, R.J., Strauss, J.H., Griffin, D.E., 1993. Viral determinants of age-dependent virulence of Sindbis virus for mice. *J. Virol.* 67, 4605-4610.
- Ueno, R., Kuno, S., 1987. Dextran sulphate, a potent anti-HIV agent in vitro having synergism with zidovudine. *Lancet* 329, 1379-1379.
- Uhlmann, F., Lottspelch, F., Nasmyth, K., 1999. Sister-chromatid separation at anaphase onset is promoted by cleavage of the cohesin subunit Scc1. *Nature* 400, 37-42.
- Urbinati, C., Chiodelli, P., Rusnati, M., 2008. Polyanionic drugs and viral oncogenesis: a novel approach to control infection, tumor-associated inflammation and angiogenesis. *Molecules* 13, 2758-2785.
- Vaheri, A., 1964. Heparin and related polyionic substances as virus inhibitors. *Acta Pathol. Microbiol. Scand.* 18 (Suppl.), 171.
- Varki, A., Schauer, R., 2009. Sialic acids, in: Varki, A., Cummings, R., Esko, J., Freeze, H., FP, S., Bertozzi, C., Hart, G., Etzler, M., (Eds.), *Essentials of Glycobiology*. 2nd Edition. New York: Cold Spring Harbor Laboratory Press.

- Velculescu, V.E., Zhang, L., Vogelstein, B., Kinzler, K.W., 1995. Serial analysis of gene expression. *Science* 270, 484-487.
- Velculescu, V.E., Zhang, L., Zhou, W., Vogelstein, J., Basrai, M.A., Bassett, D.E., Hieter, P., Vogelstein, B., Kinzler, K.W., 1997. Characterization of the yeast Transcriptome. *Cell* 88, 243-251.
- Vera-Bravo, R., Ocampo, M., Urquiza, M., García, J.E., Rodríguez, L.E., Puentes, A., López, R., Curtidor, H., Suárez, J.E., Torres, E., Guzmán, F., Díaz, D., Cortes, J., Bravo, M.M., Cómbita, A.L., Orozco, O., Patarroyo, M.E. 2003. Human papillomavirus type 16 and 18 L1 protein peptide binding to VERO and HeLa cells inhibits their VLPs binding. *Int. J. Cancer* 107, 416-424.
- Vignuzzi, M., Stone, J.K., Andino, R., 2005. Ribavirin and lethal mutagenesis of poliovirus: Molecular mechanisms, resistance and biological implications. *Virus Res.* 107, 173-181.
- Volpi, N., Linhardt, R.J., 2010. High-performance liquid chromatography-mass spectrometry for mapping and sequencing glycosaminoglycan-derived oligosaccharides. *Nature Protocols* 5, 993-1004.
- Vrublevskaya, V.V., Kornev, A.N., Smirnov, S.V., Morenkov, O.S., 2002. Cell-binding properties of glycoprotein B of Aujeszky's disease virus. *Virus Res.* 86, 7-19.
- Wachinger, M., Kleinschmidt, A., Winder, D., Von Pechmann, N., Ludvigsen, A., Neumann, M., Holle, R., Salmons, B., Erfle, V., Brack-Werner, R., 1998. Antimicrobial peptides melittin and cecropin inhibit replication of human immunodeficiency virus 1 by suppressing viral gene expression. *J. Gen. Virol.* 79, 731-740.
- Wang, S.M., Lei, H.Y., Huang, M.C., Su, L.Y., Lin, H.C., Yu, C.K., Wang, J.L., Liu, C.C., 2006. Modulation of cytokine production by intravenous immunoglobulin

- in patients with Enterovirus 71-associated brainstem encephalitis. *J. Clin. Virol.* 37, 47–52.
- Wang, S.M., Lei, H.Y., Huang, K.J., Wu, J.M., Wang, J.R., Yu, C.K., Su, I.J., Liu, C.C., 2003. Pathogenesis of enterovirus 71 brainstem encephalitis in pediatric patients: Roles of cytokines and cellular immune activation in patients with pulmonary edema. *J. Infect. Dis.* 188, 564-570.
- Wang, Y.F., Chou, C.T., Lei, H.Y., Liu, C.C., Wang, S.M., Yan, J.J., Su, I.J., Wang, J.R., Yeh, T.M., Chen, S.H., Yu, C.K., 2004. A mouse-adapted enterovirus 71 strain causes neurological disease in mice after oral infection. *J. Virol.* 78, 7916-7924.
- Ward, T., Pipkin, P.A., Clarkson, N.A., Stone, D.M., Minor, P.D., Almond, J.W., 1994. Decay-accelerating factor CD55 is identified as the receptor for echovirus 7 using CELICS, a rapid immuno-focal cloning method. *EMBO J.* 13, 5070-5074.
- Watanabe, W., Konno, K., Ijichi, K., Inoue, H., Yokota, T., Shigeta, S., 1994. MTT colorimetric assay system for the screening of anti-orthomyxo- and anti-paramyxoviral agents. *J. Virol. Methods* 48, 257-265.
- Wen, Y.Y., Chang, T.Y., Chen, S., Li, C., Liu, H., 2003. Comparative study of enterovirus 71 infection of human cell lines. *J. Med. Virol.* 70, 109-118.
- Weng, K.F., Chen, L.L., Huang, P.N., Shih, S.R., 2010. Neural pathogenesis of Enterovirus 71 infection. *Microbes and Infect.* 12, 505-510.
- Weng, T.Y., Chen, L.C., Shyu, H.W., Chen, S.H., Wang, J.R., Yu, C.K., Lei, H.Y., Yeh, T.M., 2005. Lactoferrin inhibits Enterovirus 71 infection by binding to VP1 protein and host cells. *Antiviral Res.* 67, 31-37.

- Wilkinson, B., Chen, J.Y.F., Han, P., Rufner, K.M., Goularte, O.D., Kaye, J., 2002. TOX: An HMG box protein implicated in the regulation of thymocyte selection. *Nat. Immunol.* 3, 272-280.
- Wu, B.W., Pan, T.L., Leu, Y.L., Chang, Y.K., Tai, P.J., Lin, K.H., Horng, J.T., 2007. Antiviral Effects of *Salvia miltiorrhiza* (Danshen) Against Enterovirus 71. *Am. J. Chin. Med.* 35, 153-168.
- Wu, K.X., Ng, M.M.L., Chu, J.J.H., 2010. Developments towards antiviral therapies against Enterovirus 71. *Drug Discovery Today* 15, 1041-1051.
- WuDunn, D., Spear, P.G., 1989. Initial interaction of herpes simplex virus with cells is binding to heparan sulfate. *J. Virol.* 63, 52-58.
- Xu, H.X., Zeng, F.Q., Wan, M., Sim, K.Y., 1996. Anti-HIV triterpene acids from *Geum japonicum*. *J. Nat. Prod.* 59, 643-645.
- Yamayoshi, S., Yamashita, Y., Li, J., Hanagata, N., Minowa, T., Takemura, T., Koike, S., 2009. Scavenger receptor B2 is a cellular receptor for Enterovirus 71. *Nat. Med.* 15, 798-801.
- Yan, J.J., Su, I.J., Chen, P.F., Liu, C.C., Yu, C.K., Wang, J.R., 2001. Complete genome analysis of Enterovirus 71 isolated from an outbreak in Taiwan and rapid identification of Enterovirus 71 and coxsackievirus A16 by RT-PCR. *J. Med. Virol.* 65, 331-339.
- Yang, B., Chuang, H., Yang, K.D., 2009. Sialylated glycans as receptor and inhibitor of enterovirus 71 infection to DLD-1 intestinal cells. *Virol. J.* 6, art. no. 141.
- Yang, V.C., Linhardt, R.J., Bernstein, H., 1985. Purification and characterization of heparinase from *Flavobacterium heparinum*. *J. Biol. Chem.* 260, 1849-1857.

- Yasin, B., Pang, M., Turner, J.S., Cho, Y., Dinh, N.N., Waring, A.J., Lehrer, R.I., Wagar, E.A., 2000. Evaluation of the inactivation of infectious herpes simplex virus by host-defense peptides. *Eur. J. Clin. Microbiol. Infect. Dis.* 19, 187–194.
- Ypma-Wong, M.F., Dewalt, P.G., Johnson, V.H., Lamb, J.G., Semler, B.L., 1988. Protein 3CD is the major poliovirus proteinase responsible for cleavage of the P1 capsid precursor. *Virology* 166, 265 - 270.
- Yun, S., Lee, S.H., Yoon, S.R., Kim, M.S., Piao, Z.H., Myung, P.K., Kim, T.D., Jung, H., Choi, I., 2011. TOX regulates the differentiation of human natural killer cells from hematopoietic stem cells in vitro. *Immunol. Lett.* 136, 29-36.
- Zamore, P.D., Tuschl, T., Sharp, P.A., Bartel, D.P., 2000. RNAi: double-stranded RNA directs the ATP-dependent cleavage of mRNA at 21 to 23 nucleotide intervals. *Cell* 101, 25-33.
- Zautner, A.E., Korner, U., Henke, A., Badorff, C., Schmidtke, M., 2003. Heparan sulfates and coxsackievirus-adenovirus receptor: each one mediates Coxsackievirus B3 PD infection. *J. Virol.* 77, 10071-10077.
- Zeisel, M.B., Fofana, I., Fafi-Kremer, S., Baumert, T.F., 2011. Hepatitis C virus entry into hepatocytes: molecular mechanisms and targets for antiviral therapies. *J. Hepatol.* 54, 566-576.
- Zheng, Z.M., He, P.J., Caueffield, D., Neumann, M., Specter, S., Baker, C., Bankowski, M., 1995. Enterovirus 71 isolated from China is serologically similar to the prototype E71 BrCr strain but differs in the 5prime-noncoding region. *J. Med. Virol.* 47, 161-167.
- Zhou, A., Paranjape, J.M., Hassel, B.A., Nie, H., Shah, S., Galinski, B., Silverman, R.H., 1998. Impact of RNase L overexpression on viral and cellular growth and death. *J. Interferon Cytokine Res.* 18, 953–961.

- Zhou, S., Liu, R., Baroudy, B.M., Malcolm, B.A., Reyes, G.R., 2003. The effect of ribavirin and IMPDH inhibitors on hepatitis C virus subgenomic replicon RNA. *Virology* 310, 333–342.
- Zhu, W., Li, J., Liang, G., 2011. How does cellular heparan sulfate function in viral pathogenicity? *Biomed. Environ. Sci.* 24, 81-87.
- Zimring, J.C., Goodbourn, S., Offermann, M.K., 1998. Human herpesvirus 8 encodes an interferon regulatory factor (IRF) homolog that represses IRF-1-mediated transcription. *J. Virol.* 72, 701-707.